2017

Molecular Targets of Atropine- and Mamba Toxin 3-Mediated Inhibition of Form-Deprivation Myopia in the Chick: A Case of Mistaken Receptor Identity?

Carr, Brittany Jane

UNIVERSITY OF CALGARY

Molecular Targets of Atropine- and Mamba Toxin 3-Mediated Inhibition of Form-Deprivation Myopia in the Chick: A Case of Mistaken Receptor Identity?

by

Brittany Jane Carr

A THESIS
SUBMITTED TO THE FACULTY OF GRADUATE STUDIES
IN PARTIAL FULFILMENT OF THE REQUIREMENTS FOR THE
DEGREE OF DOCTOR OF PHILOSOPHY

GRADUATE PROGRAM IN NEUROSCIENCE

CALGARY, ALBERTA

APRIL, 2017

Abstract

Myopia is a refractive disorder characterized by the inability to see distant objects clearly. It is the most common childhood vision disorder, and the leading cause of adult visual impairment world-wide. Myopia prevalence is rising rapidly; it is estimated that 2.5 billion people will be affected by 2030, and any degree of myopia increases the risk of blindness-inducing comorbidities.

There are no universally accepted pharmaceutical therapies to slow myopia progression, but some success has been found with the muscarinic acetylcholine receptor (mAChR) antagonist atropine. There remains a paucity of investigations into the ocular signalling cascades modulated by atropine-treatment. Research in this area has been based on the *assumption* that because atropine, and a few other mAChR antagonists, inhibit myopia at extremely high concentrations, mAChRs *must* regulate myopia progression. Regulation of eye growth by mAChRs has *never* been proven conclusively.

Here, I report that myopia-inhibition by atropine is *dependent* on induction of nitric oxide (NO), and that exogenous NO is sufficient to inhibit experimentally-induced form-deprivation myopia (FDM) on its own. In addition, I provide evidence that *disproves* the assumption that mAChRs are responsible for atropine- and mamba toxin 3-mediated myopia-inhibition in the chick. First, I demonstrate that alpha$_2$-adrenoceptor (ADRA2) agonists can dose-dependently inhibit FDM. Second, I show that myopia-inhibiting mAChR antagonists can bind to, and block signalling by, human alpha$_{2A}$-adrenoceptors (ADRA2A). Furthermore, I show that the relative inhibitory potencies (pIC_{50}'s) of myopia-inhibiting mAChR antagonists at ADRA2A correlate better with their reported abilities to inhibit FDM in the chick than their relative pIC_{50}'s at human and chicken mAChR M_4.

My data further our understanding of how the eye may know how large to grow. They provide two novel alternative targets for anti-myopia therapies (NO & ADRA2s), both of which would eliminate the most significant side-effects of atropine-treatment. They provide a range in which mAChR antagonists should be expected to act in a "specific" manner at human and chicken mAChR M_4, and reinforce the need for caution in attributing the effects of high concentration drug to a specific receptor target.

Preface

In this thesis, I set out to determine the important downstream signalling molecules involved in myopia inhibition by atropine; I focussed on the role of nitric oxide in regulation of eye growth and inhibition of FDM in the chick. I also wanted to provide evidence that atropine may inhibit experimentally-induced myopia in the chick through an unexpected mechanism; one that does not depend on actions mediated through mAChRs, but alpha$_2$-adrenoceptors instead. For this, I used both *in vivo* animal experiments to study the effects of alpha$_2$-adrenoceptor ligands on FDM, and *in vitro* receptor pharmacology to study the functional characteristics of mAChR antagonist action at human and chicken mAChR M_4 and alpha$_{2A}$-adrenoceptors. I performed these experiments with the hope that I will be able to provide insight into the mechanisms responsible for myopia inhibition by atropine and other mAChR antagonists. I also aimed to further our understanding of homeostatic mechanisms involved in regulation of eye growth, which is an important fundamental process in visually-driven organisms that we still know very little about.

Acknowledgements

Mentors

I wish to thank my mentors for their hard work, guidance, and support throughout the entirety of my thesis. ***Dr. Bill Stell***: Where to start? I have been in your lab for SEVEN YEARS?! It's difficult to believe it's been that long. You have always provided me with the personal freedom to grow, while at the same time giving me a solid foundation to fall back on. You have taught me to be a scientist: how to think critically, how to write, how to deal with a terrible review, and how to celebrate. Your mentorship has helped shape me into the person I am today; maybe a little too much because sometimes we're so similar it's a little scary. Words cannot express my gratitude. Thank you for taking me on, for believing in me, for providing me with the opportunities I needed to succeed, and for encouraging me to capitalize on my own curiosity. I feel so lucky and so grateful to have had to opportunity to work beside you for so long. ***Dr. Morley Hollenberg***: Thank you for giving me the opportunity to work in your lab, and for believing in my data, even when I didn't. ***Dr. Koichiro Mihara***: I cannot thank you enough for your hard work and dedication to the receptor pharmacology experiments. Thank you for encouraging me, and for providing the help I needed to get through the hard times when things just weren't working. Thank you for never giving up, and for pushing me to do the same. I could not have accomplished what I did in this thesis without your guidance, patience, and drive to complete the work to the best of your abilities. ***Dr. Ebba Kurz***: Thank you for serving on my committee, for providing your lab staff to help me to get started on my receptor pharmacology experiments, and for asking the hard questions to push me to do my best. ***Dr. Grant Gordon***: Thank you for serving on my committee, for providing your honest opinion on the life of an academic researcher, and for giving me tips on how to secure a post-doctoral position. ***Dr. Neil Nathanson***: Thank you for providing the cM_4 receptor clone, for answering my questions about receptor pharmacology, and for providing excellent feedback on my data and multiple manuscripts. Your exceptional support, even though I am not your student, is greatly appreciated. ***Dr. Mark Giembycz***: Thank you for acting as an examiner on my candidacy exam and my thesis dissertation defense, for making the time to discuss my data and provide guidance on the direction of my

experiments, and for providing the CRE-Luc construct that gave me my first positive results in four years.

Additional Supporters

I wish to thank ***Drs. Torben Bech-Hansen, Sarah McFarlane***, ***Carol Schuurmans***, and ***Richard Wilson*** for being there for me when I needed advice, and for offering your help and resources whenever required. ***Dr. Mahmoud Saifeddine***: Thank you for teaching me how to perform Ca^{2+}-sensing assays, and for always being a friendly, cheerful presence in the lab. ***Dr. Rithwik Ramachandran***: I want to thank you for helping me with my mock candidacy exam (along with ***Vadim Iablokov***), and for providing your input on multiple manuscripts. Thank you for your expertise and advice with how to best measure functional cell responses, and THANK YOU for suggesting that I try a different method of cAMP measurement, and providing that method to me. You saved my thesis. I wish to thank ***Dr. Keith Sharkey*** for acting as an examiner during my candidacy exam and for providing antibody samples to our lab, and ***Dr. Bob French*** for taking on the role of neutral chair during my candidacy. I also wish to thank ***Dr. Ray Turner*** for his approval and support in providing tuition costs for the Canadian Light Microscopy Course. Finally, I wish to thank ***Dr. Frank Schaeffel*** for acting as the external examiner for my thesis dissertation defense.

Core Support

Animal Care Staff: I wish to thank ***Onilea Matheson*** for taking such exceptional care of our chicks; I am sure they are as fond of you as you are of them. I also wish to thank the rest of the animal care team for providing incomparable care for our chicks and for helping to keep things running smoothly. *Live Cell Imaging Facility*: I wish thank ***Dr. Pina Colarusso***, ***Jen (Amon) Poirier***, ***Axinia Doering***, and ***Rima-Marie Wazen*** of the Live Cell Imaging Facility for their expertise and encouragement. Imaging on the Olympus IX81 FV1000 Laser Scanning Confocal Microscope was supported by the Live Cell Imaging Facility, funded by the Snyder Institute for Chronic Disease at the Cumming School of Medicine, University of Calgary. *Core DNA Services*: I wish to thank ***Dr. Shuyuan Yu***, ***Maria Loskot***, ***Heidi Huettler***, and ***Shelly Wegener*** of the University of Calgary Core DNA Services Laboratory. Your skills were integral for my receptor pharmacology studies,

and I am so happy to have had you as our lab neighbours. *University of Calgary Health Sciences Campus*: Finally, I want to thank the entire faculty at the University of Calgary Health Sciences Campus. It has been so amazing to work in a community that is all too willing to provide guidance and support to anyone, no matter the field or institute.

Family & Friends

Last, but not least, I wish to thank my family and friends for providing never-ending support and encouragement, even if they did not always understand what I was up to in the lab. I could not have made it this far without you. To my University friends – ***Rami Halabi, Jonathan Yang, Qing Shi,*** and ***Derek Waldner***: Thank you for being there to talk science, and for assisting me in reaching my research goals, and for reviewing my thesis before submission (***Derek Waldner***). Thank you for being my friends and for sharing the good times, on and off campus.

Funding

This project was funded by a Natural Sciences and Engineering Research Council of Canada (NSERC) Discovery Grant (RGPIN/131-2013) and the Foundation Fighting Blindness Canada EYEGEYE Research Training Fund (*Dr. William K. Stell*); a Canadian Institutes of Health Research (CIHR) grant (MOP13759), with ancillary funding from Prostate Cancer Canada, The Calgary Prostate Cancer Centre and the Calgary Motorcycle Ride for Dad (*Dr. Morley D. Hollenberg*); and an NSERC PGS-D award (PGSD2-476058-2015), Dr. D. Grant Gall Graduate Traineeship, Queen Elizabeth II Scholarships, and Odd Fellow Rebekah Visual Research Fund Awards (*Brittany J. Carr*).

Contributions

This thesis in its entirety was written by myself, with limited editorial comments and suggestions from ***Dr. Bill K. Stell*** (entire), ***Dr. Morley D. Hollenberg*** (entire), ***Dr. Neil M. Nathanson*** (**Chapter 5**), and ***Mr. Derek Waldner*** (entire). All experiments were designed and performed by myself, with the following exceptions: The D-Arg dose response data and half of the data for the SNP and L-Arg dose-response studies were performed previously by ***Dr. Bill Stell***; SNP and L-Arg dose response curves were replicated by

myself and combined with previous data for final publication (**Chapter 3**). CRISPR knockout of mAChR M_3, creation of the human-chicken α_{2A}-adrenoceptor chimera, and periodic transformation and cloning of receptors were completed by ***Dr. Koichiro Mihara*** (**Chapter 5** & **Appendix A3**). *Regardless of the contributions of others, I take full responsibility for the design and conduct of the experiments, and for the resulting data and my interpretations of them, as reported here.*

Published Materials

Data from **Chapter 3** have been published in the open access journal ***Scientific Reports***[1]; no special permission is required to reproduce them in this thesis. The work benefitted from the helpful comments of two anonymous reviewers. I thank them for their differing perspectives on my writing-style and thought-processes underlying experimental designs and interpretation of the results; my manuscript is stronger for it. Data from **Chapter 4** (Carr BJ & Stell WK. IOVS 2016; 57: ARVO E-Abstract 4738) and **Chapter 5** (Carr BJ et al. IOVS 2017; 58: ARVO E-Abstract 5465) have been published previously in abstract form (© Association for Research in Vision and Ophthalmology - ARVO). **Figures 1.4**, **1.5**, **1.6,** and **5.7** contain data from previously published studies that are not my own. **Figure 1.4**: Strang et al. 2010. *Investigative Ophthalmology and Visual Science* (© ARVO), McBrien et al. 2009. *Molecular Vision*, and Fischer et al. 1998. *Journal of Comparative Neurology* (© John Wiley & Sons, Inc.). **Figure 1.5**: Woldemussie et al. 2007. *Visual Neuroscience* (© Cambridge University Press) and Harun-Or-Rashid et al. 2014. *Investigative Ophthalmology and Visual Science* (© ARVO). **Figure 1.6**: Fischer et al. 1999. *Journal of Comparative Neurology* (© John Wiley & Sons, Inc.), Wilson et al. 2011. *Visual Neuroscience* (© Cambridge University Press), and Tekmen-Clark and Gleason. 2013. *Visual Neuroscience* (© Cambridge University Press). **Figure 5.7**: Kukkonen et al. 2004. *Journal of Biological Chemistry* (© American Society for Biochemistry and Molecular Biology). I thank the publishers for providing permission to reproduce these data in my thesis.

To patience,

perseverance,

and embracing the unknown.

Table of Contents

Abstract ... **ii**

Preface ... **iii**

Acknowledgements ... **iv**

Dedication ... **viii**

List of Figures and Tables ... **xii**

List of Abbreviations and Symbols ... **xiv**

Chapter 1: Introduction ... **1**

Myopia: Clinical Aspects and Health Care Burden ... 1

The Role of Genes in Myopia Development ... 3

Chick Models of Experimentally-Induced Myopia ... 5

Visual Regulation of Eye Growth ... 6

The Retina: Visual Processing Circuitry and Regulation of Eye Growth ... 11

Ocular Muscarinic Acetylcholine Receptors ... 18

Ocular Alpha$_2$-Adrenoceptors ... 22

Nitric Oxide ... 25

Dopamine ... 31

Thesis Aims ... 32

Chapter 2: Materials & Methods for Chick Experiments ... **33**

Animals & Ethics Statement ... 33

Induction of Form-Deprivation Myopia and Intravitreal Injections ... 34

Measurements ... 35

Data Analysis ... 36

Tissue preparation and Histology (Toluidine Blue) ... 36

Chapter 3: Nitric Oxide is Necessary for Atropine-Mediated Inhibition of FDM in Chicks, and Sufficient to Inhibit FDM by Itself ... **37**

Abstract ... 37

Introduction ... 38

Results ... 39

Normal Ocular Growth and Myopia-Development after Application of Form-Diffuser Goggles ... 39

Inhibition of Form-Deprivation Myopia by NO-Sources ... 41

Effects of L-Arg and SNP on Retinal Integrity ... 45

Inhibition of FDM by Atropine and NOS-Specific Blockade of Inhibition 49
Discussion 56
Methods 60
Drugs for Intravitreal Injection 60
Rationale for Drug Selection 61
Immunolabelling (LEP-100 & GRL2) 62
Chapter 4: Alpha$_2$-Adrenoceptor Agonists Inhibit FDM in the Chick 63
Abstract 63
Introduction 64
Results 65
Effect of Clonidine on Form-Deprivation Myopia in Chicks 65
Effect of Guanfacine on Form-Deprivation Myopia in Chicks 67
Effect of Yohimbine on Form-Deprivation Myopia in Chicks 69
Effect of Yohimbine on Prevention of FDM by Goggle-Removal in Chicks 71
Discussion 74
Methods 77
Drugs for Intravitreal Injection 77
Rationale for Drug Selection 78
Chapter 5: Myopia-Inhibiting Muscarinic Receptor Antagonists Also Block Signalling through Alpha$_{2A}$-Adrenoceptors 79
Abstract 79
Introduction 80
Results 82
Human mAChR M_4 (M_4) 82
Chicken mAChR M_4 (cM_4) 84
mAChR antagonist potency at human α_{2A}-adrenergic receptor (hADRA2A) 88
Controls 91
Discussion 93
Distribution of Drugs Within Ocular Tissues After Different Delivery Methods 93
mAChR Antagonists at M_4, cM_4, and hADRA2A, and Correlations with Myopia-Inhibition 94
Difference in Binding of MT3 at M_4 Versus cM_4 96
Methods & Materials 101

DNA and Expression Vectors 101
CRISPR/Cas9 Knock-Down of mAChR M_3 102
Cell Culture and Transfection Protocols 103
cAMP Accumulation Assay and Antagonist IC_{50} Curves 104
Data Analysis 104
Chapter 6: Implications of the Studies Performed & Where Can We Go from Here? 106
Could There Be Two Separate Growth-Regulating Pathways in the Chick? 112
Bibliography 114
Appendix A1: Does Spiperone Block Myopia-Inhibition by Atropine? 133
Appendix A2: Inhibition of FDM by Guanfacine: Mechanism? 139
Appendix A3: Attempts to Clone a Functional Chicken Alpha$_{2A}$-Adrenoceptor ... 152
Copyright Permissions 161

List of Figures and Tables

Figure 1.1.....2
Figure 1.2.....7
Figure 1.3.....12
Figure 1.4.....20
Figure 1.5.....24
Figure 1.6.....29

Figure 2.1.....34

Figure 3.1.....40
Figure 3.2.....42
Figure 3.3.....44
Figure 3.4.....46
Figure 3.5.....48
Figure 3.6.....51
Figure 3.7.....53

Figure 4.1.....66
Figure 4.2.....68
Figure 4.3.....70
Figure 4.4.....72

Figure 5.1.....83
Figure 5.2.....85
Figure 5.3.....86
Figure 5.4.....89
Figure 5.5.....91
Figure 5.6.....92
Figure 5.7.....98
Figure 5.8.....100

Figure A1.1.....135
Figure A2.1.....141
Figure A2.2.....143
Figure A2.3.....145
Figure A2.4.....150
Figure A3.1.....154
Figure A3.2.....156
Figure A3.3.....159

Table 3.1.....54
Table 3.2.....55
Table 3.3.....60

Table 4.1.....73
Table 4.2.....78

Table 5.1.....87
Table 5.2.....90

Table A1.1.....136
Table A1.2.....138
Table A2.1.....146–147
Table A2.2.....151
Table A3.1.....154

List of Abbreviations and Symbols

6-OHDA	6-Hydroxydopamine
AA	Amino Acid(s)
AC	Amacrine Cell
ADRA2A	Alpha$_{2A}$-Adrenoceptor
AL	Axial Length
Ala (A)	Alanine
Arg (R)	Arginine
Asn (N)	Asparagine
Asp (D)	Aspartic Acid
ATR	Atropine Sulfate
ccADRA2A	Chick Chimera Alpha$_{2A}$-Adrenoceptor (Human N-terminus: AA 1-46)
CCh	Carbachol
ChAT	Choline Acetyltransferase
CHRD	Choroid
Clon	Clonidine Hydrochloride
cM$_4$	Chicken Muscarinic Acetylcholine Receptor Subtype M$_4$
CN	Cone Photoreceptor(s)
CNS	Central Nervous System
CRE-Luc	cAMP Response Element Driven Luciferase Vector: (pGL4.29[luc2P/CRE/Hygro])
CRISPR	Clustered Regularly Interspaced Short Palindromic Repeats
CR-M3	Lenti-X HEK 293T cells with a CRISPR knock-out of mAChR M3
CVS	Centrifugal Vision System
Cys (C)	Cysteine
D	Diopter
d	Difference in Mean Values: Experimental Eye Minus Control Eye
dAL	Difference in Mean Axial Lengths
dED	Difference in Mean Equatorial Diameters
dRE	Difference in Mean Refractive Errors
dWW	Difference in Mean Wet Weights
DA	Dopamine

DIC	Dicyclomine
DMEM	Dulbecco's Modified Eagle's Medium
DMSO	Dimethyl Sulfoxide
D-NMMA	D-N^G-monomethyl arginine
ED	Equatorial Diameter
ED_{50}	The half maximal effective concentration of a ligand
EDTA	Ethylenediaminetetraacetic Acid
FDM	Form-Deprivation Myopia
GAG	Glycosaminoglycan
Gfcn	Guanfacine Hydrochloride
Glu (E)	Glutamic Acid
Gln (Q)	Glutamine
Gly (G)	Glycine
GPCR	G Protein-Coupled Receptor
hADRA2A	Human $Alpha_{2A}$-Adrenoceptor
HC	Horizontal Cell
HIM	Himbacine
His (H)	Histidine
Ile (I)	Isoleucine
INL	Inner Nuclear Layer
ION	Isthmo-Optic Nucleus
IOTr	Isthmo-Optic Tract
IPL	Inner Plexiform Layer
K_d	The equilibrium dissociation constant of a radioactively-labelled ligand
K_i	Equilibrium dissociation constant of an inhibitory ligand
L-Arg	L-Arginine
LASIK	Laser-Assisted In Situ Keratomileusis
Leu (L)	Leucine
LGN	Lateral Geniculate Nucleus
LIM	Lens-Induced Myopia
L-NAME	L-NG-Nitroarginine methyl ester

L-NIO	N^G-(1-Iminoethyl)-L-ornithine
L-NMMA	L-N^G-monomethyl arginine
Luc_N	Normalized CRE-Luc Expression
Lys (K)	Lysine
M_4	Human Muscarinic Acetylcholine Receptor Subtype M_4
mAChR	Muscarinic Acetylcholine Receptor
MC	Müller Cell
Met (M)	Methionine
MEP	Mepenzolate Bromide
MT3	Mamba Toxin 3 (also known as m4-toxin in early reports)
NO	Nitric Oxide
NOS	Nitric Oxide Synthase
NOSi	Nitric Oxide Synthase Inhibitor(s)
OD	Right Eye
OPL	Outer Plexiform Layer
OS	Left Eye or Outer Segment
OU	Both Eyes
OXY	Oxyphenonium Bromide
P7, P13	Post-hatch day 7, 13, etc.
PBS	Phosphate-buffered saline
PG1,6	Post-goggling day 1, 6, etc.
Phe (F)	Phenylalanine
pIC_{50}	Negative logarithm of the half maximal inhibitory concentration (molar)
PR	Photoreceptor
Pro (P)	Proline
PRZ	Pirenzepine Dihydrochloride
QNB	3-Quinuclidinyl Benzilate
RA	Retinoic Acid
RD	Rod Photoceptors
RE	Refractive Error
RLuc	Constitutively Driven *Renilla* Luciferase (Vector: pRL-TK)

RPE	Retinal Pigment Epithelium
SCL	Sclera
Ser (S)	Serine
SNP	Sodium Nitroprusside or Single Nucleotide Polymorphism
Thr (T)	Threonine
TRP	Tropicamide
Trp (W)	Tryptophan
Tyr (Y)	Tyrosine
UV	Ultraviolet
Val (V)	Valine
WW	Wet Weight
YOH	Yohimbine Hydrochloride

Chapter 1: Introduction

Humans, like other diurnal organisms, are distinctly dependent on our sense of vision. Our eyes are highly specialized organs; they collect light signals from our external environment, interpret the incoming stimuli, and then process them into a language that can be transmitted to and understood by the brain. While structural development of the eyes is largely controlled by genetics and occurs before birth, our visual perception of the world is created by collaboration between retinal circuitry and the brain. Thus, complex visual skills such as depth perception, edge detection, object tracking, and judging distances must be learned, and are fine-tuned during the post-natal period from birth to 24 months and beyond. This relationship between visual development and how we view our external environment is also significant in dictating how the eye will grow. Emmetropization is the process by which the rate of eye growth is regulated, so that the focal point of the refractive image formed by the cornea and the lens is focussed on the retinal photoreceptors. Although genetics may provide a blueprint as to how large an eye should be, eye-growth is exceedingly susceptible to visually-regulated changes[2]. Certain conditions in our visual environment can override genetics, and hamper the eyes' ability to self-regulate growth. Failure of emmetropization can lead to refractive disorders, called ametropias. Ametropias are the most common visual disorders in children and adults, but little is known about the mechanisms that control emmetropization. Thus, it is difficult to prevent significant refractive errors caused by improper growth of the eye. This is becoming a greater concern, as a specific type of ametropia – myopia – is quickly becoming a global health concern, due to its ever-increasing prevalence and significant health care burden.

Myopia: Clinical Aspects and Health Care Burden

Myopia, or near-sightedness, is characterized by the inability to see distant objects clearly. It is caused by failure of emmetropization that leads to *overgrowth* of the eye, so that the focal point of the refractive image created by the cornea and the lens falls short of the retinal photoreceptors (**Fig. 1.1**).

Figure 1.1: Simple Refractive Errors of the Eye

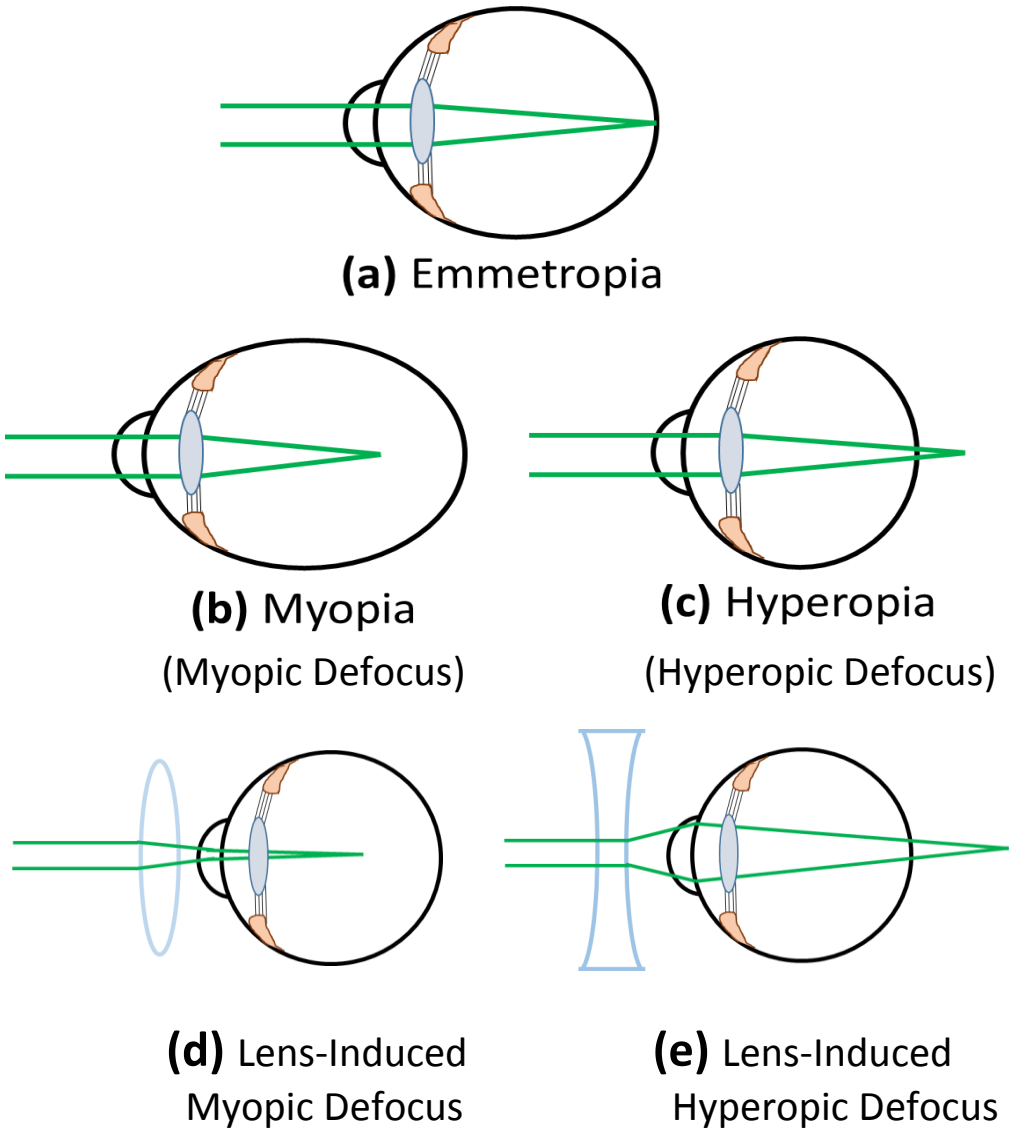

Figure 1.1: Exaggerated simple refractive errors (ametropias) caused by abnormal eye growth. Emmetropia (normal vision) is the state of refraction where light is focussed perfectly on retinal photoreceptors (a). Myopia (near-sightedness) occurs when the axial length of the eye is too long, and light is focussed in front of the photoreceptors (b). Hyperopia (short-sightedness) occurs when the axial length of the eye is too short, and light is focussed behind the photoreceptors (c). Refractive error can be modified using lenses; in an emmetropic eye, positive lenses induce myopic defocus (d), and negative lenses to induce hyperopic defocus (e).

Today, myopia onset is occurring earlier on in life and more frequently in most populations studied[3]. The underlying biological cause of myopia is unknown, and there is no widely-accepted therapy to prevent its onset and progression; symptoms can only be mitigated using optical corrections such as lenses (spectacle or contact) or surgical methods (LASIK). If left untreated, moderate myopia is the leading cause of visual impairment worldwide, and high myopia (defined as a negative refractive error of ≤ -6.00 D) is associated with a significantly increased risk of macular degeneration, retinal detachment, cataracts, and glaucoma[4]. The most common form of myopia, and the focus of this thesis, is spontaneous-onset or school-age myopia (referred to as "myopia" from now on). It is diagnosed early in most children, and progresses slowly until the growth of the eye growth stabilizes, usually by mid-teens to early 20s. The resulting final refractive error normally ranges from -1.50 D – -5.50 D, but can progress into high myopia. The health care burden of myopia worldwide, already in excess of USD $200 billion annually, is likely to increase as the population of myopic individuals grows, and some estimate that 2.5 billion people (1/3 of the world's population) will have some degree of myopia by 2030[3].

The Role of Genes in Myopia Development

The role of genes versus environment has always been a major controversy in myopia research, and recent evidence suggests that regulation of eye growth is most likely dependent on a combination of both. Myopia prevalence varies greatly in different ethnic and geographical populations[4]. Recent studies surveying myopia prevalence in American preschool children (aged 6–72 months) reported a prevalence of 1.2% in non-Hispanic whites, 3.7% in Hispanics, 3.98% in Asians, and 6.6% in African Americans[5,6]. When older children are surveyed, the difference between ethnic populations is even more profound; a study performed in Australian children reported a 500% discrepancy in myopia prevalence between European Caucasian children (8.3%) and East Asian Children (42.3%) aged 12 yrs., but this difference decreased to a 330% difference by the age of 17 (17.7% in European Caucasians compared to 59.1% in children of East Asian ethnicity)[7].

Twin studies and parental myopia studies were conducted to try to assess the role of genetics in development of myopia. Twin studies have shown that the correlation of

incidence of myopia is significantly higher in monozygotic twins than dizygotic twins; age and the methods used to gather and analyze the data are important, as correlations of myopia incidence can range from r = 0.11 to 0.94 depending on the study[8]. There is strong evidence to suggest that myopiagenic risk is dependent on the refractive state of a person's parents; a person is more likely to become myopic when they have two myopic parents, compared with one myopic parent, compared with two emmetropic parents[9-13], and this risk of becoming myopic is independent of environmental factors such as excessive near-work[9,10].

Recent advances in technology have permitted genome-wide association studies (GWAS), which have revealed a correlation between certain genes and an increased risk of myopia. The recently published Consortium for Refractive Error and Myopia (CREAM) study is the largest international genome-wide meta-analysis on myopia and refractive error, which compiled data from 32 studies encompassing Europe, the United States, Australia and Asia (n=45,758)[14]. Twenty-four new loci were identified that were associated with up to a ten-fold increased risk of myopia. Sixteen new loci were found in European populations, eight of which overlapped with Asian populations, and two of the loci had been identified previously (*GJD2* and *RASGRF1*)[15]. Later studies identified single nucleotide polymorphisms (SNPs) adjacent to an additional thirteen genes[16-20]. The genes identified by the CREAM consortium and others are associated with a large variety of functions such as neurotransmission (*GJD2, GRIA4, RASGRF1, RBFOX1/A2BP1*), ion transport (*KCNQ5, CD55, CACNA1D, KCNJ2, CHRNG, MYO1D*), retinoic acid metabolism (*RDH5, RORB, CYP26A1*), extracellular matrix remodeling (*LAMA2, BMP2*) and eye development (*PRSS56, SIX6, CHD7, ZIC2*), providing significant evidence that the root causes of myopia may arise from a plethora of (unrelated) disorders. SNPs and their associated genes have also been examined for gene/environment and early or late myopia onset interactions[21]. Although the data revealed an association between ten genes and early onset (age $\leq$ 7.5 yrs) and six genes and late onset (age > 7.5 yrs) myopia, evidence for gene/environmental interactions was scarce; only one SNP (rs7829127) associated with *ZMAT4* – a zinc finger protein with currently unknown function – had a significant interaction with near work that stood up to stringent repetition. Genes alone cannot account

for the rapid increase in myopia prevalence that is being observed world-wide[3,22], however, and they cannot explain why myopia can be experimentally induced in a plethora of animal models that do not develop myopia naturally[23].

Chick Models of Experimentally-Induced Myopia

Most identified risk factors of myopia development can be categorized as environmental influences, such as increased socioeconomic status, residing in an urban environment, higher education and IQ, increased time spent performing near work, and increased time spent indoors[4]. In order to understand the etiology of myopia, and the role that these risk factors might play in its development, scientists have used animal models to test some of the most popular hypotheses about how myopia development occurs. Animal models of myopia demonstrate clearly that although genetics may determine myopia susceptibility, environmental factors are powerful modifiers of eye growth that can override genetic predispositions.

The first reported animal model of myopia was discovered accidentally in non-human primates during investigations into the cortical effects of monocular visual deprivation. Suturing the eyelids of young macaques resulted in high levels of axial myopia[24], and the longer the period of visual deprivation, the greater amount of resultant refractive error[25]. After the establishment of the "deprivation model" of myopia in primates, reports of experimentally-induced deprivation myopia in chicken followed soon after, with translucent diffuser goggles replacing lid suture[26]. When myopia is induced by depriving the eye of clear (form) vision, either by lid suture or by affixing a frosted diffuser over the eye, it is called form-deprivation myopia (FDM). FDM acts as an "open-loop" stimulator of eye growth; significant uncorrectable blur of the visual image results in excessive axial elongation of the eye as long as the form-deprivation stimulus is present. Once the deprivation stimulus is removed, the eye will stop growing. A few years after the discovery of experimentally-induced FDM, it was reported that affixing negative lenses over the eye also caused axial myopia, as the eye will grow to compensate for the refractive error imposed onto the retina by the negative lens[27]. This type of experimental myopia is called lens-induced myopia (LIM). It is considered to be a "closed-loop system" because the eye

will grow only as large as it needs to be to overcome the refractive error imposed by the negative lens. Once this happens, the eye will stop growing, even when the lens is left affixed over the eye. Conversely, when a positive lens is affixed over the eye, axial elongation slows, resulting in a smaller axial length and a hyperopic refractive error[28]. This indicates that the retina can detect direction of defocus and compensate correctly[2], but how it does this is still unknown.

Although both models of experimentally-induced myopia result in a significant negative refractive error, it is controversial whether they work through the same biological mechanisms[29]. FDM is thought to work primarily through retinal signalling, with very little influence from the brain[2,30,31]. The primary evidence for this is that severing of the optic nerve seems to have no effect on the ability of the eye to develop deprivation myopia[30], and form-deprivation of half of the visual field results in FDM only in areas that correspond visually-deprived retina[31]. In contrast, severing of the optic nerve does seem to have a small, but significant effect on the development of LIM[32]. Certain drug treatments also reveal a difference between the FDM and LIM paradigms; 6-hydroxydopamine (6-OHDA) and mamba toxin 3 (MT3) both prevent FDM, but have little or no effect on the development of LIM[33,34].

Many of the drug treatments used to inhibit experimental myopia are not expected to exert prolonged effects ($\leq$ 3 hrs), but this is not as significant a concern as one would think. It only takes about 2 hrs per day of unimpeded vision to "rescue" the eye from myopiagenic effects of diffusers[35] and negative lenses[36]. Thus, if anti-myopia drug treatments mimic the effects of clear vision, it would be expected that they too only need to modulate retinal signalling for up to 2 hrs to prevent myopia. Eyes can also "recover" from experimentally-induced myopia upon removal of the FDM or LIM stimulus and return to an emmetropic refractive state, if the animal is young enough[37].

Visual Regulation of Eye Growth

Our perception of our external environment is dependent on the passage of the visual image through many ocular components before the visual image is eventually focussed on the

retina, therefore defects in any ocular component (**Fig. 1.2**) can have a significant impact on emmetropization.

Figure 1.2: Gross Anatomy of the Human Eye

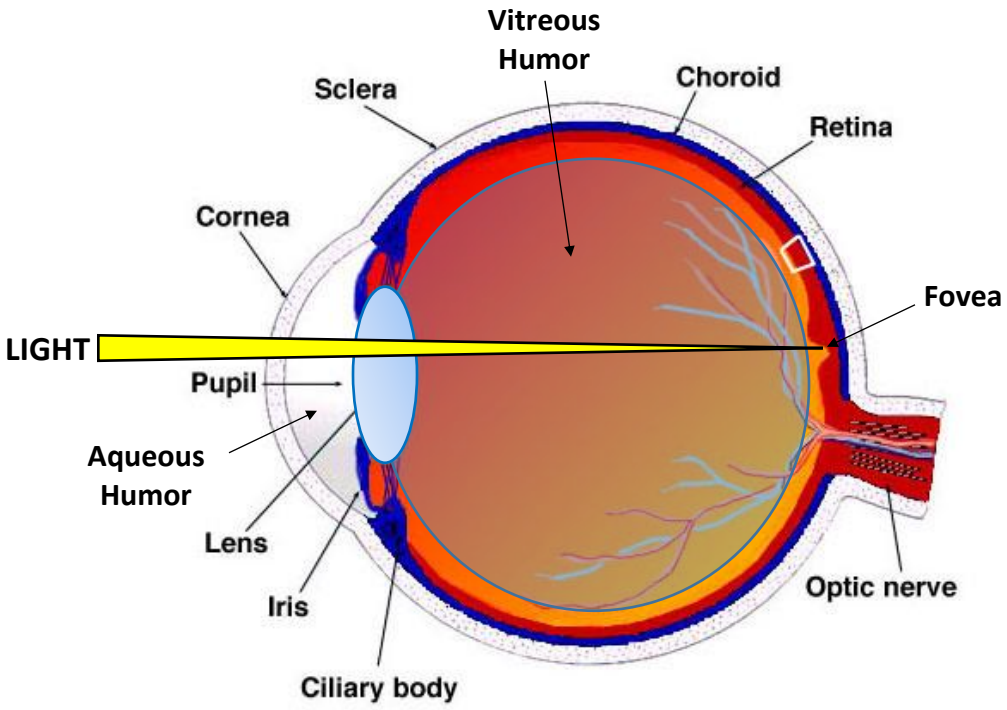

Figure 1.2: Gross anatomy of the human eye. Reproduced and modified from the online textbook Webvision (http://webvision.med.utah.edu/imageswv/sagitta2.jpeg) with permission.

When we gaze into the human eye, the first structure we see is the transparent cornea, a specialized extension of the sclera – the tough outside covering of the eye. The cornea contributes about 2/3 of the total focussing power of the eye (in humans), and its purpose, along with the crystalline lens, is to refract the visual image in such a way that its focus lies on the retinal photoreceptors. Some animals, such as chickens and pigeons, possess corneal-accommodative mechanisms, which permit up to 9 diopters (D) of changes in refractive power[38,39]. Corneal focus in humans is fixed, however, so we must rely solely on lenticular accommodation – changes in the shape of the lens – to adjust the focal point of near and distant objects to the correct area of the retina. This is achieved through the actions

of the ciliary muscle, which is a smooth muscle that contracts and relaxes to cause changes in the thickness and curvature of the lens. There is a limit to the focussing power of the cornea and the lens (in humans, about 65 D), so the axial length of the eye (or depth of the vitreal chamber) can also play an important role in determining whether the refractive image will ultimately be focussed correctly onto the photoreceptors; failure of the globe to grow to the correct size is one way that ametropias can occur (**Fig. 1.1**).

Another structure in the eye that can contribute significantly to changes in refractive error is the vascular choroid layer, which contains blood vessels, smooth muscle (vascular and avascular), sympathetic, parasympathetic, and nitrergic innervation, secretory cells, and lymphatic vessels[40]. Generally, the function of the choroid is to supply the outer retina with oxygen and nutrients, and to remove metabolic waste, but significant changes in choroidal thickness can be correlated with changes in refractive error in certain species[40]. If the eye is presented with hyperopic defocus imposed by negative lens wear (**Fig. 1.1e**) – a myopiagenic stimulus – the choroid will thin, but if myopic defocus is imposed by positive lens wear (**Fig. 1.1d**) – an anti-myopiagenic stimulus – the choroid will thicken. This thickening/thinning response of the choroid is most pronounced in birds, which possess very large lymphatic "lacunae", but it also occurs to varying degrees in mammalian models such as guinea pigs[41], marmosets[42], and macaques[43]. It is unknown whether this behavior has a direct or passive effect on emmetropization, but it is important to note that choroidal thickness also changes in response to treatment with eye growth-regulating drugs – thickening upon treatment with anti-myopia drugs such as mAChR antagonists[44] and dopamine agonists[45], and thinning in response to treatment with nitric oxide synthase (NOS) inhibitors, which may cause greater myopia susceptibility[40,46-48] and (Chakraborty et al. IOVS 2016; 57: E-Abstract 4742). The choroid can synthesize and secrete numerous growth factors, some of which have been implicated in control of ocular growth such as TGF-β[49-53] and retinoic acid[54-62], and studies support it having a direct effect on scleral growth. For example, when scleral tissues are co-cultured with choroids from eyes that are undergoing experimentally-induced myopia, the rate of glycosaminoglycan (GAG) synthesis is increased[63], but when co-cultured choroids are undergoing recovery from experimentally-induced myopia GAG synthesis is decreased[64-

[66]. Retinoic acid (RA) could be a possible mediator of these effects; its synthesis is increased during positive-lens wear and recovery from FDM[58,67,68], and increased RA results in inhibition of proteoglycan production and scleral chondrocyte and fibroblast proliferation[58,59,67].

The sclera is the tough outer tunic of the eye, and its structure differs between mammals and birds. Mammalian sclera is formed from a single fibrous layer, made up of collagen and some elastic fibres, while avian sclera contains a fibrous layer similar to mammalian sclera and a cartilaginous layer, which helps to give it more stiffness and structure. When chicks undergo FDM, there is a thinning of the fibrous sclera and thickening of the cartilaginous sclera[50]. This is due to an increase in chondrocyte proliferation and secretion of extracellular matrix, which can be controlled differentially by growth factors[69]. Mammals also experience thinning of the fibrous sclera during experimentally-induced myopia, and in the absence of a stabilizing cartilage component, this thinning can result in "scleral creep", where the destabilized sclera becomes more prone to stretching in response to mechanical forces[69-71]. Destabilization of the sclera and the resultant creep does seem to play a role in experimentally-induced myopia, as well as human myopia. People with moderate to severe myopia have thinner sclera with reduced glycosaminoglycan and collagen contents[72-74], and experimentally-induced myopia in tree shrews can result in an up 200% increase in creep rate due to scleral destabilization caused by changes in growth factor expression[71,75,76].

There have been a few attempts to investigate whether correcting scleral destabilization can prevent myopia progression in animals and humans. One study utilized polymer foam in rabbits and human test subjects[77]. Foam-treatment stimulated an increase in collagen biosynthesis, resulting in greater scleral tensile strength and elasticity (in rabbits). In humans, foam-treatment resulted in scleral stabilization in 79.6% of patients at one year (26.6% in non-treated controls) with 52.9% remaining stable at the 4-9 yr follow up (11% of non-treated controls). Although effective, liquid polymeric foam has its drawbacks; 100% of treated patients complained of eye pain and pressure, and formation of inflammatory granulomas at the injection site. The injection procedure is also dangerous;

scleral puncture can occur and some failed attempts resulted in cysts that required surgical removal. Surgical intervention in which strips of donor sclera were fastened to the posterior globe was also tested[77]; 95.7% of patients' refractive errors stabilized in the first year, and 71.9% remained stable 7 years or more after the operation. Complications included scleral perforation and subsequent choroidal hemorrhage, tenonitis, and strabismus requiring further surgical intervention. Much like the polymer foam, the drawbacks of scleral reinforcement surgery may outweigh the benefits. More recent studies have attempted to use scleral cross-linking techniques, either by riboflavin-UVA or glyceraldehyde, popularized by keratoconus therapies[78-81]. Evidence in animal models suggests that this may be an effective way to strengthen destabilized sclera and inhibit myopia[82,83]. There are significant caveats to scleral cross-linking too, however, which have impeded its acceptance as a valid anti-myopia therapy[84]. The posterior sclera is difficult to access without extremely invasive surgery, it is too difficult to tightly regulate the cross-linking effect to areas only where it is needed, and UVA light is extremely damaging to retinal photoreceptors[79,85]. Measures this extreme with a high risk of danger to the patient would hardly be considered to treat slowly progressing, mild to moderate, or perhaps even most cases of high myopia.

The remaining eye structures are not strongly linked to regulation of eye growth. The aqueous humor contains a clear fluid that is synthesized by the ciliary epithelium of the ciliary body. It is located in the space between the cornea and the lens, and serves primarily to regulate intraocular pressure (IOP) and maintain the shape of the globe. It may also provide some nutrition to the cornea and lens, and normalizes the refractive index along the pathway that light must travel to reach the retina. The vitreous humor is more gel-like, and is located between the lens and the retina. Its functions are similar to those of the aqueous humor; it helps to provide hydrostatic pressure in the globe, and normalizes the refractive index inside the eye. The iris is a circular fibrovascular tissue that forms the pupil. It aids in regulating the amount of light that enters the eye, the depth of field, and limits the amount of out-of-focus light entering the eye (when pupils are constricted). Pupil size can significantly affect retinal blur, which could have a myopiagenic effect, but the

majority of results from research investigating the correlation between pupil size and myopia risk fail to demonstrate a significant link[86].

The Retina: Visual Processing Circuitry and Regulation of Eye Growth

Visual perception begins in the retina – a complex and highly organized neural tissue that lies at the back of the eye (**Fig. 1.3**).

Figure 1.3: Retinal Neuronal Organization

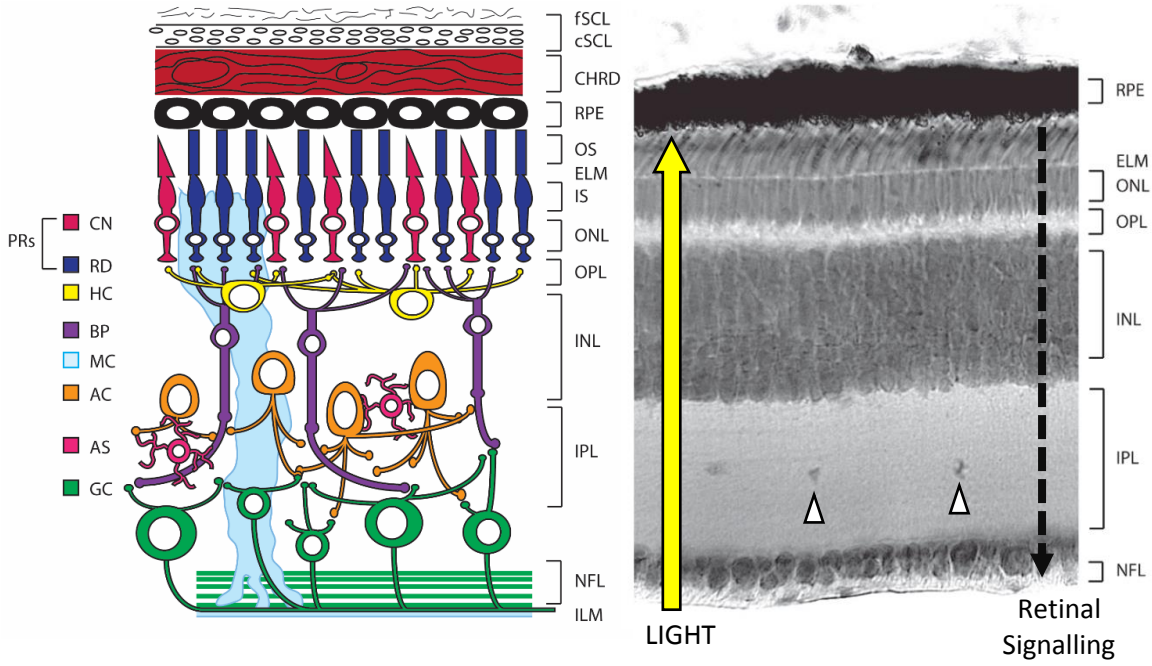

Figure 1.3: Cartoon representation (left) and toluidine blue-stained micrograph of chick retina (right). All vertebrate retinas are made up of five different classes of neurons – photoreceptors (PRs) which comprise rods (RD) and cones (CN), horizontal cells (HC), bipolar cells (BP), amacrine cells (AC), and ganglion cells (GC) – and glial cells – Müller cells (MC) and astrocytes (AS; white arrowheads on the micrograph). The retina is organized into distinct layers – the outer nuclear layer (ONL) contains PR nuclei, the outer plexiform layer (OPL) contains synapses between PRs, HCs, and BPs, the inner nuclear layer (INL) contains cell bodies for HCs, ACs, BPs, MCs, and AS, and the inner plexiform layer (IPL) contains synapses between BPs, ACs, and GCs. Additional notable structures are: the sclera (SCL) which comprises both cartilaginous-type (cSCL) and fibrous-type (fSCL) in birds, the choroid (CHRD), the retinal pigment epithelium (RPE), outer segments of photoreceptors (OS), the external limiting membrane (ELM) which is the area between PR OS and PR inner segments (IS), the nerve fibre layer (NFL) which comprises ganglion cell axons and makes up the optic nerve, and the internal limiting membrane (ILM) which is created by tight junctions between Müller cell endfeet and a basal lamina.

The retina is part of the central nervous system (CNS), and it is derived from neural ectoderm during development. Although it may seem to be a simple tissue – it is only 200-300 μm in width and comprises five different classes of neurons – signal processing by the retina is remarkably complex[87,88]. The retina possesses the neuronal circuitry necessary for intricate processing and interpretation of visual stimuli; thus, it is the logical origin tissue for emmetropic signalling cascades[2]. The position of the retina in the eye might be considered "backwards", because light must first pass by all other retinal neurons before interacting with the photoreceptors. The retina is a highly metabolic tissue, however, so this configuration allows close contact with the RPE and choroid, which supply nutrients, enable recycling of the visual pigment, and remove waste. Once light hits the outer segments of the photoreceptors, its energy is converted into a chemical signal by the process of phototransduction, which begins visual perception.

The Photoreceptors and Phototransduction

Rods and cones comprise the photoreceptor layer. Rods are highly sensitive photoreceptors; they mediate vision in low-light (scotopic) conditions and are able to detect a single photon of light, but visual perception mediated by the rod system has low spatial resolution and cannot signal colour vision. Rod circuitry in the retina is relatively simple. There is only one type of light receptor molecule (rhodopsin) and generally rods synapse onto type of bipolar cell (rod ON-bipolar). In mammals, rods "piggyback" onto cone signalling pathways by synapsing onto rod bipolar cells, which then synapse with a specialized amacrine cell called the AII (A2) amacrine cell. The AII amacrine is connected via gap junctions onto cone bipolar cells, which then relay the signal via synaptic transmission to the ganglion cells. An AII-like amacrine cell has not yet been identified in birds, even though the change in retinal signalling with light- and dark-adaptation in the chick occurs similarly to that of mammals[89]. In the human retina, rods outnumber cones 20:1, but we still possess high resolution colour vision because our central vision is mediated by the fovea – a specialized pit in the retina that has a high concentration of tightly-packed cones. The cones pathway mediates vision under bright-light (photopic) conditions, has high spatial resolution, and contains the necessary circuitry components to encode colour vision. Cone circuitry in the retina is much more complex than rods. There are many different types of opsins, which respond best to different wavelengths of light – unlike rods which respond best to spectra that peak around 500 nm. Humans possess cone-opsins that are sensitive to long-, medium-, or short-wavelength light that are the origins for red, green, or blue colour vision, respectively, while other animals can possess additional opsins – birds, teleost fish, and honey bees possess a fourth cone-opsin that is sensitive to UV light – or fewer opsins – mice possess only short- and medium-wavelength-sensitive opsins. Cones can signal through at least 11 different types of bipolar cell (in mouse), each with their own output characteristics[87] (discussed in further detail below).

Photoreceptors are the first step in capturing light and transducing it into a signal that can be passed between retinal neurons. This process – called phototransduction – occurs in the outer segments of rods and cones, which possess a large number of membranous discs, each tightly packed with the light-detecting receptor - rhodopsin in rods and opsin in

cones[90]. Rods and cone photoreceptors are different from most neurons in that they are somewhat depolarized (-30 mV) and continuously release the excitatory neurotransmitter glutamate when they are "at rest" (in darkness). When light activates the rods or cones, they become *more* polarized (-60 mV), and discontinue the release of glutamate. Phototransduction is initiated when a photon of light interacts with an opsin (the receptor) which causes it to undergo a conformational change, resulting in activation of transducin (the $G_{i/o}$-coupled protein) by catalysis of GDP to GTP. Once activated, transducin will then activate phosphodiesterase (PDE6), which hydrolyses the second messenger cGMP. This causes the closure of cGMP-gated channels in the membrane of the photoreceptor, increased polarization, and the cessation of glutamate release. Another feature unique to photoreceptors and bipolar cells is the ability to coordinate glutamate release with the amount of light hitting the photoreceptors in a graded fashion, instead of the simple all-or-none responses commonly seen throughout the CNS. Graded signalling of retinal rods, cones, and bipolar cells is the result of specialized ribbon synapses[91], which tether large pools of neurotransmitter vesicles near the action zone and enables very fast, precise, and sustained neurotransmitter release. Like other neurons, transmitter release by the ribbon synapses is mediated by changes in the concentration of intracellular Ca^{2+}, and in the rods, cones, and bipolar cells, the channels responsible for regulating Ca^{2+}-flow across the cell membrane are the voltage-dependent L-type Ca^{2+} channels. L-type Ca^{2+} channels are high voltage-activated and have long-lasting currents – i.e., their voltage-dependent *inactivation* is slow. They are sensitive to small changes in membrane voltage, enabling them to fine-tune the influx of Ca^{2+}, and consequently, the release of vesicle-bound neurotransmitter from the ribbon synapses. L-type Ca^{2+} channels are also subject to regulation by endogenous modulators that are associated with regulation of eye growth; such as nitric oxide and dopamine[92].

Photoreceptors also contain gap junctions. Cone-cone connections contain connexin 36 (CX36, CX35 in chicks) and help to improve signal-to-noise ratios by up to 80%, improving the sensitivity and fidelity of the cone signals at the expense of a slightly blurred visual image[93]. Electrical coupling also exists between rods-rods, rods-OFF-BP cells, and rods-cones. Rod-cone coupling may also be mediated by CX35/36, and is regulated by

circadian changes in retinal dopamine. During the day, increasing dopamine results in the activation of dopamine D_2/D_4 autoreceptors, which decrease cAMP and PKA activity, resulting in decreased coupling between rod-cone photoreceptors. Decreased coupling between rods and cones would result in a visual image with higher spatial resolution, at the cost of loss of sensitivity. This loss of sensitivity is minor, however, because saturation of the rod photoreceptors under photopic illumination would render the rod signalling stream mostly useless anyway. Interestingly, recent work has demonstrated that intravitreal injection of a mimetic peptide that causes uncoupling of CX35/36 containing gap junctions – as do dopamine and nitric oxide – is protective against FDM in the chick (Teves et al.[94] and Teves M, et al. IOVS 2014; 55: E-Abstract 3036).

Bipolar Cells: ON- and OFF-Retinal Signalling Pathways

Bipolar cells are interneurons; they receive chemical neurotransmission from the photoreceptors and relay the signal, in a graded fashion due to the presence of ribbon synapses, to the ganglion cells[95]. Generally, bipolar cell responses are categorized as either "ON" or "OFF", which refers to the response of bipolar cells to light – i.e., they either "turn ON" (depolarize) or "turn OFF" (hyperpolarize). Mammalian ON-bipolar cells terminate in the inner lamina of the inner plexiform layer, but in non-mammalian vertebrates this is not a hard-and-fast rule. ON-bipolar cells are "sign-inverting" and *depolarize* in response to light, because glutamate signalling in these cells is mediated by metabotropic glutamate receptors (mGluR6), which regulate the non-selective cation channel TRPM1. Upon light stimulation, deactivation of mGluR6-signalling due to discontinuation of glutamate release causes the TRPM1 channel to open, resulting in positive ion flow into the bipolar cell, and subsequent depolarization. Mammalian OFF-bipolar cells terminate in the outer lamina of the inner plexiform layer; again, this is not always the case in non-mammalian vertebrates. OFF-bipolar cells are "sign-conserving" and *hyperpolarize* in response to light; they contain ionotropic AMPA/Kainate glutamate channels which allow positive ions to flow into the cell when glutamate is present. Thus, light-induced cessation of glutamate release from the rods and cones will cause the AMPA/Kainate channels to close, preventing the flow of positive ions into the cell. Recent anatomical investigations have revealed the presence of at least 12-13 different subtypes of bipolar cells in rabbit[96] and mouse[97]. Each

of these bipolar cells express a distinct set of receptors and ion channels, terminate in distinct sublamina of the IPL, and have unique intracellular signalling mechanisms which code for different retinal responses[95]. Bipolar cell signals are also affected by feedback from horizontal cells and amacrine cells (see below). Thus, bipolar cells act as integration stations[95], as well as conduits to pass signals from the photoreceptors to the ganglion cells.

Horizontal and Amacrine Cells: Lateral Signal Processing and Inhibitory Feedback

Horizontal cells are interneurons that serve to modulate signalling input from the photoreceptors to the bipolar cells, primarily through inhibitory feedback to the bipolar cell. The interconnectivity of horizontal cells with multiple photoreceptor and bipolar cells helps to create a centre-surround receptive field, which acts to "sharpen" bipolar cells signals via lateral inhibition – a process by which strongly excitatory signals are enhanced by the inhibition of weak excitatory signals from the surrounding neurons. Gap junctions also exist in horizontal cells, and evidence suggests that changes in coupling state between these gap junctions may be involved with control of eye growth. Daytime-like conditions such as illumination with bright light[98-100], increased retinal dopamine or dopamine agonism[45,101-118], and increased nitric oxide[1] are protective against experimental myopia, and cause uncoupling of horizontal cell gap junctions[119,120].

Amacrine cells are the visual processing powerhouses of the retina and the most likely origin of eye growth-regulating signalling molecules[2]. There are as many as 30 different confirmed subtypes of amacrine cells, and it is likely that more remain to be discovered[121,122]. Primarily, amacrine cells provide inhibitory feedback to bipolar cells via GABA- and glycine-mediated signalling, but they can also contact and provide feedback to other amacrine cells and ganglion cells[87,122]. They are sensitive to environmental changes in movement[123] and retinal blur[88], and they synthesize and release a large variety of neurotransmitters and neuromodulatory molecules, most of which have functions that are yet to be discovered. Amacrine cells synthesize and release signalling molecules that are associated strongly with regulation of eye growth, such as dopamine and nitric oxide (discussed in detail below), and peptide hormones (VIP, glucagon, somatostatin, and neurotensin)[121].

Retinal Ganglion Cells: The Conduit to the Brain

The final neurons in the retinal visual pathway are the ganglion cells, spiking neurons whose axons comprise the optic nerve. Ganglion cell firing patterns are highly specific, and heavily influenced by feedback from the amacrine cells[87]. They are the final output from the retina to the brain, thus they must be able to process and encode a large amount of complex visual data. Recent classification techniques have identified about 30 individual subtypes of ganglion cell (in mice)[124] based on anatomy and function, reinforcing the expectation that a multitude of output channels from ganglion cells are required for effective visual perception. Ganglion cell axons must transduce chemical signals from the retina into electrical signals that can then travel the long distance to the brain, where they terminate on the pretectum, the lateral geniculate nucleus and superior colliculus[125].

The role of ganglion cell signalling in myopia is probably best understood via experiments that seek to eliminate input from the optic nerve to the brain, either by treatment with toxins that block signal propagation along the axon (tetrodotoxin, TTX) or surgical ablation. In the case of FDM, signalling through the optic nerve does not seem to play a significant role in elongation of the vitreal chamber across the globe[126,127] or in localized retinal areas[30]. There does seem to be a difference between ablation of optic nerve signalling by TTX or surgery; toxin-treated eyes can still emmetropize and recover accurately from myopia[126], while eyes that have had surgical ablation tend to become hyperopic[30,128]. In regards to LIM, the effects of optic nerve ablation are more controversial. One study reported that surgical sectioning of the optic nerve completely ablates the development of LIM in the chick, while TTX does not eliminate LIM completely[129]. Subsequent studies utilizing the same surgical methods, however, reported either reduced effect LIM[32], or no reduction in LIM[130] as a result of optic nerve section. Clearly, further experimentation is required to come to a final conclusion about the role of the ganglion cell axons in LIM.

An additional neuronal pathway that has fibre tracts running through the optic nerve is the centrifugal visual system (CVS)[131]. Creating a circular loop from the retina, to the isthmo-optic nucleus (ION)[132], and back again via efferent fibres[133] (also called centrifugal fibres

or retinopetal fibres), the CVS is especially well-defined in birds[134,135], but also exists in mammalian retinas[136]. The function of the CVS is still not well understood, and many hypotheses have been put forward regarding acting as a modulator of gaze stabilization and pecking behavior in ground-feeding birds, visual attention by adjusting the gain or adaptive properties of retinal processing, and acting as a sensor to detect potentially predatory shadows in the sky (review[131]). There have also been studies investigating the effects of ION-lesion on refractive error. Unilateral lesions of the ION and isthmo-optic tract (IOTr) that sufficiently disrupted the efferent fibres (> 80% lesion success) resulted in a tendency of chicks exposed to normal vision to develop hyperopia in the eye contralateral to the lesion, compared to sham controls, after 7 days post-surgery; by 21 days post-surgery, the hyperopic eyes had effectively recovered, and were either emmetropic or slightly myopic compared to the sham controls[137]. This is the same behavior that is seen in chicks with surgical disruption of the optic nerve[30,128]. Interestingly, the efferent fibres use nitric oxide (NO) as a signalling messenger[138-140], and NO is involved in regulation of eye growth[1,46-48,110] (and **Chapter 3**, discussed in detail below). Perhaps, then, the differences observed between FDM and LIM may be mediated by the CVS, and/or processes that involve NO.

Ocular Muscarinic Acetylcholine Receptors

There are five subtypes of mAChRs (in mammals): M_1, M_3 & M_5 receptors are G_q-coupled (stimulate phospholipase C beta), and M_2 & M_4 subtypes are G_i-coupled (inhibit adenylyl cyclase)[141]. Chickens lack an M_1 orthologue; instead, their M_2 subtypes takes on M_1-like characteristics, such as affinity for pirenzepine[142]. Fischer et al. localized mAChRs in chick eye tissues using affinity-purified antibodies to chicken muscarinic receptors M_2, M_3 and M_4 (cM_2, cM_3, cM_4). Immunoreactive sites for cM_2 were present only in the retina; with weak labelling in amacrine cells, OPL, and four distinct strata in the IPL. Outside the retina, cM_3 was localized to muscle and epithelial cells in the ciliary body, the retinal pigment epithelium (RPE), and choroidal blood vessels. It was also present in roughly two-thirds of bipolar cells, puncta in the outer plexiform layer, and sparsely scattered amacrine cells in the INL and GCL. Ocular immunoreactive sites for cM_4 included the ciliary epithelium, choroidal blood vessels, and cell bodies in the ciliary ganglion. Retinal cM_4-reactive sites comprised most amacrine and ganglion cells and a thin striatum in the IPL (**Fig. 1.4**)[143]. In

mammals, the presence of M_1-M_5 mAChRs in the retina, choroid, sclera, iris, and ciliary body has been confirmed using RT-PCR amplification of mRNA and immunolocalization in tree shrew[144], and rabbit[145]. Retinal mAChR expression patterns for tree shrew and rabbit are similar to each other, and to expression patterns in the chick. M_1-like expression is most prevalent in the OPL, IPL, GCL, and inner retina, M_2-like immunoreactivity was more diffuse and localized to the INL and IPL, M_3-like labelling is most prevalent in some subsets of inner nuclear neurons and the OPL. M_4- and M_5-like expression is diffuse and localized to puncta in the OPL and inner retina and some GCs. M_4-like expression differs most greatly between the rabbit (localized to puncta in the INL and GCL), tree shrew (weak diffuse labelling), and chick (strong labelling in cell bodies in the INL and GCL and obvious lamina in the IPL) (**Fig. 1.4**).

Figure 1.4: Localization of Retinal Muscarinic Receptors

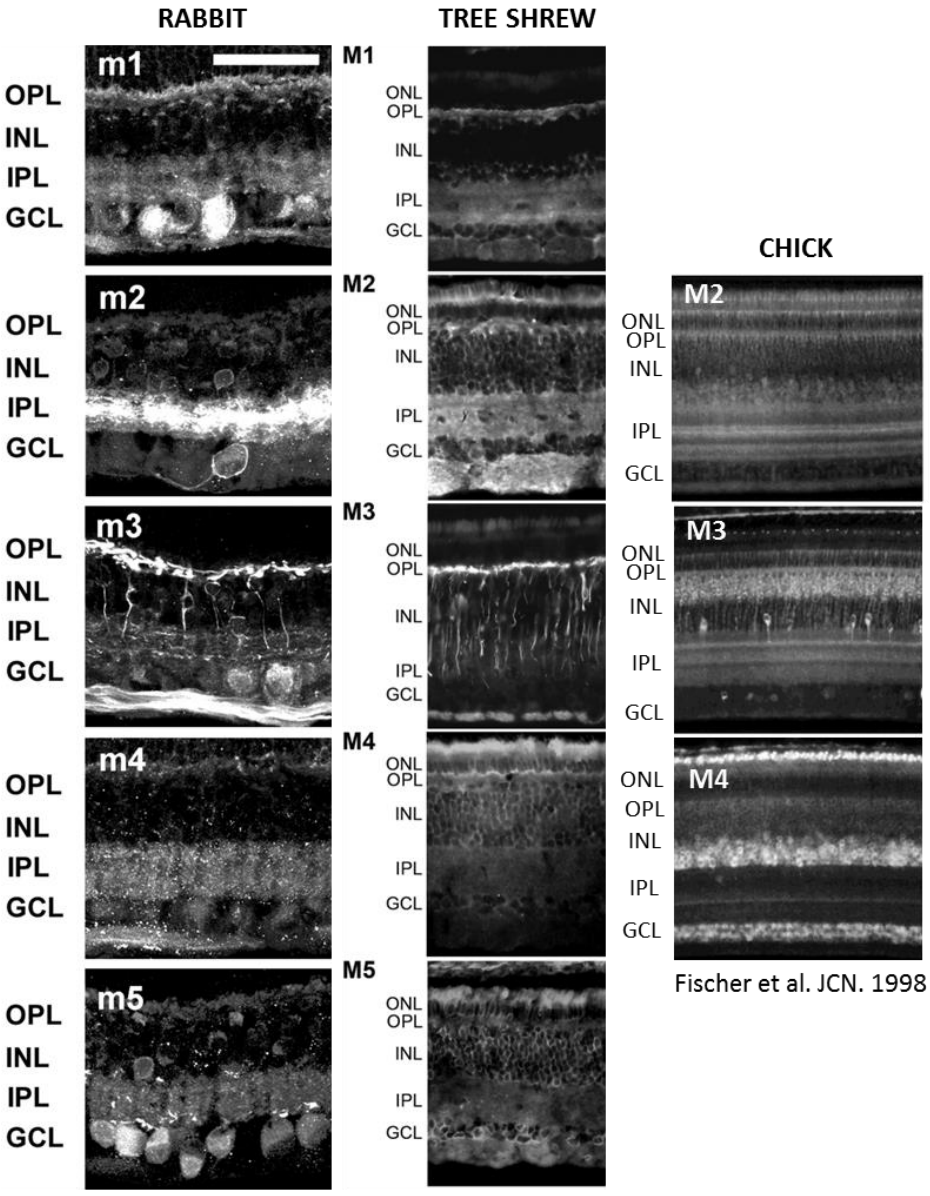

Figure 1.4: Reported expression patterns of retinal mAChRs in rabbit (left), tree shrew (middle), and chick (left). Chicks do not have an M_1-type mAChR subtype, and cM_5 has not been localized in the chick retina. Modified and reproduced with permission from Strang et al. (2010). *Investigative Ophthalmology and Visual Science* (© Association for Research in Vision and Ophthalmology - ARVO), McBrien et al. (2009). *Molecular Vision*, and Fischer et al. (1998). *Journal of Comparative Neurology* (© John Wiley & Sons, Inc.).

The endogenous neurotransmitter for mAChRs is acetylcholine (ACh), which is synthesised and released in the retina by cholinergic starburst amacrine cells. These amacrine cells are best known for their role in directional sensitivity of certain ganglion cells[123], though it may involve GABAergic, rather than cholinergic, function of those cells. In addition to modulation of directionally-sensitive ganglion cell responses, activation of mAChR subtypes can have effects on visual processing. Activation of M_2- and M_4-type mAChRs has been reported to result in increased NO in the salamander retina[146] and decreased dopamine release in the guinea pig[147]. Activation of M_1- and M_3-type mAChRs have also been reported to be correlated with an increase in ocular NO and cGMP synthesis in the rat[148], as well as an increase in intracellular Ca^{2+} in rabbits[149] – a generally excitatory response. Interestingly, additional work has demonstrated retinal effects that are opposite to these reports. Inhibition of myopia by atropine, a mAChR antagonist, seems to be dependent on the presence of ocular NO[1], which is unexpected if M_2/M_4 and M_1/M_3 mAChR activation results in increased NO[146,148]. There have also been studies that demonstrated M_1 mAChRs may be coupled to inhibition of adenylyl cyclase[150] – a generally inhibitory response. The most likely explanation for these differences is that signal processing in the retina is extremely complex, especially in the inner plexiform layer where amacrine cells, bipolar cells, and ganglion cells all make connections, and it is possible that each of these experiments may be targeting different cell populations with varying functions. In addition, the actions of endogenous NO are probably highly localized, so that bulk targeting of NOS likely can cause many changes whereas circuit activation could be more specific. Non-retinal functions of mAChR-signalling in the eye are to mediate contraction of the ciliary muscle – which controls accommodation – and the pupilloconstrictor muscle – which controls the amount of light that enters the eye. Muscarinic control of accommodation and pupil size does not apply to all animals, however, as the chick ciliary and pupilloconstrictor muscles are controlled by nicotinic receptors instead[151].

The role of mAChRs in eye growth is poorly understood and heavily dependent on *assumptions* that atropine and other mAChR antagonists inhibit myopia by action at muscarinic receptors alone. There is a significant amount of evidence to refute this

assumption[152]. Only a few muscarinic antagonists prevent myopia in humans[153-158] and animal models[159-161], and an extremely high concentration is required. Interestingly, the most potent anti-myopia drug found to date (in chick[34,161]), a subtype of green mamba toxin termed mamba toxin 3 (also known as muscarinic toxin 4 or MT3), has nearly equal high inhibitory potencies for mAChR M_4, α_{1A}-, α_{1D}-, and α_{2A}-adrenoceptors[162,163]. In addition, the results of studies investigating the involvement of mAChRs in the prevention of FDM using techniques other than drugs have been controversial. Protein and mRNA expression studies utilizing radioligand binding and real-time PCR techniques have found no change in mAChR receptor density or gene expression for any subtype in the retina or choroid of chick[164] or tree shrew[144], even when there is significant development of myopia. One study did report a significant upregulation of M_1 and M_4 mRNA in the guinea pig after 21 days of myopia development, but the results of this study are questionable as the mRNA levels were measured after a much longer period of time than is needed to induce significant refractive error in guinea pigs (6-11 days)[165,166]. There has also been a genetic polymorphism study investigating the effects of SNPs on *CHRM1* (the gene for mAChR M_1), which claimed a high correlation between *CHRM1* polymorphisms and the development of high myopia[167]. This study was later refuted[168], however, and the largest GWAS study ever performed on the correlation between genetic polymorphisms and myopia risk did not find a significant association with any mAChR gene[14,21,169]. Considering that the *best* evidence we have for muscarinic receptor involvement in prevention of myopia is that a select few muscarinic antagonists inhibit myopia only when used at extremely high concentrations, it is surprising that there have been no studies to search for possible non-muscarinic binding of these drugs, which could reveal novel targets for pharmacological prevention of myopia. We attempted to address this significant gap in the literature by examining whether atropine – and other myopia inhibiting mAChR antagonists – may bind to non-mAChRs, specifically α_{2A}-adrenoceptors (**Chapter 5**).

Ocular Alpha$_2$-Adrenoceptors

It is very likely that myopia-inhibiting mAChR antagonists such as atropine and MT3 inhibit eye growth through non-specific binding to an unknown target receptor, and adrenoceptors are a possible target. Adrenoceptors are also members of the GPCR family,

and are closely related to muscarinic receptors in structure and function[170]. There are α- and β-subtypes of adrenoceptors, but the focus of this thesis will be on the α-subtype due to the high affinity of MT3 at α_{1A}-, α_{1D}-, and α_{2A}-adrenoceptors, and the suspicion that atropine may also interact with α-adrenergic receptors when applied at concentrations similar to those used to prevent myopia[171,172]. Using pharmacological and genetic characterization, the alpha subtypes of adrenoceptors can be broken down further into α_1-type receptors ($_{A/C,B,D)}$ which are activated by phenylephrine and inhibited by prazosin, coryanthin and WB-4101, and α_2-type receptors ($_{A/D,B,C}$) which are activated by UK 14-304 (brimonidine), clonidine, and guanfacine, and inhibited by yohimbine, rauwolscine, and idazoxan; it is generally accepted now that α_{1A} and α_{1C} are the same receptor. Alpha$_{2A}$- and α_{2D} are also accepted as the same receptor subtype, with the former being the human receptor and the latter being the rat orthologue[173].

There is some older evidence that epinephrine may act as a neurotransmitter in the rat retina. It has been localized to amacrine cell populations by immunolocalization of antibodies raised against phenyletholamine N-methyltransferase (PNMT)[174] and retinal epinephrine levels have been reported to rise upon exposure of the retina to light[175]. Although, it may only account for 5% of the total catecholamine signalling that occurs[176], and there is no modern evidence that epinephrine is an important retinal signalling molecule. The presence of norepinephrine in the eye has also been confirmed, but it is thought to mediate sympathetic innervation of choroidal blood vessels, and not to play a significant role in retinal neurotransmission or visual processing[177]. More recent studies performed in rat, human, and primate tissue have localized α_{2A}-adrenoceptors (ADRA2A) to the non-pigmented ciliary body, cornea and conjunctiva, as well as ganglion cells, amacrine cells (INL and displaced), and putative horizontal amacrine cells in the inner nuclear layer[178] (**Fig. 1.5**). In the transgenic mouse, ADRA2A was localized to the outer plexiform layer, horizontal cells, inner nuclear layer, inner plexiform layer, and the retinal ganglion cell layer (Rao SS et al. IOVS 2011; 52: ARVO E-Abstract 2059). Little recent research has investigated the localization of α_2-adrenoceptors in chick ocular tissues. One study reported the presence of ADRA2A on Müller cells (Costa GV, et al. IOVS 2012; 53: ARVO E-Abstract 6545), which was later seemingly confirmed in embryonic chick[179].

Unfortunately, I was unable to replicate the reported binding patterns using the same antibody (Abcam #ab92650, but with a different lot number) in post-natal chick (**Fig. 1.5**).

Figure 1.5: Localization of Retinal Alpha$_{2A}$-Adrenoceptors

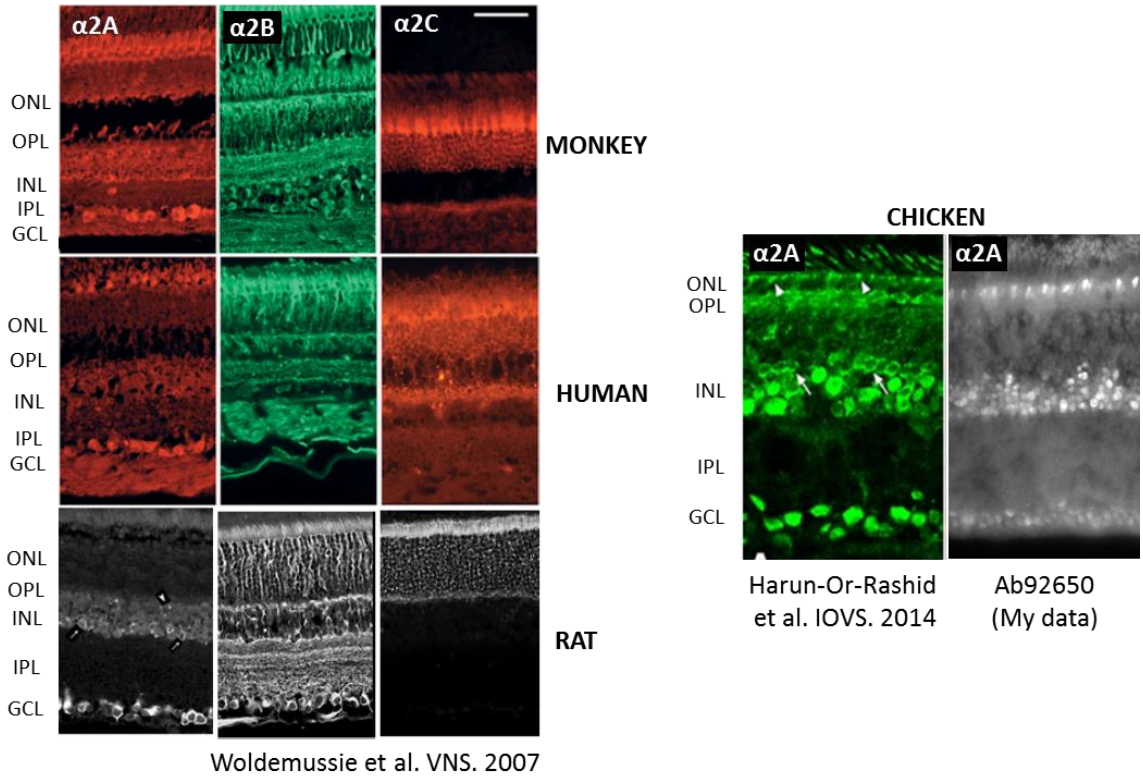

Figure 1.5: Retinal expression patterns of α_{2A}-, α_{2B}-, and α_{2C}-adrenoceptors in human, monkey, rat, and chicken. Although labelling in the chick looks similar, I was unable to obtain cytoplasmic labelling with ab92650 as was reported previously, all labels in my tissues were nuclear. Modified and reproduced from with permission from Woldemussie E, et al. (2007). *Visual Neuroscience* (© Cambridge University Press) and Harun-Or-Rashid et al. (2014). *Investigative Ophthalmology and Visual Science* (© Association for Research in Vision and Ophthalmology - ARVO).

Alpha$_2$-adrenoceptors already have an established role in the eye; they are implicated in the pathogenesis of glaucoma, which shares a high correlation with the presence of high myopia[180,181], and α_2 agonists are clinically-approved for management of intraocular pressure (IOP). In addition to reducing IOP, there is evidence that α_2-agonists are neuroprotective – especially for retinal ganglion cells, which are highly susceptible to damage in pathologic conditions such as glaucoma. The exact mechanism of protection is unknown; however, there is evidence that the α_2-agonist brimonidine can modulate the influx of extracellular Ca^{2+} though L-type Ca^{2+} channels in the inner plexiform layer[182]. Blocking of these channels by brimonidine prevents excessive buildup of intracellular Ca^{2+} and protects retinal ganglion cells from Ca^{2+}-induced excitotoxicity. Another possible mechanism for neuroprotection by ADRA2 agonism is upregulation of basic fibroblast growth factor (bFGF) in photoreceptors[183,184] (in rat), or the activation of the ERK signalling pathway in Müller cells[179] (in chick). Finally, activation of Müller cells with norepinephrine results in the subsequent upregulation of mRNA and protein expression of the neuroprotective molecule brain-derived neurotrophic factor (BDNF), which is strongly protective of amacrine and ganglion cells[185]. Brimonidine has also been implicated in the regulation of nitric oxide synthase in retinal arterioles where it may activate endothelial nitric oxide synthase (eNOS), resulting in vasodilation of *in vitro* retinal arterioles in pig. During this study, the presence of α_{2A} receptor mRNA in retinal arterioles and retinal neural tissue was confirmed using RT-PCR[186]. It is important to note, however, that there are no intraretinal blood vessels in the chick retina. The modulation of eNOS, or any NOS isoform, by adrenergic ligands is particularly interesting, because synthesis and release of nitric oxide has been strongly linked with reduction of eye growth[1] (see below and **Chapter 3**).

Nitric Oxide

Nitric oxide (NO) is a small-molecule gas that can act as a retinal neuromodulator. It is synthesized on-demand by the enzyme nitric oxide synthase (NOS), of which there are three isoforms: neuronal NOS (nNOS or NOS1), endothelial NOS (eNOS or NOS3), and inducible NOS (iNOS or NOS2). Regulation of NO synthesis and release via eNOS or nNOS is dependent on increased intracellular calcium, which then binds to calmodulin

(CaM). The resultant Ca^{2+}/CaM complex must bind to the eNOS/nNOS enzyme for activation and subsequent conversion of L-arginine to NO. iNOS is constitutively active, thus synthesis and release of NO via iNOS is dependent on transcriptional regulation of the iNOS enzyme. A final NOS isozyme is mtNOS (mitochondrial NOS), which as the name suggests is present in the mitochondria of many cells and tissues; its expression is also under the regulation of Ca^{2+} concentrations[187]. NO signalling in the retina is mediated primarily through soluble guanylate cyclase (sGC) and activation of cGMP[188], which can then interact with cyclic nucleotide-gated channels (CNGs) such as those that control influx of Na^{+} ions into rods and cones during phototransduction. Another way that NO can exert modulatory effects in the retina is via S-nitrosylation or tyrosine-nitration, which are protein modification processes similar to phosphorylation[189,190]. In addition, recent evidence supports the possibility that NO signalling can occur independently of these canonical pathways by modulating cationic TRP channels[191].

Nitric oxide can be toxic due to its ability to act as a reactive oxygen species, so its presence in cells is under strict regulation and has a short half-life; thus, it can be difficult to localize or label directly. The enzymatic activity of NOS requires the cofactor nicotinamide adenine dinucleotide phosphate (NADPH), so a labelling method in many past studies utilized the NADPH-diaphorase reduction of tetrazolium salts to create a dark stain, which could reveal NOS-containing cells with almost Golgi impregnation-like clarity. NADPH-diaphorase staining does not discern between different isoforms of NOS, thus it is necessary to double-label using isoform-specific antibodies to determine the NOS isoform present. In the chick retina, Fischer et al. found NADPH-diaphorase staining in four different types of amacrine cells (types 1-4) as well as in some ganglion cells, efferent fibres and efferent target cells, both plexiform layers, photoreceptor ellipsoids, and Müller cells (**Fig. 1.6**). There was also NADPH-positive labelling outside of the retina in the retinal pigmented epithelium (RPE), axon bundles and smooth muscle of the choroid, and scleral chondrocytes; nNOS was present in the amacrine cells, ganglion cells, and efferent fibres and target cells, but was absent from photoreceptors and Müller cells. Outside the retina, nNOS was present in the choroid, but absent from the RPE and scleral chondrocytes[139].

Later studies utilizing NADPH and nNOS labeling in conjunction with neurobiotin-filling of neurons labeled with fluorescence-conjugated streptavidin, identified significant differences in neuronal labelling between the dorsal and ventral retina in the chick, which were not reported previously[140]. The heaviest staining (either NADPH or nNOS) was present in the ganglion cell layer in dorsal retina, but in the inner nuclear and plexiform layers in the ventral retina. They also found many individually labelled neurons, and of the 15 putative nitrergic neuronal types six were ubiquitously expressed throughout the retina. They consisted of two types of displaced ganglion cell, three types of amacrine cells – light, bistratified, and knob, which corresponded to the types 1-3 amacrine cells reported by Fischer et al.[139], and a lightly-stained soma in the ganglion cell layer; whether this cell is a ganglion cell or a displaced amacrine cell remains unclear. The remaining cells, nicknamed "regional cells" were expressed in distinct quadrants of the retina. Cells found only in the ventral retina consisted of bullwhip cells, efferent fibre and amacrine target cells, small and large axon-bearing amacrine cells, and a Brn-3 (ganglion cell marker) positive ganglion cell. In the dorsal retina, there was an nNOS positive, Brn-3 negative ganglion cell, and two cells called large- and small-diffuse cells were restricted to an equatorial band separating the dorsal and ventral retinas (**Fig. 1.6**).

The results of Fischer et al.[139] and Wilson et al.[140] were again confirmed, with some discrepancies, by Tekmen-Clark and Gleason[192], who used a combination of NOS-isoform specific antibodies and 4-amino-5-methylamino-2′,7′-difluorofluorescein diacetate (DAF-FM) labeling. DAF-FM is a non-fluorescent reagent that forms a fluorescent benzotriazole upon reaction with NO, which can then be detected using fluorescence microscopy. Similar to NADPH-diaphorase, DAF-FM does not label specific NOS isoforms, but the fluorescent label is unaffected by fixation and can be used in combination with NOS isoform-specific immunocytochemistry. DAF-FM label was detected in chick photoreceptors, horizontal, amacrine, ganglion, and Müller cells, and in efferent synapses. nNOS immunoreactivity was reported to be present in all cells except horizontal and Müller cells. Tekmen-Clark and Gleason verified Wilson's report that nNOS localization differed between the dorsal and ventral retina, and determined that it was possible that the work by Fisher failed to detect nNOS in photoreceptors due to loss of photoreceptor signal in the dorsal quadrant[192].

It is also possible that the photoreceptor signal may represent mitochondrial NOS. There is a high concentration of mitochondria in inner segment ellipsoids of photoreceptors, and it appears that there may be some ellipsoid-like structures scattered throughout the mostly diffuse photoreceptor signal (**Fig. 1.6**). They also reported strong expression of eNOS- and iNOS-specific labels in photoreceptors, horizontal, amacrine, and Müller cells. These results may not be totally conclusive, however, as the authors themselves admit that they were unable to co-localize DAF-FM signal reliably with their reported eNOS- and nNOS-like immunoreactivity[192] (**Fig. 1.6**).

Figure 1.6: Retinal Localization of NADPH and NOS isozymes

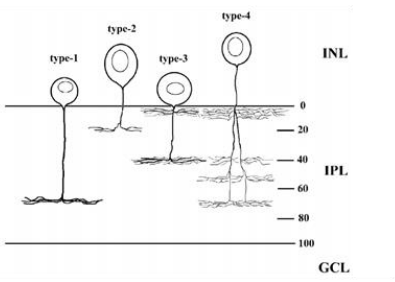

Efferent fibres (large arrowheads, left) and four neuronal types (right) that were both nNOS- and NADPH-positive in central chick retina.

(Fischer et al. *J Comp Neurol*. 1999)

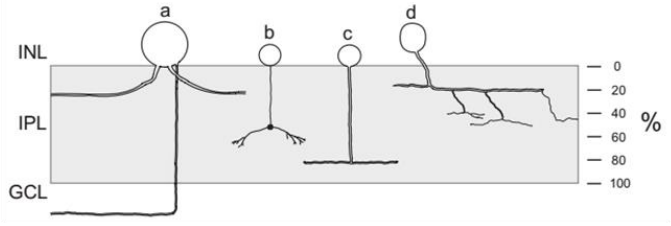

"Nonregional" nitrergic cell types. The knob (b), light (c), and bistratified cell (d) correspond to the Type-1, Type-2, and Type-3 amacrines reported previously by Fischer et al.

(Wilson et al. *Vis Neurosci*. 2011)

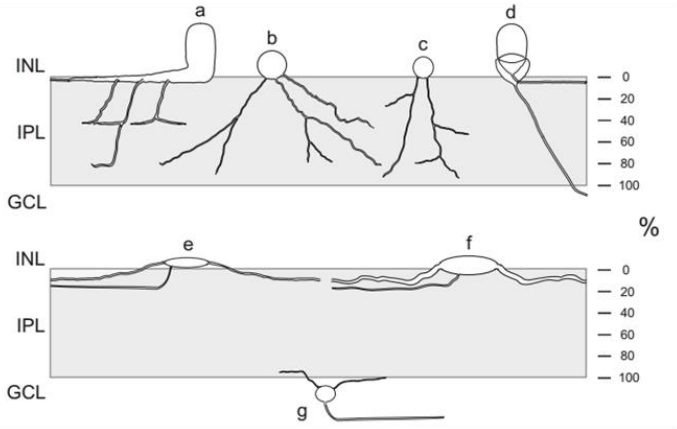

"Regional" nitrergic amacrine cells. Bullwhip (a), efferent fibre (d), small axon-bearing (e), and large axon-bearing (f) are confined to the ventral retina. The large- (b) and small- (c) diffuse cells are confined to an equatorial band, and the Brn3-positive ganglion cell (g) is confined to the ganglion call layer.

(Wilson et al. *Vis Neurosci*. 2011)

nNOS (red) and DAF-FM (green) double-label

(Tekmen-Clark & Gleason. Vis Neurosci. 2013)

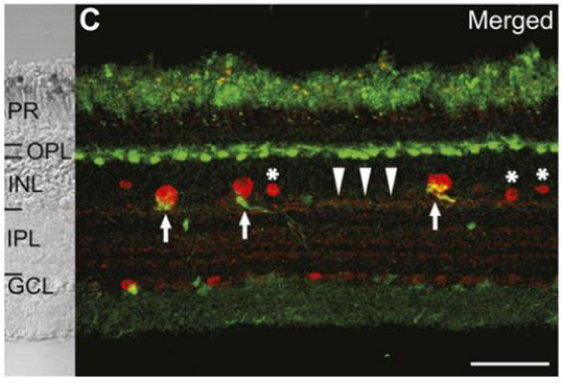

eNOS (red) and DAF-FM (green) double-label

(Tekmen-Clark & Gleason. Vis Neurosci. 2013)

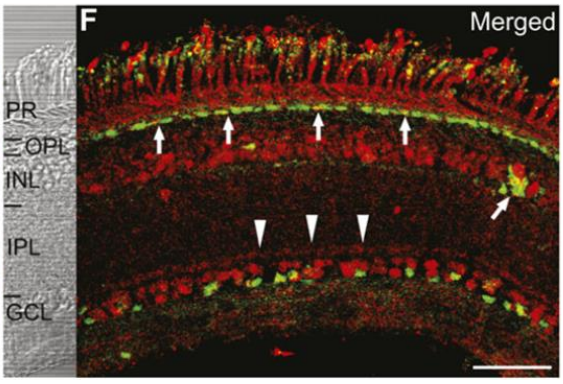

Figure 1.6. Representation of primary amacrine cell types identified by NADPH or nNOS immunolabelling by Fischer et al. (top), Wilson et al. (middle), and by DAF-FM or nNOS/eNOS immunolabelling by Tekmen-Clark & Gleason (bottom). Results from Fischer et al. and Wilson et al. corresponded well, with identifiable labelling in efferent neurons and their fibres and three amacrine cell types that were expressed throughout the retina (termed Types-1–3 by Fischer et al. or knob, light, and bistratified by Wilson et. al.). The bottom diagram shows nitric oxide labelling by DAF-FM (green) co-localized with nNOS (left) or eNOS (right) antibodies; there is little overlap between the supposed NO signal labelled with DAF, and the antibody-labelled cell bodies. Modified and reproduced, with permission from Fischer et. al. (1999). *Journal of Comparative Neurology* (© John Wiley & Sons, Inc.), Wilson et. al. (2011). *Visual Neuroscience* (© Cambridge University Press), and Tekmen-Clark & Gleason. (2013). *Visual Neuroscience* (© Cambridge University Press).

NO in the eye is most famously considered to be a "light-adaptive" signalling molecule. When applied to the retina, NO donors mimic the adaptational effects of increased illumination[193], while inhibitors of nitric oxide synthase (NOS) – the enzyme that generates NO from L-arginine – mimic the functional effects of decreased illumination in light-adapted chicks[194]. NO synthesis and release are increased by intense or intermittent (flickering) illumination[195,196], which can then result in uncoupling of gap junctions between horizontal cells[197], and between bipolar cells and AII amacrine cells[198] (in mammals). In regards to myopia, it has been reported that NOS-inhibitors block the prevention of experimentally-induced FDM normally elicited by daily periods of unobstructed vision[47] and treatment with the dopamine D_2 agonist quinpirole[110]. Pharmacological inhibition of NOS in mice increased susceptibility to FDM (Chakraborty et al. IOVS 2016; 57: E-Abstract 4742). We have demonstrated that intravitreal injections of NO donors such as L-arginine (L-Arg) and sodium nitroprusside (SNP) significantly inhibit FDM in a dose-dependent manner, and that intravitreal injection of NOS inhibitors prevents atropine-mediated myopia inhibition[1] (**Chapter 3**).

Dopamine

Dopamine is the primary retinal catecholamine neurotransmitter. It is synthesized and released from tyrosine hydroxylase-containing amacrine cells (all species) and is present in interplexiform neurons in some species (teleost fishes, toads, and some mammals, missing from birds; reviews[199,200]). There are five subtypes of dopamine receptors, which belong to the G protein-coupled receptor family. D_1-type receptors are made up of D_1 and D_5 which couple to G_s (activation of adenylyl cyclase) and D_2-type receptors (D_2, D_3, & D_4) which couple to G_i (inhibition of adenylyl cyclase). Dopamine also acts as a light-adaptive signalling molecule in the retina. It plays a significant role in reducing conductance of gap junctions between rods and cones[120], and horizontal cells[197], which aids in increasing the spatial resolution of the visual image under photopic conditions. There is significant evidence that supports a role of dopamine as a negative regulator of eye growth in the chick[102,107,113,115,116,118] and mammalian models[103-106,201]. Dopamine content in form-deprived eyes is decreased (during daytime) compared to eyes with unrestricted vision[118]. Intravitreal injection of dopamine agonists prevents FDM[112,108], while injection of dopamine antagonists before unrestricted vision blocks myopia prevention[108]. There is also evidence that retinal dopamine metabolism is sensitive to modulation by drugs that are known to prevent myopia. In chicks, intravitreal injection of atropine caused large increases in dopamine release from the retina and increased concentration of the dopamine metabolite DOPAC[116]. In addition to blocking the effects of apomorphine in myopia inhibition[112], the dopamine D_2 antagonist spiperone can inhibit myopia-prevention by the cholinomimetic diisopropylfluorophosphate[202] and MT3[203], which are assumed to work through the mAChR system. The effects of dopamine agonism and atropine are not additive, thus it is possible that atropine and dopamine may act at different points of a common pathway to prevent myopia[102,115]. Interestingly, there is evidence of a relationship between NO and DA, and reports suggest that they may work serially in the *same* pathway – with dopamine upstream of nitric oxide – to regulate light adaptation-induced cone photomechanical movement in teleost fish[204], light-evoked nitric oxide release[205], and myopia inhibition[110] (and Moinul P, et al. IOVS 2012; 53: ARVO E-Abstract 3434).

Thesis Aims

I ventured to investigate the mechanism of mAChR antagonist inhibition of myopia in a multiplicity of ways. First, I chose to investigate the respective roles of nitric oxide (NO) and dopamine (DA) in atropine-mediated myopia inhibition. We do not yet know any of the downstream signalling cascades that may be activated or inhibited by atropine-treatment. Because these two molecules have been closely linked with modulation of eye growth, it was logical to test whether they could be mediators of myopia inhibition by atropine. I found that NO is necessary for inhibition of myopia by atropine, and sufficient to inhibit myopia on its own (**Chapter 3**), but was unable to determine conclusively whether dopamine signalling through D_2 receptors was also necessary for atropine-mediated myopia inhibition (**Appendix A1**).

There is significant evidence that myopia inhibition by atropine may be the result of a non-mAChR-mediated mechanism[152]. Therefore, I chose to investigate the possibility that α_{2A}-adrenoceptors (ADRA2A) could be responsible for myopia inhibition by certain mAChR antagonists. ADRA2A is the dominant α_2-adrenoceptor in the CNS[173], and MT3 – the most potent anti-myopia agent found to date – has a nearly equally high affinity and inhibitory potency at this receptor subtype as it does for mAChR M4 (in human)[162,163]. I showed that α_2-adrenoceptor agonists – clonidine and guanfacine – could inhibit myopia in a dose-dependent manner at concentrations similar to those required by atropine, and that the ADRA2A antagonist yohimbine might inhibit myopia prevention by unobstructed vision (**Chapter 4**; Carr BJ & Stell WK. IOVS 2016; 57: ARVO E-Abstract 4738). I then followed up by demonstrating that mAChR antagonists that inhibit myopia bind to, and inhibit signalling by, transiently transfected α_{2A}-adrenoceptors at potencies that closely mimic their relative effects on FDM in the chick[159] (**Chapter 5**).

Chapter 2: Materials & Methods for Chick Experiments

Animals & Ethics Statement

Animal use protocols were approved by the Health Sciences Animal Care Committee of the University of Calgary (Protocol# M10008 & AC14-0134), and were carried out in accordance with the CCAC Guide to the Care and Use of Experimental Animals and the ARVO Statement for the Use of Animals in Ophthalmic and Vision Research. White Leghorn cockerels (*Gallus gallus domesticus*) were purchased from Rochester Hatchery (Shaver & Bovan strains; Westlock, Alberta, Canada) or Clark's Poultry (Lohmann strain; Brandon, Manitoba, Canada) and delivered on post-hatching day one (P1). They were housed at the University of Calgary Health Sciences Animal Resource Centre (HSARC) at 26°C, on a 12:12 light-dark schedule (lights on at 06:00), and given chick chow and water *ad libitum*. Mean illuminance in the housing and lab areas was 350-500 lux (as measured by a UNI-T 5URG1 luminometer), provided by conventional indoor fluorescent lamps (Sylvania Octron®XP®ECO3, 6500K, spectral power **Fig. 2.1**). The units "lux" correspond to human-sensitive spectra, and are therefore not corrected for the different spectral sensitivity of chickens, which possess UV sensitive cones; chicken-specific illuminance units are termed "chicken-lux" or "clux"[206].

Figure 2.1: Spectral Distribution of Fluorescent Lighting in the HSARC

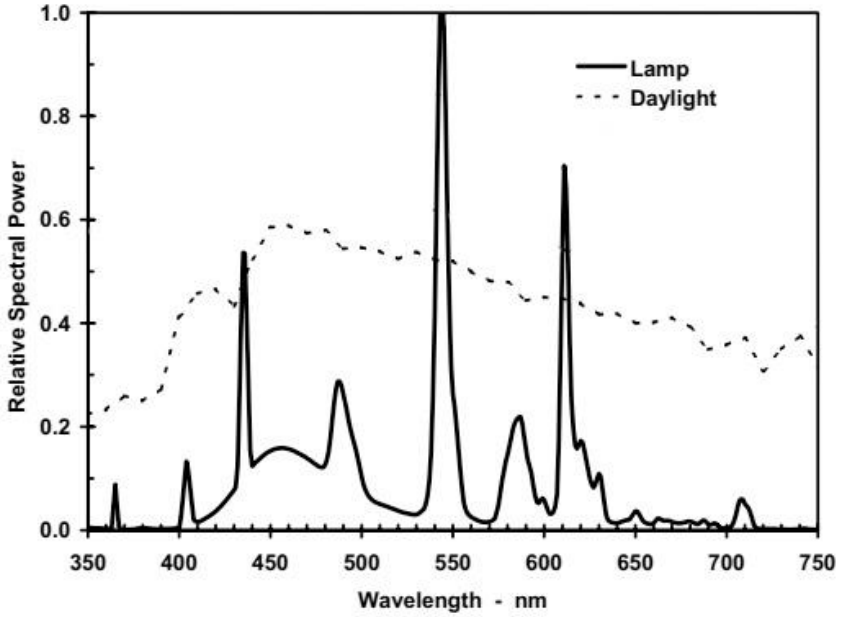

Figure 2.1: Spectral power distributions of Sylvania Octron®XP®ECO3 fluorescent lamp and daylight at 6500 K; correlated color temperature. Modified and reproduced with permission © Osram Sylvania.

Induction of Form-Deprivation Myopia and Intravitreal Injections

Experimental FDM was induced starting on days P7-P8 by affixing translucent diffuser goggles over the right eye (OD) using contact cement; the left eye (OS) was left untouched to serve as a non-occluded, vehicle-injected, within-animal control. Goggles remained in place throughout the experiment and during injections; small triangular vents in the top of the goggles provided needle access and promoted air circulation, without significantly diminishing the form-deprivation effect. Beginning one day after goggle application, intravitreal injections were performed at the same time each day (beginning at 12:00 pm-2:00 pm), every other day, in order to minimize the chicks' discomfort and any growth-retarding effects of needle-puncture[113]. Chicks were anesthetized with 1.5% isofluorane in 50:50 O_2:N_2O, the upper eyelids were cleaned externally with 70% ethanol, and drugs were injected using a 26-gauge needle attached to a 25 µL Hamilton Gastight syringe. The needle

was inserted approximately 6 mm deep, through eyelid and sclera, into the dorsal quadrant of the eye, and 20 µL of solution was injected rapidly into the vitreous. Post-injection, the needle was held in place for few seconds, and then slowly withdrawn to prevent backflow. The needle was then rinsed in 70% ethanol before the next injection; dedicated syringes and needles were used for each treatment group. The same injection site was not used for subsequent injections, to minimize local scarring and backflow through the injection holes. After injections, chicks were returned to their cage to recover.

Measurements

Refractive error (± 0.5 D) was measured without cycloplegia using a streak retinoscope (Model 18100; WelchAllyn, ON, Canada) and trial lenses; working distance was approximately 0.5 m, and no correction was made for distance or the small-eye artefact. Subsequently, chicks were euthanized by intraperitoneal injection of 240 mg/mL Euthanyl (pentobarbital sodium; CDMV, Saint-Hyacinthe, PQ, Canada), followed by decapitation. Eyes were removed, extraocular tissues were dissected away, and then the globe was placed in a Petri dish supported by a PBS-dampened paper towel for viewing either perpendicular to the optic axis (for axial length) or on-axis with the corneal side up (for equatorial diameter). Axial length was defined as the distance from front of cornea to back of sclera, and equatorial diameter was defined as the mean of the maximum and minimum diameters ($[d_{max} + d_{min}] / 2$), due to the ellipsoid shape of chick eyes. Measurements (± 0.01 mm) were made with digital calipers (Model 58-6800-4; Mastercraft). Both the globe and calipers were viewed under a dissecting microscope, and the caliper arms were closed until they just barely touched the surfaces of the eye. Wet weight of the eye (± 0.001 g) was measured using a digital balance (PL200; Mettler). Measurement bias was minimized by blinding the experimenter to the chick's treatment, and by recording refractive error separately from biometric parameters. Recorded values for axial length and equatorial diameter were the average of three separate measurements, which were typically completed within 30 seconds per eye; therefore, any changes in dimensions or weight due to handling and drying were negligible.

Data Analysis

Drug treatments were found not to affect control eyes; therefore, the effects of treatment are expressed as the mean difference between values for the experimental eye (goggled, drug-injected) and control eye (open, vehicle-injected) ± standard deviation (SD). Statistical analysis was performed using One-Way ANOVA with Tukey's post hoc test (Prism V6.02; GraphPad Software, Inc., LaJolla CA, USA) unless specified otherwise; data were deemed significant at $p < 0.05$.

Tissue preparation and Histology (Toluidine Blue)

Eyes were hemisected through the equator, the vitreous was removed, and the anterior eye was discarded. Posterior eye cups were fixed in 4% paraformaldehyde + 3% sucrose in 0.1 M phosphate buffer, pH 7.4, for 0.5 hrs (25°C), and then washed three times (15 min each) in PBS and cryoprotected in 0.1 M phosphate buffer + 30% sucrose for 2-4 days at 4°C. For cryosectioning, eye cups were soaked in Optimal Cutting Temperature (OCT; VWR) for 15 min (25°C) and then quick-frozen by dipping the mold containing OCT into a dry ice/ethanol bath; care was taken to make sure that no ethanol came in contact with the OCT. Sections were cut at 12-14 µm, thaw-mounted onto Fisherbrand Superfrost Plus slides, briefly heat-fixed on a hot plate (40°C, 10 min), ringed with rubber cement to create a hydrophobic barrier, and stored at -20°C. *Toluidine Blue* – Slides were warmed (25°C), washed three times (15 min) in PBS, and incubated under 0.1% (w/v) Toluidine blue[207]. After 2 min, the stain was removed, the slides were washed in PBS until the wash solution ran clear, and then the samples were mounted under cover-slips in a 4:1 solution of glycerol:water. Toluidine blue-labeled slides were imaged in bright-field using a Zeiss epi-illumination microscope with 25x Neo-Fluar water-immersion objective, NA = 0.8, and digital camera (Model RT3; SPOT Imaging, Division of Diagnostic Instruments, Inc., Sterling Heights, Michigan, USA).

Chapter 3: Nitric Oxide is *Necessary* for Atropine-Mediated Inhibition of FDM in Chicks, and *Sufficient* to Inhibit FDM by Itself

Abstract

Atropine inhibits myopia progression in humans and animals, but the downstream signalling cascades are unknown. In this chapter, I show that myopia-prevention by atropine requires the production of nitric oxide (NO), and that NO alone is sufficient to inhibit FDM in the chick.

FDM was induced in P7 chicks by diffusers over the right eye (OD); the left eye (OS) remained ungoggled. On post-goggling (PG) days 1, 3, and 5, OD received intravitreally 20 µL of vehicle (PBS), or vehicle plus: NO source: L-Arg (60-6,000 nmoles) or SNP (10-1,000 nmoles); atropine (240 nmoles); NOS inhibitors (NOSi): L-NIO or L-NMMA (6 nmoles); negative controls: D-NMMA (6 nmoles) or D-Arg (10 µmoles); or atropine plus L-NIO, L-NMMA, or D-NMMA. OS received vehicle. On day PG6, refractive error (RE), axial length (AL), equatorial diameter (ED), and wet weight (WW) were measured.

PBS-injected goggled eyes developed significant FDM which was inhibited by L-Arg (ED_{50} = 400 nmoles) and SNP (ED_{50} = 20 nmoles), but not D-Arg. High dose SNP, but not L-Arg, was toxic to the retina/RPE. Atropine (240 nmoles) inhibited FDM as expected. Simultaneous injection of L-NIO or L-NMMA with atropine blocked myopia-inhibition dose-dependently, while simultaneous injection of D-NMMA with atropine did not block myopia inhibition.

Blockade of atropine-mediated myopia inhibition by NOS inhibitors is likely to be specific to loss of NO induction, instead of off-target effects of NOSi treatment. Intraocular NO inhibits myopia dose-dependently and is obligatory for inhibition of myopia by atropine, and acts as an important "stop" signalling molecule in regulation of eye growth. These data have been accepted for publication prior to thesis submission in the open access journal Scientific Reports[1]. As per the licence-to-publish agreement, ownership of copyright in the article remains with us, so no additional permissions are required to reproduce them here.

Introduction

Atropine is effective against myopia in avian and mammalian animal models, in which it mainly inhibits the exaggerated axial elongation that occurs during myopia development. Current literature leaves a large gap in our understanding of the mechanism of action of mAChR antagonist-regulation of eye size; there is consensus that the mechanism underlying retardation of axial length elongation by atropine most likely does not rely on paralysis of accommodation[151], but the rest remains largely unknown. In addition to not knowing the target receptor or target tissues involved in myopia inhibition by atropine, we also do not know the downstream signalling cascades that may be activated (or inactivated) when it is applied to the eye.

One signalling cascade that could be involved in regulation of eye growth would be activation of nitric oxide synthase (NOS) and production of ocular nitric oxide (NO). NO is considered to be a "light-adaptive" signalling molecule; it is known to mediate some light-adaptive changes in the retina[208-211], and its synthesis and release are increased by intense or intermittent (flickering) illumination[195,196]. When applied to the retina, NO donors mimic the adaptational effects of increased illumination[193], while inhibitors of NOS – the enzyme that generates NO from L-arginine – mimic the functional effects of decreased illumination in light-adapted chicks[194]. Recently, increased environmental illumination has been reported to protect against myopia in animals[98,212] and children[100,213,214], and it has been reported that NOS-inhibitors block the prevention of experimentally-induced FDM normally elicited by daily periods of unobstructed vision[47]. In mouse, treatment with the NOS inhibitor resulted in an increased susceptibility to FDM (Chakraborty et al. IOVS 2016; 57: E-Abstract 4742). Taking this evidence into consideration, we tested the hypothesis that increased ocular nitric oxide synthesis is (i) sufficient to prevent FDM on its own, and (ii) necessary for atropine-mediated myopia prevention in the chick. A preliminary report of our findings was presented previously (Carr B, et al. IOVS 2013; 54: E-Abstract 3677 © ARVO).

Results

Normal Ocular Growth and Myopia-Development after Application of Form-Diffuser Goggles

Data are represented as absolute values ± SD. Control eyes (open, vehicle) from all treatment groups exhibited a mean hyperopic refractive error of 3.2 ± 0.8 D and axial length of 9.55 ± 0.18 mm at the end of the treatment period. There was no significant difference between these parameters of control eyes in any of the treatment groups (One-Way ANOVA, p=0.8807); therefore, they were used as same-animal standards for comparison of effects in treated eyes, minimizing any confounding effects of inter-individual differences. Goggled eyes that received saline injections developed significant myopia, exhibiting increases in negative refractive error (RE), axial length (AL), equatorial diameter (ED), and wet weight (WW) compared to those parameters in contralateral control eyes (RE: -14.36 ± 2.7 D vs. 3.2 ± 0.8 D; AL: 10.10 ± 0.22 mm vs. 9.55 ± 0.18 mm; ED: 13.14 ± 0.26 mm vs. 12.83 ± 0.2 3mm; WW: 0.831 ± 0.039 g vs. 0.756 ± 0.032 g; $p < 0.0001$, unpaired *t*-test, two-tailed; n = 35-38). This verified that our goggles induced significant axial myopia and increased eye size in these animals, even with repeated intravitreal injections (**Fig. 3.1**).

Figure 3.1: Effect of Diffuser Goggles on Development of FDM in Chicks

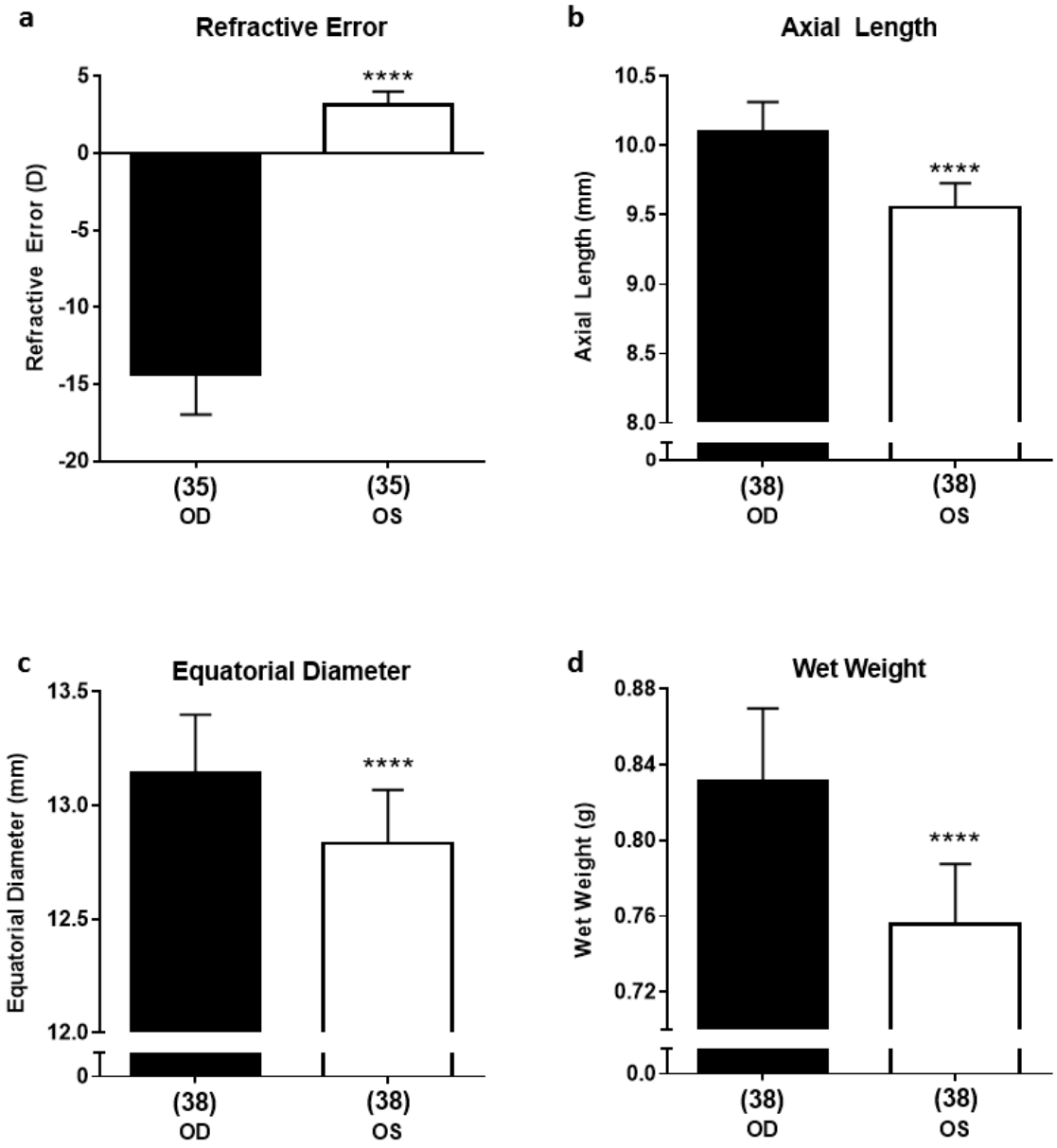

Figure 3.1: Refractive and biometric interocular differences between goggled (form-deprived right eye: OD) and non-goggled (open left eye: OS) eyes, after injecting phosphate-buffered saline (PBS) 3 times, at 48-hr intervals. Monocular form-deprivation of chicks in this study caused the expected responses: a large negative shift in refractive error (**a**), and modest but highly significant increases in total axial length (**b**), circular-equivalent equatorial diameter (**c**), and wet weight (**d**), in the goggled eyes. Data are represented as mean ± SD. ***Statistics***: ****$p < 0.0001$, unpaired Student's t-test; sample sizes (n) are denoted in brackets below each column.

Inhibition of Form-Deprivation Myopia by NO-Sources

Data are represented as the mean difference between values for the experimental eye minus those for the control eye ± SD. L-Arg (pH 7), at 60-6,000 nmoles (maximum vitreal concentrations 0.3-30 mM), decreased the effects of the diffuser goggle in a dose-dependent manner (n = 10-17), with an ED_{50} = 400 nmoles (maximum vitreal concentration 2 mM) (**Fig. 3.2a,b**). At a dose of 10 µmoles, D-Arg – which does *not* serve as a source of NO – did not alter the axial growth or refraction of normal or form-deprived eyes (**Fig. 3.2c,d**, n = 5-6). To validate further that myopia inhibition by L-arginine is mediated by an increase in NO, we tested the effect of simultaneous injection of 6 nmoles L-NMMA with 600 nmoles of L-Arg; addition of L-NMMA resulted in a complete blockade of myopia inhibition by L-Arg (**Fig. 3.2e,f**, n = 5-10).

Figure 3.2: Effects of L-Arg, D-Arg, and L-Arg + L-NMMA on FDM in Chicks

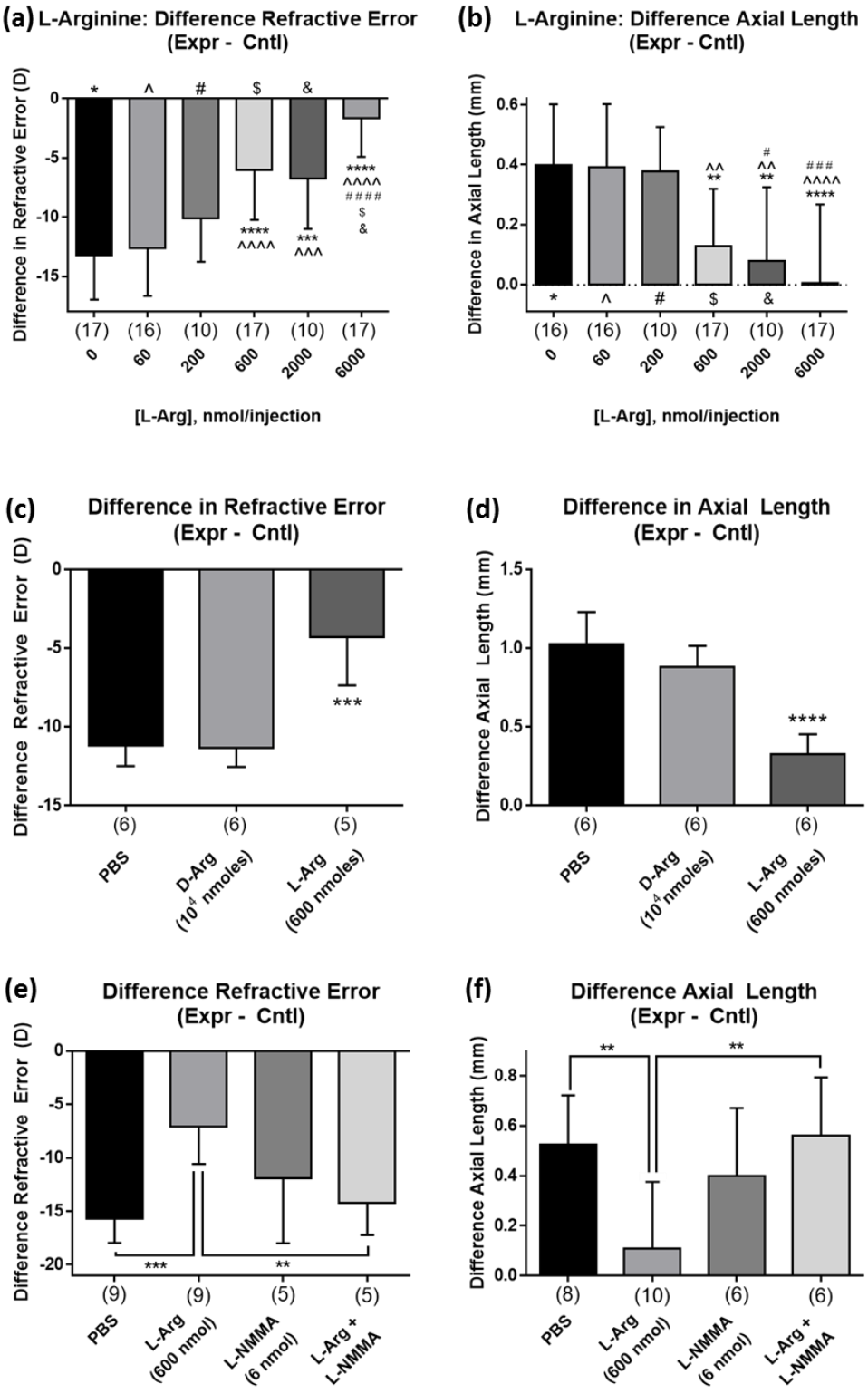

Figure 3.2: The effect of L-Arg on FDM in chicks, and control experiments. Doses represent the number of moles of drug injected, per injection, 3 times at 48-hr intervals. L-Arg dose-dependently inhibited the development of myopic refractive error and axial elongation in goggled eyes (**a,b**). D-Arg had no effect (**c,d**), and L-NMMA blocked myopia inhibition by L-Arg (**e,f**). Control eyes were not affected by drugs delivered to the goggled eyes. ***Abbreviations***: **L-Arg**: L-arginine; **D-Arg**: D-arginine; **L-NMMA**: L-N^G-monomethyl arginine. ***Symbols:*** asterisk (*): comparison to PBS-treatment, unless specified otherwise (**e-f**); caret (^): comparison to 60 nmoles; pound (#): comparison to 200 nmoles; dollar ($): comparison to 600 nmoles; ampersand (&): comparison to 2000 nmoles (**a-d**). ***Statistics:*** •••• $p < 0.0001$, ••• $p < 0.001$, •• $p < 0.01$, • $p < 0.05$; One-Way ANOVA + Tukey's post-hoc. Data are represented as the means of the difference in values for the experimental eye minus those for the control eye, ± SD; sample sizes (n) are denoted in brackets below each column.

In previous experiments performed in our lab, SNP at 10-1,000 nmoles (maximum vitreal concentrations 0.05-5 mM), decreased myopia development dose-dependently, with ED_{50} = 20 nmoles (maximum vitreal concentration 100 µM; n = 6) (**Fig. 3.3**). Eyes treated with the highest dose of SNP (1,000 nmoles) were extremely hyperopic to the point where we could not measure the refractive error accurately (hence, ≥ 15 D), and had significantly shortened axial lengths, which is typically an indicator of drug toxicity. To confirm this, I repeated the treatment with the highest- and ED_{50}-doses of SNP, and performed basic histological examination of eyes with Toluidine blue staining and immunolabelling for macrophage markers. As expected, retinas from highly shortened SNP-treated eyes were grossly abnormal (**Figs 3.4 & 3.5**).

Figure 3.3: Effect of SNP on FDM in Chicks

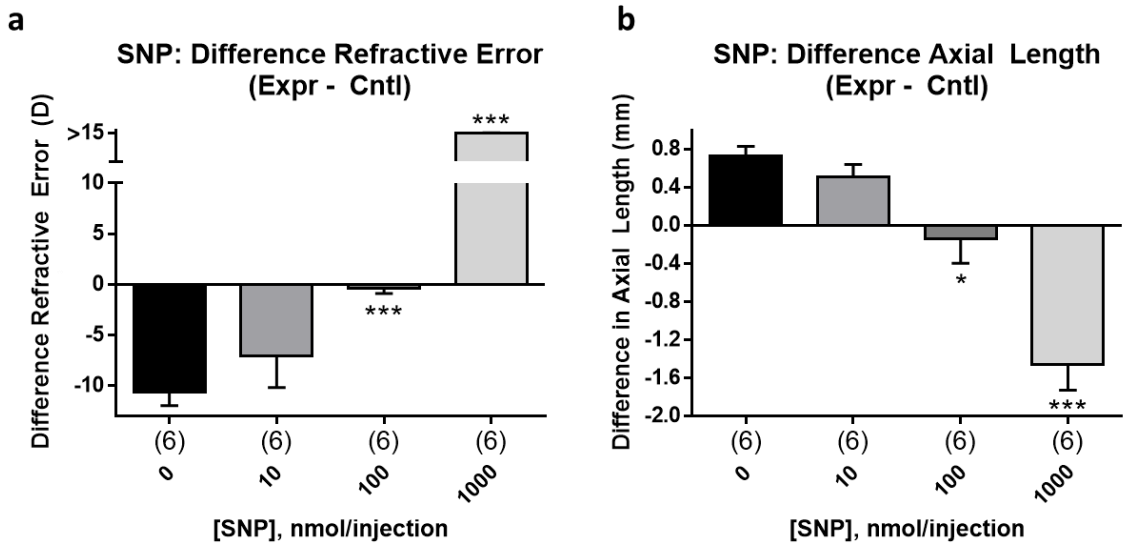

Figure 3.3: The effects of NO-donor (SNP), on FDM in chicks; doses represent the number of moles of drug injected, per injection, 3 times at 48-hr intervals. SNP dose-dependently inhibited the development of myopic refractive error (**a**) and excessive axial elongation (**b**) in goggled chick eyes; control eyes were not affected by drugs delivered to the goggled eyes. The excessively positive refractive error and shortened axial length seen in the highest treatment group (1000 nmoles) is indicative of retinal damage. ***Abbreviations***: **SNP**: sodium nitroprusside. ***Symbols***: asterisk (*): comparison to effect of PBS-treatment. ***Statistics***: $^{***}p < 0.001$, $^{*}p < 0.05$; Kruskal-Wallis + Dunn's post-hoc. Data are represented as the means of the difference in values for the experimental eye minus those for the control eye, ± SD; sample sizes (n) are denoted in brackets below each column.

Effects of L-Arg and SNP on Retinal Integrity

Toluidine blue: At the ED_{50} (400 nmoles) and maximum (6,000 nmoles) doses, L-Arg caused no obvious retinal damage; scattered small pigment aggregates were detected in the outer nuclear layer (ONL) at the highest dose, but not in controls (**Fig. 3.4a,b**). At ED_{50} of SNP (20 nmoles), pigment aggregates were more abundant in both treated and control eyes, but retinal and RPE structure remained largely intact (**Fig. 3.4c,d**). Retina and RPE of eyes treated with the maximum dose of SNP (1,000 nmoles) were severely degenerated, with complete loss of outer retinal layers and significant distortion of inner layers (**Fig. 3.4e**); ONL pigment aggregates were larger and more frequent in fellow control eyes (than were seen in the control eyes of ED_{50} dose), indicating possible contralateral-eye effects of high-dose SNP (**Fig. 3.4f**). *Immunolabelling:* LEP-100 (an indicator of phagocytosis) in control eyes was apparent in the basal RPE, retinal bacillary layer (photoreceptor outer and inner segments), outer plexiform layer, and putative microglia/macrophages[215] and astrocytes in the inner retina (**Fig. 3.5c**); the activated leukocyte marker, GRL2, only weakly labeled the basal RPE (**Fig. 3.5f**). L-Arg at any dose tested, and SNP at ED_{50}, caused no change in these labelling patterns (**Fig. 3.5b,e**). Retinas heavily damaged by maximum-dose SNP were intensely labelled for LEP-100 and GRL2, and red autofluorescence was abundant in putative RPE remnants (**Fig. 3.5a,d**).

Figure 3.4: Effects of ED_{50} and Maximum Doses of L-Arg and SNP on Retinal Integrity

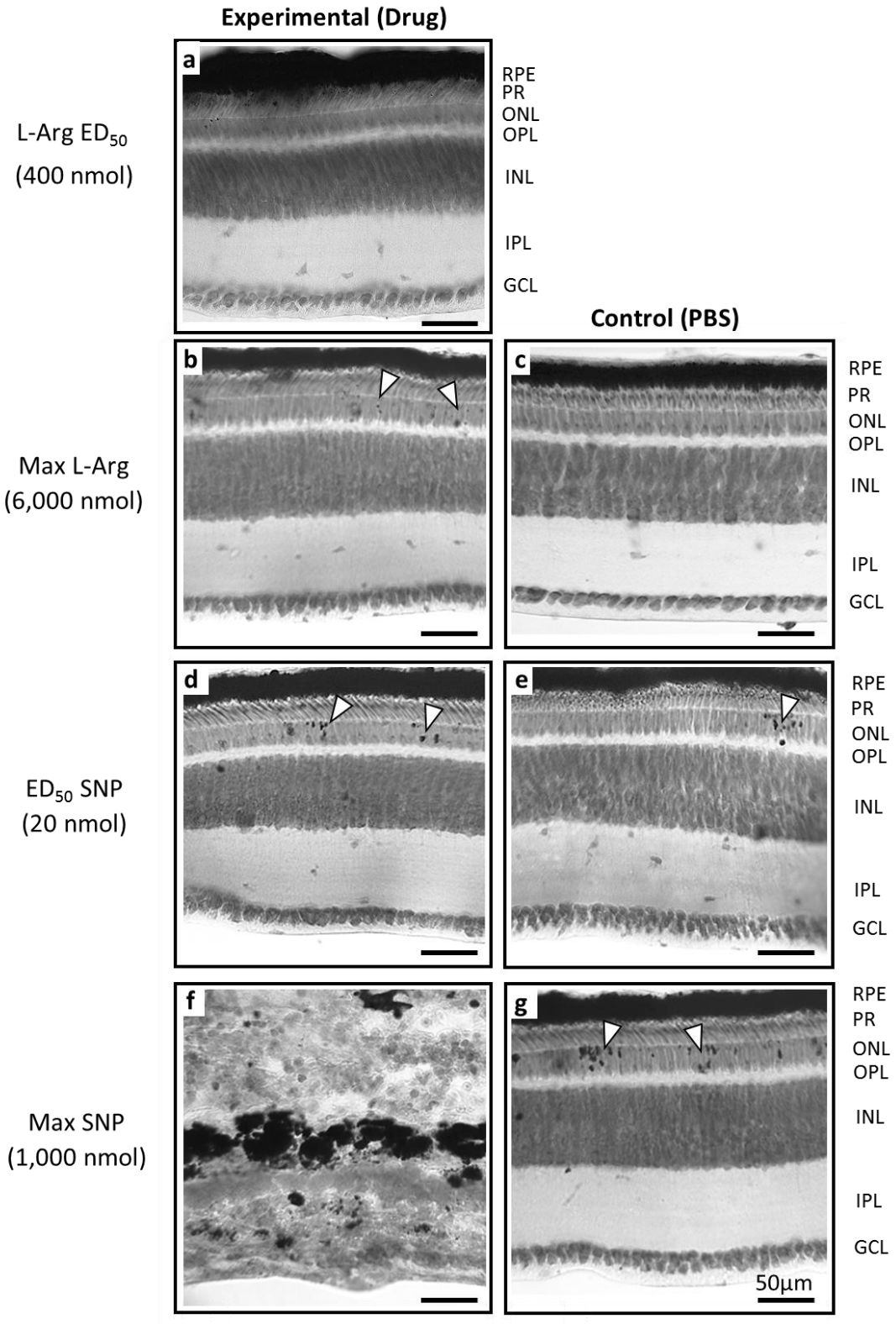

Figure 3.4: Transmission light micrographs of Toluidine blue-stained retinas treated with L-Arg and SNP, and their contralateral PBS-treated controls. There was no obvious damage to retinal or RPE structure in eyes treated with either the ED_{50} or the maximum dose of L-Arg (**a-c**), but small pigment deposits were present in the ONL (white arrowheads) that were not seen in the PBS-only control (**c**). At the ED_{50} of SNP, there was an increase in the small pigment deposits in the ONL (white arrowheads), in treated (**d**) and control (**e**) tissues; otherwise, the structure of the retina and RPE remained largely unaffected. At the maximum concentration of SNP, there was massive degeneration of the retina and RPE, with complete loss of the photoreceptor and ONL/OPL; INL and GCL were still detectable, but distorted (**f**). Contralateral control eyes (**g**) had a significant increase in pigment in the ONL; but the structure of the retina and RPE remained intact. ***Abbreviations:*** **RPE**: retinal pigment epithelium; **PR**: photoreceptor inner and outer segments (bacillary layer); **ONL**: outer nuclear layer; **OPL**: outer plexiform layer; **INL**: inner nuclear layer; **IPL**: inner plexiform layer; **GCL**: ganglion cell layer. Neo-Fluar water-immersion objective (25x, NA 0.8). Scale bar = 50 µm.

Figure 3.5: Immunolabelling of LEP-100 and GRL2 in Chick Retinas Treated with ED_{50} and Maximum Doses of L-Arg and SNP

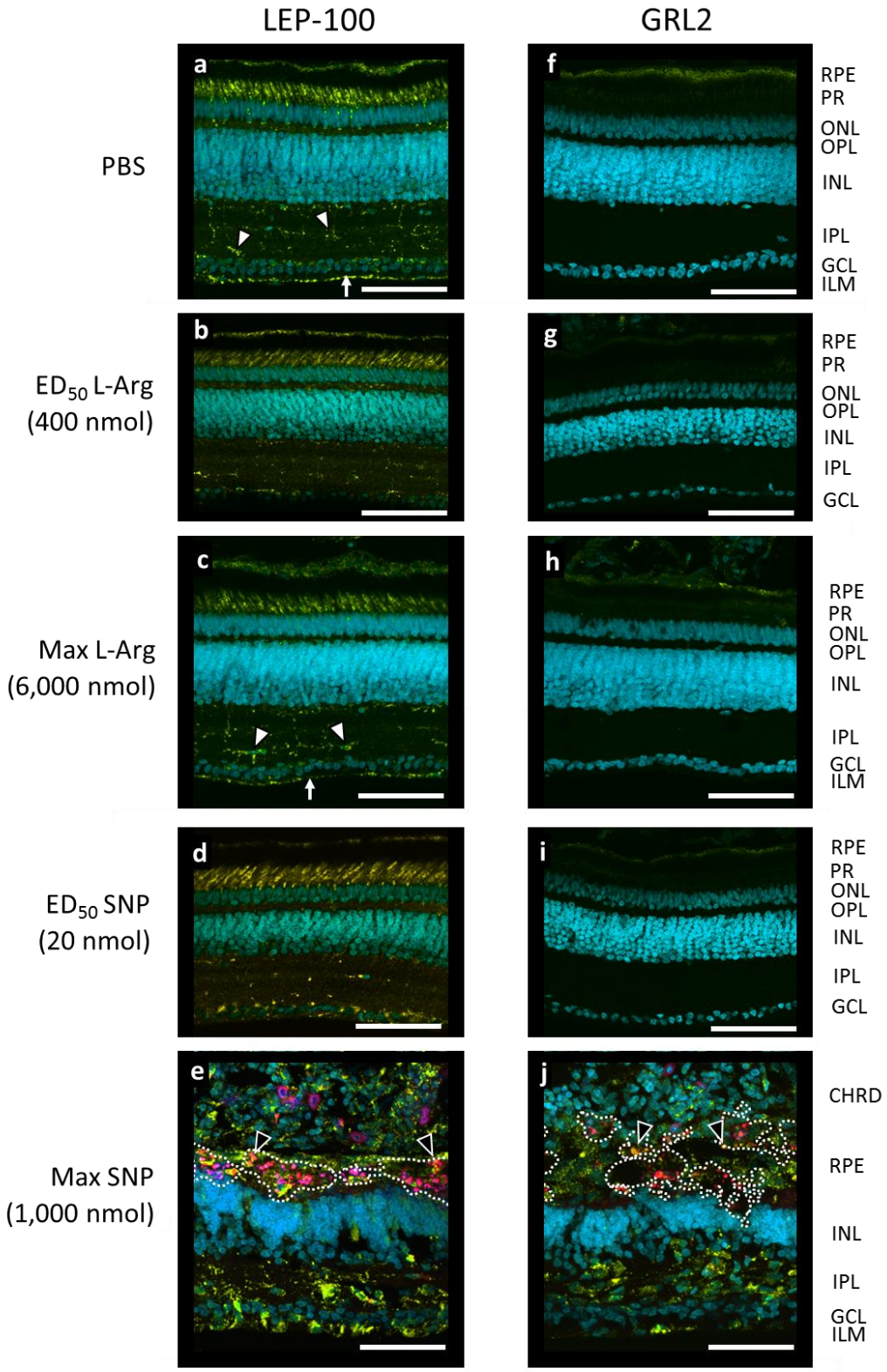

Figure 3.5: Fluorescence micrographs of retinal sections, labeled yellow-green for LEP-100 or GRL2 and teal-blue for nuclei (DAPI); RPE and pigmented structures, which we located in bright-field images, are outlined with white dotted lines. In retinas treated with the maximal dose of SNP (**e,j**), intense LEP-100 and GRL2 signals were found in the IPL, near the inner limiting membrane, and in the choroid; a significant amount of red autofluorescence (pseudo-colored pink) was detected in what are most likely the pigmented remnants of the RPE, some of which were co-localized with the LEP-100 and GRL2 signals (black arrowheads). In all other tissues tested, there was no significant fluorescence in the red channel, and LEP-100 and GRL2 labelling patterns did not differ according to treatment group. LEP-100 signal was present in the basal RPE, bacillary layer (PR), putative microglia/macrophage in the IPL (white arrowheads), and probable astrocytes at the internal limiting membrane (white arrows) in max L-Arg- and PBS-treated retina (**a,c**). GRL2 signal was not detected in undamaged retina (**e,f**). ***Abbreviations:*** **CHRD**: choroid; **RPE**: retinal pigment epithelium; **PR**: photoreceptor inner and outer segments (bacillary layer); **ONL**: outer nuclear layer; **OPL**: outer plexiform layer; **INL**: inner nuclear layer; **IPL**: inner plexiform layer; **GCL**: ganglion cell layer; **ILM**: inner limiting membrane. Images are maximum-intensity Z-stack projections of the entire thickness of retinal sections (12-14 µm, 1.5 µm/slice), oil-immersion objective (40x, NA = 1.3); scale bar = 50µm.

Inhibition of FDM by Atropine and NOS-Specific Blockade of Inhibition

Data are represented as the means of the difference (d) in values for the experimental eye minus those for the control eye, ± SD. All outcomes are listed in **Table 3.1**, statistical p-values are listed in **Table 3.2**, and data are visualized in **Fig. 3.6**. Intravitreal atropine (240 nmoles) significantly inhibited FDM-induced refractive error and axial elongation (dRE: -8.0 ± 2.1 D vs. -17.7 ± 1.5 D, $p_{(PBS)} < 0.0001$, n = 34; dAL: 0.35 ± 0.2 mm vs 0.54 ± 0.20 mm, $p_{(PBS)} = 0.0006$, n = 39). Intravitreal injection of NOS inhibitors (6 nmoles; L-NIO and L-NMMA) had no significant effect on the development of FDM; the dRE closely matched that of vehicle controls, and were significantly different from that of atropine-treated eyes (L-NIO, dRE: -16.0 ± 2.5 D, $p_{(atro)} < 0.0001$, n = 10; L-NMMA, dRE: -15.6 ± 2.6 D, $p_{(atro)} < 0.0001$, n = 10), and NOS-inhibition did not affect FD-induced changes in

dAL (L-NIO, dAL: 0.55 ± 0.2 mm, $p_{(PBS)}$ = 0.054, n = 12; L-NMMA, dAL: 0.56 ± 0.2 mm, $p_{(PBS)}$ = 0.1149, n = 12). Upon close examination of the data, treatment with NOS inhibitors seemed to result in a greater amount of FDM when compared to vehicle-treated controls, but this difference was not significant. The mean dRE of eyes injected with D-NMMA (6 nmoles) was only slightly less negative than that of controls (dRE: -14.8 ± 6.3 D, $p_{(PBS)}$ = 0.033, n = 16), but very different from that of atropine-treated eyes ($p_{(atro)}$ < 0.0001). The mean dAL of D-NMMA-injected eyes was not significantly different from that of atropine-treated eyes (dAL: 0.49 ± 0.2 mm; $p_{(atro)}$ = 0.1917, n = 17).

Simultaneous injection of NOS inhibitors with atropine interfered with myopia inhibition (atropine + L-NIO: dRE: -15.6 ± 2.6 D, $p_{(atro)}$ < 0.0001, n = 12; dAL: 0.61 ± 0.2 mm, $p_{(atro)}$ = 0.002, n = 12; atropine + L-NMMA: dRE: -17.7 ± 2.1 D, $p_{(atro)}$ < 0.0001, n = 9; dAL: 0.56 ± 0.2 mm, $p_{(atro)}$ = 0.0321, n = 12). In contrast, D-NMMA (the biologically inactive enantiomer) had no effect on myopia-prevention by atropine (atropine + D-NMMA: dRE: -8.05 ± 2.0 D, $p_{(PBS)}$ < 0.0001, n = 16; dAL: 0.30 ± 0.1 mm, $p_{(PBS)}$ = 0.0012, n = 17). None of the treatments had a significant effect on equatorial diameter or wet weight (**Table 3.1**). To validate these results, we evaluated the effect of decreasing concentrations of L-NMMA on atropine-mediated inhibition of myopia; 60 and 600 pmol L-NMMA (n = 9-11) had no effect on atropine's ability to prevent FDM, while 6 nmoles L-NMMA (n = 7) blocked inhibition of myopia by atropine (**Fig. 3.7**).

Figure 3.6: Effects of Atropine, L-NIO, L-NMMA, D-NMMA, and Their Combination on FDM in Chicks

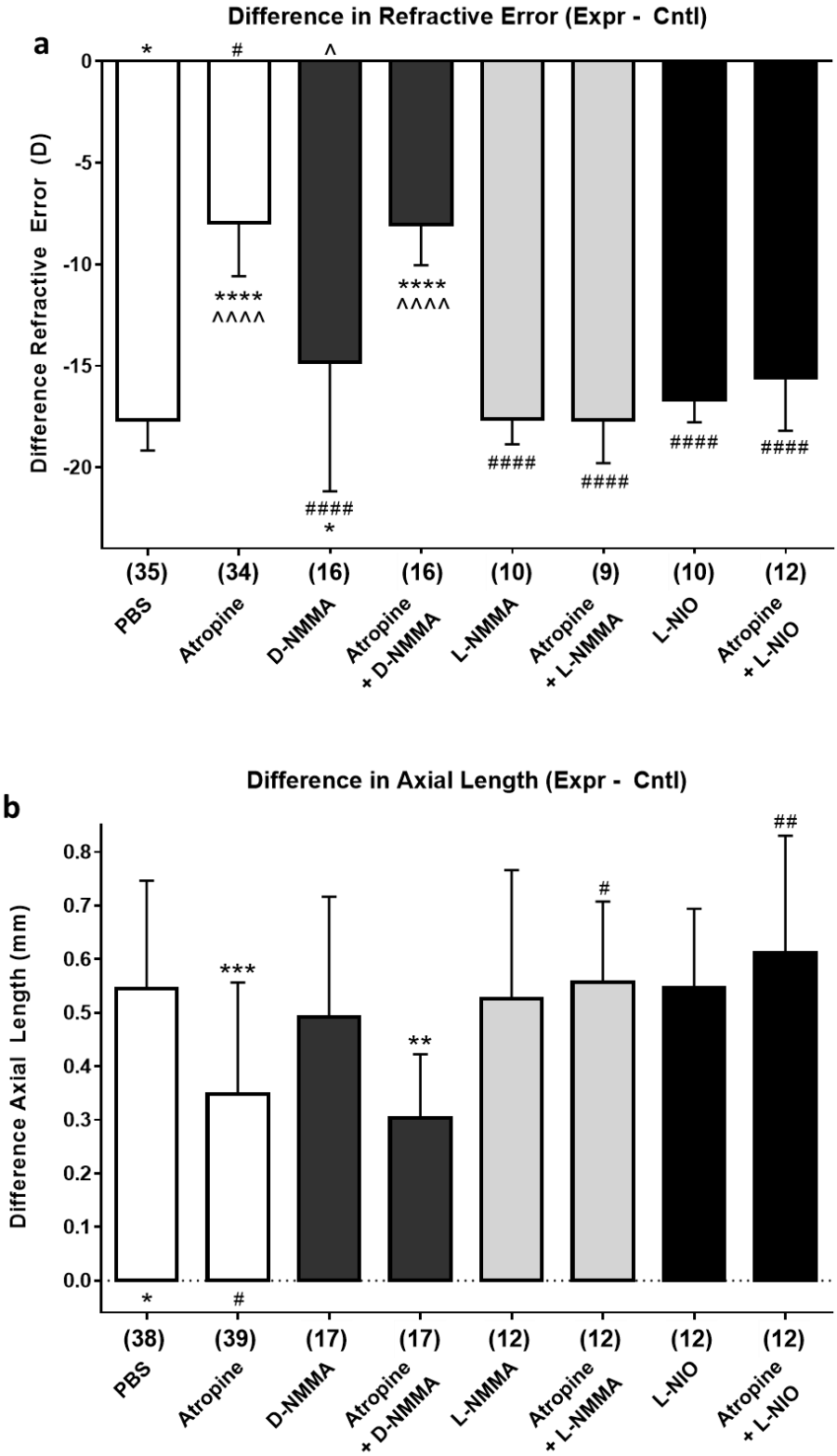

Figure 3.6: The effects of atropine (240 nmoles), NOS inhibitors (6 nmoles; L-NIO, L-NMMA), D-NMMA (6 nmoles), and the combination of atropine + NOS inhibitors (L-NIO, L-NMMA), or atropine + D-NMMA on refractive error (**a**) and axial length (**b**); doses represent the number of moles of drug injected, per injection, 3 times at 48-hr intervals. ***Abbreviations***: **L-NIO**: N^G-(1-Iminoethyl)-L-ornithine; **L-NMMA**: L-N^G-monomethyl arginine; **D-NMMA**: D-N^G-monomethyl arginine. ***Symbols***: asterisk (*): comparison to effect of PBS-treatment; pound (#): comparison to effect of atropine-treatment; caret (^): comparison to effect of D-NMMA-treatment. ***Statistics***: •••• $p < 0.0001$, ••• $p < 0.001$, •• $p < 0.01$, • $p < 0.05$; One-Way ANOVA + Tukey's post-hoc. Data are represented as the means of the difference in values for the experimental eye minus those for the control eye, ± SD; sample sizes (n) are denoted in brackets below each column.

Figure 3.7: Dose-Dependent Effects of L-NMMA on Prevention of Myopia-Inhibition by Atropine

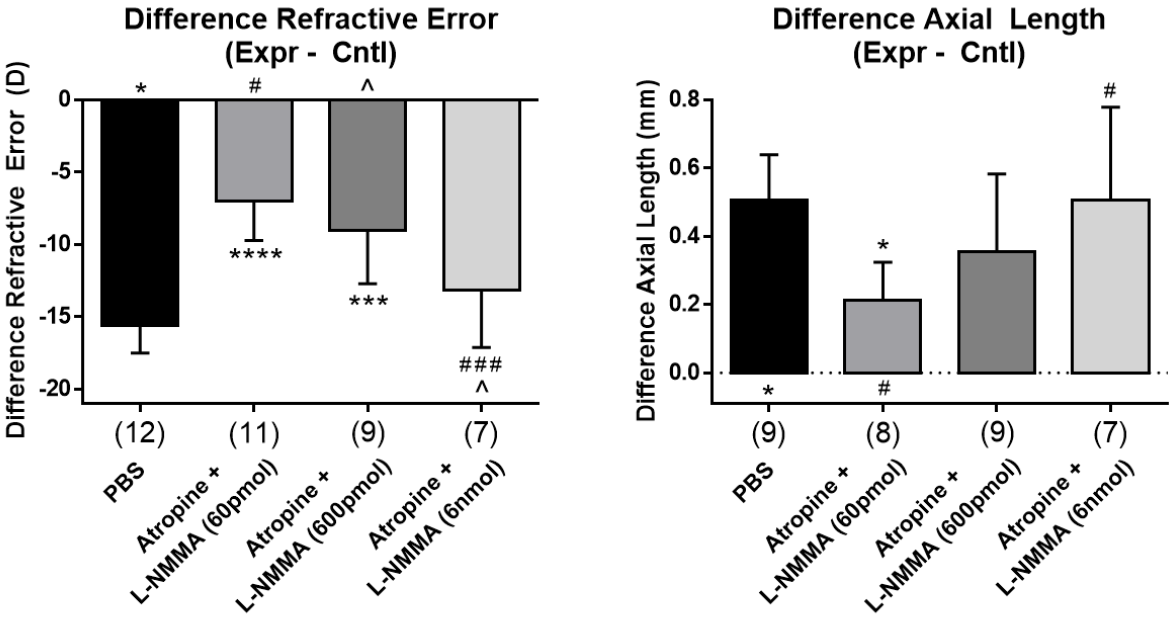

Figure 3.7: Dose-dependent effects of L-NMMA on atropine-mediated myopia inhibition on refractive error (**a**) and axial length (**b**). As the concentration of L-NMMA is decreased from 6 nmoles to 60 pmol, its ability to block myopia inhibition by atropine (240 nmoles) is lost. ***Abbreviations***: **L-NMMA**: L-N^G-monomethyl arginine. ***Symbols:*** asterisk (*): comparison to effect of PBS-treatment; pound (#): comparison to 60 pmol; caret (^): comparison to 600 pmol. ***Statistics:*** $^{\bullet\bullet\bullet\bullet}$ $p < 0.0001$, $^{\bullet\bullet\bullet}$ $p < 0.0001$, $^{\bullet}$ $p < 0.05$; One-Way ANOVA + Tukey's post-hoc. Data are represented as the means of the difference in values for the experimental eye minus those for the control eye, ± SD; sample sizes (n) are denoted in brackets below each column.

Table 3.1: The effects of atropine (240 nmoles), NOS inhibitors (6 nmoles), and D-NMMA (6 nmoles) on the mean difference between experimental (goggled) eyes and control (non-goggled) eyes of various eye parameters.

Treatment	dRE (D)	dAL (mm)	dED (mm)	dWW (g)
PBS	-17.7 ± 1.5	0.54 ± 0.20	0.31 ± 0.23	0.075 ± 0.033
Atropine (Atro)	-8.0 ± 2.6	0.35 ± 0.21	0.30 ± 0.16	0.087 ± 0.030
L-NIO	-16.0 ± 2.5	0.55 ± 0.15	0.33 ± 0.18	0.085 ± 0.018
Atro + L-NIO	-15.6 ± 2.6	0.61 ± 0.22	0.38 ± 0.20	0.100 ± 0.028
L-NMMA	-15.6 ± 2.6	0.56 ± 0.24	0.21 ± 0.25	0.062 ± 0.040
Atro + L-NMMA	-17.7 ± 2.1	0.56 ± 0.15	0.39 ± 0.20	0.082 ± 0.039
D-NMMA	-14.8 ± 6.3	0.49 ± 0.22	0.38 ± 0.22	0.080 ± 0.035
Atro + D-NMMA	-8.0 ± 2.0	0.30 ± 0.12	0.34 ± 0.16	0.081 ± 0.016

*dRE: difference refractive errors; dAL: difference axial lengths; dED: difference equatorial diameters; dWW: difference wet weights. Values represented as mean ± SD.

Table 3.2: Adjusted p-values (One-Way ANOVA + Tukey's post hoc) for all significantly different means of the difference between eyes for refractive error (dRE) and axial lengths (dAL) from atropine-, NOS inhibitor-, and D-NMMA-treatment experiments.

Treatment Groups	**dRE**	**dAL**
PBS vs. Atropine (Atro)	< 0.0001	0.0006
PBS vs. D-NMMA	0.0331	
PBS vs. Atro + D-NMMA	< 0.0001	0.0012
Atro vs. D-NMMA	< 0.0001	
Atro vs. L-NMMA	< 0.0001	
Atro vs. Atro + L-NMMA	< 0.0001	0.0321
Atro vs. L-NIO	< 0.0001	
Atro vs. Atro + L-NIO	< 0.0001	0.0019
D-NMMA vs. Atro + D-NMMA	< 0.0001	
Atro + D-NMMA vs. L-NMMA	< 0.0001	0.0173
Atro + D-NMMA vs. Atro + L-NMMA	< 0.0001	
Atro + D-NMMA vs. L-NIO	< 0.0001	0.0281
Atro + D-NMMA vs. Atro + L-NIO	< 0.0001	0.0013

*dRE: difference refractive errors; dAL: difference axial lengths

Discussion

In these experiments, we tested whether NO plays a role in regulation of eye growth and atropine-mediated prevention of FDM. As hypothesized, atropine and NO-sources inhibited FDM in a dose-dependent manner, and NOS-inhibitors blocked the atropine-mediated inhibition of myopia. In contrast, D-NMMA – an enantiomer that is inactive at NOS – had no effect; therefore, the blockade of myopia-prevention by NOS inhibitors is likely due to the stereospecific actions of these L-Arg analogs at NOS, rather than non-specific effects of arginine-like compounds via other molecular targets and processes[216].

Histological examination of retinas treated with L-Arg at all doses, and SNP at ED_{50}, revealed no significant damage to retina and RPE. At the maximum applied dose of SNP, however, we observed massive destruction of both tissues and dramatic changes in the associated choroid. Eye growth (specifically, size of the sclera) is controlled by retinal activity, relayed through the RPE and choroid[2]. Therefore, the damage observed in these tissues likely explains the arrest of elongation, highly positive refractive error, and shortened axial length of these SNP-treated eyes – indicating, coincidentally, that *signalling by the retina/RPE and/or the choroid constitutively promotes ocular elongation during the post-hatching period of rapid growth*. The intense labelling for LEP-100 and GRL2 in the IPL and choroid, and the appearance of red autofluorescence in RPE-choroid at the highest dose of SNP, likely indicate increased macrophage activation[215], phagocytosis of cell debris[217], and gliosis.

Nitric oxide is synthesized by the enzyme nitric oxide synthase (NOS), of which there are three isoforms: neuronal NOS (nNOS/NOS1) and endothelial NOS (eNOS/NOS3) are expressed constitutively and require calcium for activation, while inducible NOS (iNOS/NOS2) is transcriptionally regulated, and thus has calcium-independent activity. NADPH-diaphorase activity and nNOS-like immunoreactivity can be found in all major cell types in the chick retina and choroid[139,140,192] and are co-localized consistently in approximately 15 types of retinal neurons; they may be absent from RPE and scleral chondrocytes[139]. Localization of eNOS and iNOS in ocular tissues has been reported as widespread expression in the chick retina[192], but these results may not be conclusive, as the

authors were unable to reliably co-localize endogenously generated NO signal with eNOS- and iNOS-like immunoreactivity. As reported by us in the present paper, intravitreal delivery of NO sources (L-Arg and SNP) significantly inhibited FDM, while blockade of NO-synthesis prevented myopia-inhibition by atropine and L-Arg. These results support the role of nitric oxide as a "stop" signal in regulation of eye growth, and are in agreement with previous studies that either directly[47,110] (and Chakraborty et al. IOVS 2016; 57: E-Abstract 4742) or indirectly[98,213] link changes in ocular NO synthesis with differential effects on myopia.

The evidence for direct interaction between ACh and modulation of NOS in the retina is sparse and conflicting. Oxotremorine is reported to increase immunoreactive cGMP via mAChR M2 in salamander retina[146], and via mAChR M1/M3 in rat[148]. And, while induction of NO is reported to enhance light-evoked release of ACh from amacrine cells in the rabbit[218], it *inhibits* high K^+-evoked release of ACh in the rat[219]. In the chick, no studies such as these have been published. Given the limited information currently available in the literature, we can only speculate as to the pathways and mechanisms by which atropine might induce NO synthesis in the retina (or other ocular tissues). Direct Pathway/Excitation: If atropine *does* work via mAChRs, its targets would likely be M_2/M_4, which are G_i-coupled and generally produce inhibitory effects when activated by ACh[220]. Here, muscarinic antagonism by atropine would cause cellular excitation and depolarization by blocking the constitutive inhibitory activity of the mAChR target(s). The resulting cellular excitation would in turn increase the concentration of intracellular calcium that can drive NO synthesis by stimulating constitutive nNOS or eNOS. Indirect Pathway/Disinhibition: If atropine were working via mAChR subtypes $M_1/M_3/M_5$ it might increase NO concentrations indirectly, by disrupting inhibitory circuitry in the inner retina. Atropine would block its target receptor on an inhibitory interneuron, resulting in decreased release of the inhibitory neurotransmitter and depolarization of whatever cell was targeted by that interneuron – in this case, a cell containing NOS. Depolarization would lead to an increase in intracellular calcium and subsequent activation of eNOS or nNOS, resulting in myopia inhibition. It is important to note that chickens do not have an M1 subtype

equivalent receptor[221]; instead, the chick M2-like receptor has a motif that gives it M1-like affinity for pirenzepine[142].

Alternatively, we suggest the compelling hypothesis that it is not the interaction of atropine with mAChRs *per se* that is responsible for growth inhibition, but instead either interaction with off-target (i.e., non-mAChR) receptors, or atropine-induced release of signalling molecules in the retina, that ultimately cause retardation of ocular growth. A good case can be made for the latter scenario. Schwahn et al. have shown that, *in vivo*, intravitreal injection of myopia-inhibiting concentrations of atropine results in an increase in retinal dopamine content 3 hrs after treatment. They also showed that, *in vitro*, infusion of high-concentration atropine (500 μM) into the medium surrounding an RPE-retina preparation in an infusion chamber resulted in a massive release of dopamine from the retina 30 min after perfusion (> 200% over baseline)[116]. In agreement with this, immunoreactive chick M_4 receptors are expressed universally by retinal dopaminergic neurons (100% of neurons studied, n = 75)[143]. Increasing retinal dopamine synthesis and release is well known to have strong myopia-inhibiting effects[112,118], and apomorphine, a nonselective dopamine agonist, inhibits LIM and FDM[45,112]. Co-administration of atropine plus apomorphine does not result in an increased effect, however, leading Schmid et al. to suggest that these drugs may work at different points in the same pathway[115].

The mechanism through which dopamine prevents myopia is also unclear, but evidence suggests that it too may stimulate the synthesis and release of NO[110] (and Moinul, et al. IOVS 2012; 53: E-Abstract 3434). Considering the evidence, atropine could act in the retina to inhibit myopia by causing the release of dopamine, which in turn stimulates the synthesis and release of NO. It remains to be determined how this release of dopamine and subsequent NO synthesis may inhibit ocular growth, but NO is known to serve many functions in the retina. One of these – the regulation of cell-cell coupling via gap junctions – has been implicated in myopia-inhibition by studies in our group (Teves M, et al. IOVS 2014; 55: E-Abstract 3036 and Teves[94]). Alternatively, release of NO could inhibit myopia quite simply by causing relaxation of the non-vascular smooth muscle cells in the choroid; these cells are hypothesized to possibly by involved in regulation of choroidal thickness by

either contracting to squeeze fluid out of the large lymphoid lacunae (causing choroidal thinning) or relaxing to allow fluid to drain back into the lacunae (causing choroidal thickening)[40]. Thickening of the choroid by NO-mediated relaxation of non-vascular smooth muscle cells this would push the retina forward resulting in myopic defocus, which is powerfully protective against further axial elongation[222]. Muscarinic-independent signalling mechanisms such as could provide an explanation for some of the curiosities of the relationship between ACh, mAChRs, and eye growth. It could explain why no significant changes are seen in mAChR expression and regulation during induction of FDM[164], and why destroying > 90% of ChAT-positive cells and enzyme activity (leaving dopaminergic amacrine cells intact) has little effect on the eye's ability to grow normally or respond to form-deprivation and atropine-treatment[223].

The existing evidence leaves no question that atropine prevents experimentally-induced myopia in chicks. Our data have confirmed this effect, while supporting for the first time an important role for NO in this process. The retina is the most likely candidate target tissue for atropine-mediated effects on myopia; it contains many kinds of cells and receptors with which atropine could interact, and it is recognized as the visual processing powerhouse of the eye, which drives the regulation of eye growth[2]. It is less likely that atropine would have a strong effect on either the choroid or the sclera, because of loss by diffusion, binding in the vitreous and retina, and limited penetration of the blood-retina barrier formed by the RPE. In addition, FDM is mediated by changes in function in local retinal circuits[31], which cause local changes in signalling. However, the retina is not the only possible site of atropine's anti-myopia action. Some evidence is consistent with an extra-retinal action of atropine[44,223] – with the choroid being a likely alternative target. The choroid relays growth-regulating signals from RPE to sclera[28,50] and it too contains cells which express mAChRs[30,31] and NOS[40]. Furthermore, the requirement of such a high dose of atropine to inhibit myopia is consistent with the limited ability of drugs to pass from vitreous to choroid.

More work is required to determine the mechanism by which atropine can prevent myopia, but its dependence on NO is an important clue, suggesting possible new treatment options.

Targeting NO instead of mAChR mechanisms would allow us to control human myopia without the M_3-mediated side effects of photophobia, glare, and loss of accommodation, and might allow us to use more dilute drug concentrations, alleviating allergic side-effects. Light-therapy may be a better option, as it is linked to an increase in ocular NO[195,196] and protection against myopia development[100,213]. This approach would not require special equipment or expose the subject to the potentially serious side-effects of pharmaceuticals. Thus, the focus on NO as the therapeutic mediator could lead to a paradigm shift in the treatment of myopia.

Methods

The animal ethics statement and common methods for induction of FDM, intravitreal injections, eye biometric measurements, statistical analysis, and preparation of eye tissues for histology are described previously in **Chapter 2**.

Drugs for Intravitreal Injection

Drugs, commercial sources, and the molar amounts delivered per injection are listed in Table 3.3. Drugs were dissolved in phosphate-buffered saline (PBS) (Gibco 14190-144; ThermoFisher Scientific) at room temperature. Stock solutions were made fresh on injection day one, and aliquots were quick-frozen, stored at -20°C, and used only for the duration of one experiment (six days) so as to avoid loss of drug activity due to prolonged storage. The concentrations tested were based on previously published data[47,110,224] and preliminary results from our own dose-response studies in this specific strain of chick (Shavers).

Table 3.3: Agents employed in the present studies.

Drug	Source	Cat#	Amt/Injection (Syringe)
Atropine Sulfate	Sigma-Aldrich	A0257	240 nmoles
L-arginine•HCl	Sigma-Aldrich	A5006	60-6000 nmoles
D-arginine•HCl	Sigma-Aldrich	A2646	10 µmol
L-NIO	Sigma-Aldrich	I134	6 nmoles
L-NMMA (acetate)	Cayman Chemicals	10005031	6 nmoles
D-NMMA (acetate)	Cayman Chemicals	14186	6 nmoles
Sodium nitroprusside	Sigma-Aldrich	71778	10-1000 nmoles

Rationale for Drug Selection

L-arginine (L-Arg) increases intraocular NO by supplementing the endogenous L-Arg substrate for NOS, thus boosting NO-synthesis at local sources; in contrast, sodium nitroprusside (SNP) releases NO spontaneously and diffusely, without restriction to sites of local NO synthesis, release, and action. The best-known effect of these drugs is vasodilation caused by NO-activation of soluble guanylyl cyclase and subsequent cGMP-mediated smooth muscle relaxation[225,226]. However, we do not yet know enough about the role of NO in the retina to say whether these vasodilatory effects might underlie myopia prevention; it is not likely for the chick model, as the avian retina is avascular. N^G-(1-Iminoethyl)-L-ornithine (L-NIO), and L-N^G-monomethyl arginine (L-NMMA) are analogues of L-Arg, which (unlike L-NAME) are transported readily into nitrergic cells by the L-Arg transporter, bind to the active site of NOS, and competitively inhibit L-Arg binding and NO synthesis[224]. D-N^G-monomethyl arginine (D-NMMA), an enantiomer of L-NMMA, is arginine-like but has insignificant NOS-inhibiting activity, and is a negative control for the stereospecific action of L-NMMA at NOS. D-arginine serves a similar experimental role, acting as a negative control for L-Arg.

Calculation of ED_{50} for L-Arginine and SNP

The 50% effective dose (ED_{50}) for L-arg and SNP was calculated by graphing curve-fitted linear regressions of the mean ± SEM of the transformed molar concentration values from the L-arg and SNP dose-response studies (GraphPad Prism, Version 6.07, LaJolla, CA,

USA). Data were visualized as bar graphs instead of dose-response curves (**Figs. 3.2 & 3.3**) to emphasize the differences between the high, middle, and low drug doses, and to keep formatting consistent across FDM drug-studies.

Immunolabelling (LEP-100 & GRL2)

For detecting signs of damage by immunolabelling, we used two monoclonal mouse antibodies (both known to be specific for application to chicken tissues) from the Developmental Studies Hybridoma Bank (DSHB; University of Iowa, Ames, IA, USA): anti-LEP-100 (lysosomal membrane glycoprotein, cv24)[227] and anti-GRL2 (activated leukocyte cell-surface glycoprotein GRL2)[217], which are markers for microglia/macrophages[215,228] and activated phagocytes/granulocytes[229], respectively. Sections were warmed, washed (3 x 15 min in PBS with gentle shaking), and then incubated overnight at 25°C in LEP-100 (1:50) or GRL2 (1:500) antibodies, diluted in PBS + 0.025% Triton X-100. After incubation, the slides were washed in PBS and then incubated under 1:1000 AF488 donkey anti-mouse secondary antibody (Jackson ImmunoResearch Laboratories, Inc., West Grove, PA, USA) for 2 hrs. Slides were washed again in PBS, and mounted using Fluoroshield mounting medium + DAPI (Abcam Inc., Toronto, ON, Canada). LEP-100- and GRL2-labeled slides were imaged using a laser-scanning confocal microscope (Model FV1000; Olympus Corporation of the Americas, Center Valley, PA, USA) with a 40x oil-immersion objective (NA = 1.3). Image post-processing was performed using Adobe Photoshop CS5 (Adobe Systems Incorporated, San Jose, CA, USA).

Chapter 4: Alpha$_2$-Adrenoceptor Agonists Inhibit FDM in the Chick

Abstract

The putative "myopia-controlling" receptor is thought to be mAChR M_4, because MT3 can inhibit FDM in chicks at a far lower concentration than atropine (2.5 µM vs. 10 mM, respectively). These concentrations are still very high when considering the reported potency of these drugs for the M_4 receptor (pIC_{50}: MT3 = 8.79 versus atropine = 9.9)[162,230], and any drug can act at unintended targets when applied at high doses. Evidence suggests that atropine can interact with α-adrenoceptors (ADRAs) at concentrations ≥ 1 µM (in rat)[171,172], while MT3 has nearly equal inhibitory potency at mAChR M_4 as it does at α_{2A}-, α_{1A}-, and α_{1D}-adrenoceptors (human receptors)[162,163]. We tested the hypothesis that ADRAs are involved in eye growth by intravitreal injection of ADRA2 agonists clonidine (clon) and guanfacine (gfcn), and ADRA2A antagonist yohimbine (yoh).

The right eyes of chicks (age P7) were goggled with diffusers to induce FDM; left eyes served as controls. 20 µL of PBS, or 2, 20, or 200 nmoles clon, gfcn, or yoh was injected intravitreally on days P8, P10, and P12. On day P13, refractive error (RE) and axial length (AL), equatorial diameter (EQ), and wet weight (WW) were measured. Experimental procedures for the myopia-rescue paradigm were the same as above, but with the addition of goggle-removal immediately after injection of yoh for a period of 2 hrs. Control eyes were not affected by any treatment, so the interocular difference was taken as the measure of treatment effect (± SD; One-Way ANOVA).

For clon, 200 nmoles was the only dose that effectively inhibited FDM. All doses of gfcn significantly inhibited the negative refractive error, but only 20 & 200 nmoles significantly inhibited axial elongation. Yohimbine had no effect on FDM, but 200 nmoles partially inhibited emmetropization induced by goggle removal.

These data are the first to report that ADRA agonists can inhibit FDM at concentrations similar to those used for atropine. They were published previously in abstract form (Carr & Stell. IOVS 2016; 57: ARVO E-Abstract 4738), which led to an advisory position on a small pilot study investigating the effects of apraclonidine on myopia in children, in collaboration with Dr. Jaime Tejedor (Hospital Ramón y Cajal, Madrid, Spain).

Introduction

In this chapter, we begin to address the question of possible ocular receptor targets of mAChR antagonist-mediated myopia inhibition. There is significant evidence that atropine may not inhibit myopia through a mAChR-mediated mechanism[152]. Most mAChR antagonists do not inhibit myopia, in chicks, even very potent ones such as QNB, mepenzolate, or dicyclomine[159]. Significant changes in eye size do not result in significant changes in mRNA[144] or protein[164] expression of any mAChR subtype in the retina, nor do they result in changes in the concentration of retinal acetylcholine, or its metabolite choline[231]. Ablating over 90% of choline acetyltransferase (ChAT)-producing amacrine cells – the only known source of retinal ACh – has no effect on the eye's ability to achieve emmetropia, nor does it impair myopia-inhibition by atropine[223]. Results such as these have led to arguments that favour a non-retinal mechanism of atropine-mediated myopia inhibition, with mAChR binding in the choroid or sclera suggested as the most likely alternative. There is no change in mAChR mRNA or protein expression in the choroid or the sclera upon experimental induction of myopia[144,164] either, however, and although it has been shown that atropine can inhibit scleral glycosaminoglycan (GAG) synthesis *in vitro*, an extremely high concentration (10-100 μM) is required[232].

No drug is perfectly "specific" for a single receptor, and a primary consequence of application of high concentrations of drug is the increased risk of binding to "off-target" receptors, especially when thresholds of $\geq 10^{-7}$ M are surpassed. It is surprising, then, that there has been very little suggestion of possible non-mAChR targets of atropine-treatment of myopia, and even less research on this topic. As it stands, mAChR M_4 has been deemed the putative myopia-controlling receptor because mamba toxin 3 (MT3) is "highly specific" for mAChR M_4[233], and inhibits myopia (in chicks) at a much lower concentration than is required by atropine (2.5-10 μM[34,161] vs. 10 mM, respectively). While it is true that MT3 has inhibitory potency at the M_4-receptor (pIC_{50} = 8.79-9.08), that is not its only high-affinity target; at human receptors, it binds with equally high potency to α_{1A}- (pIC_{50} = 8.84-8.86), α_{1D}- (pIC_{50} = 7.88-8.13), and α_{2A}-adrenoceptors (pIC_{50} = 8.49-8.51), and with moderately-high potency to α_{1B}- (pIC_{50} = 7.57-7.68), α_{2C}- (pIC_{50} = 7.29-8.82), and mAChR M_1 (pIC_{50} = 6.22-6.71)[162,163]. It has been suggested that MT3 may be a non-competitive

(allosteric) inhibitor of α-adrenoceptors, and a competitive (orthosteric) inhibitor of M_4[163]. Because of the high activity of MT3 at α-adrenoceptors, I decided to test whether α_2-adrenoceptors agonists – clonidine and guanfacine – or antagonist – yohimbine – can affect FDM in chicks.

Results

Refractive error, eye biometrics, and statistical p-value data for all treatment groups are summarized in **Table 4.1**.

Effect of Clonidine on Form-Deprivation Myopia in Chicks

Data are represented as the means of the difference (d) in values for the experimental eye minus those for the control eye, ± SD, and are visualized in **Fig. 4.1**. Intravitreal clonidine (200 nmoles) significantly inhibited FD-induced refractive error, axial elongation, and increased equatorial diameter induced by goggle-wear compared to PBS controls (dRE: -2.2 ± 3.4 D vs. -12.0 ± 3.8 D, $p < 0.0001$, $n = 10$; dAL: 0.002 ± 0.2 mm vs 0.43 ± 0.2 mm, $p = 0.0004$, $n = 10$; dEQ: 0.21 ± 0.1 mm vs. 0.38 ± 0.2 mm, $p = 0.0495$, $n = 10$); there was no effect on overall wet weight of the eyes. For 2 nmoles and 20 nmoles clonidine, induced negative refractive error and axial length elongation were decreased compared to controls, but not significantly (2 nmoles: dRE: -10.7 ± 2.8 D, dAL: 0.31 ± 0.2 mm and 20 nmoles: dRE: -9.2 ± 2.0 D, dAL: 0.34 ± 0.2 mm; **Fig. 4.1**).

Figure 4.1: Effect of Clonidine on FDM in Chicks

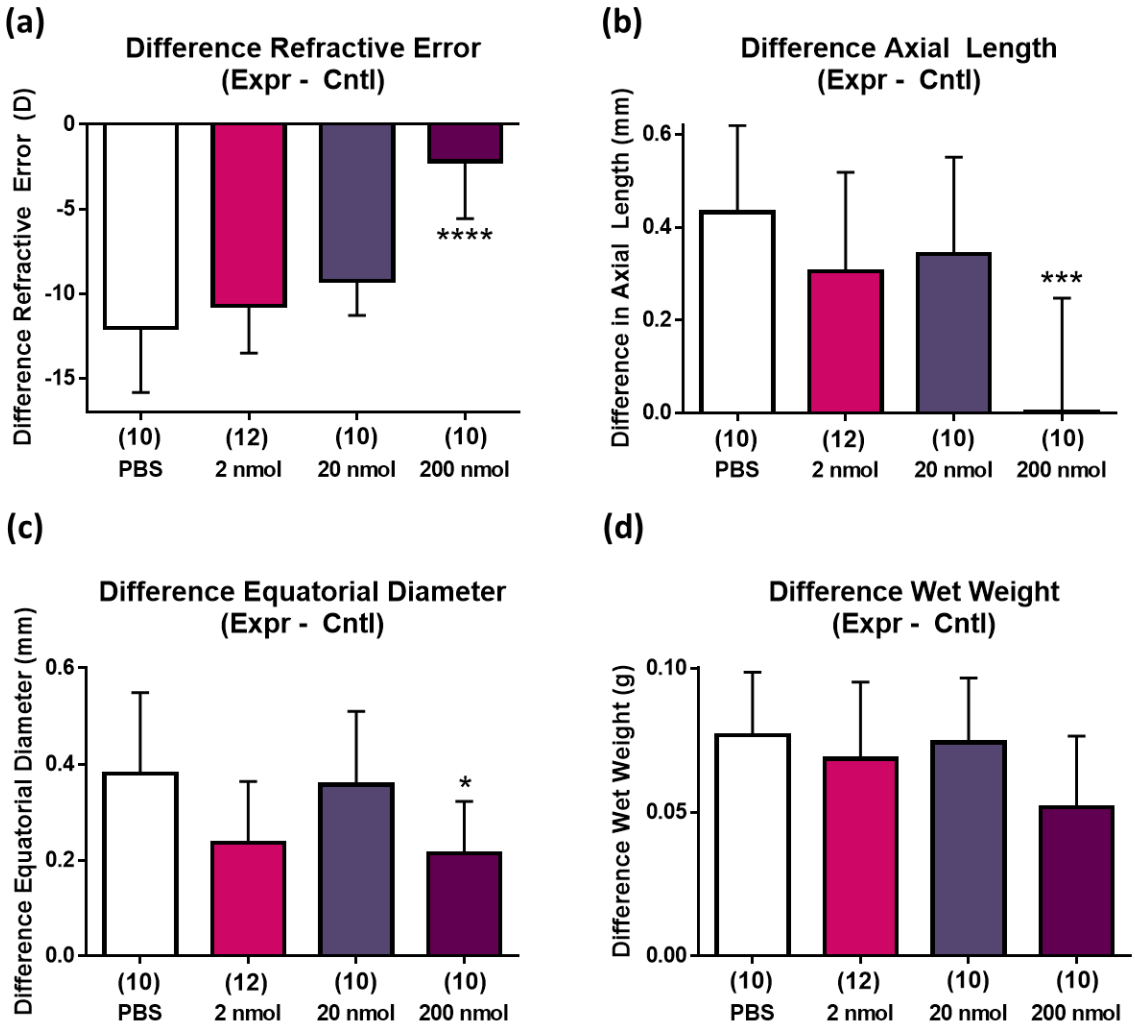

Figure 4.1: Effects of intravitreal injection of clonidine on FDM in chicks. 200 nmoles clonidine significantly inhibited the induced difference in refractive error (**a**), axial length (**b**), and equatorial diameter (**c**), but not wet weight (**d**) compared to PBS-controls. There was no significant effect of 2 or 20 nmoles clonidine-treatment. ***Statistics***: **** $p < 0.0001$, *** $p < 0.001$, * $p < 0.05$; One-Way ANOVA + Tukey's post-hoc. Data are represented as the means of the difference in values for the experimental eye minus those for the control eye, ± SD; sample sizes (n) are denoted in brackets below each column.

Effect of Guanfacine on Form-Deprivation Myopia in Chicks

Data are represented as the means of the difference (d) in values for the experimental eye minus those for the control eye, ± SD, and are visualized in **Fig. 4.2**. Intravitreal guanfacine (2, 20, and 200 nmoles) significantly inhibited FD-induced difference in refractive error compared to PBS-controls (PBS: -16.5 ± 1.7 D, n = 10; 2 nmoles: -9.8 ± 5.2D, p = 0.0004, n = 11; 20 nmoles: -8.6 ± 2.9 D, p < 0.0001, n = 12; 200 nmoles: -8.2 ± 3.0 D, p < 0.0001, n = 12), but only 20 and 200 nmoles significantly inhibited thr difference in axial elongation (PBS: 0.71 ± 0.16 mm, n = 10; 2 nmoles: 0.55 ± 0.27 mm, p = 0.3063, n = 11; 20 nmoles: 0.43 ± 0.16 mm, p = 0.0175, n = 11; 200 nmoles: 0.34 ± 0.20 mm, p = 0.0007, n = 12; **Fig. 4.2a,b**). There was no significant effect of guanfacine-treatment on difference in equatorial diameter or wet weight in any treatment group (**Fig. 4.2c,d**).

Figure 4.2: Effect of Guanfacine on FDM in Chicks

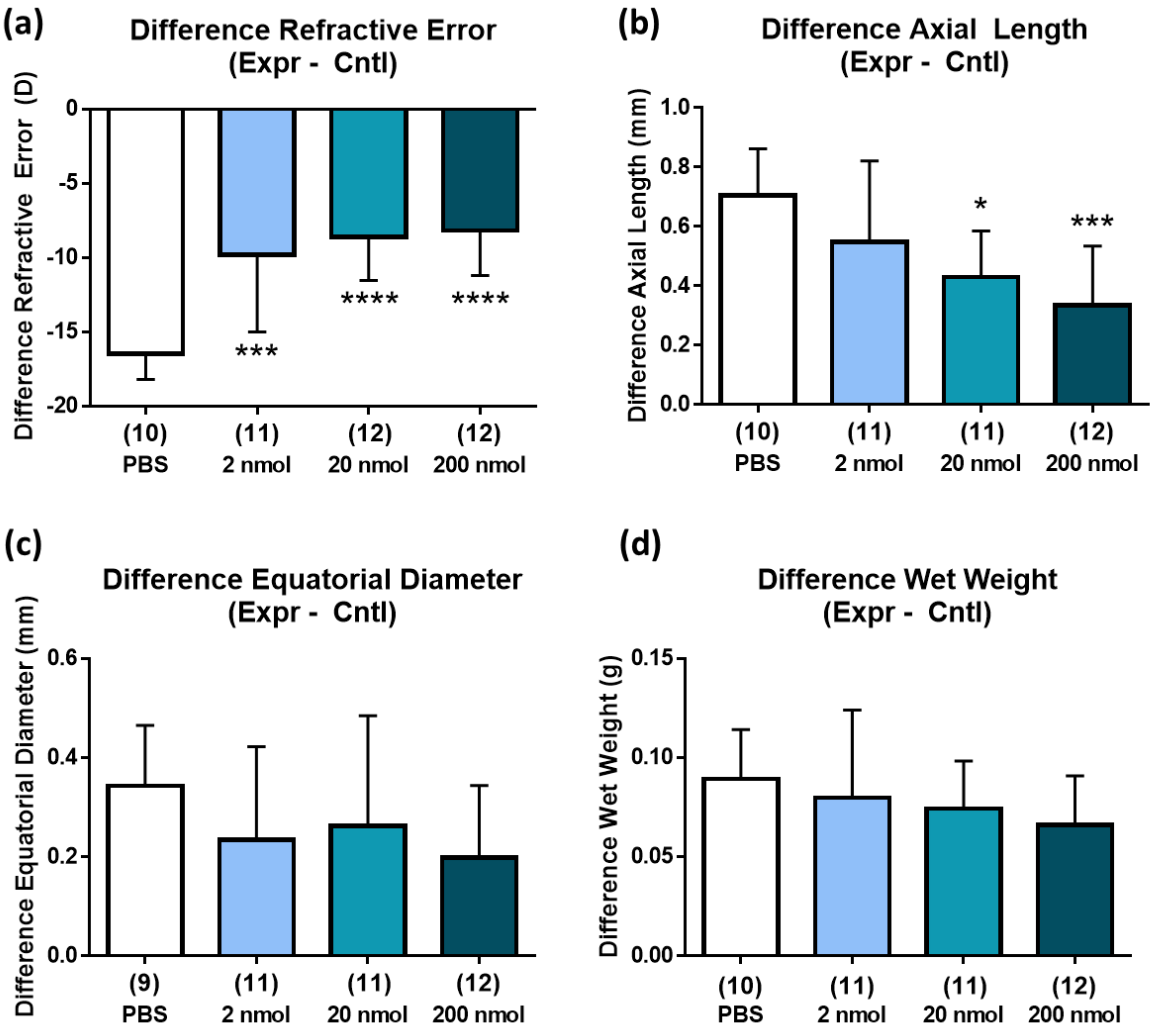

Figure 4.2: Effect of guanfacine (2, 20, and 200 nmoles) on FDM in chicks. All concentrations significantly inhibited the induced negative refractive error (**a**), but only 20 and 200 nmoles resulted in a significant reduction of axial length (**b**). There was no treatment effect on the difference in equatorial diameter (**c**) or wet weight (**d**). ***Statistics***: **** $p < 0.0001$, *** $p < 0.001$, * $p < 0.05$; One-Way ANOVA + Tukey's post-hoc. Data are represented as the means of the difference in values for the experimental eye minus those for the control eye, ± SD; sample sizes (n) are denoted in brackets below each column.

Effect of Yohimbine on Form-Deprivation Myopia in Chicks

Intravitreal injection of yohimbine had no significant effect on development of FDM in any treatment group (**Fig. 4.3**, n = 17-21). Goggle removal for > 2hrs/day can completely inhibit experimentally-induced FDM in chicks[35]; because ADRA2 agonism was successful in inhibiting FDM, and because it is expected that agonists and antagonists should have opposing effects on FDM, I decided to test whether antagonism with yohimbine could block inhibition of myopia mediated by clear vision.

Figure 4.3: Effect of Yohimbine on FDM in Chicks

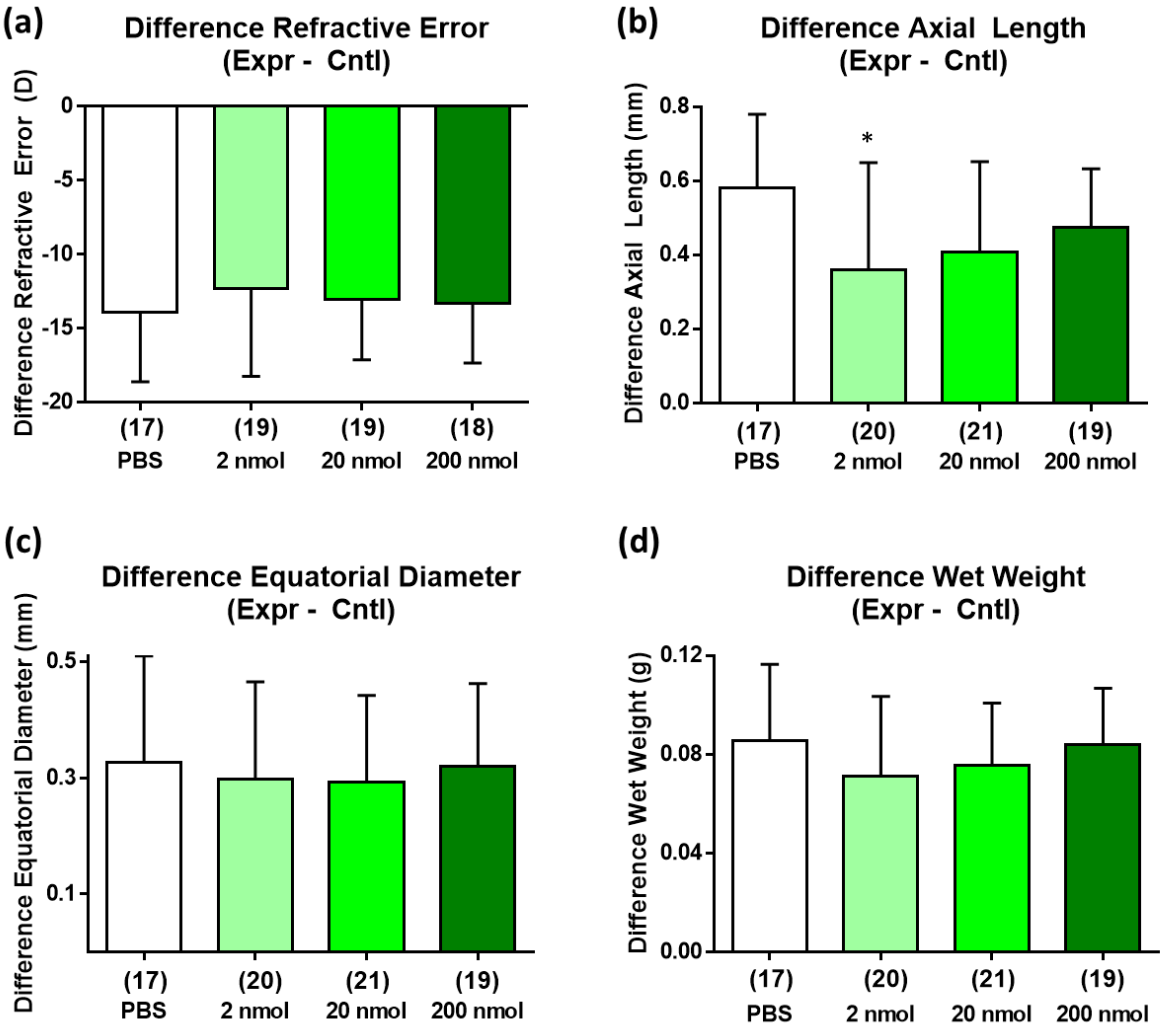

Figure 4.3: There was no significant effect of yohimbine-treatment (2, 20, or 200 nmoles) on the difference in refractive error (**a**), equatorial diameter (**c**), or wet weight (**d**) in form-deprived chick eyes; eyes treated with 2 nmoles yoh showed a small, but significant, decrease in axial length (**b**). ***Statistics***: * $p < 0.05$; One-Way ANOVA + Tukey's post-hoc. Data are represented as the means of the difference in values for the experimental eye minus those for the control eye, ± SD; sample sizes (n) are denoted in brackets below each column.

Effect of Yohimbine on Prevention of FDM by Goggle-Removal in Chicks

Yohimbine-treatment (200 nmoles) resulted in partial blockade of emmetropization induced by clear vision compared to PBS-controls (PBS: -4.53 ± 1.2 D; 200 nmoles: -7.90 ± 3.3 D, $p = 0.0341$, $n = 10$). This trend was paralleled in the axial length measurements, but results were not significant most likely due to high variability of axial length in the PBS-controls (**Fig. 4.4**). Lower concentrations (2 and 20 nmoles) had no significant effect. These results are promising, but further replication is required.

Figure 4.4: Effect of Yohimbine on Myopia-Prevention by Goggle-Removal in Chicks

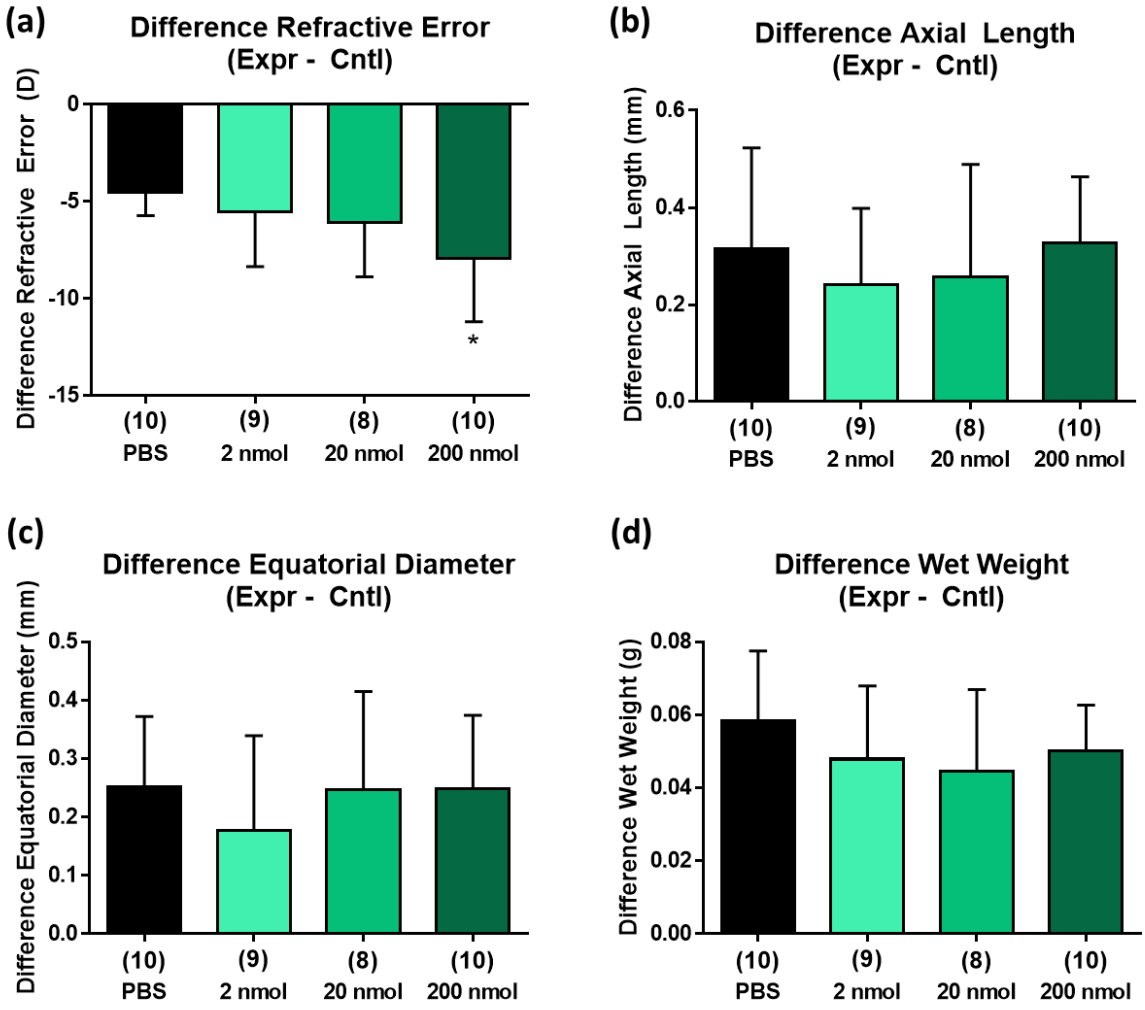

Figure 4.4: The effect of yohimbine on myopia recovery induced by goggle-removal in chicks. There was a small, but significant blockade of myopia recovery as measured by refractive error compared to PBS-controls (**a**), but there was no significant effect on axial elongation (**b**), equatorial diameter (**c**), or wet weight of eyes (**d**). ***Statistics***: * $p < 0.05$; One-Way ANOVA + Tukey's post-hoc. Data are represented as the means of the difference in values for the experimental eye minus those for the control eye, ± SD; sample sizes (n) are denoted in brackets below each column.

Table 4.1: Summarized data for all experiments performed. Number of replicates and statistical p-values ($p < 0.05$ in bold) are listed below treatment outcomes.

Clon	**PBS (n)**	**2 nmoles (n, p-value vs. PBS)**	**20 nmoles (n, p-value vs. PBS)**	**200 nmoles (n, p-value vs. PBS)**
dRE	-12.0 ± 3.8 D (10)	-10.7 ± 2.8 D (10, p = 0.7475)	-9.2 ± 2.0 D (12, p = 0.1895)	-2.2 ± 3.4 D (10, **p < 0.0001**)
dAL	0.43 ± 0.19 mm (10)	0.31 ± 0.21 mm (12, p = 0.5178)	0.34 ± 0.21 mm (10, p = 0.7847)	0.002 ± 0.24 mm (10, **p = 0.0004**)
dEQ	0.38 ± 0.17 mm (11)	0.24 ± 0.13 mm (12, p = 0.0856)	0.35 ± 0.15 mm (10, p = 0.9821)	0.21 ± 0.11 mm (10, **p = 0.0495**)
dWW	0.0766 ± 0.022 g (10)	0.0684 ± 0.027 g (12, p = 0.8579)	0.0741 ± 0.022 g (10, p = 0.9956)	0.0517 ± 0.025 g (10, p = 0.1147)

Gfcn	**PBS (n)**	**2 nmoles (n, p-value vs. PBS)**	**20 nmoles (n, p-value vs. PBS)**	**200 nmoles (n, p-value vs. PBS)**
dRE	-16.5 ± 1.7 D (10)	-9.8 ± 5.2 D (11, **p = 0.0004**)	-8.6 ± 2.9 D (12, **p < 0.0001**)	-8.2 ± 3.0 D (12, **p < 0.0001**)
dAL	0.71 ± 0.16 mm (10)	0.55 ± 0.27 mm (11, p = 0.3063)	0.43 ± 0.16 mm (11, **p = 0.0175**)	0.34 ± 0.20 mm (12, **p = 0.0007**)
dEQ	0.34 ± 0.12 mm (9)	0.23 ± 0.19 mm (11, p = 0.5137)	0.26 ± 0.22 mm (11, p = 0.7319)	0.20 ± 0.15 mm (12, p = 0.2569)
dWW	0.0892 ± 0.025 g (10)	0.0798 ± 0.044 g (11, p = 0.8971)	0.0744 ± 0.024 g (11, p = 0.6890)	0.0659 ± 0.025 g (12, p = 0.3032)

Yoh (FDM)	**PBS (n)**	**2 nmoles (n, p-value vs. PBS)**	**20 nmoles (n, p-value vs. PBS)**	**200 nmoles (n, p-value vs. PBS)**
dRE	-13.9 ± 4.7 D (17)	-12.3 ± 5.9 D (19, p = 0.7537)	-13.1 ± 4.0 D (19, p = 0.9523)	-13.3 ± 4.0 D (18, p = 0.9837)
dAL	0.58 ± 0.20 mm (17)	0.36 ± 0.29 mm (20, **p = 0.0247**)	0.41 ± 0.24 mm (21, p = 0.1102)	0.47 ± 0.15 mm (19, p = 0.5291)
dEQ	0.33 ± 0.18 mm (17)	0.30 ± 0.17 mm (20, p = 0.9411)	0.29 ± 0.15 mm (21, p = 0.9137)	0.32 ± 0.14 mm (19, p = 0.9987)
dWW	0.0855 ± 0.031 g (17)	0.0710 ± 0.032 g (20, p = 0.4019)	0.0754 ± 0.025 g (21, p = 0.6852)	0.0840 ± 0.023 g (19, p = 0.9983)

Yoh (Recovery)	**PBS (n)**	**2 nmoles (n, p-value vs. PBS)**	**20 nmoles (n, p-value vs. PBS)**	**200 nmoles (n, p-value vs. PBS)**
dRE	-4.5 ± 1.2 D (10)	-5.5 ± 2.8 D (9, p = 0.8397)	-6.1 ± 2.8 D (8, p = 0.6107)	-7.9 ± 3.3 D (10, **p = 0.0341**)
dAL	0.32 ± 0.21 mm (10)	0.24 ± 0.16 mm (9, p = 0.8203)	0.26 ± 0.23 mm (8, p = 0.9077)	0.33 ± 0.14 mm (10, p = 0.9986)
dEQ	0.25 ± 0.12 mm (10)	0.18 ± 0.16 mm (9, p = 0.6756)	0.25 ± 0.17 mm (8, p = 0.9999)	0.25 ± 0.13 mm (10, p > 0.9999)
dWW	0.0583 ± 0.019 g (10)	0.0479 ± 0.020 g (9, p = 0.6237)	0.0445 ± 0.022 g (8, p = 0.4167)	0.0500 ± 0.013 g (10, p = 0.7545)

Discussion

The data presented here provide the first evidence of inhibition of FDM by clonidine and guanfacine in the chick. It also seems that yohimbine might inhibit myopia-rescue by clear vision, though further investigation is required. The concentration required by these ligands to cause changes in development of FDM and myopia recovery do not differ significantly from those of atropine, however, so we cannot attribute their ability to modulate changes in eye size specifically to α_2-adrenoceptors.

The results from these studies are representative of a central fallacy in the myopia-research field – i.e., that the results from high-concentration drug treatments (≥ 1 mM) can be attributed to a specific receptor or system in the eye. It is possible that the requirement for high concentration drug *in vivo* could be due to factors other than non-specific drug interactions, such as loss of drug due to diffusion through the vitreal fluids or choroidal blood supply, binding of the drug to free-floating proteins that are abundant in the vitreous body, or anatomical impediments to drug access to the target cells/receptors such as the blood-retina barrier or slow diffusion through the gel-like vitreous body. Results obtained by high concentration drug *in vitro*[44,232] cannot be explained by mechanisms such as these, however, and non-specific ligand binding is the more likely explanation. *In vivo* studies investigating the distribution of radioactively-labelled ligands after intravitreal injection found that the concentration of [^{3}H]-spiperone in the retina was 25% of that in the original injection at time points ≤ 30 min, and 8% at 1-24 hrs[112]. Another study investigating the distribution of [^{3}H]-pirenzepine after intravitreal injection yielded similar results; drug levels peaked at 1 hr (6% in the retina, 1.5% in the choroid, and 2.5% in the sclera), and the distribution of [^{3}H]-pirenzepine remained similar to peak levels even after 24 hrs (3.6% in the retina, 2.6% in the choroid, and 0.6% in the sclera)[234]. Thus, a concentration of 2 nmoles (100 µM) at the lowest level of distribution in ocular tissues would approach, but still be above, the theoretical threshold for "certain specificity" (retina = 6 µM, choroid = 1.5 µM, sclera = 600 nM).

If we cannot attribute the effects of high concentration drug (clonidine, guanfacine, atropine) to a specific receptor or system, what is the point of performing these types of

experiments? For one, they allow us to test the possible downstream signalling mechanisms of these treatments. Studies by others have indicated an important role of dopamine in myopia-inhibition by ligands such as atropine[116] – which causes an increase in synthesis and release of retinal dopamine – and MT3[203] – whose myopia inhibiting effect is blocked by simultaneous injection of the D_2-type antagonist spiperone (5 nmoles). Although the effect of the myopia-inhibiting drug may be non-selective, we can still block those effects using drug concentrations that are more likely to be acting at their intended targets. In **Chapter 3**, we showed that myopia inhibition by atropine (240 nmoles) is blocked by simultaneous injection of a nitric oxide synthase inhibitor (L-NIO or L-NMMA; 6 nmoles)[1] (and Carr & Stell. IOVS 2016; 57: ARVO E-Abstract 4738).

Myopia-inhibition using high-concentration drug may also be able to tell us about whether there may be multiple emmetropia-regulating pathways in the eye. Strange results have been obtained while investigating the effects 6-hydroxydopamine (6-OHDA), a catecholamine-specific toxin, on form-deprivation and lens-induced experimental myopia. In the chick, a single intravitreal injection of 6-OHDA is sufficient to block FDM, but it has no effect on LIM[33,235,236]. This led the authors to suggest that perhaps there are multiple growth-controlling pathways in the chick retina[33,237]. While the role of accommodation in control of eye growth has been shown to be less important than previously thought[151,238], it still may be possible that multiple pathways exist, and that they may involve reciprocal signalling between retinal dopaminergic and adrenergic systems. It has been demonstrated that retinal α_2-adrenoceptors may regulate the activity of tyrosine hydroxylase (TH) – the rate limiting enzyme in dopamine synthesis[239]. Intraperitoneal (i.p.) and intravitreal injection (i.i.) of yohimbine (i.p: 3.2 µmoles; i.i: 2 nmoles) in dark-adapted rats resulted in an increase in TH activity. This effect was partially antagonized by simultaneous administration of clonidine (7.5 µmoles), which by itself had no effect on TH activity in dark-adapted rats. When yohimbine was administered at light onset, it caused increased TH activity, and this effect was again partially antagonized by clonidine, which by itself caused a decrease in TH activity when applied at light onset. Application of apomorphine (4.1 µmoles) at light onset had no effect on TH activity; thus, the authors concluded that the effects of clonidine and yohimbine were not entirely the result of non-specific binding

to dopamine D_2 receptors, but mediated by a combination of α_2-adrenoceptor- and D_2-related mechanisms. Results similar to these have been observed in the prefrontal cortex (pFC) of rats. Norepinephrine can bind to D_2-like receptors with high affinity[240-242], and treatment with ADRA2 agonist clonidine results in decreased extracellular dopamine, while ADRA2 antagonism causes an increase in extracellular dopamine[243-246]. Modulation of α_2-adrenoceptors by dopamine has also been reported in smooth muscle strips taken from the guinea pig fundus, where dopamine may antagonize cholinergic-induced muscle contractions through an α_2-adrenoceptor mediated mechanism[247].

The finding that high-dose clonidine and guanfacine inhibit FDM, while yohimbine may inhibit myopia rescue by unobscured vision, produces more questions than answers. The literature supports the hypothesis that clonidine and guanfacine should exacerbate or have no effect on FDM, and that yohimbine should inhibit it. Possibly our results could have arisen via a significant species-difference in the way dopamine affects retinal visual processing in rats (rod-dominated) and chicks (cone-dominated). In support of this hypothesis, there is some evidence to suggest that although increased retinal dopamine inhibits myopia in both chick and guinea pig models, it may do so through action at different dopamine receptors (D_2 in chick[112], and D_1 in guinea pig[106]). Although there is precedent for modulation of dopaminergic signalling in the retina by α_2-adrenoceptors, it would be naïve at this point to attribute the anti-myopia effects of clonidine and guanfacine seen here to ADRA2s specifically. More likely, is that non-specific or even toxic effects of clonidine on FDM are responsible; only the highest dose was effective in inhibiting FDM (200 nmoles), while doses that more closely matched those used in previous experiments[239] (2 nmoles, 20 nmoles) were ineffective. In the case of guanfacine, the lower two doses did have a significant effect on refractive error, so it is more difficult to explain why, if these drugs were working through α_2-adrenoceptors, we would end up with results that were the opposite of those that were hypothesized. Much more experimentation is required. We need to show that myopia-inhibition by these drugs is not due to toxicity, by allowing treated eyes to emmetropize normally after goggle removal, and we need to repeat the yohimbine ungoggling experiments to determine whether the results are valid. Finally, it would be interesting to test whether lower concentration clonidine and guanfacine injection before

goggle-removal would block the myopia-inhibiting effects of unobscured vision. There is strong evidence that retinal dopamine is integral in this process[108], and if previously reported results are true, I would hypothesize that clonidine-treatment should reduce TH activity upon onset of "activating" stimuli, such as light onset[45] or removal of deprivation goggles.

Atropine-treatment to combat myopia is far from perfect, and there are many side-effects that limit its acceptance as a valid therapy. If we could determine where atropine acts – its target tissue or receptor – then we could possibly decrease the amount of drug required to inhibit myopia, and eliminate serious side-effects. The data presented in this chapter are far from proving that ADRAs are a valid target receptor for anti-myopia therapies. They provide yet another class of drugs that can inhibit myopia at high concentration, and in doing so support the argument that we should not be so carefree in attributing the effects of high concentration drug to a specific system.

Methods

The animal ethics statement and common methods for induction of FDM, intravitreal injections, eye biometric measurements, statistical analysis, and preparation of eye tissues for Toluidine blue staining are described previously in **Chapter 2**. Chicks used in these experiments were of Shaver and Bovan strains (Rochester Hatchery, Westlock, AB).

Drugs for Intravitreal Injection

Drugs, commercial sources, and the molar amounts delivered per injection are listed in **Table 4.2**. Drugs were dissolved in phosphate-buffered saline (PBS) (Gibco 14190-144; ThermoFisher Scientific) at room temperature; yohimbine and guanfacine required gentle heating to dissolve fully at the highest concentration (200 nmoles). Solutions were made fresh for each set of injections. Concentrations tested were based on a log dose range of those required for atropine-mediated myopia inhibition.

Table 4.2: Agents employed in the present studies.

Drug	Source	Cat#	Amt/Injection (Syringe)
Clonidine•HCl	Sigma-Aldrich	C7897	2, 20, 200 nmoles
Guanfacine•HCl	Sigma-Aldrich	G1043	2, 20, 200 nmoles
Yohimbine•HCl	Sigma-Aldrich	Y3125	2, 20, 200 nmoles

Rationale for Drug Selection

Clonidine and guanfacine are α_2-adrenoceptor agonists, but clonidine does have known action at imidazoline receptors as well. Despite the action of clonidine at imidazoline receptors, it was chosen because it is one of the most common α_2-adrenoceptor agonists used, and there is precedent for neuroprotective and TH-regulating effects of clonidine in the retina (in rats)[183,184,239]. Guanfacine was chosen because is has a higher specificity for the α_{2A}-adrenoceptor subtype, and less activity at imidazoline receptors. Clonidine and guanfacine have also been used to induce sleepiness and tonic immobility in chicks[248-251], and I observed that chicks injected intravitreally with clonidine and guanfacine in my experiments were dozy compared to the saline-injected controls. Yohimbine was chosen as the antagonist because it is water soluble, thus has a lower risk of precipitating once injected into the vitreous, and has higher affinity for the α_2-adrenoceptor subtype. Previously reported affinities for clonidine and yohimbine at human and chicken receptors are recorded in **Table 5.2**, but I was unable to find affinity binding data for guanfacine in avian tissues.

Chapter 5: Myopia-Inhibiting Muscarinic Receptor Antagonists Also Block Signalling through Alpha$_{2A}$-Adrenoceptors

Abstract

Although atropine is a potent muscarinic acetylcholine receptor (mAChR) antagonist, it may inhibit myopia through non-mAChR means[152]. There is evidence that atropine may act at α-adrenoceptors[171,172], and the most potent myopia-inhibiting ligand found to date (MT3) has nearly equal affinity at human mAChR M_4, α_{1A}- and α_{2A}-adrenoceptors[162,163].

Human M_4 (M_4), chicken M_4 (cM_4), or human α_{2A}-adrenoceptor (hADRA2A) clones were transiently co-transfected with cAMP response element luciferase vector (CRE-Luc) and constitutively active *Renilla* luciferase vector (RLuc) into HEK293T cells. The ability of increasing concentrations of antagonist (ATR: atropine, MT3: mamba toxin 3, HIM: himbacine, PRZ: pirenzepine, TRP: tropicamide, OXY: oxyphenonium, QNB; DIC: Dicyclomine & MEP: Mepenzolate) to inhibit agonist-induced CRE-Luc expression was measured using the Dual-Glo® Luciferase Assay System (Promega). Normalized data were graphed as curve-fitted log dose-responses and pIC_{50} values were obtained from nonlinear regression analysis.

Relative pIC_{50} at M_4/cM_4 were as follows: QNB (9.94/9.51) > ATR (9.41/9.15) ≤ OXY (9.40/9.25) > MEP (8.85/8.45) > HIM (7.98/8.25) > DIC (7.82/7.39) > PRZ (7.63/7.31) > TRP (6.81/6.61); antagonist potencies at M_4 compared to cM_4 were not significantly different *with the exception* of MT3 (8.08/6.35, $p<0.0001$, unpaired t-test, two tailed). At hADRA2A, calculated pIC_{50}s were MT3 (7.81) > HIM (4.78) > ATR (4.34) > QNB (3.58) = OXY (3.33) > MEP (3.10) = PRZ (3.062) > TRP (2.83); DIC had no effect.

We confirmed high affinity of MT3 at hADRA2A and mAChR M_4, and showed that mAChR antagonists can affect hADRA2A signalling when applied in high concentrations. pIC_{50} data for these ligands at hADRA2A, but not M_4/cm_4, correlate well with their reported abilities to inhibit FDM in chicks[159], and there is a significant difference in the affinity of MT3 at M_4 compared to cM_4. This data has been accepted for publication in abstract form (Carr BJ et al. IOVS 2017; ARVO E-Abstract © ARVO; in press).

Introduction

As myopia prevalence continues to rise, so does the need for an effective therapy. Atropine can inhibit myopia in children[153], but it has significant mAChR M_3-mediated side effects – mydriasis, photophobia, and loss of accommodation due to paralysis of the ciliary muscle – which are severe enough to prevent FDA approval in North America. Because atropine is a mAChR antagonist, it is *assumed* that it prevents myopia through a mAChR-mediated action. It has been suggested that mAChR M_4 must be the myopia-controlling receptor because "highly-specific" mAChR antagonists himbacine and mamba toxin 3 (MT3), which have selectivity for M_4 mAChR over other mAChR subtypes[160,233], inhibit myopia in the chick at far lower concentrations than are required by atropine. A conclusive link between mAChR systems in the eye and atropine-mediated inhibition of myopia has never been demonstrated. There is significant evidence to support the possibility that myopia inhibition may not involve mAChRs at all[152]. High-concentration atropine is required to prevent myopia (0.1-10 mM), even though it has a very high affinity for mAChRs (pK_i = 9.6-9.9; 125-250 pM)[252,230], and just because himbacine can inhibit myopia at grossly excessive concentrations (ED_{50} = 190 mM)[160] and MT3 can inhibit myopia at greatly reduced concentrations compared to atropine (2.5-10 μM)[161], it does not mean that they do so through mAChR M_4. Applying drugs at a concentration greater than 10^{-7} M will most certainly result in off-target effects, no matter the "selectivity" profile of that drug; the reported ED_{50} of himbacine for myopia inhibition exceeds this threshold by 190,000x. In addition, just because a ligand is "selective" for a certain receptor in a given class, it does not mean that the ligand will not bind freely to receptors outside of that class. MT3 is a perfect example of this, because even though it is touted as being "highly specific" for mAChR M_4, it is in fact quite promiscuous. Studies on its binding behavior at human receptors have shown that it also has a high potency at α_{1A}- and α_{2A}-adrenergic receptors (pK_i: M_4 = 8.79 ± 0.06/9.08 ± 0.02, α_{1A} = 8.86 ± 0.14/8.84 ± 0.02, α_{2A} = 8.49 ± 0.06/8.51 ± 0.3), moderate potency at α_{1B}- and α_{2C}-adrenergic receptors (α_{1B} = 7.57 ± 0.22/7.68 ± 0.02, α_{2C} = 7.29 ± 0.13/8.82 ± 0.2), and low potency at mAChR M_1 (6.71 ± 0.14/6.22 ± 0.04)[162,163]. There is some speculation that atropine may also have antagonist activity at α-adrenergic receptors[171,172], although the specific subtypes ($\alpha_{1A,B,C}$ or $\alpha_{2A,B,C}$) to which it may bind remain unknown.

Chicks are a popular animal model for myopia drug studies; they are inexpensive and docile, have large eyes for easy drug delivery, and results from chick experiments can usually be replicated in mammals and non-human primates. There have been relatively few studies on the binding of most mAChR antagonists to muscarinic receptors in avian tissues, and chick retinal structure and receptor proteins can be significantly different from those of mammals. For example, chickens lack a mAChR M_1 orthologue; instead they have cM_2 receptors with an M_1-like high affinity for pirenzepine[142]. Thus, although chickens may be a very useful model organism for determining whether a drug will prevent myopia, they may be less useful when attempting to determine the mechanism through which myopia-inhibiting drugs work. Experiments utilizing most mAChR antagonists to prevent FDM in the chick are based only on the *assumption* that these ligands work the same way at avian receptors as they do at human receptors. When non-selective drugs such as atropine are used, species differences are likely not a significant problem, as receptor orthosteric binding sites are highly conserved between receptors and species. Instead, species-differences become a more significant factor as more selective or allosteric ligands (such as MT3) are utilized; allosteric binding sites are generally much less conserved than orthosteric sites (which aids in selectivity of drugs), and substitution of even a single amino acid can have a significant impact on ligand-receptor binding characteristics[253].

To investigate further possible mechanisms of mAChR antagonist-mediated myopia inhibition, we decided to test whether mAChR antagonists have similar functional characteristics at chicken and human mAChR M_4, and whether they can bind to, and inhibit signalling by, α_{2A}-adrenoceptors. We hypothesized that (i) there will be little correlation between potency of mAChR antagonists at M_4 and cM_4 and their ability to inhibit myopia, and (ii) that drugs that prevent FDM will have significant activity at α_{2A}-adrenergic receptors, while drugs that do not inhibit myopia will have no discernable binding at α_{2A}-adrenergic receptors. We chose to investigate the binding of mAChR antagonists to α_{2A}-adrenoceptors because MT3 has a high affinity to these receptors, and α_2 agonists – clonidine and guanfacine – inhibit FDM in the chick (Carr & Stell. IOVS 2016; 57: ARVO E-Abstract 4738; **Chapter 4**).

Results

Human mAChR M_4 (M_4)

Carbachol (CCh)-treatment of transiently-transfected cells resulted in an increased induction of CRE-Luc (maximum 87-fold increase) with a pED_{50} = 5.25; 10 µM was selected as the fixed-agonist concentration, as it resulted in a submaximal induction of CRE-Luc (ca. 80% of maximum response). Ranked relative pIC_{50} values of mAChR antagonists from highest to lowest potency were QNB (9.94 ± 0.03) > Atropine (9.41 ± 0.05) ≥ Oxyphenonium (9.40 ± 0.04) > Mepenzolate (8.85 ± 0.03) > MT3 (8.08 ± 0.08) > Himbacine (7.98 ± 0.08) > Dicyclomine (7.82 ± 0.11) > Pirenzepine (7.63 ± 0.07) > Tropicamide (6.81 ± 0.05) (**Fig. 5.1**; n = 3-4 duplicates). Inhibitory constants, estimated from these data by the method of Cheng & Prusoff ($IC_{50}/([A]/EC_{50})$; $pK_i(CP)$)[254], are in good agreement with previously published affinity binding data (pK_i) of these ligands at either human M_4 receptor or mammalian tissues (**Table 5.1**), and demonstrate a high variability of potency for different mAChR antagonists at the M_4 receptor in our system.

Figure 5.1: mAChR Antagonism at Human M_4
(n = 3-4, duplicates)

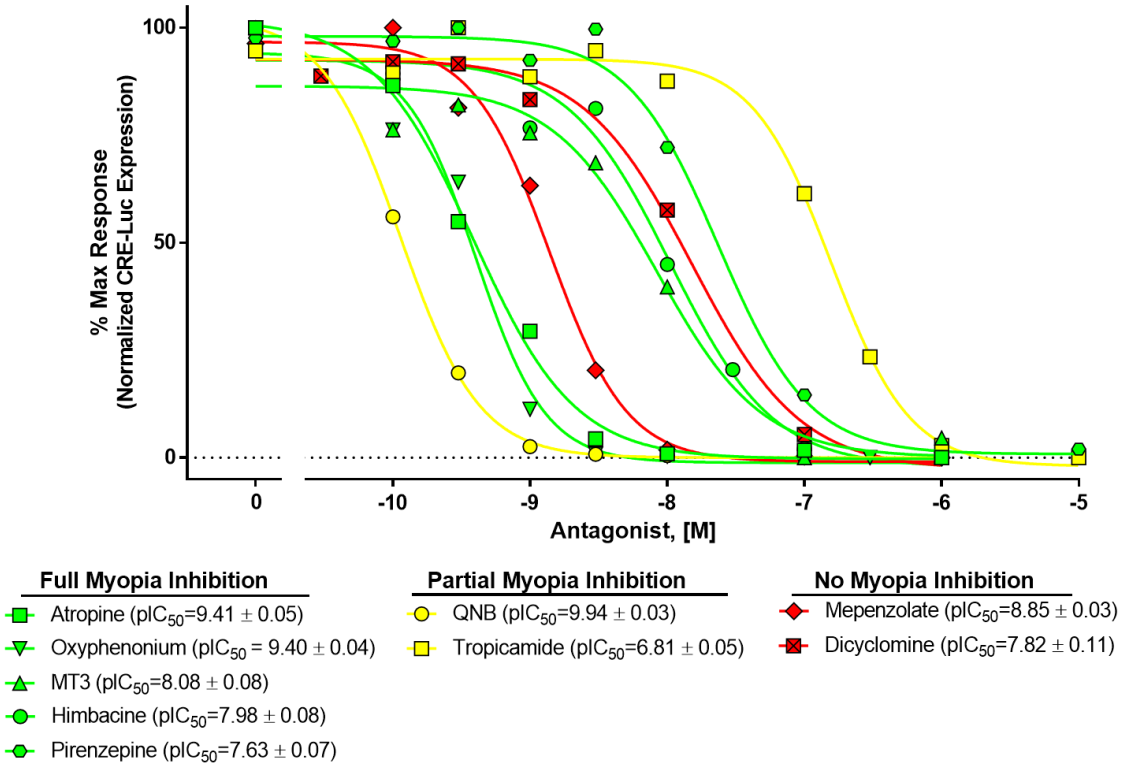

Figure 5.1: Inhibitory potencies of various mAChR antagonists at the human M_4 receptor. Antagonists are categorized into full myopia inhibition (green), partial myopia inhibition (yellow), and no myopia inhibition (red) according to previously published research[159-161]. Under each category, antagonists are ranked in descending order from most to least potent in our receptor assay (pIC_{50} ± SEM).

Chicken mAChR M_4 (cM_4)

CCh-treatment resulted in an increased induction of CRE-Luc (maxiumum 287-fold increase) similar to results reported previously[220], with a $pED_{50} = 5.72$; 10 µM was chosen as the fixed concentration as it gave a submaximal activation of CRE-Luc induction (ca. 90% of maximum response). The behavior of antagonists at the cM_4 receptor did not mimic perfectly their behavior at human M_4. Ranked relative pIC_{50} values from highest to lowest potency were QNB (9.51 ± 0.03) > Oxyphenonium (9.25 ± 0.05) > Atropine (9.15 ± 0.07) > Mepenzolate (8.45 ± 0.07) > Himbacine (8.25 ± 0.07) > Dicyclomine (7.39 ± 0.10) > Pirenzepine (7.31 ± 0.11) > Tropicamide (6.61 ± 0.10) > MT3 (6.35 ± 0.12) (**Fig. 5.2**; n = 3-4 duplicates). These data are the first to provide functional IC_{50} values for all drugs tested in the avian model, the first to investigate drug-receptor relationships for oxyphenonium, mepenzolate, and MT3 in the avian model, and the first to investigate binding behavior of dicyclomine and tropicamide at the cM_4 receptor. The IC_{50} data for atropine, QNB, and pirenzepine are in good agreement with previously published K_i values obtained by utilizing the same receptor clone[142,255] (**Table 5.1**). Although most drugs acted similarly at the cM_4 receptor as they did at the M_4 receptor, MT3 in particular contradicted the assumption that drug affinity remains the same between species, as it was 56-times more potent at M_4 than at cM_4 ($pIC_{50} = 8.08 \pm 0.08$ vs. 6.35 ± 0.12, respectively; **Fig. 5.3**).

Figure 5.2: mAChR Antagonism at Chicken cM_4
(n = 3-4, duplicates)

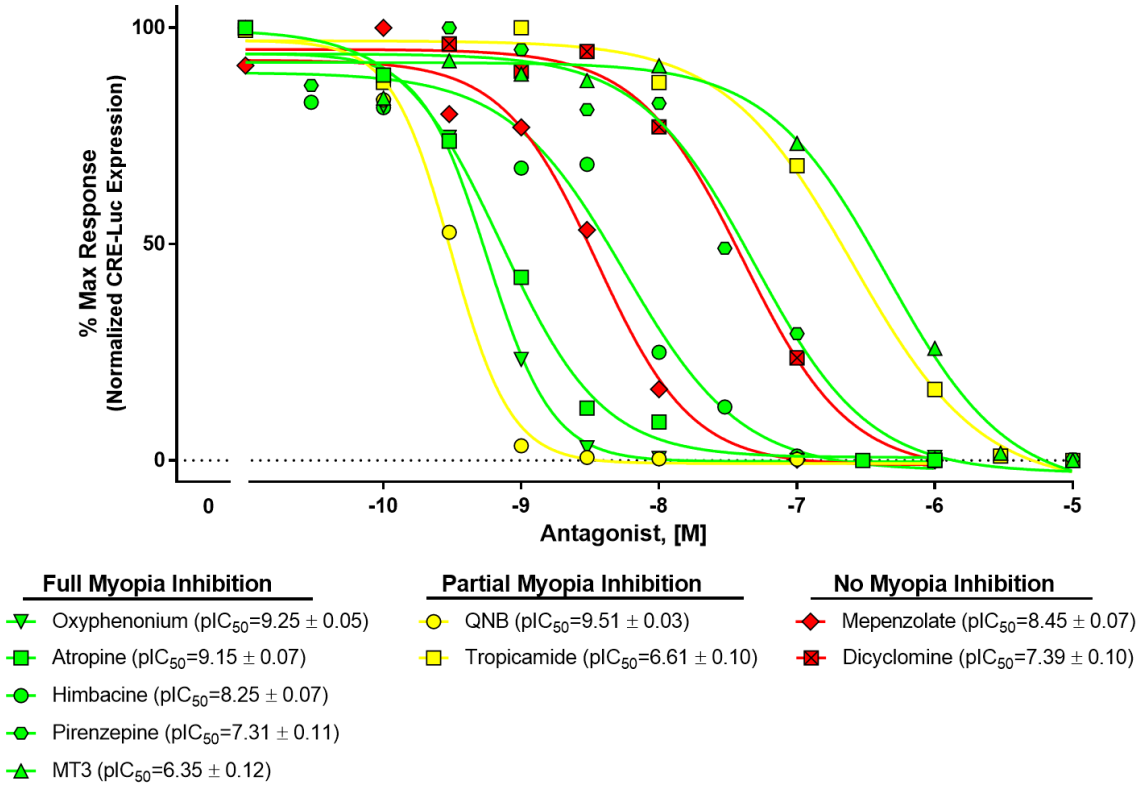

Figure 5.2: Inhibitory potencies of various mAChR antagonists at the chicken cM_4 receptor. Antagonists are categorized into full myopia inhibition (green), partial myopia inhibition (yellow), and no myopia inhibition (red) according to previously published research[159-161]. Under each category, antagonists are ranked in descending order from most to least potent in our receptor assay (pIC_{50} ± SEM).

Figure 5.3: mAChR Antagonism at Human M_4 Versus Chicken cM_4 (n = 3-4, duplicates)

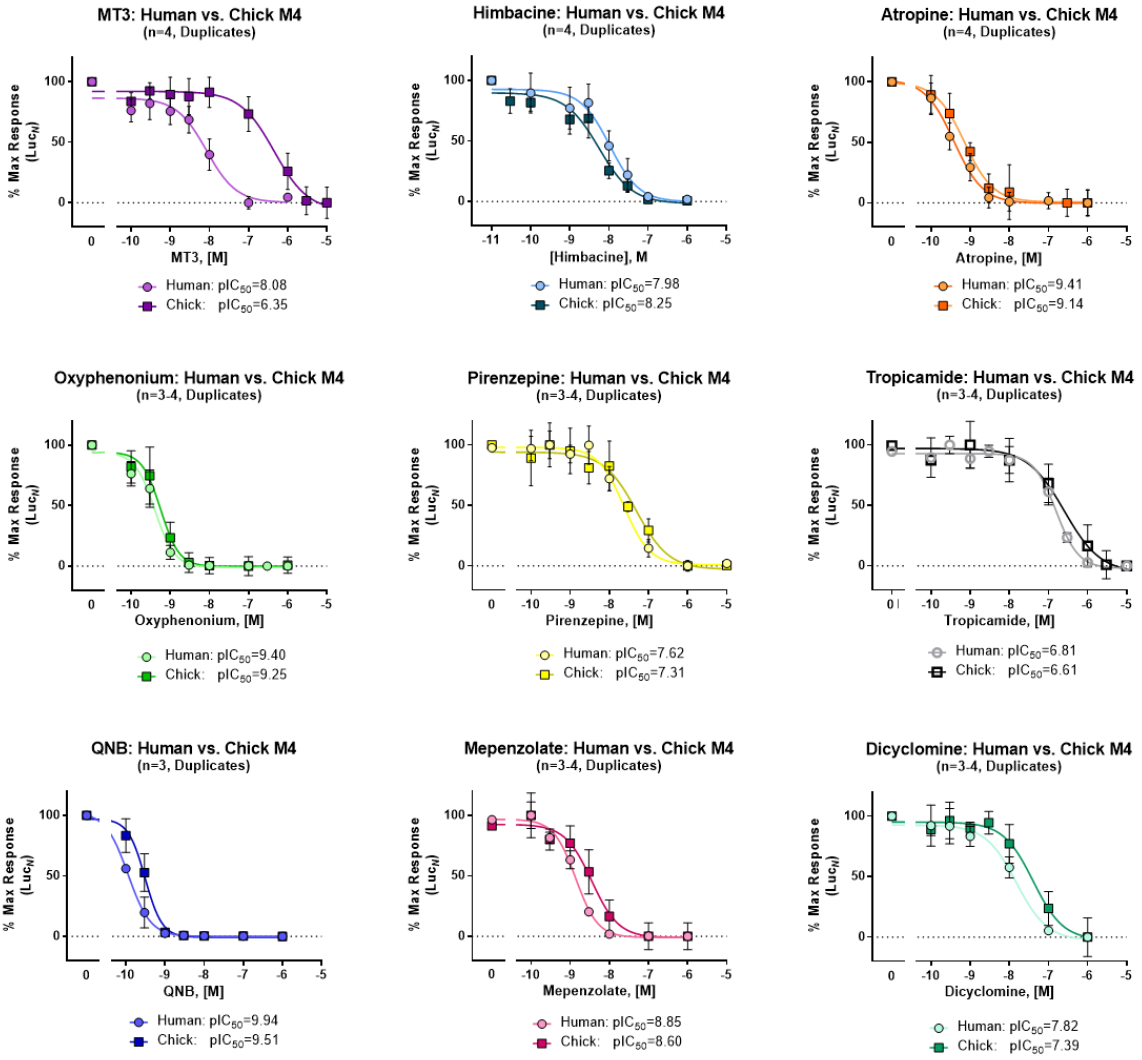

Figure 5.3: Fitted IC_{50} curves (error bars represent ± SEM) for mAChR antagonists at human M_4 versus chicken cM_4 receptors. The only antagonist that exhibited a significant difference in potency between human and chicken receptors was MT3 ($p < 0.0001$, unpaired t-test, two-tailed; top left).

Table 5.1: Binding data for muscarinic antagonists tested at mAChR M_4 and cM_4 in our assay. pIC_{50} (Study) were the data determined by our binding assay, pK_i (CP) (Study) data were calculated from the IC_{50} values in our assay by the method of Cheng and Prusoff[254], and pKi (Literature) are data from previously published studies. Maximum inhibition achieved by all antagonists was 100%. ***Abbreviations:*** Est. [Vit]: estimated vitreal concentrations required for myopia-inhibition in chick.

Muscarinic Antagonists at mAChR M_4 and cM_4						
Drug	pIC_{50} (Study) *Human ^Chick	pK_i (CP) (Study) *Human ^Chick	pK_i (Literature) *Human ^Avian	Inhibits Myopia Est. [Vit]	Source	Cat #
Atropine Sulfate	*9.41 ± 0.05 ^9.15 ± 0.07	*9.66 ^9.87	*9.6[a]-9.9[b] ^9.2-9.4[c]	Yes[l] 0.1-10 mM	Sigma	A0257
Mamba Toxin 3 (MT3)	*8.08 ± 0.08 ^6.35 ± 0.12	*8.32 ^7.07	*8.7[d,e] ^N/A	Yes[m,n] 0.25-2.5 µM	Peptides International	PMT-4410-s
Himbacine	*7.98 ± 0.8 ^8.25 ± 0.07	*8.25 ^8.97	*8.1[f] ^8.2[g]	Yes[g] 17-33 mM	Enzo Life Sciences	ALX-550-061
Oxyphenonium • Br	*9.40 ± 0.04 ^9.25 ± 0.05	*9.64 ^9.97	*9.8-10[h] ^N/A	Yes[l] 1-10 mM	Sigma	O5501
Pirenzepine • 2HCl	*7.63 ± 0.07 ^7.31 ± 0.11	*7.87 ^8.03	*7.1[a]-7.8[b] ^8.2-8.4[c]	Yes[l] 10 mM	Sigma	P7412
3-Quinuclidinyl Benzilate (QNB)	*9.94 ± 0.03 ^9.51 ± 0.03	*10.19 ^10.23	*9.5[a] ^10-10.5[c]	Partial[l] 0.74 mM	Sustainable Scientific	BR-143013
Tropicamide	*6.81 ± 0.05 ^6.61 ± 0.10	*7.05 ^7.33	*7.8[f] ^7.2[i]	Partial[l] 10 mM	Sigma	T9778
Mepenzolate • Br	*8.85 ± 0.03 ^8.45 ± 0.07	*9.10 ^9.17	*N/A ^N/A	No[l] 1-10 mM	Sigma	M5651
Dicyclomine • HCl	*7.82 ± 0.11 ^7.39 ± 0.10	*8.06 ^8.11	*6.8-7.3[h] ^8.3[g]	No[l] 1-10 mM	Sigma	D7909

Muscarinic Agonism mAChR M_4 and cM_4						
	pED_{50} (Study)	pK_i (CP)	pED_{50} (Literature)	Inhibits Myopia	Source	Cat #
Carbamoylcholine • Cl (Carbachol)	*5.25 ± 0.03 ^5.72 ± 0.05	N/A	*4.9[j]-5.4[a] ^5.3-5.5[k]	No 1-10 mM	Tocris	2810

a. Kashihara et al. 1992. *Life Sci*
b. Moriya et al. 1999. *Life Sci*
c. Tietje & Nathanson. 1991. *J Biol Chem*
d. Jolkkonen et al. 1994. *FEBS Lett*
e. Näreoja et al. 2011. *Br J Pharmacol*
f. Lazareno et al. 1993. *Br J Pharmacol*
g. Cottriall et al. 2001. *Neuroreport*
h. Eglen & Whiting. 1987. *Br J Pharmacol** *Guinea pig
i. Lazareno et al. 1990. *Mol Pharmacol*
j. Wood et al. 1999. *Br J Pharmacol*
k. Tietje et al. 1990. *J Biol Chem*
l. Luft et al. 2003. *Invest Ophthalmol Vis Sci*
m. McBrien et al. 2011. *Ophthalmic Physiol Opt*
n. Nickla et al. 2015. *Curr Eye Res*

mAChR antagonist potency at human α_{2A}-adrenergic receptor (hADRA2A)

Clonidine (clon)-treatment of cells transiently transfected with human ADRA2A resulted in increased CRE-Luc (maximum 26-fold increase) with a $pED_{50} = 6.37$; 1 µM was chosen as the fixed concentration as it gave a submaximal activation of CRE-Luc (ca. 78% of maximum response). Although increased cAMP is not the usual response to agonist treatment of a G_i-coupled receptor, this effect has been reported previously in CHO cells transfected with hADRA2A[256]; this should not significantly affect results from our assay, as we are comparing relative values of mAChR antagonism of clon-mediated effects at hADRA2A. The pIC_{50} for yohimbine, an α_2-adrenergic antagonist, was calculated as 8.28 ± 0.12, which falls in the middle of previously published K_i data for yohimbine at hADRA2A[257-259]. Ranked relative pIC_{50} values for mAChR antagonists at the hADRA2A receptor, from highest to lowest potency, were MT3 (7.81 ± 0.11) > himbacine (4.78 ± 0.23) > atropine (4.34 ± 0.11) > QNB (3.58 ± 0.37) > oxyphenonium (3.33 ± 0.17) > mepenzolate (3.10 ± 0.12) > pirenzepine (3.062 ± 0.07) > tropicamide (2.83 ± 0.09); we were unable to obtain a full inhibitory response for QNB (maximum inhibition = 81.7%) and mepenzolate (maximum inhibition = 68.3%), and dicyclomine had no detectable activity at hADRA2A at the concentrations tested (**Fig. 5.4**; Table 5.2; n = 3-4 duplicates). These data are in good agreement with previously published reports about the affinity of MT3 for the hADRA2A receptor[162,163], and demonstrate that atropine and himbacine may bind to hADRA2A, albeit with very low potency.

Figure 5.4: mAChR Antagonism at Human ADRA2A (n = 3-4, duplicates)

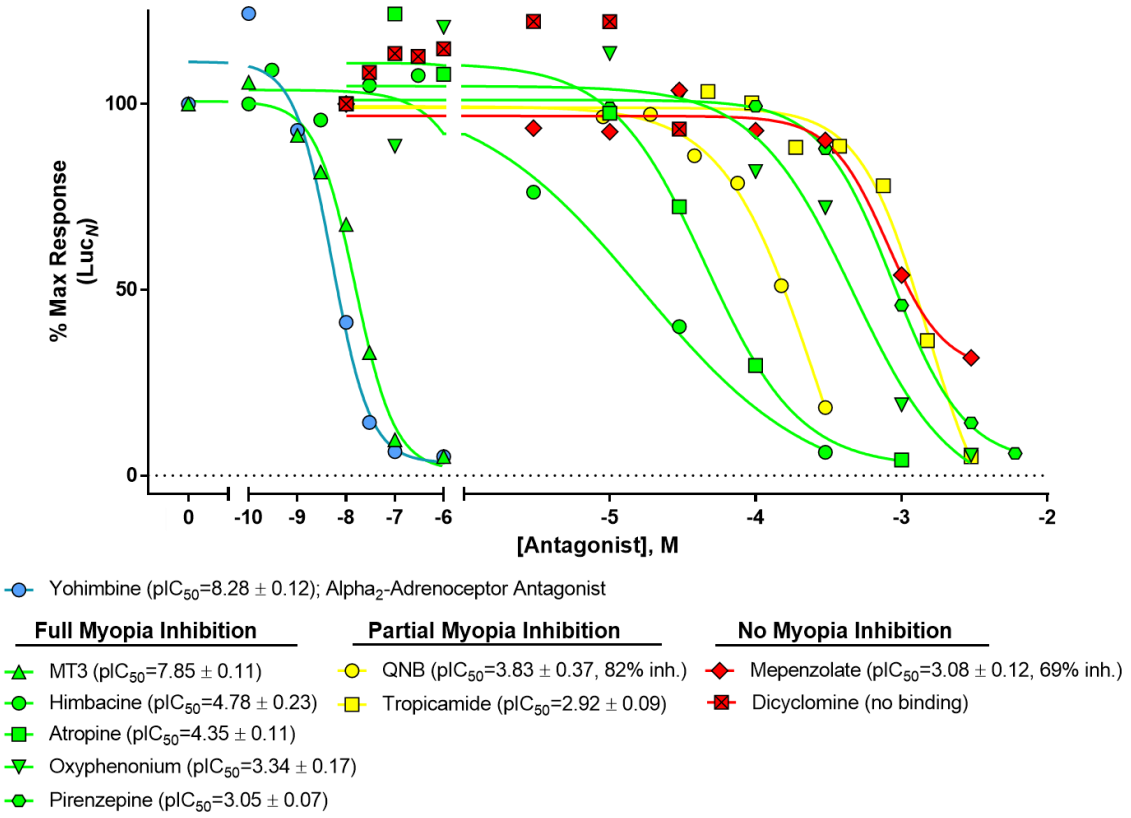

Figure 5.4: Potencies of various mAChR antagonists at the human hADRA2A receptor. We confirmed high potency of yohimbine (blue), an α_2-adrenoceptor antagonist, at hADRA2A (pIC_{50} = 8.28 ± 0.12). Muscarinic antagonists are categorized into full myopia inhibition (green), partial myopia inhibition (yellow), and no myopia inhibition (red) according to previously published research[159-161]. Under each category, antagonists are ranked in descending order from most to least potent in our receptor assay (pIC_{50} ± SEM).

Table 5.2: Binding data for α_2-adrenergic drugs and mAChR antagonists at human α_{2A}-adrenoceptor (hADRA2A). pIC_{50} (Study) were the data determined by our binding assay, pK_i (CP) (Study) data were calculated from the IC_{50} values in our assay by the method of Cheng and Prusoff[254], and pKi (Literature) are data from previously published studies. Maximum inhibition achieved was 100%, unless indicated otherwise by percent values in parentheses under the reported pIC_{50}. ***Abbreviations:*** Est. [Vit]: estimated vitreal concentrations required for myopia-inhibition in chick.

Alpha$_2$-Adrenergic Drugs at ADRA2A						
Drug	pK_i /pED_{50} (Study) (Human)	pK_i (CP) (Study) (Human)	pK_i /pED_{50} (Literature) *Human ^Avian	Inhibits Myopia Est. [Vit]	Source	Cat #
Yohimbine ● HCl (Antagonist; pK_i)	8.28 ± 0.12	8.65	*8.2-9.4[a-c] ^9.2[d]	No 0.01-1 mM	Sigma	Y3125
Clonidine ● HCl (Agonist; pED_{50})	6.37 ± 0.12	N/A	*6.8-7.2[e] ^8.4[f]	Yes[j] 0.01-1 mM	Sigma	C7897

Muscarinic Antagonists at human ADRA2A						
Drug	pIC_{50} (Study) (Human)	pKi (CP) (Study) (Human)	pK_i (Literature) (Human)	Inhibits Myopia Est. [Vit]	Source	Cat #
Atropine Sulfate	4.34 ± 0.11	4.71	5.88[g]	Yes[k] 0.1-10 mM	Sigma	A0257
Mamba Toxin 3 (MT3)	7.81 ± 0.11	8.18	8.5[h,i]	Yes[l,m] 0.25–2.5 µM	Peptides International	PMT-4410-s
Himbacine	4.78 ± 0.23	5.15	N/A	Yes[n] 17–33 mM	Enzo Life Sciences	ALX-550-061
Oxyphenonium • Br	3.33 ± 0.17	3.70	N/A	Yes[k] 1–10 mM	Sigma	O5501
Pirenzepine • 2HCl	3.06 ± 0.07	3.43	N/A	Yes[k] 10 mM	Sigma	P7412
3-Quinuclidinyl Bezilate (QNB)	3.58 ± 0.37 (81.7%)	3.95	N/A	Partial[k] 0.74 mM	Sustainable Scientific	BR-143013
Tropicamide	2.83 ± 0.09	3.20	N/A	Partial[k] 10 mM	Sigma	T9778
Mepenzolate • Br	3.10 ± 0.12 (68.3%)	3.47	N/A	No[k] 1–10 mM	Sigma	M5651
Dicyclomine • HCl	No Binding	N/A	N/A	No[k] 1–10 mM	Sigma	D7909

a. Ruuskanen et al. 2005. *Br J Pharmacol*
b. Laurila et al. 2007. *Br J Pharmacol*
c. Zheng et al. 2000. *Bioorg Med Chem Lett*
d. Bylund et al. 1988. *J Neurochem*
e. Newman-Tancredi et al. 1998. *Naunyn Schmiedebergs Arch Pharmacol*
f. Randall et al. 1983. *Biochem Pharmacol*
g. Chang et al. 1995. *Eur J Pharmacol*
h. Näreoja et al. 2011. *Br J Pharmacol*
i. Blanchet et al. 2014. *Biochimie*
j. Carr et al. IOVS 2016; 57: ARVO E-Abstract
k. Luft et al. 2003. *Invest Ophthalmol Vis Sci*
l. McBrien et al. 2011. *Ophthalmic Physiol Optics*
m. Nickla et al. 2015. *Curr Eye Res*
n. Cottriall et al. 2001. *Neuroreport*

Controls

Three different control experiments were conducted in order to verify that changes in CRE-Luc were related to transfected receptor-mediated changes in intracellular cAMP and not other signalling pathways. Cells were transfected with the pcDNA™3.1+ plasmid only; there was no significant change in cAMP levels in response to carbachol (CCh)- or clonidine (clon)-treatment (n = 3 duplicates, **Fig. 5.5**). In order to verify that changes in cAMP were not the result of Ca^{2+}-dependent pathways, calcium ionophore (CI A23187) and Phorbol 12-myristate 13-acetate (PMA) were tested. CI A23187-treatment results in an increase in intracellular Ca^{2+} which could cause activation of Ca^{2+}-dependent cyclase and increased cellular cAMP independent of receptor activation (**Fig. 5.6a; 1**), and PMA is an activator of protein kinase C, a phosphatase that could act on cAMP Response Element Binding protein (CREB) causing increased luminescence without the presence of elevated cellular cAMP (**Fig. 5.6a; 2**). There was no significant change in Luc_N with treatment of either CI A23187 (1 µM) or PMA (10 µM) when compared to agonist-treatment in transfected cells (**Fig. 5.6b**; n = 3 duplicates).

Figure 5.5: Agonist Action at pcDNA™3.1(+) Empty Vector (n = 3, duplicates)

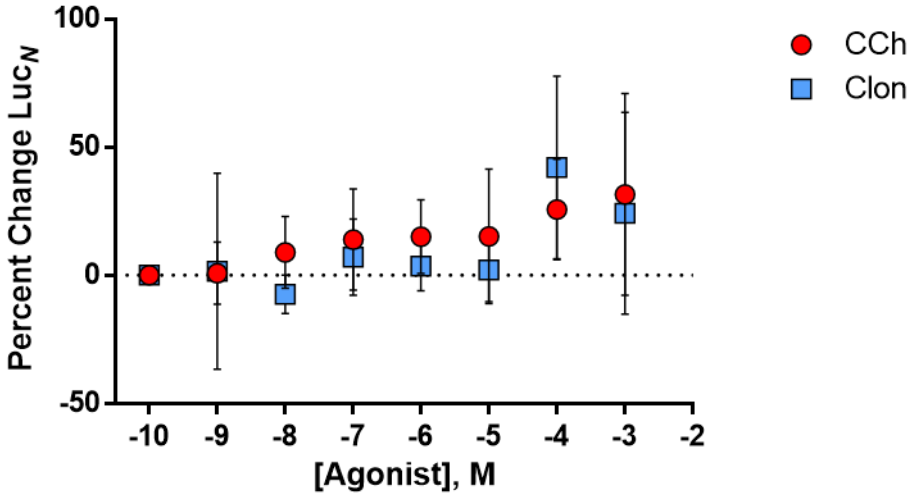

Figure 5.5: Percent change of normalized luciferase (Luc_N) upon agonist-treatment (carbachol: CCh; clonidine: clon) of cells co-transfected with empty pcDNA™3.1+ vector, CRE-Luc, and RLuc vectors.

Figure 5.6: Lack of CREB-Activation by Calcium-Dependent Pathways (n = 3, duplicates)

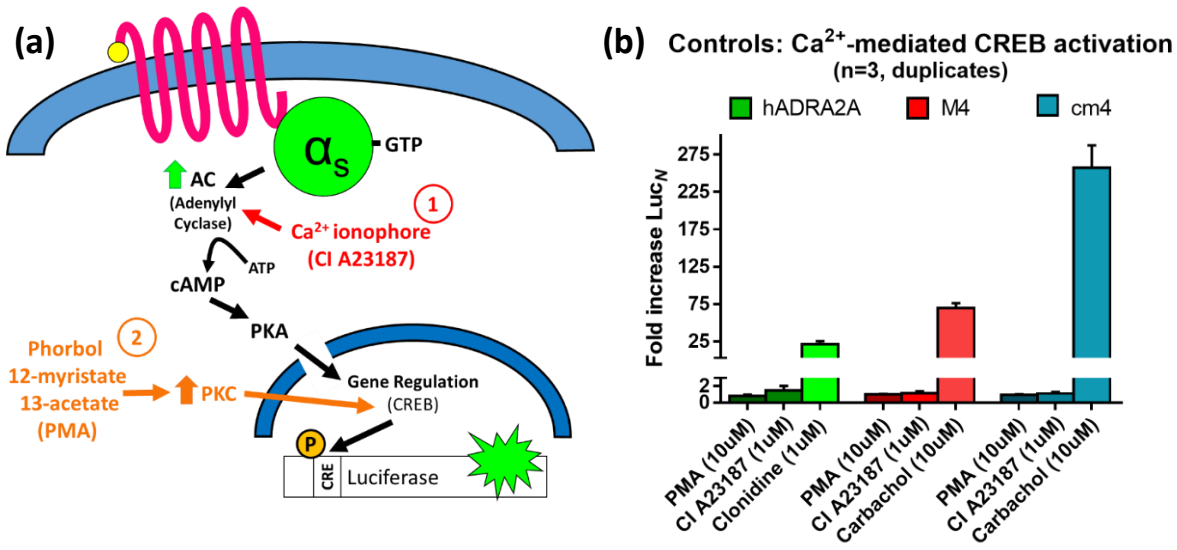

Figure 5.6: Schematic demonstrating calcium-dependent pathways that could lead to activation of cAMP and increased expression of CRE-Luc without requiring receptor activation, and the theorized sites of action of CI A23187 (1) and PMA (2) **(a)**. Fold increase normalized luciferase (Luc_N) of cells co-transfected with receptor clone (hADRA2A, M_4, or cM_4), CRE-Luc, and RLuc upon treatment with activators of calcium-dependent adenylyl-cyclase (calcium ionophore; CI A23187), protein kinase C activator (Phorbol 12-myristate 13-acetate; PMA), and receptor agonist (carbachol or clonidine) **(b)**.

Discussion

Distribution of Drugs Within Ocular Tissues After Different Delivery Methods

In humans, myopia inhibition by atropine is delivered in the form of daily treatment with topical eye drops, which require concentrations of 0.01-1% to be effective[153]. Under experimental conditions, delivery of a single dose of 2% [^{3}H]-atropine to the conjunctival sac of rabbits resulted in a distribution of 0.05% of the original concentration in the choroid and 0.008% of the original concentration in the retina one hour after instillation[260]; [^{3}H]-pirenzepine (2%) was also tested, and final concentrations were half those calculated for atropine[260]. Distribution of atropine after multiple doses has not been determined, but distribution studies of topical [^{14}C]-brimonidine in rabbit and monkey eyes have estimated that the retina/choroid contains approximately 0.05-0.7% of the original drug concentration, depending on whether the drug was applied once with radioactivity measured after two hours (0.05%), or after a multiple topical dosing regimen (2x/day for 14 days; 0.7%); it was reported also that the concentration of radioactivity was greater in pigmented ocular tissues (RPE, iris, ciliary body, choroid/retina) than non-pigmented ones[261]. Other studies investigating the distribution after topical application of a carbonic anhydrase (CA) inhibitor dorzolamide – which has a significantly different structure and chemical properties than [^{14}C]-brimonidine – reported similar concentrations of 0.04-0.06% of the original drug concentration in the retina/choroid, depending on the dosing regimen in Wistar rats and rabbits[262,263]. Thus, if we estimate conservatively that topical delivery of multiple doses of atropine to the retina/choroid is similar to that of multiple doses of brimonidine and dorzolamide, then a 0.01-1% dose would result in approximate retinal/choroidal concentrations of 70 nM – 7 µM atropine at 0.05% of the original solution. Concentrations such as these are still very likely to result in non-mAChR off-target effects in the retina/choroid, as they are roughly 350-35,000 times the previously reported affinity of atropine at mAChR M_4 (125-250 pM)[230,252] and 180 times that of the IC_{50} determined by our experiments (385 pM).

In chicks, where intravitreal injection is the usual method of delivery, estimates for the final concentration in the retina vary widely[159,161]. However, if we look to studies investigating the ocular distribution of intravitreally-injected radioactively labelled drug

there is greater consensus. In one study, the concentration of [^{3}H]-spiperone in the retina after intravitreal injection was found to be 25% of the original injection at time points ≤ 30 min, and 8% at 1-24 hrs[112]. A similar study investigating the distribution of [^{3}H]-pirenzepine after intravitreal injection found that drug levels peaked at 1hr, and were measured to be 6% in the retina, 26% in the vitreous, 1.5% in the choroid, and 2.5% in the sclera[234]. Taking into account these levels of conservation of activity and the extremely high concentrations used for intravitreal injection of drugs (1-100 mM)[159], it is highly likely that the amount of drug delivered to the retina and other ocular tissues after intravitreal injection is more than enough to result in binding of off-target (non-mAChR) receptors. This off-target binding could easily explain the requirement for high concentration mAChR antagonist (0.001-10 mM) to elicit myopia inhibition in humans and animal models[159-161], the finding that only a few mAChR antagonists are effective against myopia[159], and the seemingly paradoxical discovery that cholinergic amacrine cells are not required for visual emmetropization, development of FDM in chicks, or effective prevention of FDM with atropine treatment[223]. Even MT3, which has been successful at inhibiting myopia at much lower concentrations than atropine (2.5-10 μM), is not immune to off-target effects. It has significant activity at human α-adrenoceptors at low- to mid-nanomolar concentrations[162,163]; and even diluted by diffusion through the vitreous, its concentration would still be greater than 100x the concentration required for action at its target receptors, which would be more than enough to achieve non-specific effects at non-mAChRs.

mAChR Antagonists at M_4, cM_4, and hADRA2A, and Correlations with Myopia-Inhibition

Results obtained from our experiments agree with previously published data about the binding characteristics of mAChR antagonists at the M_4 and cM_4 receptors (**Table 5.1**). Interestingly, these data do not correlate well with the reported abilities of these drugs to inhibit myopia in children or animal models. Atropine, the current gold standard for myopia prevention, has a very high affinity at M_4 and cM_4, but extremely high concentrations are required to achieve a ~50% effect in humans[153] and animals[151,159,264]. Oxyphenonium also has a very high affinity for M_4 and cM_4, and it too requires high concentrations to inhibit FDM in the chick[159]; it has not been tested in humans. QNB has the highest potency in our assay for both M_4 and cM_4, but it only partially inhibits myopia in the chick[159], and

mepenzolate and dicyclomine have no effect on myopia in the chick, despite inhibitory potencies for M_4 and cM_4 in the lower nanomolar range[159]. In contrast, tropicamide (pK_i = 7.1-7.3), and pirenzepine (pK_i = 7.8-8.0) are effective at inhibiting myopia in humans[156] and animals[159,234], yet have a significantly lower affinity for M_4 and cM_4 receptors than other ligands tested. One possibility for this is that pirenzepine has a preference for M_1 receptor subtypes, thus would not bind as effectively to M_4, while tropicamide is reported to be only moderately-selective for mammalian M_4[265]. Most interesting is the behavior of the three-finger toxin, MT3. While we were able to confirm that MT3 has a high potency for the M_4 receptor, we also demonstrated that its potency is significantly decreased at the cM_4 receptor. This result does not support published studies that conclude that cM_4 is the putative myopia-controlling receptor based upon the significantly decreased concentrations of MT3 required for myopia inhibition in chick[34,161], when atropine, QNB, oxyphenonium, dicyclomine, and mepenzolate – all of which have a greatly increased potency in inhibiting cM_4-receptor mediated responses over MT3 – require a much larger concentration of drug to achieve equal effectiveness as MT3, or have no myopia-inhibiting effect. One could argue that these results do not eliminate M_4/cM_4 as the myopia-controllers because there may be conflicting effects of activating both G_q-coupled and G_i-coupled subtypes of mAChRs – which have opposing effects – when using a broad-spectrum drug such as atropine or oxyphenonium. MT3 does not bind solely to M_4, however, and will act on human mAChR M_1 with a pKi = 6.22–6.71 (200-600 nM), in addition to α-adrenoceptors pK_i for α_{1A} = 8.84–8.86 (1 nM); α_{1B} = 7.57-7.68 (~24 nM); α_{2A} = 8.49–8.51 (3 nM); α_{2C} = 7.29–8.82 (9 nM)[162,163]. These pK_i values fall well within the range of expected drug concentration to reach the retina/choroid after intravitreal injection of 2.5 µM MT3 – i.e., 6-8% retention of activity (as discussed in the previous paragraph) would yield a concentration of 150–200 nM – which does not rule out the possibility of that MT3 may inhibit myopia by binding to M_1 and/or α-adrenoceptors.

We confirmed previous reports of high affinity MT3 binding to hADRA2A (pIC_{50} = 7.81), and demonstrated that atropine and himbacine can bind with low potency to hADRA2A. All other mAChR antagonists had low potency at hADRA2A, but we were able to achieve 100% inhibition of clonidine-mediated effects with oxyphenonium, tropicamide, and

pirenzepine – drugs that fully inhibit myopia in the chick. The maximum inhibitory effects achieved by QNB (partial myopia inhibition) and mepenzolate (no myopia inhibition) were 81.7% and 68.3% respectively, and dicyclomine (no myopia inhibition) had no discernable effect at the concentrations tested. These results do correlate better with myopia-inhibition by mAChR antagonists in the chick[159], and because extreme concentrations were used (10-100 mM), there would easily be sufficient drug delivered to the retina/choroid to elicit binding at these off-target receptors, even at the low efficacies determined by our experiments. There is a caveat to these results, however. Although we have shown that some mAChR antagonists will bind hADRA2A at extreme concentrations, we have not ruled out any other mAChR or α-adrenoceptor subtypes, or non-mAChR/non-adrenergic receptor targets. We cannot eliminate or include any of the receptors tested for a role in myopia-inhibition with this kind of data, because we cannot determine for certain all of the possible targets accessed by using high drug doses.

Difference in Binding of MT3 at M_4 Versus cM_4

The muscarinic subtype M_4 has gained favour as "myopia-controlling" receptor, largely because of the effects of MT3 – which has been hailed as "highly specific for M_4" – on FDM in the chick model organism[34,161]. When attempting to assign functional consequences to a particular ligand across species however, it is important to consider the mechanism of binding of that ligand to its target receptor. Generally, orthosteric binding sites are highly conserved (100%) between receptors of the same class and between species. Thus, in order to achieve a greater specificity of binding, ligands such as MT3 will bind to residues that are less conserved, usually in the extracellular loops 2 and 3 (EL2 and EL3) of the target GPCRs[253]. There is a wide variety of mamba toxins from *Dendroaspis angusticeps* (East African green mamba) which have greatly different affinities for mAChR subtypes (MT1-MT7), but if we examine their amino acid sequences they are remarkably similar[253,266]. Thus, it is logical to assume that subtype specificity of these ligands should depend on the presence of very few amino acid residues.

There is little information available about the structure-function relationship of MT3 at mAChRs, but MT7 has been extensively studied because of its remarkably high affinity

for the M_1-receptor, which is more than 1000-fold greater than its affinity at all other subtypes. Through construction of M_1:M_3 chimeras and mutagenesis of M_4, it has been determined that MT7 selectivity is dependent on a small number of residues on the M_1 receptor[253]; namely, Glu^{170}, Tyr^{179}, and Glu^{397}. Muscarinic M_1 is the only receptor that has a negatively-charged Glu^{170} in EL2 (M_3-M_4: Lys^{170}) and Glu^{397} in EL3 (M_3: Lys^{397}, M_4: Asp^{397}), and it was determined that Glu^{170} is *necessary* for MT7 recognition and affinity; all M_3 constructs with a positively-charged Lys^{170} had no discernable functional interaction with MT7 (**Fig. 5.7**; M_3 & M_4). Substitution of Lys^{397} in EL3 in place of Glu^{397} in M_3-Glu^{170} constructs resulted in a ~10-times decrease in affinity of MT7 (**Fig. 5.7**; M1:M3-IV vs. M_1). These M_1:M_3 chimera data were corroborated by mutagenesis studies in M_4, in which substitution of Lys^{170} to Glu^{170} was again required for functional binding of MT7, but leaving a negative residue (Asp^{397}) in EL3 did not have a significant effect on the apparent functional K_i of MT7 compared to native M_1 (**Fig. 5.7**; M4ELY)[253]. Another important residue for MT7 affinity to M1 is Tyr^{179} in EL2 (M_3-M_4: Phe^{179}). Mutagenesis of M_3-Glu^{170} constructs to contain a Tyr^{179} instead of Phe^{179} resulted in a 30- to 90-times increased affinity of MT7, which implicates the Tyr hydroxyl (-OH) group as having a significant impact on MT7 affinity at M_1 (**Fig. 5.7**; M3ELA-E vs. M3ELAY-E and M3ELAQ-E vs. M3ELAQY-E). Interestingly, these residue substitutions (i.e. Glu→Lys, Tyr→Phe) would be considered "highly conserved" by the default protein scoring matrix (BLOSUM62) used as the default for many bioinformatics programs. Thus, data such as these highlight the importance of amino acid charge in dictating protein-protein interactions *in vivo*, and demonstrate the need for careful manual analysis of consequences induced by changes in amino acid sequence.

Figure 5.7: MT7 is Dependent on Few Residues for Binding to mAChR M_1

Receptor Sequence Comparisons

	outer loop 2	outer loop 3
	170	397
M1	WQYLVG**E**RTVLAGQC**Y**IQFLSQ...	...CKDCVP**E**TL
	213	523
M3	WQYFVGKRTVPPGECFIQFLSE...	...CDSCIPKTF
M1:M3-IV	WQYLVG**E**RTVLAGQCYIQFLSQ...	...CDSCIPKTF
M3ELA-E	WQYFVG**E**RTVLAGECFIQFLSE...	...CDSCIP**E**TF
M3ELAY-E	WQYFVG**E**RTVLAGEC**Y**IQFLSE...	...CDSCIP**E**TF
M3ELAQ-E	WQYFVG**E**RTVLAG**Q**CFIQFLSE...	...CDSCIP**E**TF
M3ELAQY-E	WQYFVG**E**RTVLAG**Q**C**Y**IQFLSE...	...CDSCIP**E**TF
M4	WQFVVGKRTVPDNQCFIQFLSN...	...CQSCIPDTV
M4ELY	WQFVVG**E**RTVLDNQC**Y**IQFLSN...	...CQSCIPDTV

Functional Characteristics of Expressed Receptor Constructs

Receptor construct	Control		MT7
	Carbachol EC_{50}	Max. increase in $[Ca^{2+}]_i$	Functional inhibition App. K_i
	μM	*nM*	*nM (n)*
M1	2.9 ± 0.9	279 ± 43	1.31 ± 0.36 (5)
M3	2.1 ± 0.3	369 ± 22	ND
M1:M3-IV	1.7 ± 0.1	276 ± 19	10.71 ± 0.37 (3)
M3ELA-E	73.6 ± 16.6	183 ± 21	23.25 ± 6.76 (2)
M3ELAY-E	9.7 ± 0.3	292 ± 22	0.26 ± 0.04 (4)
M3ELAQ-E	31.5 ± 12.6	193 ± 44	19.54 ± 3.62 (3)
M3ELAQY-E	8.1 ± 2.1	352 ± 19	0.72 ± 0.35 (4)

Radioligand Binding Data of Expressed Receptor Constructs

Receptor construct	Control		IC_{50} MT7 NMS displacement
	K_d [^{3}H]NMS	B_{max}	
	pM	*fmol/mg of protein*	*nM*
M1	361 ± 52	858 ± 38	0.50 ± 0.06
M3	207 ± 65	1770 ± 59	ND
M4	93 ± 18	424 ± 15	ND
M4ELY	83 ± 14	343 ± 11	1.45 ± 0.69

Modified from: Anu Kukkonen et al. J. Biol. Chem. 2004;279:50923-50929

Figure 5.7: Receptor sequence comparisons, functional characteristics, and radioligand binding data for M_1:M_3-receptor chimeras and mutants utilized in studies by Kukkonen et al.[253] to determine important residues for MT7 affinity at M_1. This research was originally published in the Journal of Biological Chemistry by Kukkonen A, Peräkylä M, Akerman KE, Näsman J. Muscarinic toxin 7 selectivity is dictated by extracellular receptor loops. *J. Biol. Chem*. 2004; 279: 50923-9. © the American Society for Biochemistry and Molecular Biology. No special permissions are required to reproduce the work here.

Another three-finger toxin from *Dendroaspis*, fasciculin (FAS), has high species-selectivity for acetylcholinesterase (AChE), which is dependent on only a few residues. Fasciculins (FASI-III) bind with high affinity to AChE in mammals and fish, but not with avian, insect, or reptilian AChE, or the closely-related butyrylcholinesterase (BuChE). Crystallography studies of AChE from *Torpedo californica* (Pacific electric ray) determined that, of the many residues that interact in the FAS-II-AChE complex, substitution of $Tyr^{70} \rightarrow Asp^{70}$ or $Trp^{279} \rightarrow Arg^{279}$, Ala^{279}, or Val^{279} resulted in a loss of affinity for FAS-II at $AChE^{267}$. These results were complemented by studies utilizing mouse AChE, in which mutagenesis of the *Torpedo californica* equivalent aromatic residues to their BuChE counterparts ($Tyr^{72} \rightarrow Asn^{72}$, $Tyr^{124} \rightarrow Gln^{124}$, and $Trp^{286} \rightarrow Arg^{286}$) individually reduced FAS-II affinity to AChE significantly (10^2-10^6-fold), while triple-mutation caused a loss of affinity equal to eight orders of magnitude; compellingly, the loss of affinity caused by triple mutation matches the reported affinity for FAS-II at $BuChE^{268}$.

Taking these data for three-finger toxins into consideration, we may assume that specificity of MT3 binding to M_4 may also be determined by very few amino acid residues. Unfortunately, there are no data on the amino acids required for binding of MT3 to any receptor (personal communication with Dr. Denis Servent), so we cannot comment on the exact resides that may be involved. However, chicken and human M_4 share only a 71.4–72.7% identity for allosteric binding areas in EL3 and EL2, respectively (**Fig. 5.8**), and as demonstrated above, even "highly conserved" amino acid substitutions (according to the BLOSUM62 matrix) can have significant effects on the functional behavior and binding affinity of MTs at their target receptors. It is likely, then, that the decreased activity of MT3 at cM_4 is caused by amino acid differences in EL2 and EL3 compared to those of M_4. That all other drugs tested in our assay did not differ significantly in their functional characteristics between M_4 and cM_4 is consistent with the fact that they are all known to be orthosteric inhibitors of ACh at mAChRs, and the reported orthosteric binding site of mAChR M_4[269] is 100% conserved between human and chick receptor (**Fig. 5.8**).

Figure 5.8: Orthosteric and Allosteric Binding Sites of M_4 and cM_4

Figure 5.8: BLAST sequence comparison data for human and chicken mAChR M_4. Orthosteric binding site residues[269] are highlighted in red, while reported allosteric residues[269] and extracellular loops 2 and 3 are highlighted in blue. BLAST comparison results for whole receptor and individual analysis of EL2 and EL3 are displayed on the left.

Atropine is still the best pharmacological tool we have to combat the progression of childhood myopia, but its mAChR M_3-mediated side effects and the high concentration requirement for treatment limit its acceptance as an approved therapy. The lack of knowledge of the mechanism of atropine's actions prevents the generation of more effective interventions with fewer side-effects. The data presented here make a compelling case for continued investigation into non-mAChR explanations for atropine-mediated myopia inhibition, with α-adrenoceptors as a distinct possibility. The assumption that atropine inhibits myopia via mAChR M_4 (or any mAChR) is not supported by the pharmacological analyses presented in this study. Examination of the potencies of mAChR antagonists on M_4 and cM_4 receptors makes it difficult to reconcile the non-correlation between the extreme potentcy of broad-spectrum, orthosteric mAChR antagonists such as QNB, dicyclomine, mepenzolate, and their inability to inhibit myopia in the chick. The behaviors of mAChR antagonists at the α_{2A}-adrenoceptor correlate better with myopia inhibition, but this is just one possible receptor target out of many, and much more investigation is required before recommending a drastic change in treatment paradigms. The benefits of understanding the true target receptors of atropine in myopia inhibition are obvious: more effective therapies with fewer side-effects and less demanding treatment regimens. In the case of α-adrenoceptors there are already many drugs targeted to them (i.e., brimonidine for glaucoma-treatment) that are approved for topical use in the human eye, so transition into clinical trials would be more efficient than for experimental ligands such as MT3. The field of myopia pharmacology has grown stagnant, and the benefits of continued investigation into the key players of regulation of eye growth would contribute significantly to our understanding of the fundamental homeostatic mechanisms of vision, and could lead to greatly improved therapies to combat the growing threat of global myopia prevalence.

Methods & Materials

DNA and Expression Vectors

All receptor clones were expressed in a pcDNA™3.1+ vector (Invitrogen, ThermoFisher Scientific, Waltham, MA, USA). The chicken M_4 (cM_4) genomic clone was a gift from Dr. Neil Nathanson[255], and the human M_4 (M_4; MAR0400000) and alpha$_{2A}$-adrenergic

(hADRA2A; AR0A2A0000) receptor clones were purchased from the cDNA Resource Center (Bloomsburg University Foundation, Bloomsburg, PA, USA). The cAMP response element luciferase vector (CRE-Luc; pGL4.29[luc2P/CRE/Hygro]) and the constitutively active Renilla luciferase control vector (RLuc; pRL-RK) were purchased from Promega (Madison, WI, USA).

CRISPR/Cas9 Knock-Down of mAChR M_3

All cell media, serum, transfection materials, culture flasks, and multiwell plates were purchased from ThermoFisher Scientific (Waltham, MA, USA) unless specified otherwise. CRISPR knockout of M_3 in Lenti-X HEK 293T cells (LX293T; Clontech, Mountain View, CA, USA) was performed to ensure mAChR ligand-mediated effects on cAMP were the result of activity at transfected, and not endogenous receptors; stable CRISPR M_3-knockout LX293T cells are referred to as CR-M_3 cells. The knockout design and procedures used to derive the CR-M_3 cells from the wild-type LX293T cells were as described by Sanjana et al.[270] and Shalem et al.[271] using the GeCKO CRISPR protocol (https://www.addgene.org/crispr/libraries/geckov2/). Three sets of genome-specific sgRNA sequences of mAChR M_3 (F to R) were chosen from the GeCKOv2 Human Library, and both strands of oligonucleotides were synthesized for each target sequence (F_A:CACCGgtcacaagcgcgcacccgagc, R_A: AAACgctcgggtgcgcgcttgtgacC; F_B:CACCGgcggtaccaccgatgaccctc, R_B:AAACgagggtcatcggtggtaccgcC; F_C: CACCGgcgctttcttaacgggcatcc, R_C: AAACggatgcccgttaagaaagcgcC); lower case sequences are target sequences of the M_3 genomic locus and the upper case sequences are flanking sequences for cloning. Both strands of the oligonucleotides were annealed and inserted in BsmBl restriction enzyme sites under a U6 promoter in a CRISPR/CAS9 vector (lentiCRISPR v2), a gift from Feng Zhang (Addgene plasmid #52961, Cambridge, MA, USA). The lentiCRISPR v2 plasmids containing three M_3-targeting sequences were mixed and transfected using Lipofectamine LTX Reagent. The transfected cells were maintained in the presence of 5mg/ml puromycin to select for knockout cells, and once established, stable-knockout CR-M_3 cells were re-suspended in high glucose DMEM + 10% DMSO and frozen in liquid nitrogen for future use. CR-M_3 cells were used as the background cells for all experiments, and M_3-receptor knockdown was verified periodically using a Ca^{2+}-

monitoring assay. Briefly, cells were grown in 75 cm^2 flasks until 80% confluent, lifted in enzyme-free buffer (PBS + 1 mM EDTA), and then resuspended in 1 mL Fluo-4 calcium-imaging dye. Dye-treated cells were incubated with gentle shaking for 15-30 min, washed free of excess Fluo-4 indicator, and then diluted 1:10 into individual plastic cuvettes containing Hank's Balanced Salt Solution (HBSS) plus 1.5 mM Ca^{2+}. Cells were then treated with various concentrations of carbachol to verify knock-out of M_3-receptor; changes in intracellular Ca^{2+} and concomitant increases in fluorescence were monitored using an Aminco Bowman series II fluorescence spectrophotometer using AB2 software. Intracellular calcium-dependent fluorescent signals were monitored using an excitation wavelength of 480 nm and an emission wavelength at 530 nm, and were expressed as a percentage of the emission fluorescence caused by 2 µM calcium ionophore A23187.

Cell Culture and Transfection Protocols

CR-M_3 cells were grown in high glucose DMEM supplemented with 10% fetal bovine serum, 1 mM sodium pyruvate, and 5 µg/mL Plasmocin™ (InvivoGen, San Diego, CA, USA) in a 5% CO_2 environment at 37°C. Cells were maintained at < 80% confluency and passaged with PBS containing enzyme-free EDTA (1 mM) plus mild trypsinization (90 µL of 0.25% trypsin-EDTA/25 cm^2 T-flask) to optimize homogeneity during re-plating. Transfection was performed in 12 well plates at 30% confluency; for each well to be transfected, 4 µL of Lipofectamine LTX was diluted in 50 µL Opti-MEM® reduced serum medium, vector cDNAs (CRE-Luc [180 ng], RLuc [160 ng] and receptor genomic clones [160 ng]) were mixed in a separate aliquot of 50 µL Opti-MEM®. The LTX and DNA solutions were then combined (1:1 ratio) and incubated at room temperature for 5 min. The LTX-DNA complexes were then added (100 µL of LTX-DNA complex/well) with gentle mixing, and the cells were allowed to grow in 5% CO_2 at 37°C. Medium was changed to supplemented DMEM without selection after a minimum of 8 hrs exposure to transfection medium. At 24 hrs post-transfection, cells were seeded (7500 cells/well) into white, clear-bottom, tissue-treated 96 well plates, fed with supplemented DMEM without selection, and allowed to grow overnight.

cAMP Accumulation Assay and Antagonist IC_{50} Curves

At 48 hrs post-transfection, the cell medium was aspirated and replaced with various concentrations of antagonist diluted in FluoroBrite™ DMEM with a fixed concentration of agonist (50 µL/well); treated cells were incubated for 4 hrs at 37°C + 5% CO_2. The fixed agonist concentration (carbachol: 10 µM; clonidine: 1 µM) was chosen on the basis of preliminary concentration dose-response studies, and represented a submaximal activation of normalized CRE-Luc luminescence (Luc_N). The choice of antagonists for testing was based on availability and previously published reports of their ability to prevent FDM in the chick (**Table 5.1**). All drug stock solutions (10 mM) were made using sterile dH_2O, with the exception of QNB (5 mM) and himbacine (9 mM), which were dissolved in 100% and 90% methanol (MeOH), respectively. We did not exceed the maximum concentration of MeOH that did not cause obvious cell death, as determined by ROUT statistical analysis, which was 6%.

Changes in intracellular cAMP were measured indirectly using the Dual-Glo® Luciferase Assay System and protocol (Promega). Drug-treated cells and Dual-Glo® assay reagents were allowed to equilibrate to room temperature, and then an equivalent volume of Dual-Glo® Luciferase Reagent (50 µL) was added to each sample well. The plate was incubated for 10 min at room temperature with moderate shaking to ensure complete cell lysis. After incubation, CRE-Luciferase (CRE-Luc) levels were measured using a Victor X4 Spectrophotometer (PerkinElmer). Once CRE-Luc measurements were complete, 50 µL of the Dual-Glo® Stop-and-Glo® Reagent was added to each of the sample wells, the ten-minute incubation with shaking was repeated, and then the levels of *Renilla* luciferase (RLuc, normalizing control) in the wells were measured in the same order, using the same spectrophotometer.

Data Analysis

Raw *Renilla* luminescence data (RLuc; normalization control) were first subjected to outlier detection using ROUT analysis with a 1% false detection rate (Graphpad Prism v6.07, La Jolla, CA). Any flagged data were removed along with their corresponding CRE-Luc values; these data usually represented significantly decreased RLuc because of cell

death. Remaining CRE-Luc data were normalized to RLuc (CRE-Luc/RLuc = Luc_N), and then either fold change Luc_N (agonist-treatment: (treated-well – well without agonist) ÷ well without agonist) or the percent maximum response (antagonist-treatment: (treated well ÷ well without antagonist) * 100) was calculated. For graphing and IC_{50} calculations, molar concentrations were graphed on the x-axis, transformed using the algorithm X = Log(X), and then nonlinear regression analysis was performed. Graphical data are represented as curve-fitted linear regressions of the mean ± SEM of the transformed molar concentration values. For simplicity, inhibitory potency (IC_{50}) data are reported as the negative logarithm of the molar concentrations of the IC_{50} (pIC_{50}) ± SEM (GraphPad Prism, Version 6.07, LaJolla, CA, USA); n = 3-4 duplicates.

Chapter 6: Implications of the Studies Performed & Where Can We Go from Here?

In this thesis, I ventured to investigate possible mechanisms that may underlie myopia inhibition by atropine and a few other mAChR antagonists. I attempted to do this by identifying important downstream signalling molecules (**Chapter 3 & Appendix A1**), and by investigating possible off-target effects of high-concentration mAChR antagonists (**Chapter 4** & **Chapter 5**). First, I showed that nitric oxide is required for myopia inhibition by atropine in the chick, and that it can inhibit myopia dose-dependently on its own (**Chapter 3**). Little is known about the signalling cascades that are affected by atropine treatment, and these results demonstrate an important link between increased ocular nitric oxide and myopia inhibition. Second, I am the first to report that α_2-adrenoceptor agonists can affect the development of FDM in the chick (**Chapter 4**). Although clonidine and guanfacine *do* inhibit FDM (at high concentrations), I cannot speculate on mechanism due to the likelihood of off-target or even toxic effects. These experiments demonstrate that attributing an experimental outcome – i.e., inhibition of FDM – to the expected drug receptor targets when that drug is applied at large doses is problematic. They identified yet another class of drug that inhibits FDM at high concentration, but has paradoxical results regarding the possible mechanism(s) that may be attributed to their expected receptor targets[152,272]. Finally, we showed that myopia-inhibiting mAChR antagonists can bind to ADRA2A at concentrations similar to those required to inhibit FDM in the chick[159] (**Chapter 5**). This novel finding not only reinforces the fact that high-concentration drug can have unexpected effects *in vivo*, but also provides a range of concentrations within which these particular mAChR antagonists *should* act in a specific manner. Specific caveats and suggested follow-up experiments for each chapter are discussed in greater detail below.

Downstream Signalling Molecules of Atropine-Mediated Myopia Inhibition

Although our data are the first to show clearly that NO can mediate myopia prevention in the chick – both by itself and during atropine-treatment – we did not demonstrate that atropine treatment directly results in upregulation of NO synthesis and release in the retina or any other ocular tissues. This interesting question could be addressed by assaying the expression of NO in the eye after atropine-treatment using DAF-FM[273]. Determining

whether atropine causes directly an upregulation of NO, and pinpointing the cell types that may be involved using immunocytochemical markers, would be valuable in furthering our knowledge of the retinal circuitry and signalling molecules that may underlie myopia inhibition. We do not know how increased NO may result in slowed eye growth, but there is at least some indirect evidence for a few different possibilities. First, increased NO is known to result in uncoupling of gap junctions between retinal horizontal cells, rods and cones, and amacrine cells; this is associated with a switch from a dark-adapted to light-adapted state of the retina, and increased contrast sensitivity and spatial resolution of the visual system. Interestingly, intense light exposure is associated with myopia prevention; thus, it is possible that upregulation of NO may mediate the functional consequences of intense light – i.e., uncoupling of gap junctions – in form-deprived eyes to inhibit myopia. Further evidence for a role of gap junction uncoupling in myopia inhibition is that intravitreal injection of a mimetic peptide designed to block coupling of gap junctions containing connexin 36 (35 in birds) results in light-adaptive-like changes in retinal processing – i.e., increased sensitivity to contrast and high spatial frequencies – and inhibits the development of FDM (Teves[94] and Teves M, et al. IOVS 2014; 55: E-Abstract 3036).

Determining whether dopamine is involved in atropine-mediated myopia inhibition is an important next step. I attempted to do this by simultaneous injection of the dopamine D_2 receptor antagonist spiperone and atropine in form-deprived chicks (**Appendix A1**); the results I obtained were inconclusive. It is expected that spiperone should prevent myopia inhibition by atropine, as it blocks myopia inhibition by "mAChR antagonists" MT3 in the chick (Arumugam B et al. IOVS 2010; 51: ARVO E-Abstract 1195) and MT7 in the tree shrew (Arumugam B et al. IOVS 2012; 53: ARVO E-Abstract 3431), and by apomorphine[112], and goggle removal[108]. If my results, which show a trend towards no role of dopamine D_2-signalling in atropine-mediated myopia inhibition, were confirmed by additional experiments, it would be a very surprising revelation. A speculative explanation for lack of effect of blockade of dopaminergic D_2 signalling could be that there are two separate pathways through which the eye may achieve emmetropization: one involving atropine-nitrergic mediated mechanisms, and one controlled by MT3-dopaminergic mediated mechanisms. This would not be entirely unexpected in a diurnal animal that is

highly dependent on acute vision such as the chick; redundancy of emmetropic mechanisms would help to ensure the best vision possible, and thus increase the odds of survival.

Study Limitations

High dose SNP (1000 nmoles) caused a light-sensitivity reaction in the treated eye. Chicks were hesitant to open their drug-injected eye approximately 5-10 min after injection under normal room light (ca. 500 lux), while no effect was seen for the saline-injected control eye. This sensitivity response was not permanent; chicks were monitored after injection of SNP, and it was found that after 2 hrs the chicks' behavior returned to normal. There was no visual damage to the sensitized eyes, and chicks responded to visual cues (feeding, movement towards the injected eye) normally.

After my work was published, I was alerted to a study that reported that D-NMMA and D-arginine (D-Arg) do not readily enter the cell through the L-arginine (L-Arg) transporter, unlike L-NMMA and L-NIO[274]. This means that the negative effects seen by our assay – i.e., the inability to inhibit FDM by D-Arg and the inability of D-NMMA to inhibit myopia prevention by atropine – may not have been because they are the wrong enantiomer, but instead because they could not as readily enter the target cell(s) to elicit any effect. An additional study was found that reported that D-NMMA does interact with the L-Arg transporter, but at a concentration ca. 20x higher than that required by L-NMMA[275]. Thus, the better negative control experiment involving D-NMMA may have been to test concentrations 20x greater than those required by L-NMMA to inhibit myopia-inhibition by atropine (150 nmoles vs. 6 nmoles). For D-Arg, a concentration of 10,000 nmoles were tested, which is 25x that of the ED_{50} of L-Arg (400 nmoles), and no effect on development of FDM was seen. Therefore, I feel that I can safely conclude that, at least in the case of D-Arg, the negative effect on myopia inhibition was due to the sterospecificity of D-Arg, and not because it could not penetrate the cell. Unfortunately, I was unable to find binding data for D-NMMA at any NOS enzyme.

A-scan ultrasound would have allowed us to measure the relevant internal axial dimensions of the eye – such as vitreous chamber depth, which is more informative than overall eye length, or choroidal thickness, which has been correlated with changes in myopia development due to treatment with muscarinic drugs[44] and nitric oxide synthase inhibitors[46,47]. It would have been useful to compare such results with those in previous studies, which utilized a different NOS inhibitor (L-NAME) whose mechanism of action may differ from that of L-NMMA or L-NIO[224]. This is true also of the experiments involving clonidine and guanfacine; because we are the first to report their ability to inhibit FDM in the chick, it would have been informative to know whether they induce changes in choroidal thickness when they are injected into the eye. Unfortunately, high-resolution ultrasonography was not available to us during the course of this thesis. This does not change our conclusions about the data gathered; myopia development primarily occurs via increased axial length[2], which can be reliably measured using the methods outlined in this thesis.

Alpha-Adrenoceptor Agonist Inhibition of FDM and Off-Target Binding of Muscarinic Antagonists to Alpha$_{2A}$-Adrenoceptor

We have demonstrated that two additional agents – clonidine and guanfacine – inhibit FDM in the chick at high concentration (**Chapter 4**), and that myopia-inhibiting mAChR antagonists can bind to the human ADRA2A receptor when applied at concentrations assumed to be required for myopia inhibition in the chick (**Chapter 5**). Although these data do not establish for certain that atropine and MT3 inhibit myopia via ADRA2A, neither they do not rule out the possibility. They address an important flaw in research investigating the role of mAChRs in myopia inhibition – the *assumption* that drugs such as MT3 and atropine inhibit myopia exclusively through mAChRs – and demonstrate that you cannot always attribute the effects of high concentration drug to its canonical target receptor. Alpha$_{2A}$-adrenoceptor is just one possible off-target receptor out of many; MT3 also interacts with α_{1A}-, α_{1B}-, α_{1D}-, and α_{2C}-adrenoceptors and mAChR M_1. These are just the receptor targets that we know of, and we cannot be sure that MT3 (or any other ligand) will not interact with any other receptor in the eye, unless it is specifically tested. Taken together, these data establish strongly that investigation into possible off-target

mechanisms of established treatment regimes is not a frivolous undertaking, but may provide the opportunity to discover novel therapeutic targets.

These data, regarding the binding behavior of mAChR antagonists at mAChR M_4, cM_4, and hADRA2A, should be of interest to researchers within and outside the field of myopia research. They provide some of the first reports of binding behavior of mAChR antagonists at cM_4 (MT3, oxyphenonium, and mepenzolate), and confirm binding behavior of mAChR antagonists at M_4. There is little literature on non-specific effects of any drug, and our data quantify the off-target binding behaviors of a number of mAChR antagonists at two particular human receptors. They should increase awareness of mAChR antagonist concentrations that we can safely call "selective" and those that should be viewed with marked discretion. We confirmed that binding of orthosteric ligands is not likely to differ between species, but that caution should be used in assuming that binding characteristics of selective – or allosteric – ligands will also be the same when used in different species (**Chapter 5; MT3**). This is not unexpected, but often overlooked; selective ligands bind to less conserved areas – such as the extracellular loops – where the amino acid structure may differ significantly enough between species to result in significant changes of binding behavior[253,266,268].

Study Limitations

We were unable to get successful expression of a functional chicken ADRA2A (cADRA2A) receptor (**Appendix A3**), so we were unable to measure the off-target binding of mAChR antagonists to this receptor type. This was disheartening, as the chicken is the most common myopia model, and information on off-target binding in this organism would have helped to complete our data set. Most regrettable about our inability to get functional expression of cADRA2A is that we could not determine whether MT3 has similar inhibitory potency at ADRA2A in chicken and human, or whether it is significantly different, like we saw at human mAChR M_4.

The amount of clonidine and guanfacine required for myopia-inhibition in the chick were in the same range as those required by atropine (2, 20, and 200 nmoles). Thus, we cannot

attribute the anti-myopia ability of these drugs to the α_2-adrenoceptors, any more than we can contribute the anti-myopia ability of atropine to mAChR M_4. In the case of clonidine, myopia inhibition did not occur until intravitreal injection of 200 nmoles, so the likelihood that it is acting at its intended target to inhibit myopia is low. Action at the choroid, and not the retina/RPE could account for the requirement of high-concentration drug, but at this point it would not be much use to extend the range into lower concentrations; no effect at 2 or 20 nmoles was observed. Although we did not detect any obvious toxic effects of clonidine- or guanfacine-treatment via histological examination (Toluidine blue), we did not test whether treated eyes could recover from FDM and return to emmetropia once the form diffusers were removed. This is an important experiment, because it would provide additional evidence that myopia inhibition by these drugs is not caused by toxicity – as was seen in the highly shortened eyes treated with high dose SNP (**Chapter 3**).

Guanfacine did have a significant effect on the difference in refractive error and axial length at lower concentrations than clonidine (2 & 20 nmoles), which is still in excess of what should be required for "specific" action at ADRA2A – i.e., K_d of gfcn in rat brain homogenate at assumed α_2-adrenoceptors is 1.77 ± 0.24 nM[276], versus assumed concentrations of 6 µM in the retina, and 1.5 µM in the choroid[234] after intravitreal injection of 2 nmoles gfcn in the chick eye. Nevertheless, I decided to investigate possible mechanisms of gfcn-mediated myopia inhibition with a few pilot experiments (**Appendix A2**). First, I attempted to block myopia inhibition by gfcn using yohimbine, an α_2-adrenoceptor antagonist with selectivity for the ADRA2A subtype. When injected simultaneously with gfcn, yohimbine (6 nmoles) did not block myopia prevention. This would seem to indicate that however gfcn is inhibiting myopia, it is not doing so though ADRA2A. Second, I attempted to use L-NMMA to block myopia inhibition by gfcn, but it too failed to exert an effect. This is another surprising result; if atropine and gfcn inhibit myopia via the same mechanism, gfcn should also require activation of NOS to slow down eye growth. Myopia inhibition by gfcn and atropine at concentrations plateaus near 50%. I injected simultaneously 200 nmoles of gfcn and 200 nmoles of atropine to determine whether their effects were additive; atropine + gfcn-treatment resulted in greater myopia inhibition than either atropine or gfcn alone. Investigation into possible mechanisms of gfcn-mediated myopia inhibition has demonstrated that gfcn does not seem to be dependent

on the same mechanisms as atropine to regulate eye growth; although their mechanisms do seem to interact in some way – e.g., at a downstream integrator (possibly NO), where inputs from multiple sources may sum nonlinearly to regulate eye growth. It would be interesting to know whether gfcn-mediated myopia inhibition was dependent on signalling through the dopamine D_2 receptor, as this could further support myopia inhibition via different mechanisms for atropine, gfcn, and MT3.

Could There Be Two Separate Growth-Regulating Pathways in the Chick?

Many questions remain regarding the mechanism(s) through which atropine, MT3, clonidine, and guanfacine may inhibit FDM in the chick, but a recurring theme in this thesis is the possibility of multiple emmetropia-controlling pathways – one dependent on NO (atropine; **Chapter 3, Appendix A1**) and one that is NO-independent (gfcn; **Appendix A2**). There is little direct evidence of this occurring, but I am not the first to suggest this[237], and there is controversy about whether experimentally-induced FDM and LIM are mechanistically the same[29,109,115,277]. A single injection of 6-OHDA, a catecholamine-specific toxin, inhibited FDM but had no effect on LIM[33]. Atropine can inhibit FDM and LIM equally well[115,278], but MT3 inhibits FDM and has *no* effect on LIM. Myopia inhibition by goggle removal is prevented by dopamine antagonism in the case of FDM, but it is only partially blocked in LIM[109]. Besides differences between FDM and LIM, there are differences in results for different drug-treatments. Atropine, pirenzepine, and oxyphenonium induce choroidal thickening[44] but MT3 induces choroidal thinning[34] in the chick, even though all treatments inhibit FDM in the chick. FDM inhibition by MT3 in the chick and MT7 in the tree shrew can be blocked by antagonism of dopamine D_2-mediated signalling, but the same treatment does not seem to have an effect on FDM inhibition by atropine (**Appendix A1**). Finally, combination of gfcn and atropine resulted in a slightly increased anti-myopia effect (**Appendix A2**), but combination of atropine and apomorphine does not[115].

There are significant caveats to this hypothesis. Many of these results are not consistent with a unifying hypothesis. For example, why would 6-OHDA inhibit FDM, but have no effect on LIM, when it is supposed to kill dopaminergic neurons, whose activation inhibits

FDM and LIM? Also, why does atropine + apomorphine not result in an increased anti-myopia effect, when my data support no role of dopaminergic signalling in atropine-mediated inhibition? Clearly, results such as these cannot be easily explained easily. Retinal visual processing is extremely complex, and it is likely that past experiments did not give enough credit to the intricate computational circuitry that exists; we are just now beginning to understand the intricacies of reciprocal signalling that occurs in the retina, which makes it difficult to draw conclusions about results gained from treatment with high-concentration drug. In addition, chicks have cone-dominated retinas (compared to rod-dominated retinas of humans), and they possess visual processing and focal mechanisms that humans lack, such as significant choroidal changes in response to defocus, and corneal – as well as lenticular – accommodative mechanisms. Therefore, even if we *could* prove that birds do have multiple growth-regulating pathways, there is a distinct possibly that this could be a species-specific attribute and may not apply humans or other diurnal mammals.

Conclusion

Whether myopia inhibition by the many different reported ligands – mAChR antagonists, MT3, ADRA2 agonists, dopaminergic agonists, and NO sources to name a few – occurs through the same mechanism, remains to be determined; the target receptors, signalling cascades, and even target tissues for these agents remain unknown. Data reported here further support a role for NO in myopia inhibition, and may provide a mechanism for myopia prevention by intense outdoors light. I have contributed significantly to the literature regarding behavior of mAChR antagonists at known target receptors – M_4 and cM_4 – and possible off-target receptors – ADRA2A, which could possibly be novel therapeutic targets for anti-myopia therapies. It is our hope that these data will be helpful in i) shifting the perception of the role of mAChRs in myopia prevention from a commonly accepted assumption to one that is regarded with greater caution, and ii) guiding evidence-based design of more accurate and informative drug-treatment experiments in future studies.

Bibliography

1 Carr, B. J. & Stell, W. K. Nitric Oxide (NO) Mediates the Inhibition of Form-Deprivation Myopia by Atropine in Chicks. *Scientific Reports* **6**, 9, doi:10.1038/s41598-016-0002-7 (2016).

2 Wallman, J. & Winawer, J. Homeostasis of eye growth and the question of myopia. *Neuron* **43**, 447-468, doi:10.1016/j.neuron.2004.08.008 (2004).

3 Dolgin, E. The myopia boom. *Nature* **519**, 276-278, doi:10.1038/519276a (2015).

4 Foster, P. J. & Jiang, Y. Epidemiology of myopia. *Eye (Lond)* **28**, 202-208, doi:10.1038/eye.2013.280 (2014).

5 Prevalence of myopia and hyperopia in 6- to 72-month-old african american and Hispanic children: the multi-ethnic pediatric eye disease study. *Ophthalmology* **117**, 140-147.e143, doi:10.1016/j.ophtha.2009.06.009 (2010).

6 Wen, G. *et al.* Prevalence of myopia, hyperopia, and astigmatism in non-Hispanic white and Asian children: multi-ethnic pediatric eye disease study. *Ophthalmology* **120**, 2109-2116, doi:10.1016/j.ophtha.2013.06.039 (2013).

7 French, A. N., Morgan, I. G., Burlutsky, G., Mitchell, P. & Rose, K. A. Prevalence and 5- to 6-year incidence and progression of myopia and hyperopia in Australian schoolchildren. *Ophthalmology* **120**, 1482-1491, doi:10.1016/j.ophtha.2012.12.018 (2013).

8 Dirani, M. *et al.* Refractive errors in twin studies. *Twin Res Hum Genet* **9**, 566-572, doi:10.1375/183242706778024955 (2006).

9 Mutti, D. O., Mitchell, G. L., Moeschberger, M. L., Jones, L. A. & Zadnik, K. Parental myopia, near work, school achievement, and children's refractive error. *Invest Ophthalmol Vis Sci* **43**, 3633-3640 (2002).

10 Ip, J. M. *et al.* Ethnic differences in the impact of parental myopia: findings from a population-based study of 12-year-old Australian children. *Invest Ophthalmol Vis Sci* **48**, 2520-2528, doi:10.1167/iovs.06-0716 (2007).

11 Lam, D. S. *et al.* The effect of parental history of myopia on children's eye size and growth: results of a longitudinal study. *Invest Ophthalmol Vis Sci* **49**, 873-876, doi:10.1167/iovs.06-1097 (2008).

12 Xiang, F., He, M. & Morgan, I. G. The impact of parental myopia on myopia in Chinese children: population-based evidence. *Optom Vis Sci* **89**, 1487-1496, doi:10.1097/OPX.0b013e31826912e0 (2012).

13 Guo, L. *et al.* Prevalence and associated factors of myopia among primary and middle school-aged students: a school-based study in Guangzhou. *Eye (Lond)*, doi:10.1038/eye.2016.39 (2016).

14 Verhoeven, V. J. *et al.* Genome-wide meta-analyses of multiancestry cohorts identify multiple new susceptibility loci for refractive error and myopia. *Nat Genet* **45**, 314-318, doi:10.1038/ng.2554 (2013).

15 Solouki, A. M. *et al.* A genome-wide association study identifies a susceptibility locus for refractive errors and myopia at 15q14. *Nat Genet* **42**, 897-901, doi:10.1038/ng.663 (2010).

16 Cheng, C. Y. *et al.* Nine loci for ocular axial length identified through genome-wide association studies, including shared loci with refractive error. *Am J Hum Genet* **93**, 264-277, doi:10.1016/j.ajhg.2013.06.016 (2013).

17 Khor, C. C. *et al.* Genome-wide association study identifies ZFHX1B as a susceptibility locus for severe myopia. *Hum Mol Genet* **22**, 5288-5294, doi:10.1093/hmg/ddt385 (2013).
18 Kiefer, A. K. *et al.* Genome-wide analysis points to roles for extracellular matrix remodeling, the visual cycle, and neuronal development in myopia. *PLoS Genet* **9**, e1003299, doi:10.1371/journal.pgen.1003299 (2013).
19 Li, Z. *et al.* A genome-wide association study reveals association between common variants in an intergenic region of 4q25 and high-grade myopia in the Chinese Han population. *Hum Mol Genet* **20**, 2861-2868, doi:10.1093/hmg/ddr169 (2011).
20 Shi, Y. *et al.* A genome-wide meta-analysis identifies two novel loci associated with high myopia in the Han Chinese population. *Hum Mol Genet* **22**, 2325-2333, doi:10.1093/hmg/ddt066 (2013).
21 Fan, Q. *et al.* Childhood gene-environment interactions and age-dependent effects of genetic variants associated with refractive error and myopia: The CREAM Consortium. *Sci Rep* **6**, 25853, doi:10.1038/srep25853 (2016).
22 Rose, K. A., Morgan, I. G., Smith, W. & Mitchell, P. High heritability of myopia does not preclude rapid changes in prevalence. *Clin Experiment Ophthalmol* **30**, 168-172, doi:10.1046/j.1442-9071.2002.00521.x (2002).
23 Schaeffel, F. & Feldkaemper, M. Animal models in myopia research. *Clin Exp Optom* **98**, 507-517, doi:10.1111/cxo.12312 (2015).
24 Hubel, D. H., Wiesel, T. N. & LeVay, S. Functional architecture of area 17 in normal and monocularly deprived macaque monkeys. *Cold Spring Harb Symp Quant Biol* **40**, 581-589, doi:10.1101/SQB.1976.040.01.054 (1976).
25 Wiesel, T. N. & Raviola, E. Myopia and eye enlargement after neonatal lid fusion in monkeys. *Nature* **266**, 66-68, doi:10.1038/266066a0 (1977).
26 Wallman, J., Turkel, J. & Trachtman, J. Extreme myopia produced by modest change in early visual experience. *Science* **201**, 1249-1251, doi:10.1126/science.694514 (1978).
27 Schaeffel, F., Glasser, A. & Howland, H. C. Accommodation, refractive error and eye growth in chickens. *Vision Res* **28**, 639-657, doi:10.1016/0042-6989(88)90113-7 (1988).
28 Diether, S. & Schaeffel, F. Long-term changes in retinal contrast sensitivity in chicks from frosted occluders and drugs: relations to myopia? *Vision Res* **39**, 2499-2510, doi:10.1016/S0042-6989(99)00005-X (1999).
29 Morgan, I. G., Ashby, R. S. & Nickla, D. L. Form deprivation and lens-induced myopia: are they different? *Ophthalmic Physiol Opt* **33**, 355-361, doi:10.1111/opo.12059 (2013).
30 Troilo, D., Gottlieb, M. D. & Wallman, J. Visual deprivation causes myopia in chicks with optic nerve section. *Curr Eye Res* **6**, 993-999, doi:10.3109/02713688709034870 (1987).
31 Wallman, J., Gottlieb, M. D., Rajaram, V. & Fugate-Wentzek, L. A. Local retinal regions control local eye growth and myopia. *Science* **237**, 73-77, doi:10.1126/science.3603011 (1987).
32 Choh, V., Lew, M. Y., Nadel, M. W. & Wildsoet, C. F. Effects of interchanging hyperopic defocus and form deprivation stimuli in normal and optic nerve-

sectioned chicks. *Vision Res* **46**, 1070-1079, doi:10.1016/j.visres.2005.08.020 (2006).

33 Schaeffel, F., Hagel, G., Bartmann, M., Kohler, K. & Zrenner, E. 6-Hydroxy dopamine does not affect lens-induced refractive errors but suppresses deprivation myopia. *Vision Res* **34**, 143-149, doi:10.1016/0042-6989(94)90327-1 (1994).

34 Nickla, D. L., Yusupova, Y. & Totonelly, K. The Muscarinic Antagonist MT3 Distinguishes Between Form Deprivation- and Negative Lens-Induced Myopia in Chicks. *Curr Eye Res* **40**, 962-967, doi:10.3109/02713683.2014.967870 (2015).

35 Napper, G. A. *et al.* The duration of normal visual exposure necessary to prevent form deprivation myopia in chicks. *Vision Res* **35**, 1337-1344, doi:10.1016/0042-6989(94)00226-C (1995).

36 Schmid, K. L. & Wildsoet, C. F. Effects on the compensatory responses to positive and negative lenses of intermittent lens wear and ciliary nerve section in chicks. *Vision Res* **36**, 1023-1036, doi:10.1016/0042-6989(95)00191-3 (1996).

37 Wallman, J. & Adams, J. I. Developmental aspects of experimental myopia in chicks: susceptibility, recovery and relation to emmetropization. *Vision Res* **27**, 1139-1163, doi:10.1016/0042-6989(87)90027-7 (1987).

38 Glasser, A., Troilo, D. & Howland, H. C. The mechanism of corneal accommodation in chicks. *Vision Res* **34**, 1549-1566, doi:10.1016/0042-6989(94)90112-0 (1994).

39 Schaeffel, F. & Howland, H. C. Corneal accommodation in chick and pigeon. *J Comp Physiol A* **160**, 375-384, doi:10.1007/BF00613027 (1987).

40 Nickla, D. L. & Wallman, J. The multifunctional choroid. *Prog Retin Eye Res* **29**, 144-168, doi:10.1016/j.preteyeres.2009.12.002 (2010).

41 Howlett, M. H. & McFadden, S. A. Spectacle lens compensation in the pigmented guinea pig. *Vision Res* **49**, 219-227, doi:10.1016/j.visres.2008.10.008 (2009).

42 Troilo, D., Nickla, D. L. & Wildsoet, C. F. Choroidal thickness changes during altered eye growth and refractive state in a primate. *Invest Ophthalmol Vis Sci* **41**, 1249-1258 (2000).

43 Hung, L. F., Wallman, J. & Smith, E. L., 3rd. Vision-dependent changes in the choroidal thickness of macaque monkeys. *Invest Ophthalmol Vis Sci* **41**, 1259-1269 (2000).

44 Nickla, D. L., Zhu, X. & Wallman, J. Effects of muscarinic agents on chick choroids in intact eyes and eyecups: evidence for a muscarinic mechanism in choroidal thinning. *Ophthalmic Physiol Opt* **33**, 245-256, doi:10.1111/opo.12054 (2013).

45 Nickla, D. L., Totonelly, K. & Dhillon, B. Dopaminergic agonists that result in ocular growth inhibition also elicit transient increases in choroidal thickness in chicks. *Exp Eye Res* **91**, 715-720, doi:10.1016/j.exer.2010.08.021 (2010).

46 Nickla, D. L. & Wildsoet, C. F. The effect of the nonspecific nitric oxide synthase inhibitor NG-nitro-L-arginine methyl ester on the choroidal compensatory response to myopic defocus in chickens. *Optom Vis Sci* **81**, 111-118, doi:10.1097/00006324-200402000-00009 (2004).

47 Nickla, D. L., Wilken, E., Lytle, G., Yom, S. & Mertz, J. Inhibiting the transient choroidal thickening response using the nitric oxide synthase inhibitor l-NAME prevents the ameliorative effects of visual experience on ocular growth in two

different visual paradigms. *Exp Eye Res* **83**, 456-464, doi:10.1016/j.exer.2006.01.029 (2006).

48 Nickla, D. L., Damyanova, P. & Lytle, G. Inhibiting the neuronal isoform of nitric oxide synthase has similar effects on the compensatory choroidal and axial responses to myopic defocus in chicks as does the non-specific inhibitor L-NAME. *Exp Eye Res* **88**, 1092-1099, doi:10.1016/j.exer.2009.01.012 (2009).

49 Chen, B. Y., Wang, C. Y., Chen, W. Y. & Ma, J. X. Altered TGF-beta2 and bFGF expression in scleral desmocytes from an experimentally-induced myopia guinea pig model. *Graefes Arch Clin Exp Ophthalmol* **251**, 1133-1144, doi:10.1007/s00417-013-2269-8 (2013).

50 Kusakari, T., Sato, T. & Tokoro, T. Visual deprivation stimulates the exchange of the fibrous sclera into the cartilaginous sclera in chicks. *Exp Eye Res* **73**, 533-546, doi:10.1006/exer.2001.1064 (2001).

51 Rohrer, B. & Stell, W. K. Basic fibroblast growth factor (bFGF) and transforming growth factor beta (TGF-beta) act as stop and go signals to modulate postnatal ocular growth in the chick. *Exp Eye Res* **58**, 553-561, doi:10.1006/exer.1994.1049 (1994).

52 Seko, Y., Shimokawa, H. & Tokoro, T. Expression of bFGF and TGF-beta 2 in experimental myopia in chicks. *Invest Ophthalmol Vis Sci* **36**, 1183-1187, doi:10.1097/00006982-199616020-00029 (1995).

53 Seko, Y., Tanaka, Y. & Tokoro, T. Influence of bFGF as a potent growth stimulator and TGF-beta as a growth regulator on scleral chondrocytes and scleral fibroblasts in vitro. *Ophthalmic Res* **27**, 144-152, doi:10.1002/(sici)1099-0844(199709)15:3<191::aid-cbf738>3.0.co;2-2 (1995).

54 Bitzer, M., Feldkaemper, M. & Schaeffel, F. Visually induced changes in components of the retinoic acid system in fundal layers of the chick. *Exp Eye Res* **70**, 97-106, doi:10.1006/exer.1999.0762 (2000).

55 Ding, Y. *et al.* Association analysis of retinoic acid receptor beta (RARbeta) gene with high myopia in Chinese subjects. *Mol Vis* **16**, 855-861 (2010).

56 Mao, J. F., Liu, S. Z. & Dou, X. Q. Retinoic acid metabolic change in retina and choroid of the guinea pig with lens-induced myopia. *Int J Ophthalmol* **5**, 670-674, doi:10.3980/j.issn.2222-3959.2012.06.04 (2012).

57 McFadden, S. A., Howlett, M. H. & Mertz, J. R. Retinoic acid signals the direction of ocular elongation in the guinea pig eye. *Vision Res* **44**, 643-653, doi:10.1016/j.visres.2003.11.002 (2004).

58 Mertz, J. R. & Wallman, J. Choroidal retinoic acid synthesis: a possible mediator between refractive error and compensatory eye growth. *Exp Eye Res* **70**, 519-527, doi:10.1006/exer.1999.0813 (2000).

59 Seko, Y., Shimokawa, H. & Tokoro, T. In vivo and in vitro association of retinoic acid with form-deprivation myopia in the chick. *Exp Eye Res* **63**, 443-452, doi:10.1006/exer.1996.0134 (1996).

60 Seko, Y., Shimizu, M. & Tokoro, T. Retinoic acid increases in the retina of the chick with form deprivation myopia. *Ophthalmic Res* **30**, 361-367, doi:10.1159/000055496 (1998).

61 Troilo, D., Nickla, D. L., Mertz, J. R. & Summers Rada, J. A. Change in the synthesis rates of ocular retinoic acid and scleral glycosaminoglycan during

experimentally altered eye growth in marmosets. *Invest Ophthalmol Vis Sci* **47**, 1768-1777, doi:10.1167/iovs.05-0298 (2006).

62 Wang, S., Liu, S., Mao, J. & Wen, D. Effect of retinoic acid on the tight junctions of the retinal pigment epithelium-choroid complex of guinea pigs with lens-induced myopia in vivo. *Int J Mol Med* **33**, 825-832, doi:10.3892/ijmm.2014.1651 (2014).

63 Marzani, D. & Wallman, J. Growth of the two layers of the chick sclera is modulated reciprocally by visual conditions. *Invest Ophthalmol Vis Sci* **38**, 1726-1739 (1997).

64 Rada, J. A., Thoft, R. A. & Hassell, J. R. Increased aggrecan (cartilage proteoglycan) production in the sclera of myopic chicks. *Dev Biol* **147**, 303-312, doi:10.1016/0012-1606(91)90288-E (1991).

65 Rada, J. A., McFarland, A. L., Cornuet, P. K. & Hassell, J. R. Proteoglycan synthesis by scleral chondrocytes is modulated by a vision dependent mechanism. *Curr Eye Res* **11**, 767-782, doi:10.3109/02713689209000750 (1992).

66 Rada, J. A. & Matthews, A. L. Visual deprivation upregulates extracellular matrix synthesis by chick scleral chondrocytes. *Invest Ophthalmol Vis Sci* **35**, 2436-2447 (1994).

67 Rada, J. A., Hollaway, L. R., Lam, W., Li, N. & Napoli, J. L. Identification of RALDH2 as a visually regulated retinoic acid synthesizing enzyme in the chick choroid. *Invest Ophthalmol Vis Sci* **53**, 1649-1662, doi:10.1167/iovs.11-8444 (2012).

68 Harper, A. R., Wang, X., Moiseyev, G., Ma, J. X. & Summers, J. A. Postnatal Chick Choroids Exhibit Increased Retinaldehyde Dehydrogenase Activity During Recovery From Form Deprivation Induced Myopia. *Invest Ophthalmol Vis Sci* **57**, 4886-4897, doi:10.1167/iovs.16-19395 (2016).

69 Truong, H. T., Cottriall, C. L., Gentle, A. & McBrien, N. A. Pirenzepine affects scleral metabolic changes in myopia through a non-toxic mechanism. *Exp Eye Res* **74**, 103-111, doi:10.1006/exer.2001.1107 (2002).

70 Phillips, J. R., Khalaj, M. & McBrien, N. A. Induced myopia associated with increased scleral creep in chick and tree shrew eyes. *Invest Ophthalmol Vis Sci* **41**, 2028-2034 (2000).

71 Siegwart, J. T., Jr. & Norton, T. T. Regulation of the mechanical properties of tree shrew sclera by the visual environment. *Vision Res* **39**, 387-407, doi:10.1016/S0042-6989(98)00150-3 (1999).

72 Curtin, B. J. Physiopathologic aspects of scleral stress-strain. *Trans Am Ophthalmol Soc* **67**, 417-461 (1969).

73 Curtin, B. J., Iwamoto, T. & Renaldo, D. P. Normal and staphylomatous sclera of high myopia. An electron microscopic study. *Arch Ophthalmol* **97**, 912-915 (1979).

74 Curtin, B. J. Pathologic myopia. *Acta Ophthalmol Suppl* **185**, 105-106, doi:10.1111/j.1755-3768.1988.tb02680.x (1988).

75 Siegwart, J. T., Jr. & Norton, T. T. Selective regulation of MMP and TIMP mRNA levels in tree shrew sclera during minus lens compensation and recovery. *Invest Ophthalmol Vis Sci* **46**, 3484-3492, doi:10.1167/iovs.05-0194 (2005).

76 McBrien, N. A. & Gentle, A. Role of the sclera in the development and pathological complications of myopia. *Prog Retin Eye Res* **22**, 307-338, doi:10.1016/S1350-9462(02)00063-0 (2003).

77 Avetisov, E. S., Tarutta, E. P., Iomdina, E. N., Vinetskaya, M. I. & Andreyeva, L. D. Nonsurgical and surgical methods of sclera reinforcement in progressive myopia. *Acta Ophthalmol Scand* **75**, 618-623, doi:10.1111/j.1600-0420.1997.tb00617.x (1997).
78 Wollensak, G. & Spoerl, E. Collagen crosslinking of human and porcine sclera. *J Cataract Refract Surg* **30**, 689-695, doi:10.1016/j.jcrs.2003.11.032 (2004).
79 Wollensak, G., Iomdina, E., Dittert, D. D., Salamatina, O. & Stoltenburg, G. Cross-linking of scleral collagen in the rabbit using riboflavin and UVA. *Acta Ophthalmol Scand* **83**, 477-482, doi:10.1111/j.1600-0420.2005.00447.x (2005).
80 Wollensak, G. & Iomdina, E. Long-term biomechanical properties after collagen crosslinking of sclera using glyceraldehyde. *Acta Ophthalmol* **86**, 887-893, doi:10.1111/j.1755-3768.2007.01156.x (2008).
81 Zhang, Y. *et al.* Comparison of riboflavin/ultraviolet-A cross-linking in porcine, rabbit, and human sclera. *Biomed Res Int* **2014**, 194204, doi:10.1155/2014/194204 (2014).
82 Chu, Y. *et al.* The Effects of Scleral Collagen Cross-Linking Using Glyceraldehyde on the Progression of Form-Deprived Myopia in Guinea Pigs. *J Ophthalmol* **2016**, 3526153, doi:10.1155/2016/3526153 (2016).
83 Dotan, A. *et al.* Scleral Cross-linking Using Riboflavin and Ultraviolet-A Radiation for Prevention of Axial Myopia in a Rabbit Model. *J Vis Exp*, e53201, doi:10.3791/53201 (2016).
84 Elsheikh, A. & Phillips, J. R. Is scleral cross-linking a feasible treatment for myopia control? *Ophthalmic Physiol Opt* **33**, 385-389, doi:10.1111/opo.12043 (2013).
85 Iseli, H. P. *et al.* Scleral cross-linking by riboflavin and blue light application in young rabbits: damage threshold and eye growth inhibition. *Graefes Arch Clin Exp Ophthalmol* **254**, 109-122, doi:10.1007/s00417-015-3213-x (2016).
86 Charman, W. N. & Radhakrishnan, H. Accommodation, pupil diameter and myopia. *Ophthalmic Physiol Opt* **29**, 72-79, doi:10.1111/j.1475-1313.2008.00611.x (2009).
87 Masland, R. H. The neuronal organization of the retina. *Neuron* **76**, 266-280, doi:10.1016/j.neuron.2012.10.002 (2012).
88 Gollisch, T. & Meister, M. Eye smarter than scientists believed: neural computations in circuits of the retina. *Neuron* **65**, 150-164, doi:10.1016/j.neuron.2009.12.009 (2010).
89 Shi, Q. & Stell, W. K. Die Fledermaus: regarding optokinetic contrast sensitivity and light-adaptation, chicks are mice with wings. *PLoS One* **8**, e75375, doi:10.1371/journal.pone.0075375 (2013).
90 Fu, Y. Phototransduction in Rods and Cones. *Webvision: The Organization of the Retina and Visual System*, (Online) http://webvision.med.utah.edu/ (2010).
91 Heidelberger, R., Thoreson, W. B. & Witkovsky, P. Synaptic transmission at retinal ribbon synapses. *Prog Retin Eye Res* **24**, 682-720, doi:10.1016/j.preteyeres.2005.04.002 (2005).
92 Barnes, S. & Kelly, M. E. Calcium channels at the photoreceptor synapse. *Adv Exp Med Biol* **514**, 465-476, doi:10.1007/978-1-4615-0121-3_28 (2002).

93 DeVries, S. H., Qi, X., Smith, R., Makous, W. & Sterling, P. Electrical coupling between mammalian cones. *Curr Biol* **12**, 1900-1907, doi:10.1016/S0960-9822(02)01261-7 (2002).
94 Benavente-Perez, A. *et al.* Abstracts from the 15th International Myopia Conference. *Eye and Vision* **3**, 1-11, doi:10.1186/s40662-016-0057-3 (2016).
95 Euler, T., Haverkamp, S., Schubert, T. & Baden, T. Retinal bipolar cells: elementary building blocks of vision. *Nat Rev Neurosci* **15**, 507-519, doi:10.1038/nrn3783 (2014).
96 MacNeil, M. A., Heussy, J. K., Dacheux, R. F., Raviola, E. & Masland, R. H. The population of bipolar cells in the rabbit retina. *J Comp Neurol* **472**, 73-86, doi:10.1002/cne.20063 (2004).
97 Wassle, H., Puller, C., Muller, F. & Haverkamp, S. Cone contacts, mosaics, and territories of bipolar cells in the mouse retina. *J Neurosci* **29**, 106-117, doi:10.1523/jneurosci.4442-08.2009 (2009).
98 Ashby, R., Ohlendorf, A. & Schaeffel, F. The effect of ambient illuminance on the development of deprivation myopia in chicks. *Invest Ophthalmol Vis Sci* **50**, 5348-5354, doi:10.1167/iovs.09-3419 (2009).
99 Ashby, R. S. & Schaeffel, F. The effect of bright light on lens compensation in chicks. *Invest Ophthalmol Vis Sci* **51**, 5247-5253, doi:10.1167/iovs.09-4689 (2010).
100 French, A. N., Ashby, R. S., Morgan, I. G. & Rose, K. A. Time outdoors and the prevention of myopia. *Exp Eye Res* **114**, 58-68, doi:10.1016/j.exer.2013.04.018 (2013).
101 Cohen, Y., Peleg, E., Belkin, M., Polat, U. & Solomon, A. S. Ambient illuminance, retinal dopamine release and refractive development in chicks. *Exp Eye Res* **103**, 33-40, doi:10.1016/j.exer.2012.08.004 (2012).
102 Feldkaemper, M. & Schaeffel, F. An updated view on the role of dopamine in myopia. *Exp Eye Res* **114**, 106-119, doi:10.1016/j.exer.2013.02.007 (2013).
103 Huang, F. *et al.* Activation of dopamine D2 receptor is critical for the development of form-deprivation myopia in the C57BL/6 mouse. *Invest Ophthalmol Vis Sci* **55**, 5537-5544, doi:10.1167/iovs.13-13211 (2014).
104 Iuvone, P. M., Tigges, M., Fernandes, A. & Tigges, J. Dopamine synthesis and metabolism in rhesus monkey retina: development, aging, and the effects of monocular visual deprivation. *Vis Neurosci* **2**, 465-471, doi:10.1017/S0952523800012360 (1989).
105 Iuvone, P. M., Tigges, M., Stone, R. A., Lambert, S. & Laties, A. M. Effects of apomorphine, a dopamine receptor agonist, on ocular refraction and axial elongation in a primate model of myopia. *Invest Ophthalmol Vis Sci* **32**, 1674-1677 (1991).
106 Jiang, L. *et al.* Effects of dopaminergic agents on progression of naturally occurring myopia in albino guinea pigs (Cavia porcellus). *Invest Ophthalmol Vis Sci* **55**, 7508-7519, doi:10.1167/iovs.14-14294 (2014).
107 Luft, W. A., Iuvone, P. M. & Stell, W. K. Spatial, temporal, and intensive determinants of dopamine release in the chick retina. *Vis Neurosci* **21**, 627-635, doi:10.1017/s0952523804214110 (2004).

108 McCarthy, C. S., Megaw, P., Devadas, M. & Morgan, I. G. Dopaminergic agents affect the ability of brief periods of normal vision to prevent form-deprivation myopia. *Exp Eye Res* **84**, 100-107, doi:10.1016/j.exer.2006.09.018 (2007).
109 Nickla, D. L. & Totonelly, K. Dopamine antagonists and brief vision distinguish lens-induced- and form-deprivation-induced myopia. *Exp Eye Res* **93**, 782-785, doi:10.1016/j.exer.2011.08.001 (2011).
110 Nickla, D. L., Lee, L. & Totonelly, K. Nitric oxide synthase inhibitors prevent the growth-inhibiting effects of quinpirole. *Optom Vis Sci* **90**, 1167-1175, doi:10.1097/opx.0000000000000041 (2013).
111 Pendrak, K. *et al.* Retinal dopamine in the recovery from experimental myopia. *Curr Eye Res* **16**, 152-157, doi:10.1076/ceyr.16.2.152.5090 (1997).
112 Rohrer, B., Spira, A. W. & Stell, W. K. Apomorphine blocks form-deprivation myopia in chickens by a dopamine D2-receptor mechanism acting in retina or pigmented epithelium. *Vis Neurosci* **10**, 447-453, doi:10.1017/S0952523800004673 (1993).
113 Rohrer, B., Iuvone, P. M. & Stell, W. K. Stimulation of dopaminergic amacrine cells by stroboscopic illumination or fibroblast growth factor (bFGF, FGF-2) injections: possible roles in prevention of form-deprivation myopia in the chick. *Brain Res* **686**, 169-181, doi:10.1016/0006-8993(95)00370-6 (1995).
114 Schaeffel, F., Bartmann, M., Hagel, G. & Zrenner, E. Studies on the role of the retinal dopamine/melatonin system in experimental refractive errors in chickens. *Vision Res* **35**, 1247-1264, doi:10.1016/0042-6989(94)00221-7 (1995).
115 Schmid, K. L. & Wildsoet, C. F. Inhibitory effects of apomorphine and atropine and their combination on myopia in chicks. *Optom Vis Sci* **81**, 137-147, doi:10.1097/00006324-200402000-00012 (2004).
116 Schwahn, H. N., Kaymak, H. & Schaeffel, F. Effects of atropine on refractive development, dopamine release, and slow retinal potentials in the chick. *Visual neuroscience* **17**, 165-176 (2000).
117 Seko, Y., Tanaka, Y. & Tokoro, T. Apomorphine inhibits the growth-stimulating effect of retinal pigment epithelium on scleral cells in vitro. *Cell Biochem Funct* **15**, 191-196, doi:10.1002/(sici)1099-0844(199709)15:3<191::aid-cbf738>3.0.co;2-2 (1997).
118 Stone, R. A., Lin, T., Laties, A. M. & Iuvone, P. M. Retinal dopamine and form-deprivation myopia. *Proc Natl Acad Sci U S A* **86**, 704-706, doi:10.1073/pnas.86.2.704 (1989).
119 Daniels, B. A. & Baldridge, W. H. The light-induced reduction of horizontal cell receptive field size in the goldfish retina involves nitric oxide. *Vis Neurosci* **28**, 137-144, doi:10.1017/s0952523810000490 (2011).
120 Bloomfield, S. A. & Volgyi, B. The diverse functional roles and regulation of neuronal gap junctions in the retina. *Nat Rev Neurosci* **10**, 495-506, doi:10.1038/nrn2636 (2009).
121 Kolb, H. Roles of Amacrine Cells. *Webvision: The Organization of the Retina and Visual System*, (Online) http://webvision.med.utah.edu (2012).
122 Masland, R. H. Cell populations of the retina: the Proctor lecture. *Invest Ophthalmol Vis Sci* **52**, 4581-4591, doi:10.1167/iovs.10-7083 (2011).

123 Famiglietti, E. V. Dendritic co-stratification of ON and ON-OFF directionally selective ganglion cells with starburst amacrine cells in rabbit retina. *The Journal of comparative neurology* **324**, 322-335, doi:10.1002/cne.903240303 (1992).
124 Sanes, J. R. & Masland, R. H. The types of retinal ganglion cells: current status and implications for neuronal classification. *Annu Rev Neurosci* **38**, 221-246, doi:10.1146/annurev-neuro-071714-034120 (2015).
125 Kandel, E., Schwartz, J. & Jessel, T. *Principles of Neural Science*. Vol. Fourth Edition (McGraw-Hill, 2000).
126 McBrien, N. A., Moghaddam, H. O., Cottriall, C. L., Leech, E. M. & Cornell, L. M. The effects of blockade of retinal cell action potentials on ocular growth, emmetropization and form deprivation myopia in young chicks. *Vision Res* **35**, 1141-1152, doi:10.1016/0042-6989(94)00237-G (1995).
127 Norton, T. T., Essinger, J. A. & McBrien, N. A. Lid-suture myopia in tree shrews with retinal ganglion cell blockade. *Vis Neurosci* **11**, 143-153, doi:10.1017/S0952523800011184 (1994).
128 Troilo, D. Experimental studies of emmetropization in the chick. *Ciba Found Symp* **155**, 89-102; discussion 102-114, doi:10.1002/9780470514023.ch6 (1990).
129 Wildsoet, C. & Wallman, J. Choroidal and scleral mechanisms of compensation for spectacle lenses in chicks. *Vision Res* **35**, 1175-1194, doi:10.1016/0042-6989(94)00233-C (1995).
130 Wildsoet, C. Neural pathways subserving negative lens-induced emmetropization in chicks--insights from selective lesions of the optic nerve and ciliary nerve. *Curr Eye Res* **27**, 371-385, doi:10.1076/ceyr.27.6.371.18188 (2003).
131 Wilson, M. & Lindstrom, S. H. What the bird's brain tells the bird's eye: the function of descending input to the avian retina. *Vis Neurosci* **28**, 337-350, doi:10.1017/s0952523811000022 (2011).
132 Wallenberg, A. Das mediale Opticusbündel der Taube. *Neurol Zbl* **17**, 532–537 (1898).
133 Ramón y Cajal, S. Nouvelles contributions à l'étude histologique de la rétine. *Journal de l'Anatomie et de la Physiologie* **32**, 481–543 (1896).
134 Cowan, W. M. & Powell, T. P. Centrifugal Fibres in the Avian Visual System. *Proc R Soc Lond B Biol Sci* **158**, 232-252, doi:10.1098/rspb.1963.0045 (1963).
135 Wolf-Oberhollenzer, F. A study of the centrifugal projections to the pigeon retina using two fluorescent markers. *Neurosci Lett* **73**, 16-20, doi:10.1016/0304-3940(87)90023-1 (1987).
136 Gastinger, M. J., Tian, N., Horvath, T. & Marshak, D. W. Retinopetal axons in mammals: emphasis on histamine and serotonin. *Curr Eye Res* **31**, 655-667, doi:10.1080/02713680600776119 (2006).
137 Dillingham, C. M., Guggenheim, J. A. & Erichsen, J. T. Disruption of the centrifugal visual system inhibits early eye growth in chicks. *Invest Ophthalmol Vis Sci* **54**, 3632-3643, doi:10.1167/iovs.12-11548 (2013).
138 Morgan, I. G., Miethke, P. & Li, Z. K. Is nitric oxide a transmitter of the centrifugal projection to the avian retina? *Neurosci Lett* **168**, 5-7, doi:10.1016/0304-3940(94)90402-2 (1994).
139 Fischer, A. J. & Stell, W. K. Nitric oxide synthase-containing cells in the retina, pigmented epithelium, choroid, and sclera of the chick eye. *J Comp Neurol* **405**, 1-

14, doi:10.1002/(SICI)1096-9861(19990301)405:1%3C1::AID-CNE1%3E3.0.CO;2-U (1999).

140 Wilson, M., Nacsa, N., Hart, N. S., Weller, C. & Vaney, D. I. Regional distribution of nitrergic neurons in the inner retina of the chicken. *Vis Neurosci* **28**, 205-220, doi:10.1017/s0952523811000083 (2011).

141 Nathanson, N. M. A multiplicity of muscarinic mechanisms: enough signaling pathways to take your breath away. *Proceedings of the National Academy of Sciences of the United States of America* **97**, 6245-6247, doi: 10.1073/pnas.97.12.6245 (2000).

142 Tietje, K. M. & Nathanson, N. M. Embryonic chick heart expresses multiple muscarinic acetylcholine receptor subtypes. Isolation and characterization of a gene encoding a novel m2 muscarinic acetylcholine receptor with high affinity for pirenzepine. *J Biol Chem* **266**, 17382-17387 (1991).

143 Fischer, A. J., McKinnon, L. A., Nathanson, N. M. & Stell, W. K. Identification and localization of muscarinic acetylcholine receptors in the ocular tissues of the chick. *J Comp Neurol* **392**, 273-284, doi:10.1002/(SICI)1096-9861(19980316)392:3%3C273::AID-CNE1%3E3.0.CO;2-Z (1998).

144 McBrien, N. A., Jobling, A. I., Truong, H. T., Cottriall, C. L. & Gentle, A. Expression of muscarinic receptor subtypes in tree shrew ocular tissues and their regulation during the development of myopia. *Mol Vis* **15**, 464-475 (2009).

145 Strang, C. E., Renna, J. M., Amthor, F. R. & Keyser, K. T. Muscarinic acetylcholine receptor localization and activation effects on ganglion response properties. *Invest Ophthalmol Vis Sci* **51**, 2778-2789, doi:10.1167/iovs.09-4771 (2010).

146 Cimini, B. A., Strang, C. E., Wotring, V. E., Keyser, K. T. & Eldred, W. D. Role of acetylcholine in nitric oxide production in the salamander retina. *J Comp Neurol* **507**, 1952-1963, doi:10.1002/cne.21655 (2008).

147 Weber, B. & Schlicker, E. Modulation of dopamine release in the guinea-pig retina by G(i)- but not by G(s)- or G(q)-protein-coupled receptors. *Fundam Clin Pharmacol* **15**, 393-400, doi:10.1046/j.1472-8206.2001.00056.x (2001).

148 Borda, E., Berra, A., Saravia, M., Ganzinelli, S. & Sterin-Borda, L. Correlations between neuronal nitric oxide synthase and muscarinic M3/M1 receptors in the rat retina. *Exp Eye Res* **80**, 391-399, doi:10.1016/j.exer.2004.09.016 (2005).

149 Baldridge, W. H. Optical recordings of the effects of cholinergic ligands on neurons in the ganglion cell layer of mammalian retina. *J Neurosci* **16**, 5060-5072 (1996).

150 Qu, Z. X., Fertel, R., Neff, N. H. & Hadjiconstantinou, M. Pharmacological characterization of muscarinic receptors mediating inhibition of adenylate cyclase activity in the rat retina. *J Pharmacol Exp Ther* **246**, 839-842 (1988).

151 McBrien, N. A., Moghaddam, H. O. & Reeder, A. P. Atropine reduces experimental myopia and eye enlargement via a nonaccommodative mechanism. *Investigative ophthalmology & visual science* **34**, 205-215 (1993).

152 McBrien, N. A., Stell, W. K. & Carr, B. How does atropine exert its anti-myopia effects? *Ophthalmic Physiol Opt* **33**, 373-378, doi:10.1111/opo.12052 (2013).

153 Chia, A. *et al.* Atropine for the treatment of childhood myopia: safety and efficacy of 0.5%, 0.1%, and 0.01% doses (Atropine for the Treatment of Myopia 2). *Ophthalmology* **119**, 347-354, doi:10.1016/j.ophtha.2011.07.031 (2012).

154 Chua, W. H. *et al.* Atropine for the treatment of childhood myopia. *Ophthalmology* **113**, 2285-2291, doi:10.1016/j.ophtha.2006.05.062 (2006).
155 Bartlett, J. D. *et al.* A tolerability study of pirenzepine ophthalmic gel in myopic children. *J Ocul Pharmacol Ther* **19**, 271-279, doi:10.1089/108076803321908392 (2003).
156 Siatkowski, R. M. *et al.* Two-year multicenter, randomized, double-masked, placebo-controlled, parallel safety and efficacy study of 2% pirenzepine ophthalmic gel in children with myopia. *J aapos* **12**, 332-339, doi:10.1016/j.jaapos.2007.10.014 (2008).
157 Tan, D. T., Lam, D. S., Chua, W. H., Shu-Ping, D. F. & Crockett, R. S. One-year multicenter, double-masked, placebo-controlled, parallel safety and efficacy study of 2% pirenzepine ophthalmic gel in children with myopia. *Ophthalmology* **112**, 84-91, doi:10.1016/j.ophtha.2004.06.038 (2005).
158 Iribarren, R. Tropicamide and myopia progression. *Ophthalmology* **115**, 1103-1104, doi:10.1016/j.ophtha.2007.11.018 (2008).
159 Luft, W. A., Ming, Y. & Stell, W. K. Variable effects of previously untested muscarinic receptor antagonists on experimental myopia. *Invest Ophthalmol Vis Sci* **44**, 1330-1338, doi:10.1167/iovs.02-0796 (2003).
160 Cottriall, C. L., Truong, H. T. & McBrien, N. A. Inhibition of myopia development in chicks using himbacine: a role for M(4) receptors? *Neuroreport* **12**, 2453-2456, doi:10.1097/00001756-200108080-00033 (2001).
161 McBrien, N. A., Arumugam, B., Gentle, A., Chow, A. & Sahebjada, S. The M4 muscarinic antagonist MT-3 inhibits myopia in chick: evidence for site of action. *Ophthalmic Physiol Opt* **31**, 529-539, doi:10.1111/j.1475-1313.2011.00841.x (2011).
162 Nareoja, K. *et al.* Adrenoceptor activity of muscarinic toxins identified from mamba venoms. *Br J Pharmacol* **164**, 538-550, doi:10.1111/j.1476-5381.2011.01468.x (2011).
163 Blanchet, G. *et al.* Polypharmacology profiles and phylogenetic analysis of three-finger toxins from mamba venom: case of aminergic toxins. *Biochimie* **103**, 109-117, doi:10.1016/j.biochi.2014.04.009 (2014).
164 Vessey, K. A., Cottriall, C. L. & McBrien, N. A. Muscarinic receptor protein expression in the ocular tissues of the chick during normal and myopic eye development. *Brain Res Dev Brain Res* **135**, 79-86, doi:10.1016/S0165-3806(02)00309-7 (2002).
165 Liu, Q., Wu, J., Wang, X. & Zeng, J. Changes in muscarinic acetylcholine receptor expression in form deprivation myopia in guinea pigs. *Molecular vision* **13**, 1234-1244 (2007).
166 Howlett, M. H. & McFadden, S. A. Form-deprivation myopia in the guinea pig (Cavia porcellus). *Vision research* **46**, 267-283, doi:10.1016/j.visres.2005.06.036 (2006).
167 Lin, H. J. *et al.* Muscarinic acetylcholine receptor 1 gene polymorphisms associated with high myopia. *Molecular vision* **15**, 1774-1780 (2009).
168 Guggenheim, J. A., Zayats, T., Hammond, C. & Young, T. L. Lumican and muscarinic acetylcholine receptor 1 gene polymorphisms associated with high

myopia. *Eye (London, England)* **24**, 1411-1412; author reply 1412, doi:10.1038/eye.2010.55 (2010).
169 Fan, Q. *et al.* Meta-analysis of gene-environment-wide association scans accounting for education level identifies additional loci for refractive error. *Nat Commun* **7**, 11008, doi:10.1038/ncomms11008 (2016).
170 Kerlavage, A. R., Fraser, C. M., Chung, F. Z. & Venter, J. C. Molecular structure and evolution of adrenergic and cholinergic receptors. *Proteins* **1**, 287-301, doi:10.1002/prot.340010403 (1986).
171 Chang, K. C. & Hahn, K. H. Is alpha-adrenoceptor blockade responsible for atropine flush? *European journal of pharmacology* **284**, 331-334 (1995).
172 Nedergaard, O. A. & Schrold, J. Presynaptic muscarinic and alpha-adrenergic receptor blocking effect of atropine on the noradrenergic neurones of the rabbit pulmonary artery. *Blood Vessels* **16**, 163-168 (1979).
173 Civantos Calzada, B. & Aleixandre de Artinano, A. Alpha-adrenoceptor subtypes. *Pharmacol Res* **44**, 195-208, doi:10.1006/phrs.2001.0857 (2001).
174 Cohen, J. & Hadjiconstantinou, M. Identification of epinephrine and phenylethanolamine N-methyltransferase activity in rat retina. *Fed Proc* **43**, 2725-2728 (1984).
175 Hadjiconstantinou, M., Cohen, J. & Neff, N. H. Epinephrine: a potential neurotransmitter in retina. *J Neurochem* **41**, 1440-1444, doi:10.1111/j.1471-4159.1983.tb00843.x (1983).
176 Hadjiconstantinou, M., Mariani, A. P., Panula, P., Joh, T. H. & Neff, N. H. Immunohistochemical evidence for epinephrine-containing retinal amacrine cells. *Neuroscience* **13**, 547-551, doi:10.1016/0306-4522(84)90247-1 (1984).
177 Forster, B. A., Ferrari-Dileo, G. & Anderson, D. R. Adrenergic alpha 1 and alpha 2 binding sites are present in bovine retinal blood vessels. *Invest Ophthalmol Vis Sci* **28**, 1741-1746 (1987).
178 Woldemussie, E., Wijono, M. & Pow, D. Localization of alpha 2 receptors in ocular tissues. *Visual neuroscience* **24**, 745-756, doi:10.1017/s0952523807070605 (2007).
179 Harun-Or-Rashid, M., Lindqvist, N. & Hallbook, F. Transactivation of EGF receptors in chicken Muller cells by alpha2A-adrenergic receptors stimulated by brimonidine. *Invest Ophthalmol Vis Sci* **55**, 3385-3394, doi:10.1167/iovs.13-13823 (2014).
180 Fong, D. S., Epstein, D. L. & Allingham, R. R. Glaucoma and myopia: are they related? *International ophthalmology clinics* **30**, 215-218 (1990).
181 Mitchell, P., Hourihan, F., Sandbach, J. & Wang, J. J. The relationship between glaucoma and myopia: the Blue Mountains Eye Study. *Ophthalmology* **106**, 2010-2015 (1999).
182 Dong, C. J., Guo, Y., Wheeler, L. & Hare, W. A. Alpha2 adrenergic receptor-mediated modulation of cytosolic Ca++ signals at the inner plexiform layer of the rat retina. *Investigative ophthalmology & visual science* **48**, 1410-1415, doi:10.1167/iovs.06-0890 (2007).
183 Wen, R., Cheng, T., Li, Y., Cao, W. & Steinberg, R. H. Alpha 2-adrenergic agonists induce basic fibroblast growth factor expression in photoreceptors in vivo and ameliorate light damage. *J Neurosci* **16**, 5986-5992 (1996).

184 Chao, H. M., Chidlow, G., Melena, J., Wood, J. P. & Osborne, N. N. An investigation into the potential mechanisms underlying the neuroprotective effect of clonidine in the retina. *Brain Res* **877**, 47-57, doi:10.1016/S0006-8993(00)02592-0 (2000).
185 Seki, M. *et al.* Muller Cells as a source of brain-derived neurotrophic factor in the retina: noradrenaline upregulates brain-derived neurotrophic factor levels in cultured rat Muller cells. *Neurochem Res* **30**, 1163-1170, doi:10.1007/s11064-005-7936-7 (2005).
186 Rosa, R. H., Jr. *et al.* Brimonidine evokes heterogeneous vasomotor response of retinal arterioles: diminished nitric oxide-mediated vasodilation when size goes small. *American journal of physiology. Heart and circulatory physiology* **291**, H231-238, doi:10.1152/ajpheart.01281.2005 (2006).
187 Ghafourifar, P. & Cadenas, E. Mitochondrial nitric oxide synthase. *Trends Pharmacol Sci* **26**, 190-195, doi:10.1016/j.tips.2005.02.005 (2005).
188 Ignarro, L. J. Signal transduction mechanisms involving nitric oxide. *Biochem Pharmacol* **41**, 485-490, doi:10.1016/0006-2952(91)90618-F (1991).
189 Marozkina, N. V. & Gaston, B. S-Nitrosylation signaling regulates cellular protein interactions. *Biochim Biophys Acta* **1820**, 722-729, doi:10.1016/j.bbagen.2011.06.017 (2012).
190 Mayer, B. *et al.* A new pathway of nitric oxide/cyclic GMP signaling involving S-nitrosoglutathione. *J Biol Chem* **273**, 3264-3270, doi:10.1074/jbc.273.6.3264 (1998).
191 Maddox, J. W. & Gleason, E. L. Nitric oxide promotes GABA release by activating a voltage-independent Ca2+ influx pathway in retinal amacrine cells. *J Neurophysiol*, jn.00803.02016, doi:10.1152/jn.00803.2016 (2017).
192 Tekmen-Clark, M. & Gleason, E. Nitric oxide production and the expression of two nitric oxide synthases in the avian retina. *Visual neuroscience* **30**, 91-103, doi:10.1017/s0952523813000126 (2013).
193 Wellard, J. W. & Morgan, I. G. Nitric oxide donors mimic the effects of light on photoreceptor melatonin synthesis. *Aust N Z J Ophthalmol* **24**, 61-63, doi:10.1111/j.1442-9071.1996.tb00998.x (1996).
194 Shi, Q. *Mechanisms of Adaptation to Mean Light Intensity in the Chick Retina*. PhD thesis, University of Calgary, (2014).
195 Hoshi, H., Sato, M., Oguri, M. & Ohtsuka, T. In vivo nitric oxide concentration in the vitreous of rat eye. *Neurosci Lett* **347**, 187-190, doi:10.1016/s0304-3940(03)00717-1 (2003).
196 Neal, M., Cunningham, J. & Matthews, K. Selective release of nitric oxide from retinal amacrine and bipolar cells. *Invest Ophthalmol Vis Sci* **39**, 850-853 (1998).
197 DeVries, S. H. & Schwartz, E. A. Modulation of an electrical synapse between solitary pairs of catfish horizontal cells by dopamine and second messengers. *J Physiol* **414**, 351-375, doi:10.1113/jphysiol.1989.sp017692 (1989).
198 Mills, S. L. & Massey, S. C. Differential properties of two gap junctional pathways made by AII amacrine cells. *Nature* **377**, 734-737, doi:10.1038/377734a0 (1995).
199 Reis, R. A., Ventura, A. L., Kubrusly, R. C., de Mello, M. C. & de Mello, F. G. Dopaminergic signaling in the developing retina. *Brain Res Rev* **54**, 181-188, doi:10.1016/j.brainresrev.2007.01.001 (2007).

200 Nguyen-Legros, J., Versaux-Botteri, C. & Vernier, P. Dopamine receptor localization in the mammalian retina. *Mol Neurobiol* **19**, 181-204, doi:10.1007/bf02821713 (1999).
201 Yan, T. *et al.* Daily Injection But Not Continuous Infusion of Apomorphine Inhibits Form-Deprivation Myopia in Mice. *Invest Ophthalmol Vis Sci* **56**, 2475-2485, doi:10.1167/iovs.13-12361 (2015).
202 Cottriall, C. L., Brew, J., Vessey, K. A. & McBrien, N. A. Diisopropylfluorophosphate alters retinal neurotransmitter levels and reduces experimentally-induced myopia. *Naunyn-Schmiedeberg's archives of pharmacology* **364**, 372-382 (2001).
203 Arumugam, B. M., N.A. The D2 antagonist spiperone prevents muscarinic antagonist control of experimentally-induced myopia in chick. *ARVO Meeting Abstracts* (2010).
204 Haamedi, S. N. & Djamgoz, M. B. Dopamine and nitric oxide control both flickering and steady-light-induced cone contraction and horizontal cell spinule formation in the teleost (carp) retina: serial interaction of dopamine and nitric oxide. *J Comp Neurol* **449**, 120-128, doi:10.1002/cne.10278 (2002).
205 Sekaran, S., Cunningham, J., Neal, M. J., Hartell, N. A. & Djamgoz, M. B. Nitric oxide release is induced by dopamine during illumination of the carp retina: serial neurochemical control of light adaptation. *Eur J Neurosci* **21**, 2199-2208, doi:10.1111/j.1460-9568.2005.04051.x (2005).
206 Kristensen, H. H. *et al.* Leg health and performance of broiler chickens reared in different light environments. *Br Poult Sci* **47**, 257-263, doi:10.1080/00071660600753557 (2006).
207 Fischer, A. J., Morgan, I. G. & Stell, W. K. Colchicine causes excessive ocular growth and myopia in chicks. *Vision Res* **39**, 685-697, doi:10.1016/S0042-6989(98)00178-3 (1999).
208 Noll, G. N., Billek, M., Pietruck, C. & Schmidt, K. F. Inhibition of nitric oxide synthase alters light responses and dark voltage of amphibian photoreceptors. *Neuropharmacology* **33**, 1407-1412, doi:10.1016/0028-3908(94)90042-6 (1994).
209 Tsuyama, Y., Noll, G. N. & Schmidt, K. F. L-arginine and nicotinamide adenine dinucleotide phosphate alter dark voltage and accelerate light response recovery in isolated retinal rods of the frog (Rana temporaria). *Neurosci Lett* **149**, 95-98, doi:10.1016/0304-3940(93)90356-P (1993).
210 Shiells, R. & Falk, G. Retinal on-bipolar cells contain a nitric oxide-sensitive guanylate cyclase. *Neuroreport* **3**, 845-848, doi:10.1097/00001756-199210000-00006 (1992).
211 Sato, M., Ohtsuka, T. & Stell, W. K. Endogenous nitric oxide enhances the light-response of cones during light-adaptation in the rat retina. *Vision Res* **51**, 131-137, doi:10.1016/j.visres.2010.10.011 (2011).
212 Wang, Y. *et al.* Exposure to sunlight reduces the risk of myopia in rhesus monkeys. *PLoS One* **10**, e0127863, doi:10.1371/journal.pone.0127863 (2015).
213 Rose, K. A. *et al.* Outdoor activity reduces the prevalence of myopia in children. *Ophthalmology* **115**, 1279-1285, doi:10.1016/j.ophtha.2007.12.019 (2008).

214 Read, S. A., Collins, M. J. & Vincent, S. J. Light Exposure and Eye Growth in Childhood. *Invest Ophthalmol Vis Sci* **56**, 6779-6787, doi:10.1167/iovs.14-15978 (2015).
215 Fischer, A. J., Scott, M. A., Zelinka, C. & Sherwood, P. A novel type of glial cell in the retina is stimulated by insulin-like growth factor 1 and may exacerbate damage to neurons and Muller glia. *Glia* **58**, 633-649, doi:10.1002/glia.20950 (2010).
216 Moretti, M. *et al.* Role of agmatine in neurodegenerative diseases and epilepsy. *Front Biosci* **6**, 341-359, doi:10.2741/710 (2014).
217 Thomas, J. L., Pourquie, O., Coltey, M., Vaigot, P. & Le Douarin, N. M. Identification in the chicken of GRL1 and GRL2: two granule proteins expressed on the surface of activated leukocytes. *Exp Cell Res* **204**, 156-166, doi:10.1006/excr.1993.1020 (1993).
218 Neal, M., Cunningham, J. & Matthews, K. Nitric oxide enhancement of cholinergic amacrine activity by inhibition of glycine release. *Invest Ophthalmol Vis Sci* **38**, 1634-1639 (1997).
219 Okada, M., Osumi, Y., Okuma, Y. & Ueno, H. Nitric oxide inhibits the release of acetylcholine in the isolated retina. *Graefes Arch Clin Exp Ophthalmol* **239**, 217-221, doi:10.1007/s004170100274 (2001).
220 Migeon, J. C. & Nathanson, N. M. Differential regulation of cAMP-mediated gene transcription by m1 and m4 muscarinic acetylcholine receptors. Preferential coupling of m4 receptors to Gi alpha-2. *J Biol Chem* **269**, 9767-9773 (1994).
221 Yin, G. C., Gentle, A. & McBrien, N. A. Muscarinic antagonist control of myopia: a molecular search for the M1 receptor in chick. *Mol Vis* **10**, 787-793 (2004).
222 Zhu, X., Winawer, J. A. & Wallman, J. Potency of myopic defocus in spectacle lens compensation. *Invest Ophthalmol Vis Sci* **44**, 2818-2827, doi:10.1167/iovs.02-0606 (2003).
223 Fischer, A. J., Miethke, P., Morgan, I. G. & Stell, W. K. Cholinergic amacrine cells are not required for the progression and atropine-mediated suppression of form-deprivation myopia. *Brain Res* **794**, 48-60, doi:10.1016/S0006-8993(98)00188-7 (1998).
224 Wellard, J. W., Miethke, P. & Morgan, I. G. Neural barriers affect the action of nitric oxide synthase inhibitors in the intact chicken retina. *Neurosci Lett* **201**, 17-20, doi:10.1016/0304-3940(94)12120-F (1995).
225 Martin, W., Furchgott, R. F., Villani, G. M. & Jothianandan, D. Phosphodiesterase inhibitors induce endothelium-dependent relaxation of rat and rabbit aorta by potentiating the effects of spontaneously released endothelium-derived relaxing factor. *J Pharmacol Exp Ther* **237**, 539-547 (1986).
226 Palmer, R. M., Ferrige, A. G. & Moncada, S. Nitric oxide release accounts for the biological activity of endothelium-derived relaxing factor. *Nature* **327**, 524-526, doi:10.1038/327524a0 (1987).
227 Fambrough, D. M., Takeyasu, K., Lippincott-Schwarz, J. & Siegel, N. R. Structure of LEP100, a glycoprotein that shuttles between lysosomes and the plasma membrane, deduced from the nucleotide sequence of the encoding cDNA. *J Cell Biol* **106**, 61-67, doi:10.1083/jcb.106.1.61 (1988).

228 Fischer, A. J., Seltner, R. L., Poon, J. & Stell, W. K. Immunocytochemical characterization of quisqualic acid- and N-methyl-D-aspartate-induced excitotoxicity in the retina of chicks. *J Comp Neurol* **393**, 1-15, doi:10.1002/(SICI)1096-9861(19980330)393:1%3C1::AID-CNE1%3E3.0.CO;2-3 (1998).

229 Thomas, J. L., Stieber, A. & Gonatas, N. Two proteins associated with secretory granule membranes identified in chicken regulated secretory cells. *J Cell Sci* **107 (Pt 5)**, 1297-1308 (1994).

230 Moriya, H. *et al.* Affinity profiles of various muscarinic antagonists for cloned human muscarinic acetylcholine receptor (mAChR) subtypes and mAChRs in rat heart and submandibular gland. *Life Sci* **64**, 2351-2358, doi:10.1016/S0024-3205(99)00188-5 (1999).

231 McBrien, N. A., Cottriall, C. L. & Annies, R. Retinal acetylcholine content in normal and myopic eyes: a role in ocular growth control? *Vis Neurosci* **18**, 571-580, doi:10.1017/S0952523801184075 (2001).

232 Lind, G. J., Chew, S. J., Marzani, D. & Wallman, J. Muscarinic acetylcholine receptor antagonists inhibit chick scleral chondrocytes. *Invest Ophthalmol Vis Sci* **39**, 2217-2231 (1998).

233 Liang, J. S. *et al.* Anti-muscarinic toxins from Dendroaspis angusticeps. *Toxicon* **34**, 1257-1267 (1996).

234 Cottriall, C. L., McBrien, N. A., Annies, R. & Leech, E. M. Prevention of form-deprivation myopia with pirenzepine: a study of drug delivery and distribution. *Ophthalmic Physiol Opt* **19**, 327-335, doi:10.1046/j.1475-1313.1999.00438.x (1999).

235 Li, X. X., Schaeffel, F., Kohler, K. & Zrenner, E. Dose-dependent effects of 6-hydroxy dopamine on deprivation myopia, electroretinograms, and dopaminergic amacrine cells in chickens. *Vis Neurosci* **9**, 483-492, doi:10.1017/S0952523800011287 (1992).

236 Schwahn, H. N. & Schaeffel, F. Chick eyes under cycloplegia compensate for spectacle lenses despite six-hydroxy dopamine treatment. *Invest Ophthalmol Vis Sci* **35**, 3516-3524 (1994).

237 Schaeffel, F. & Howland, H. C. Mathematical model of emmetropization in the chicken. *J Opt Soc Am A* **5**, 2080-2086, doi:10.1364/JOSAA.5.002080 (1988).

238 McBrien, N. A., Moghaddam, H. O., New, R. & Williams, L. R. Experimental myopia in a diurnal mammal (Sciurus carolinensis) with no accommodative ability. *J Physiol* **469**, 427-441, doi:10.1113/jphysiol.1993.sp019821 (1993).

239 Iuvone, P. M. & Rauch, A. L. Alpha 2-adrenergic receptors influence tyrosine hydroxylase activity in retinal dopamine neurons. *Life Sci* **33**, 2455-2463 (1983).

240 Lanau, F., Zenner, M. T., Civelli, O. & Hartman, D. S. Epinephrine and norepinephrine act as potent agonists at the recombinant human dopamine D4 receptor. *J Neurochem* **68**, 804-812, doi:10.1046/j.1471-4159.1997.68020804.x (1997).

241 Newman-Tancredi, A., Audinot-Bouchez, V., Gobert, A. & Millan, M. J. Noradrenaline and adrenaline are high affinity agonists at dopamine D4 receptors. *Eur J Pharmacol* **319**, 379-383, doi:10.1016/S0014-2999(96)00985-5 (1997).

242 Rivera, A. *et al.* Cellular localization and distribution of dopamine D(4) receptors in the rat cerebral cortex and their relationship with the cortical dopaminergic and noradrenergic nerve terminal networks. *Neuroscience* **155**, 997-1010, doi:10.1016/j.neuroscience.2008.05.060 (2008).
243 Gresch, P. J., Sved, A. F., Zigmond, M. J. & Finlay, J. M. Local influence of endogenous norepinephrine on extracellular dopamine in rat medial prefrontal cortex. *J Neurochem* **65**, 111-116, doi:10.1046/j.1471-4159.1995.65010111.x (1995).
244 Devoto, P., Flore, G., Pani, L. & Gessa, G. L. Evidence for co-release of noradrenaline and dopamine from noradrenergic neurons in the cerebral cortex. *Mol Psychiatry* **6**, 657-664, doi:10.1038/sj.mp.4000904 (2001).
245 Devoto, P., Flore, G., Pira, L., Longu, G. & Gessa, G. L. Alpha2-adrenoceptor mediated co-release of dopamine and noradrenaline from noradrenergic neurons in the cerebral cortex. *J Neurochem* **88**, 1003-1009, doi:10.1046/j.1471-4159.2003.02239.x (2004).
246 Devoto, P. & Flore, G. On the origin of cortical dopamine: is it a co-transmitter in noradrenergic neurons? *Curr Neuropharmacol* **4**, 115-125, doi:10.2174/157015906776359559 (2006).
247 Costall, B., Naylor, R. J. & Tan, C. C. The mechanism of action of dopamine to inhibit field stimulation-induced contractions of guinea pig stomach strips. *Naunyn Schmiedebergs Arch Pharmacol* **328**, 174-179, doi:10.1007/BF00512068 (1984).
248 Rotiroti, D., Silvestri, R., de Sarro, G. B., Bagetta, G. & Nistico, G. Evidence that behavioural and electrocortical sleep induced by guanfacine is due to stimulation of alpha 2-adrenoceptors. *J Psychiatr Res* **17**, 231-239 (1982).
249 Roach, A. G., Lefevre-Borg, F., Gomeni, R. & Cavero, I. Pharmacological evidence favoring a similarity between alpha adrenoceptors mediating sleep in chicks and cardiac presynaptic alpha-2 receptors in rats. *J Pharmacol Exp Ther* **222**, 680-687 (1982).
250 Roach, A. G., Doxey, J. C., Strachan, D. A. & Cavero, I. Sleeping times evoked by alpha adrenoceptor agonists in two-day-old chicks: an experimental model to evaluate full and partial agonists at central alpha-2 adrenoceptors. *J Pharmacol Exp Ther* **227**, 421-428 (1983).
251 Hennig, C. W., Fazio, J. K., Hughes, C. A., Castaldi, W. R. & Spencer, B. D. Duration of tonic immobility in chickens as a function of alpha-adrenergic receptor stimulation and blockade. *Pharmacol Biochem Behav* **20**, 731-738, doi:10.1016/0091-3057(84)90192-8 (1984).
252 Kashihara, K., Varga, E. V., Waite, S. L., Roeske, W. R. & Yamamura, H. I. Cloning of the rat M3, M4 and M5 muscarinic acetylcholine receptor genes by the polymerase chain reaction (PCR) and the pharmacological characterization of the expressed genes. *Life Sci* **51**, 955-971, doi:10.1016/0024-3205(92)90403-C (1992).
253 Kukkonen, A., Perakyla, M., Akerman, K. E. & Nasman, J. Muscarinic toxin 7 selectivity is dictated by extracellular receptor loops. *J Biol Chem* **279**, 50923-50929, doi:10.1074/jbc.M406424200 (2004).
254 Cheng, Y. & Prusoff, W. H. Relationship between the inhibition constant (K1) and the concentration of inhibitor which causes 50 per cent inhibition (I50) of an enzymatic reaction. *Biochem Pharmacol* **22**, 3099-3108 (1973).

255 Tietje, K. M., Goldman, P. S. & Nathanson, N. M. Cloning and functional analysis of a gene encoding a novel muscarinic acetylcholine receptor expressed in chick heart and brain. *J Biol Chem* **265**, 2828-2834 (1990).
256 Eason, M. G., Kurose, H., Holt, B. D., Raymond, J. R. & Liggett, S. B. Simultaneous coupling of alpha 2-adrenergic receptors to two G-proteins with opposing effects. Subtype-selective coupling of alpha 2C10, alpha 2C4, and alpha 2C2 adrenergic receptors to Gi and Gs. *J Biol Chem* **267**, 15795-15801 (1992).
257 Laurila, J. M. *et al.* The second extracellular loop of alpha2A-adrenoceptors contributes to the binding of yohimbine analogues. *Br J Pharmacol* **151**, 1293-1304, doi:10.1038/sj.bjp.0707330 (2007).
258 Ruuskanen, J. O. *et al.* Conserved structural, pharmacological and functional properties among the three human and five zebrafish alpha 2-adrenoceptors. *Br J Pharmacol* **144**, 165-177, doi:10.1038/sj.bjp.0706057 (2005).
259 Zheng, W. *et al.* Yohimbine dimers exhibiting binding selectivities for human alpha2a- versus alpha2b-adrenergic receptors. *Bioorg Med Chem Lett* **10**, 627-630 (2000).
260 Tigges, M. *et al.* Effects of muscarinic cholinergic receptor antagonists on postnatal eye growth of rhesus monkeys. *Optom Vis Sci* **76**, 397-407, doi:10.1097/00006324-199906000-00020 (1999).
261 Acheampong, A. A. *et al.* Distribution of brimonidine into anterior and posterior tissues of monkey, rabbit, and rat eyes. *Drug Metab Dispos* **30**, 421-429, doi:10.1124/dmd.30.4.421 (2002).
262 Inoue, J. *et al.* Effects of dorzolamide hydrochloride on ocular tissues. *J Ocul Pharmacol Ther* **20**, 1-13, doi:10.1089/108076804772745419 (2004).
263 Sugrue, M. F. Pharmacological and ocular hypotensive properties of topical carbonic anhydrase inhibitors. *Prog Retin Eye Res* **19**, 87-112, doi:10.1016/S1350-9462(99)00006-3 (2000).
264 Carr, B., Nathanson, N. & Stell, W. Atropine Prevents Myopia via a Nitric Oxide-Mediated Relay. *Invest. Ophthalmol. Vis. Sci.* **54**, 3677- (2013).
265 Lazareno, S., Buckley, N. J. & Roberts, F. F. Characterization of muscarinic M4 binding sites in rabbit lung, chicken heart, and NG108-15 cells. *Mol Pharmacol* **38**, 805-815 (1990).
266 Krajewski, J. L., Dickerson, I. M. & Potter, L. T. Site-directed mutagenesis of m1-toxin1: two amino acids responsible for stable toxin binding to M(1) muscarinic receptors. *Mol Pharmacol* **60**, 725-731 (2001).
267 Harel, M., Kleywegt, G. J., Ravelli, R. B., Silman, I. & Sussman, J. L. Crystal structure of an acetylcholinesterase-fasciculin complex: interaction of a three-fingered toxin from snake venom with its target. *Structure* **3**, 1355-1366, doi:10.1016/S0969-2126(01)00273-8 (1995).
268 Radic, Z. *et al.* Site of fasciculin interaction with acetylcholinesterase. *J Biol Chem* **269**, 11233-11239 (1994).
269 Thal, D. M. *et al.* Crystal structures of the M1 and M4 muscarinic acetylcholine receptors. *Nature* **531**, 335-340, doi:10.1038/nature17188 (2016).
270 Sanjana, N. E., Shalem, O. & Zhang, F. Improved vectors and genome-wide libraries for CRISPR screening. *Nat Methods* **11**, 783-784, doi:10.1038/nmeth.3047 (2014).

271 Shalem, O. *et al.* Genome-scale CRISPR-Cas9 knockout screening in human cells. *Science* **343**, 84-87, doi:10.1126/science.1247005 (2014).
272 Ganesan, P. & Wildsoet, C. F. Pharmaceutical intervention for myopia control. *Expert Rev Ophthalmol* **5**, 759-787, doi:10.1586/eop.10.67 (2010).
273 Eldred, W. D. & Blute, T. A. Imaging of nitric oxide in the retina. *Vision Res* **45**, 3469-3486, doi:10.1016/j.visres.2005.07.033 (2005).
274 Bogle, R. G., Moncada, S., Pearson, J. D. & Mann, G. E. Identification of inhibitors of nitric oxide synthase that do not interact with the endothelial cell L-arginine transporter. *Br J Pharmacol* **105**, 768-770, doi:10.1111/j.1476-5381.1992.tb09053.x (1992).
275 Forray, M. I., Angelo, S., Boyd, C. A. & Deves, R. Transport of nitric oxide synthase inhibitors through cationic amino acid carriers in human erythrocytes. *Biochem Pharmacol* **50**, 1963-1968, doi:10.1016/0006-2952(95)02090-X (1995).
276 Jarrott, B., Louis, W. J. & Summers, R. J. [3H]-guanfacine: a radioligand that selectively labels high affinity alpha2-adrenoceptor sites in homogenates of rat brain. *Br J Pharmacol* **75**, 401-408, doi:10.1111/j.1476-5381.1982.tb08801.x (1982).
277 Nickla, D. L. & Schroedl, F. Parasympathetic influences on emmetropization in chicks: evidence for different mechanisms in form deprivation vs negative lens-induced myopia. *Exp Eye Res* **102**, 93-103, doi:10.1016/j.exer.2012.07.002 (2012).
278 Diether, S., Schaeffel, F., Lambrou, G. N., Fritsch, C. & Trendelenburg, A. U. Effects of intravitreally and intraperitoneally injected atropine on two types of experimental myopia in chicken. *Exp Eye Res* **84**, 266-274, doi:10.1016/j.exer.2006.09.019 (2007).
279 Newman-Tancredi, A. *et al.* Actions of alpha2 adrenoceptor ligands at alpha2A and 5-HT1A receptors: the antagonist, atipamezole, and the agonist, dexmedetomidine, are highly selective for alpha2A adrenoceptors. *Naunyn Schmiedebergs Arch Pharmacol* **358**, 197-206 (1998).
280 Li, Y. P., Bang, D. D., Handberg, K. J., Jorgensen, P. H. & Zhang, M. F. Evaluation of the suitability of six host genes as internal control in real-time RT-PCR assays in chicken embryo cell cultures infected with infectious bursal disease virus. *Vet Microbiol* **110**, 155-165, doi:10.1016/j.vetmic.2005.06.014 (2005).

Appendix A1: Does Spiperone Block Myopia-Inhibition by Atropine?

Abstract

Previous reports have demonstrated that inhibition of myopia by "muscarinic antagonists" MT3 in chick and MT7 in tree shrew can be blocked by simultaneous injection of the dopamine D_2-antagonist spiperone. If the mechanisms of myopia inhibition by mamba toxins are the same as those of atropine, then spiperone should also block atropine-mediated prevention of FDM.

Form-deprivation myopia (FDM) was induced in P7 chicks by diffusers over the right eye (OD); the left eye (OS) remained ungoggled. On post-goggling (PG) days 1, 3, and 5, OD received intravitreally 20 µL of vehicle (PBS), or vehicle plus: atropine (60 nmoles); spiperone (5 nmoles); or atropine plus spiperone. On day PG6, refractive error (RE), axial length (AL), equatorial diameter (ED), and wet weight (WW) were measured.

Atropine-treatment resulted in significant inhibition of induced negative refractive error and axial elongation compared to eyes injected with PBS or spiperone alone. Addition of spiperone during atropine-treatment did not significantly diminish the inhibition of myopia development seen when atropine was used alone.

The data presented here did not support the prediction that spiperone would block the anti-myopia action of atropine, even though previous reports suggest spiperone blocks myopia inhibition by MT3[203], dopamine agonism[112], and goggle removal[108] in the chick. Possible explanations for these results include i) the spiperone used in this experiment was not active, or ii)) that atropine does not inhibit myopia through the same mechanisms as dopamine agonism or MT3/MT7. Repetition of this experiment is warranted. The finding that atropine may not depend on ocular dopamine to inhibit FDM is important, and could further significantly our understanding of the mechanisms underlying atropine-mediated myopia-inhibition.

Introduction

The downstream signalling cascades altered by atropine in myopia inhibition remain elusive, but one study has found that atropine-treatment results in a large increase in ocular dopamine release in the chick[116]. The important role of dopamine in myopia prevention has been demonstrated time and time again in the chick[102,107,113,115,116,118] and mammalian model organisms[103-106,201] (see introduction). Because both dopamine agonists and atropine inhibit myopia, simultaneous injection of apomorphine and atropine was investigated[115]; treatment with both drugs did not result in an increased myopia-inhibiting effect, leading the authors to suggest that they may work in a common pathway. Dopamine may act upstream of nitric oxide to cause myopia inhibition[110] (and Moinul P et al. IOVS 2012; 53: ARVO E-Abstract 3434). We have shown that myopia inhibition by atropine is dependent on the presence of ocular NO (**Chapter 3**), but its dependence on signalling via dopamine D_2 has not been tested. I hypothesized that blockade of dopaminergic signalling via simultaneous injection of spiperone with atropine would result in ablation of myopia inhibition.

Results

Results are reported as the difference (d) between the experimental eye and the control eye, and summarized in **Fig. A1.1** and **Table A1.1**. PBS-treated goggled eyes exhibited a large increase in negative refractive error (dRE: -15.7 ± 4.4 D), axial length (dAL: 0.57 ± 0.22 mm), equatorial diameter (dEQ: 0.30 ± 0.19 mm), and wet weight (dWW: 0.0744 ± 0.023 g), a sign of significant myopia-induction. Eyes treated with spiperone did not differ significantly from PBS-treated eyes, and had a significantly larger refractive error and axial length than atropine-treated eyes (dRE: -16.0 ± 4.2 D, n = 18, $p_{(atro)} = 0.0008$; dAL: 0.67 ± 0.25 mm, n = 18, $p_{(atro)} = 0.0009$). Atropine-treated goggled eyes had significantly lower negative refractive error (dRE: -10.1 ± 3.6 D, n = 16, $p_{(PBS)} = 0.0015$) and shorter axial length (dAL: 0.37 ± 0.20 mm, n = 16, $p_{(PBS)} = 0.0460$) than PBS-controls. Goggled eyes treated with atropine + spiperone did not differ significantly from atropine-treated eyes; they had decreased negative refractive error compared to PBS- and spiperone-treated eyes, but this difference failed to reach significance (dRE: -12.8 ± 4.8 D, n = 14, $p_{(PBS)} = 0.2375$). The decrease in axial elongation also failed to reach significance compared to PBS, but

was significantly different than spiperone (dAL: 0.44 ± 0.18 mm, n = 18, $p_{(spip)} = 0.0156$). There was no difference in equatorial diameter or wet weight for any treatment group.

A1.1: The Effects of Atropine, Spiperone, and Their Combination on FDM in Chicks

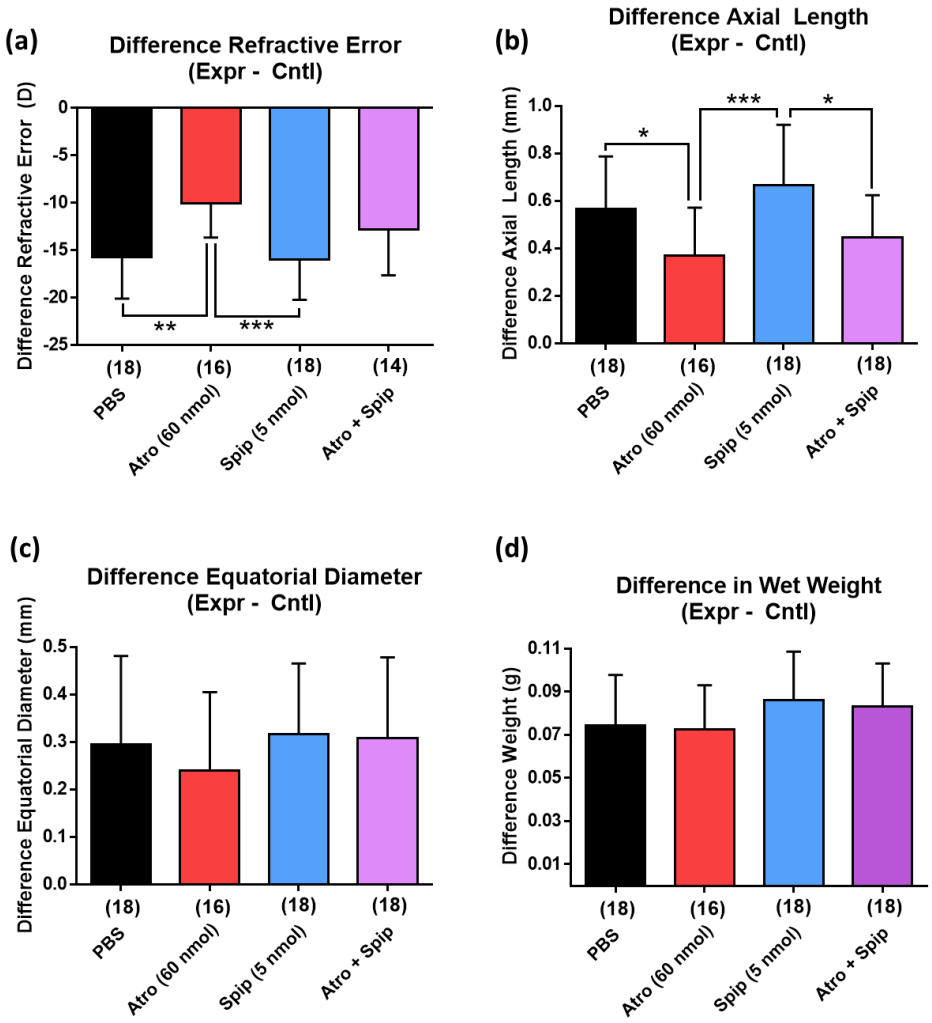

Figure A1.1 The effect of atropine (60 nmoles), spiperone (5 nmoles) and atro + spip on FDM in chicks. The addition of spip with atro did not seem to affect atropine's ability to inhibit increased negative refractive error (**a**) or axial elongation (**b**); there was no significant effect of any treatment on equatorial diameter (**c**) or wet weight (**d**) of eyes. ***Abbreviations:*** **atro**: atropine, **spip**: spiperone. ***Statistics***: $^{*}p<0.05$; $^{**}p < 0.01$, $^{***}p < 0.001$; One-Way ANOVA + Tukey's post-hoc. Data are represented as the means of the difference in values for the experimental eye minus those for the control eye, ± SD; sample sizes (n) are denoted in brackets below each column.

Table A1.1: Summarized data for refractive error, biometrics, and significant p-values for all treatment groups – atropine (60 nmoles), spiperone (5 nmoles), and atropine (60 nmoles) + spiperone (5 nmoles). ***Abbreviations:*** **atro**: atropine, **spip**: spiperone, a+s: atropine + spiperone. ***Statistics***: One-Way ANOVA + Tukey's post-hoc; number of replicates (n) and statistical p-values ($p_{(PBS)}$: comparison to PBS, $p_{(spip)}$: comparison to spiperone, $p_{(a+s)}$: comparison to atropine + spiperone) are listed below treatment outcomes.

Drug	**PBS** **(n)**	**Atropine** **(n) p-value vs. PBS**	**Spiperone** **(n) p-value vs. PBS**	**Atro + Spip** **(n) p-value vs. PBS**
dRE	-15.7 ± 4.4 D (18)	-10.1 ± 3.6 D (16) **$p_{(PBS)}$ = 0.0015** **$P_{(spip)}$ = 0.0008**	-16.0 ± 4.2 D (18)	-12.8 ± 4.8 D **(**14)
dAL	0.57 ± 0.22 mm (18)	0.37 ± 0.20 mm (16) **$p_{(PBS)}$ = 0.0460** **$p_{(spip)}$ = 0.0009**	0.67 ± 0.25 mm (18) **$p_{(a+s)}$ = 0.0156**	0.44 ± 0.18 mm **(**18)
dEQ	0.30 ± 0.19 mm (18)	0.24 ± 0.16 mm (16)	0.32 ± 0.15 mm (18)	0.31 ± 0.17 mm **(**18)
dWW	0.0744 ± 0.023 g (18)	0.0727 ± 0.020 g (16)	0.0862 ± 0.022 g (18)	0.0831 ± 0.020 g (18)

Discussion

The data presented here do not support a role for spiperone, and the dopamine D_2 receptor signalling, in atropine-mediated myopia inhibition. Given that spiperone-treatment has been very successful in blocking myopia inhibition by a number of different experimental methods[45,98,108,109,112] (and Arumugam B et al. IOVS 2010; 51: ARVO E-Abstract 1195 & Arumugam B et al. IOVS 2012; 53: ARVO E-Abstract 3431), it is surprising that it would be unsuccessful in blocking myopia inhibition by atropine as well. The first explanation for this would be that the spiperone used was no longer active; in the experimental paradigm used, there would be no way to tell whether the spiperone was working correctly because a negative result – no effect on FDM – could be obtained similarly with the active or inactive drug when spiperone was injected alone. A second, more interesting hypothesis could be that atropine is not dependent on signalling through the dopamine D_2 receptor to inhibit myopia. We did not test a broad-spectrum dopamine receptor antagonist, or a more specific D_1-type receptor antagonist, so we cannot say for sure that atropine-mediated myopia inhibition is not at all dependent on dopamine signalling. This discrepancy could be corrected by simultaneous injection of either SCH-23390 (D1-type antagonist) or

methylergonovine (broad-spectrum dopamine antagonist) with atropine to look for effects of non-D_2 dopaminergic systems on myopia inhibition. In addition, dopamine signalling may act upstream of whatever signalling cascade is activated by atropine treatment, as is seems to do with NO[110] (and Moinul P, et al. IOVS 2012; 53: ARVO E-Abstract 3434). Finally, this result could be a false negative; the parameters in atro + spip were also not significantly different from those in PBS, and the small sample size doesn't allow me to draw definitive conclusions. If atropine was found to not be affected by treatment with any dopamine antagonist, however, that result could provide evidence that atropine and MT3 may inhibit myopia through different mechanisms. It could be possible that MT3 may act through a dopaminergic-dependent pathway, and atropine could work through a nitrergic-dependent pathway for myopia inhibition. This is just speculation, however, as we know too little about the signalling cascades involved in myopia inhibition to make any conclusive statements about the underlying mechanisms.

Methods

The animal ethics statement and common methods for induction of form-deprivation myopia, intravitreal injections, eye biometric measurements, and statistical analysis are described previously (**Chapter 2**). The chickens used in these experiments were Bovans (Rochester Hatchery, Westlock, AB).

Drugs for Intravitreal Injection

Drugs, commercial sources, and the molar amounts delivered per injection are listed in **Table A1.2**. Drugs were dissolved in phosphate-buffered saline (PBS) (Gibco 14190-144; ThermoFisher Scientific) at room temperature. Stock solutions were made fresh on injection day one, and aliquots were quick-frozen, stored at -20°C, and used only for the duration of one experiment (six days) so as to avoid loss of drug activity due to prolonged storage. The concentrations tested were based on previously published data (spiperone[45,108,109]) and preliminary results from our own dose-response studies (atropine) in this specific strain of chick. Spiperone was chosen as the dopamine blocker because of the success of previous studies using spiperone to block myopia-inhibition by MT3 in chick (Arumugam B et al. IOVS 2010; 51: ARVO E-Abstract 1195), MT7 in tree shrew

(Arumugam B et al. IOVS 2012; 53: ARVO E-Abstract 3431), and apomorphine in chick[112]. Spiperone also blocks form-deprivation myopia rescue by clear vision, if injected prior to goggle removal[45,108,109].

Table A1.2: Agents employed in the present studies.

Drug	**Source**	**Cat#**	**Amt/Injection (Syringe)**
Atropine Sulfate	Calbiochem	189361	60 nmoles
Spiperone	Sigma-Aldrich	S7395	5 nmoles

Appendix A2: Inhibition of FDM by Guanfacine: Mechanism?

Abstract

Guanfacine (gfcn) inhibits FDM in the chick at high concentrations (**Chapter 4**). Because this is a novel finding, we know very little about how this may occur. This appendix chapter outlines numerous experiments performed to attempt to determine important signalling molecules and mechanisms involved in myopia inhibition by gfcn. We chose to investigate gfcn instead of clonidine because it had a significant effect at both 20 and 200 nmoles, and acted similarly to atropine in that the treatment effect seemed to plateau at 50% inhibition.

Form-deprivation myopia (FDM) was induced in P7 chicks by diffusers over the right eye (OD); the left eye (OS) remained ungoggled. On post-goggling (PG) days 1, 3, and 5, OD received intravitreally 20 µL of vehicle (PBS), or vehicle plus: gfcn (200 nmoles); yohimbine (yoh: 6 nmoles); L-NMMA (6 nmoles); atropine (atro: 200 nmoles); or gfcn + yoh, gfcn + L-NMMA, or gfcn + atro. On day PG6, refractive error (RE), axial length (AL), equatorial diameter (ED), and wet weight (WW) were measured.

Gfcn significantly inhibited FD-induced negative RE and AL in all experiments performed, except in gfcn + atro experiments, where it only significantly inhibited the difference in RE. Neither yoh nor L-NMMA had a significant effect on the ability of gfcn to inhibit FDM. Combination of gfcn + atro resulted in a significantly larger anti-myopia effect than treatment with either drug alone. There was no significant effect on the difference in equatorial diameter for any treatment, but gfcn-, yoh- and gfcn + yoh-treated eyes had a decreased wet weight compared to PBS controls.

These data are surprising. Guanfacine is an α_2-adrenoceptor (ADRA2) agonist, and if myopia inhibition were mediated through these receptors, we would expect that yohimbine, an ADRA2 antagonist, would block myopia inhibition by gfcn. In **Chapter 3**, we showed that atropine *requires* induction of ocular NO for myopia inhibition, but the same experiments with gfcn did not support a role of NO, and the effects of gfcn + atro were additive. If these data are true, it is likely that i) gfcn does not inhibit myopia via agonism at ADRA2, and ii) there are multiple emmetropization pathways in the eye.

Introduction

As demonstrated previously (**Chapter 4)**, α-adrenoceptor agonists clonidine and guanfacine inhibit FDM at high concentrations in the chick. Because this is a novel finding, we know very little about the underlying signaling mechanisms and neural pathways. In an attempt to address possible mechanisms that may underlie gfcn-mediated inhibition of FDM, I chose to investigate the effects of 1) blockade of ADRA2-signalling using the ADRA2 antagonist yohimbine, 2) blockade of NO synthesis using L-NMMA, and 3) guanfacine- and atropine-treatment in combination. We chose to investigate guanfacine, because it acts similarly to atropine in that myopia inhibition occurs at concentrations of ≥ 200 nmoles, and plateaus at roughly 50% inhibition of FDM. Clonidine did have a larger anti-myopia effect (80-100%), but it did not occur until the highest dose (200 nmoles) was used.

Results

A2.1: Yohimbine Does Not prevent Gfcn-Mediated Reduction in Axial Growth

Results are summarized in **Fig A2.1 and Table A2.1**. H_2O- and yohimbine (yoh)-treated goggled eyes developed significant myopia as measured by the difference in refractive error and axial length (dRE: H_2O: -15.1 ± 3.5 D, n = 10; yoh: -15.1 ± 0.8 D, n = 10; dAL: H_2O: 0.56 ± 0.25 mm, n = 12; yoh: 0.42 ± 0.15 mm, n = 11). Eyes treated with guanfacine (gfcn) had a significantly smaller difference in refractive error when compared to all other treatment groups (gfcn: -6.6 ± 1.7 D, n = 12; $p_{(H2O)} < 0.0001$, $p_{(yoh)} < 0.0001$, $p_{(g+y)} = 0.0009$), but axial lengths did not follow perfectly the pattern for dRE; both gfcn and gfcn + yoh had significantly smaller axial lengths than H_2O-controls (gfcn: 0.24 ± 0.2 mm, n = 11, p = 0.0014; gfcn + yoh: 0.25 ± 0.15 mm, n = 12, p = 0.0018). The difference in equatorial diameter was not significantly different between any treatment group (H_2O: 0.31 ± 0.12 mm, n = 11; gfcn: 0.18 ± 0.11 mm, n = 11; yoh: 0.24 ± 0.17 mm, n = 12; gfcn + yoh: 0.26 ± 0.19 mm, n = 11), but wet weight was significantly smaller in all treatment groups compared to H_2O-controls (gfcn: 0.0450 ± 0.022 g, n = 11, p = 0.0018; yoh: 0.0578 ± 0.030, n = 12, p = 0.0271; gfcn + yoh: 0.0603 ± 0.031, n = 12, p = 0.0461).

A2.1: The Effects of Guanfacine, Yohimbine, and Their Combination on FDM in Chicks

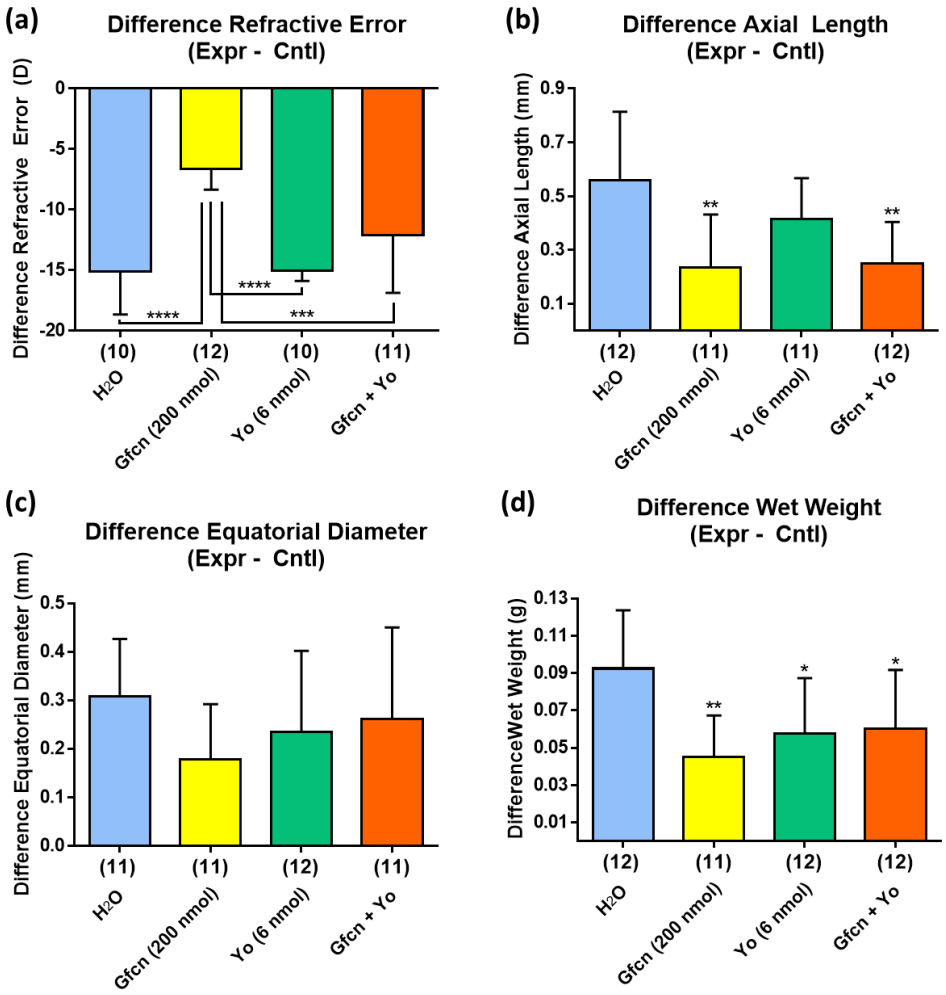

Figure A2.1: The effect of gfcn (200 nmoles), yo (6 nmoles) and gfcn + yo on FDM in chicks. Yohimbine significantly reduced the inhibition of myopic RE by guanfacine (**a**), but had no effect on axial elongation (**b**). There was no significant effect of any treatment on equatorial diameter (**c**), but the wet weights of all drug-treated eyes were smaller than H_2O controls (**d**). ***Abbreviations:*** **gfcn**: guanfacine, **yo**: yohimbine. ***Statistics***: comparison to H_2O unless specified otherwise; $^{*}p<0.05$; $^{**}p < 0.01$, $^{***}p < 0.001$; One-Way ANOVA + Tukey's post-hoc. Data are represented as the means of the differences in values for the experimental eye minus those for the control eye, ± SD; sample sizes (n) are denoted in brackets below each column.

A2.2: L-NMMA Does Not Prevent Gfcn-Mediated Inhibition of FDM

Results are summarized in **Fig A2.2** and **Table. A2.1**. Intravitreal injection of guanfacine significantly reduced the difference in refractive error (H_2O: -13.4 ± 2.1 D, n = 9 vs. gfcn: -6.77 ± 3.0 D, n = 14, p = 0.0014), axial elongation (H_2O: 0.66 ± 0.18 mm, n = 10 vs. gfcn: 0.31 ± 0.16 mm, n = 14, p = 0.0004), and wet weight (H_2O: 0.0946 ± 0.027 g, n = 10 vs. gfcn: 0.0646 ± 0.027 g, n = 14, p = 0.0179), but not equatorial diameter (H_2O: 0.27 ± 0.15 mm, n = 10 vs. gfcn: 0.26 ± 0.15 mm, n = 14) caused by application of diffuser goggles. As expected, L-NMMA had no effect on induction of FDM (dRE: -12.4 ± 4.6 D, n = 14, $p_{(gfcn)}$ = 0.0044; dAL: 0.51 ± 0.22 mm, n = 14; dEQ: 0.27 ± 0.17 mm, n = 11; dWW: 0.0714 ± 0.021 g, n = 11), but it also did not block myopia-inhibition by guanfacine; the difference in axial length was significantly smaller in gfcn + L-NMMA-treated eyes than controls (dRE: -10.0 ± 4.8 D, n = 11: dAL: 0.38 ± 0.21 mm, n = 11, $p_{(H2O)}$ = 0.0059; dEQ: 0.24 ± 0.17 mm, n = 14; dWW: 0.0706 ± 0.019, n = 14).

A2.2: The Effects of Guanfacine, L-NMMA, and Their Combination on FDM in Chicks

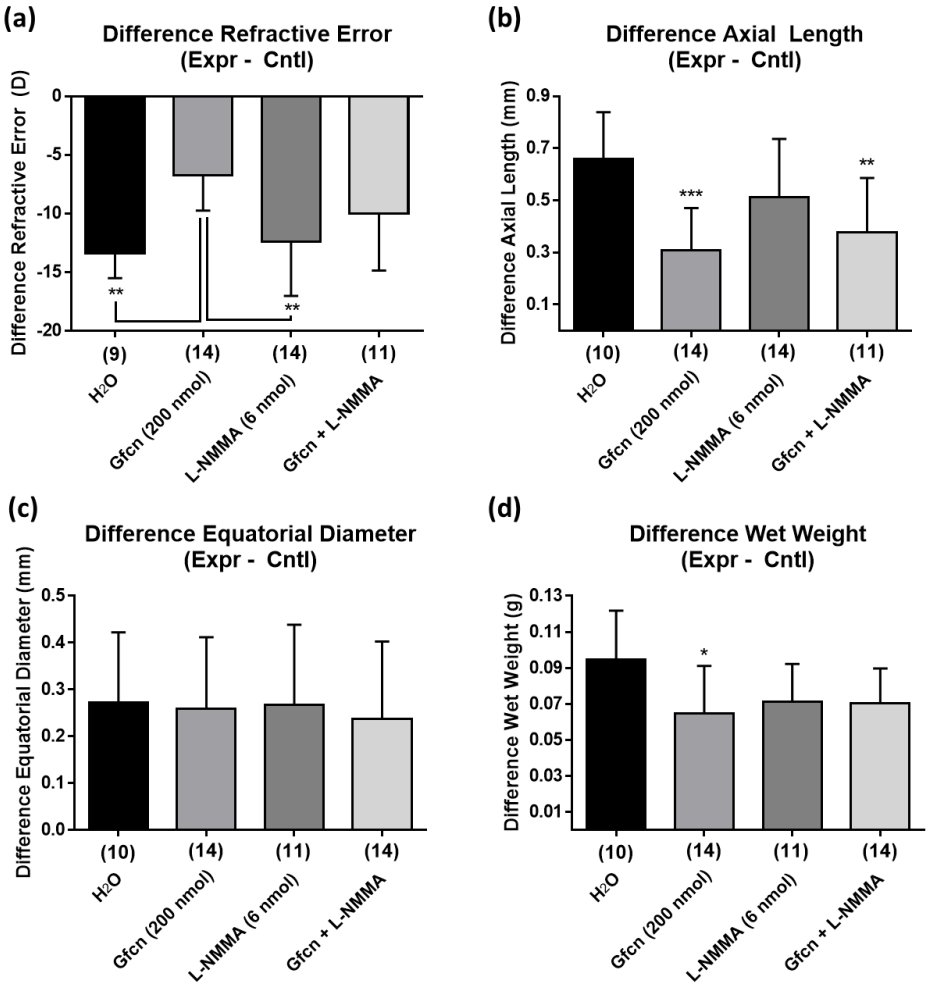

Figure A2.2: The effect of guanfacine (200 nmoles), L-NMMA (6 nmoles) and gfcn + L-NMMA on FDM in chicks. Guanfacine significantly inhibited the induction of negative refractive error (**a**), axial elongation (**b**), and increased weight (**d**) caused by diffuser goggles; there was no statistically significant effect on equatorial diameter (**c**) for any treatment. L-NMMA did not significantly affect the guanfacine-induced reduction of dRE (**a**) and dAL (**b**). ***Abbreviations:*** **H_2O**: distilled water; **gfcn**: guanfacine; **L-NMMA**: L-N^G-monomethyl arginine. ***Statistics***: comparison to H_2O unless specified otherwise; $^{*}p<0.05$; $^{**}p < 0.01$, $^{***}p < 0.001$; One-Way ANOVA + Tukey's post-hoc. Data are represented as the means of the difference in values for the experimental eye minus those for the control eye, ± SD; sample sizes (n) are denoted in brackets below each column.

A2.3: The Myopia-Inhibiting Effects of Guanfacine and Atropine Are Additive

Results are summarized in **Fig A2.3** and **Table A2.1**. Guanfacine- and atropine-treatment significantly inhibited the induced negative refractive error caused by goggle-wear (PBS: -14.8 ± 1.5 D, n = 11; gfcn: -8.1 ± 2.1 D, n = 14, $p_{(PBS)} < 0.0001$; atro: -8.4 ± 3.3 D, n = 12, $p_{(PBS)} < 0.0001$), but did not significantly reduce the difference in axial length, equatorial diameter, or wet weight of goggled eyes (dAL: PBS: 0.54 ± 0.16 mm, n = 13; gfcn: 0.38 ± 0.19 mm, n = 14; atro: 0.40 ± 0.28 mm, n = 13). Eyes treated with gfcn + atro had a significantly smaller difference in refractive error than controls and those treated with gfcn or atropine alone (dRE: -3.7 ± 3.0 D, n = 13, $p_{(PBS)} < 0.0001$, $p_{(gfcn)} = 0.0004$, $p_{(atro)} = 0.0002$), and had axial lengths that were significantly shorter than PBS-controls (dAL: 0.20 ± 0.20 mm, n = 14, $p_{(PBS)} = 0.0006$). Although gfcn + atro-treatment did reduce the mean differences in equatorial diameter (dEQ: 0.20 ± 0.13 mm, n = 14) and wet weight (0.0519 ± 0.026, n = 14), there was no statistically significant difference between any of the treatment groups for these parameters (dEQ: PBS: 0.30 ± 0.15 mm, n = 13; gfcn: 0.27 ± 0.20 mm, n = 14; atro: 0.28 ± 0.16 mm, n = 13 and dWW: PBS: 0.0765 ± 0.025 g, n = 13; gfcn: 0.0696 ± 0.021 g, n = 14; atro: 0.0657 ± 0.037 g, n = 13).

A2.3: The Effects of Atropine, Guanfacine, and Their Combination on FDM in Chicks

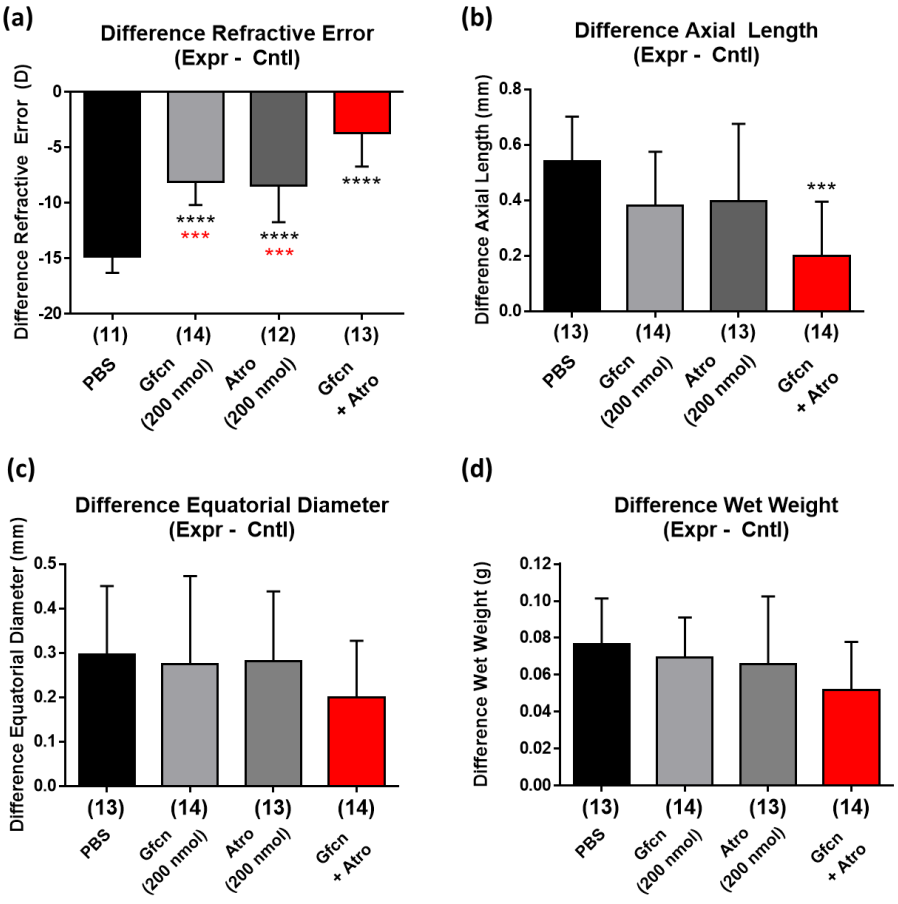

Figure A2.3: The effect of guanfacine (gfcn; 200 nmoles), atropine (atro; 200 nmoles) and gfcn + atro on FDM in chicks. Guanfacine- and atropine-treatment significantly inhibited the difference in refractive error (**a**) caused by diffuser goggles, but did not significantly affect goggle-induced changes in axial elongation (**b**), equatorial diameter (**c**), or wet eye weight (**d**). The combined effect of gfcn + atro resulted in a greater inhibition of FDM than gfcn or atropine alone; but, as usual, this effect was only statistically significant for dRE and dAL. ***Abbreviations:*** **PBS**: phosphate-buffered saline; **gfcn**: guanfacine; **atro**: atropine. ***Statistics***: black: comparison to H_2O; red: comparison to gfcn + atropine; $^{***}p < 0.001$, $^{****}p < 0.0001$; One-Way ANOVA + Tukey's post-hoc. Data are represented as the means of the difference in values for the experimental eye minus those for the control eye, ± SD; sample sizes (n) are denoted in brackets below each column.

Table A2.1: Summarized data for all experiments. Number of replicates for each treatment group (n) and statistically significant p-values (compared to groups in brackets; bold) are reported under the treatment outcomes. Data are represented as the means of the difference in values for the experimental eye minus those for the control eye, ± SD. ***Abbreviations:*** **gfcn**: guanfacine; **yoh**: yohimbine; **L-NMMA**: L-N^G-monomethyl arginine; **atro**: atropine, **G+A**: guanfacine + atropine. Experiment **A2.1** investigated the effect of yohimbine (6 nmoles) on the ability of gfcn to inhibit FDM. Experiment **A2.2** investigated the effect of NO-blockade by L-NMMA (6 nmoles) on gfcn-mediated myopia inhibition. Experiment **A2.3** investigated the effects of simultaneous injection of guanfacine (200 nmoles) and atropine (200 nmoles) on FDM in the chick.

A2.1	**H_2O** **(n)**	**Guanfacine** **(n) p-value**	**Yohimbine** **(n) p-value**	**Gfcn + Yoh** **(n) p-value**
dRE	-15.1 ± 3.5 D (10)	-6.6 ± 1.7 D (12) **$p_{(H2O)}$ < 0.0001**	-15.1 ± 0.8 D (10) **$p_{(gfcn)}$ < 0.0001**	-12.1 ± 4.8 D **(**11) **$p_{(gfcn)}$ = 0.0009**
dAL	0.56 ± 0.25 mm (12)	0.24 ± 0.20 mm (11) **$p_{(H2O)}$ = 0.0014**	0.42 ± 0.15 mm (11)	0.25 ± 0.15 mm **(**12) **$p_{(H2O)}$ = 0.0018**
dEQ	0.31 ± 0.12 mm (11)	0.18 ± 0.11 mm (11)	0.24 ± 0.17 mm (12)	0.26 ± 0.19 mm **(**11)
dWW	0.0924 ± 0.031 g (12)	0.0450 ± 0.022 g (11) **$p_{(H2O)}$ = 0.0018**	0.0578 ± 0.030 g (12) **$p_{(H2O)}$ = 0.0271**	0.0603 ± 0.031 g (12) **$p_{(H2O)}$ = 0.0461**

A2.2	**H_2O** **(n)**	**Guanfacine** **(n) p-value**	**L-NMMA** **(n) p-value**	**Gfcn + L-NMMA** **(n) p-value**
dRE	-13.4 ± 2.1 D (9)	-6.8 ± 3.0 D (14) **$p_{(H2O)}$ = 0.0014**	-12.4 ± 4.6 D (11) **$p_{(gfcn)}$ = 0.0044**	-10.0 ± 4.8 D **(**14)
dAL	0.66 ± 0.18 mm (10)	0.31 ± 0.16 mm (14) **$p_{(H2O)}$ = 0.0004**	0.51 ± 0.22 mm (11)	0.38 ± 0.21 mm **(**14) **$p_{(H2O)}$ = 0.0059**
dEQ	0.27 ± 0.15 mm (10)	0.26 ± 0.15 mm (14)	0.27 ± 0.17 mm (11)	0.24 ± 0.17 mm **(**14)
dWW	0.0946 ± 0.027 g (10)	0.0646 ± 0.027 g (14) **$p_{(H2O)}$ = 0.0179**	0.0714 ± 0.021 g (11)	0.0706 ± 0.019 g (14)

A2.3	PBS (n)	Guanfacine (n) p-value	Atropine (n) p-value	Gfcn + Atro (n) p-value
dRE	-14.8 ± 1.5 D (11)	-8.1 ± 2.1 D (13) **$p_{(PBS)} < 0.0001$** **$p_{(G+A)} = 0.0004$**	-8.4 ± 3.3 D (12) **$p_{(PBS)} < 0.0001$** **$p_{(G+A)} = 0.0002$**	-3.7 ± 3.0 D **(**13) **$p_{(PBS)} < 0.0001$**
dAL	0.54 ± 0.16 mm (13)	0.38 ± 0.19 mm (14)	0.40 ± 0.28 mm (13)	0.20 ± 0.20 mm **(**14) **$p_{(H2O)} = 0.0006$**
dEQ	0.30 ± 0.15 mm (13)	0.27 ± 0.20 mm (14)	0.28 ± 0.16 mm (13)	0.20 ± 0.13 mm **(**14)
dWW	0.0765 ± 0.025 g (13)	0.0696 ± 0.021 g (14)	0.0657 ± 0.037 g (14)	0.0519 ± 0.026 g (14)

Discussion

The results reported here are generally surprising in regards to the possible target receptor, and downstream signalling molecules involved in inhibition of FDM by guanfacine in chicks. First, if guanfacine was working through an α_2-adrenoceptor mechanism, its ability to inhibit myopia should be blocked by simultaneous injection of the high-affinity α_2-adrenoceptor antagonist, yohimbine, but this does not seem to be the case. Second, we have strong evidence that atropine requires induction of ocular NO in order to inhibit FDM in the chick[1] (and **Chapter 3**), but the addition of L-NMMA at concentrations that block atropine-mediated effects does not seem to block myopia inhibition by guanfacine; thus, it is possible that atropine and guanfacine may inhibit FDM via different retinal pathways. This hypothesis may be supported by the results of the third experiment; combination of atropine and guanfacine result in an increased myopia inhibiting effect over injection of either of the drugs alone. The lack of correlation between the difference in refractive error and the difference in axial lengths for experiments A2.1 and A2.2, as well as the lack of effect of gfcn- and atropine-treatment in experiment A2.3, can only be addressed by repetition. Experimentally-induced myopia in chicks is inherently variable, and the results from these experiments will remain inconclusive until further replicates can be obtained. For the purposes of the discussion, however, I will *assume* that the data are true, in order to address possible reasons for the seemingly noteworthy differences between guanfacine-

and atropine-mediated inhibition of FDM in chicks, and to provide insight into the mechanisms that may be responsible for these outcomes.

Inability of Yohimbine to Block Guanfacine-Mediated Myopia Inhibition

This thesis was the first to report the ability of α_2-adrenoceptor agonists – clonidine and guanfacine – to inhibit form-deprivation myopia in the chick (**Chapter 4**; Carr et al. IOVS 2016; 57: ARVO E-Abstract 4738). Like atropine, however, an extremely high concentration of drug (200 nmoles; 10 mM) must be used to achieve 50% (guanfacine) to 80% (clonidine) efficacy, and while guanfacine seems to affect FDM at concentrations $\geq$ 100 µM, clonidine had no effect on FDM until the highest dose tested. In this regard, it is not as surprising that yohimbine was unable to block myopia inhibition by guanfacine, as it is likely that guanfacine too may inhibit FDM by binding to some non-specific target in the eye. To address this issue, it would be useful to examine non-specific binding partners of high-concentration atropine, guanfacine, and clonidine, and then look for any overlapping receptors. This could be done by methods such as a pull-down assay. Another possibility is that the yohimbine used for these experiments was no longer active; because of the experimental set up, and the lack of information on the effect of yohimbine on FDM, we cannot verify the activity of intravitreally-injected yohimbine by measuring changes in eye growth caused by diffuser wear. These experiments were performed at the same time as the receptor pharmacology experiments (**Chapter 5**), however, and the same yohimbine was effective at blocking clonidine-induced increases in CRE-luciferase expression, at a concentration similar to previously published values (**Table 5.2**).

Inability of L-NMMA to Block Inhibition of FDM by Guanfacine

There is substantial evidence that induction of nitric oxide is required for myopia inhibition in the chick[46-48,110], and mouse (Chakraborty et al. IOVS 2016; 57: E-Abstract 4742), and that it is an essential signalling molecule for atropine-mediated myopia inhibition[1] (**Chapter 3**). If gfcn and atropine modulate signalling through the same receptor(s) to inhibit FDM, it would be expected that NO-signalling would also be required for myopia inhibition by gfcn. Our data do not support an important role of NO in myopia inhibition by gfcn, however, which could indicate the presence of two distinct growth- regulating

pathways. This conclusion is not outlandish; diurnal animals such as chicks are highly-dependent on in-focus vision for their survival, and redundant growth-regulating mechanisms would protect against complete failure of emmetropization. It is less likely that the L-NMMA would have no effect because the drug was old or inactive, as these experiments were performed shortly after the atropine + L-NMMA experiments, in which it had a significant effect.

Additive Effect of Guanfacine and Atropine On Myopia-Inhibition

The differences in refractive error and axial elongation for eyes treated with atropine and gfcn alone were smaller than when the drugs were injected simultaneously. This result could have two possible explanations. First, it could simply be that by combining the drugs we are essentially doubling the concentration, which may result in a stronger inhibitory effect. This is a distinct possibility; although the effects of atropine and gfcn seem to begin their plateau at concentrations ≥ 2 nmoles (**Fig. A2.4**), I have not tested concentrations > 10 mM in our particular strain of chick. Therefore, I cannot say whether higher concentrations of either drug alone could result in an increased anti-myopia effect. Second, it is possible that high concentration atropine and high concentration guanfacine may affect different myopia-inhibiting pathways in the eye (discussed in **Chapter 6**). These experiments are similar in theory to a previous study investigating the effects of combination of atropine and apomorphine, which did not find an additive effect of atropine plus apomorphine[115]. That my experiments were additive, when previous experiments using atropine plus dopamine agonism were not, supports the presence of multiple emmetropization pathways in the eye, and/or the possibility of multiple sites of action for growth-regulating processes; speculatively, for example, atropine may act in the choroid – requiring high concentration drug to reach the target receptors because of loss through diffusion and binding in non-target tissues – whereas guanfacine and dopamine action may occur in the retina – where dopamine action is mediated through dopamine receptors, and perhaps clonidine and guanfacine may act as a non-specific ligand at those same receptors.

A2.4: The Effects of Extended Doses of Atropine and Guanfacine on FDM in Chicks

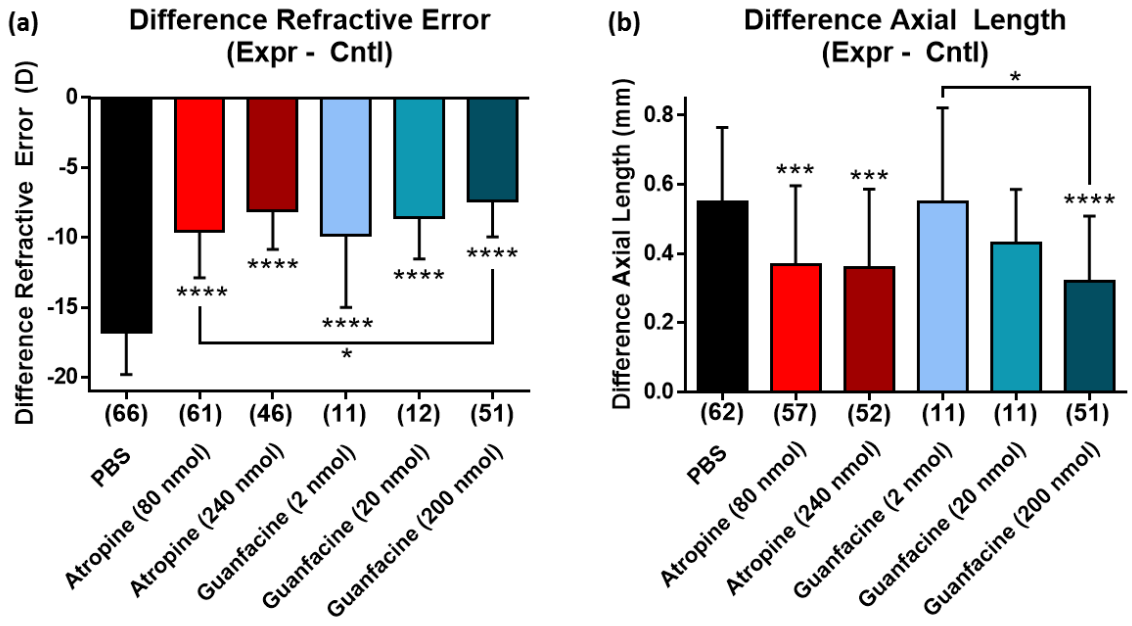

Figure A2.4: The effects of atropine (80 & 240 nmoles) and guanfacine (2, 20, and 200 nmoles) on the difference in refractive error (**a**) and axial length (**b**) induced by form-diffusers in the chick. Both atropine- and guanfacine-treatment plateau near 50% inhibition, beginning at intravitreally injected concentrations of ≥ 20 nmoles. There was no significant treatment effect on the differences in equatorial diameter or wet weight of the eyes (data not shown). ***Statistics:*** comparison to PBS-controls unless indicated otherwise by brackets; ****$p < 0.0001$, ***$p < 0.001$, *$p < 0.05$. One-Way ANOVA, Tukey's post-hoc. Data are represented as the means of the difference in values for the experimental eye minus those for the control eye, ± SD; sample sizes (n) are denoted in brackets below each column.

Methods

The animal ethics statement and common methods for induction of form-deprivation myopia, intravitreal injections, eye biometric measurements, and statistical analysis are described previously in **Chapter 2**. The chickens used in these experiments were Lohmanns (**A2.1**; Clark's Poultry, Brandon, MA) and Shavers (**A2.2** & **A2.3**; Rochester Hatchery, Westlock, AB).

Drugs for Intravitreal Injection

Drugs, commercial sources, and the molar amounts delivered per injection are listed in **Table A2.2**. Due to low solubility of guanfacine, drugs were either dissolved in sterile distilled H_2O at room temperature (gfcn + yohimbine & gfcn + L-NMMA) or sterile phosphate-buffered saline (PBS; Gibco 14190-144; ThermoFisher Scientific, WA, USA) that was slightly warmed (≤ 30°C) (gfcn + atropine). Stock solutions were made fresh for each injection and kept at room temperature until use, which was less than 1 hr. The concentrations tested were based on previously published data (atropine & L-NMMA[1]), preliminary dose-response data (guanfacine; **Chapter 4**) in this specific strain of chick, and concentrations that were estimated to be in excess of 1000x the binding affinity of guanfacine at the mammalian α_{2A}-adrenoceptor[279] (yohimbine). We chose to use yohimbine because it has affinity for the ADRA2A subtype, the most abundant subtype in the CNS, and it is water soluble, thus easily injected into the eye and poses a smaller risk of precipitating in the vitreous. We chose to investigate the effects of L-NMMA because it ablated atropine-mediated myopia inhibition and has a negative control counterpart (D-NMMA).

Table A2.2: Agents employed in the present studies.

Drug	Source	Cat#	Amt/Injection (Syringe)
Atropine Sulfate	Sigma-Aldrich	A0257	200 nmoles
Guanfacine • HCl	Sigma-Aldrich	G1043	200 nmoles
L-NMMA	Sigma-Aldrich	M7033	6 nmoles
Yohimbine • HCl	Sigma-Aldrich	Y3125	6 nmoles

Appendix A3: Attempts to Clone a Functional Chicken Alpha$_{2A}$-Adrenoceptor

The ability to compare ligand binding characteristics between human and chicken α_{2A}-adrenoceptor would have been a useful contribution to this thesis; especially because MT3 had a significantly lower potency at human vs. chicken mAChR M_4 (**Chapter 5**). Although we were unsuccessful in obtaining a functional chicken α_{2A}-adrenoceptor clone to test in parallel with the human one, it was not for lack of trying. This appendix chapter outlines the various methods we attempted in order to create a functional chicken α_{2A}-adrenoceptor (cADRA2A) clone.

A3.1: Reverse-Transcription from RNA

RNA Extraction from Chick Tissues

All reagents and kits used were from QIAgen (Hilden, Germany), unless specified otherwise. We first attempted to clone the cADRA2A receptor from RNA extracted from various chick tissues (age P1): retina/RPE, heart, kidney, and spleen. Retina/RPE RNA was purified using the RNeasy Lipid Tissue Midi kit and protocol. Two eye-cups were placed in 5 mL QIAzol Lysis Reagent and incubated at room temperature for 5 min. Chloroform (200 µL/750 µL homogenate) was added with vigorous shaking, and then incubated for 3 min at room temperature. The choloroform/homogenate solution was then centrifuged at 5000g for 15 min at 4°C, and then the upper aqueous phase was transferred into a new tube with 750 µL 70% EtOH and vortexed gently to mix. The solution was then transferred into an RNeasy column and washed once with 400 µL RW1 buffer, and then washed twice with 400 µL RPE buffer. RNA was eluted in 40 µL RNAse-free H_2O; final concentration of total RNA was 2600 ng/µL. Heart, kidney, and spleen tissues were placed into RNeasy Lysis Buffer (20 µL/ mg tissue) before homogenization using a rotor-stator homogenizer. Homogenized tissue lysate was then added to a QIAshredder column, and centrifuged, after which 750 µL of 70% EtOH was added, and the contents transferred to a RNeasy spin column. The sample was washed once with 700 µL Buffer RW1, and then twice with 500 µL Buffer RPE. RNA was eluted with 40 µL RNAse-free H_2O; final concentrations of total RNA were: heart: 520 ng/µL; kidney: 820 ng/µL; spleen: 850 ng/µL. RNA bands were checked on 1% agarose made with TBE buffer (27 g Tris base + 18.8 g boric acid + 10 mL 0.5 M EDTA + 500 mL dH_2O). 2-3 ug RNA from heart, kidney,

and spleen + 10x volume loading dye was added to each well, and gel was run at 50 mV for 45 min (**Fig. A3.1a**).

SuperScript™ III Reverse Transcriptase – cDNA Synthesis

Reagents were from Invitrogen (Thermo Fisher Scientific, Calsbad, CA, USA) unless specified otherwise. The following reagents were added to a nuclease-free tube on ice: 1 µL oligoDT (100 µM), 4 µg total RNA (retina/RPE: 2 µL, heart: 8 µL, kidney: 5 µL, spleen: 5 µL), 1 µL 10 mM dNTP, 13 µL nuclease-free dH_2O. The mixture was heated to 65°C for 5 min and then incubated on ice for 1 min before being collected by short centrifugation. The following reagents were then added: 4 µL 5X first-strand buffer, 1 µL 0.1 M DTT, 1 µL RNase out (40 units/µL), and 1 µL SuperScript™ III reverse transcriptase (200 units/µL). Contents were mixed by pipetting and then incubated at 50°C for 45 min, and then the reaction was inactivated by heating to 70°C for 15 min. The product was stored at -20°C until use, and a 1:1 conversion ratio for transcription of RNA to cDNA was assumed (estimated final concentration of 4 µg cDNA).

Polymerase Chain Reaction (PCR) – Attempted amplification of cADRA2A Clone

We then attempted to amplify the cADRA2A receptor using PCR; primers (5'-3') were based on the predicted sequence for chicken (*Gallus gallus*) ADRA2A mRNA (NCBI: XP_004942333.2; F1: ATGGAGTACCAGCGGCAGCTGGAG, R1: AACGATCCTTTTCCTCTCTCTATCCT; F2: GGGTCCGGAGAGTACCAGCGGCAGCTGGAG, R2: GGGCTCGAGTCAAACGATCCTTTTCCTCTCT; F3: TGAGAGCAAAGAGCCCATGA, R3: CCAGGCCGTTCTGCTTTTTC). Chicken beta actin (NCBI: NM_205518; F: GAGAAATTGTGCGTGACATCA, R: CCTGAACCTCTCATTGCCA) and GADPH (NCBI: NM_204305; F: GGTGGTGCTAAGCGTGTTA, R: CCCTCCACAATGCCAA) were used as housekeeping genes[280]. Two different PCR master-mix solutions were used (**Table A3.1**). Unfortunately, we were unable to get any quantifiable PCR products for any primer set (cADRA2A, chicken β-Actin, or chicken GADPH; **Fig. A3.1b**) even after multiple replications and changes to protocols.

Table A3.1: Polymerase chain reaction master-mixes and protocols used to attempt to clone the chicken α_{2A}-adrenoceptor and housekeeping genes (chicken β-Actin and GADPH).

Pfx Buffer	**Mihara Buffer**	**PCR Protocol(s)**	
45.7 µL dH_2O	48.7 µL dH_2O	95°C - 2 min	94°C - 2 min
6 µL Pfx Buffer	6 µL Mihara buffer	95°C - 20 s	94°C - 20 s
1.8 µL dNTP	1.2 µL template	63°C - 20 s	60°C - 20 s
1.2 µL MgSO4	1.2 µL primers (F and R) 0.6 µL housekeeping primers	68°C - 20 s	72°C - 15 s
1.2 µL template	0.5 µL Platinum Pfx DNA pol.	68°C - 1 min	72°C - 5 min
1.2 µL primers (F and R) 0.6 µL housekeeping primers		10°C - 30 s	10°C - 30 s
0.5 µL Platinum Pfx DNA pol.		30 cycles	40 cycles

Figure A3.1: RNA Extraction and PCR Products After Attempts to Clone cADRA2A

(a)

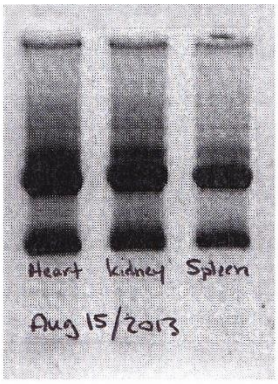

(b)

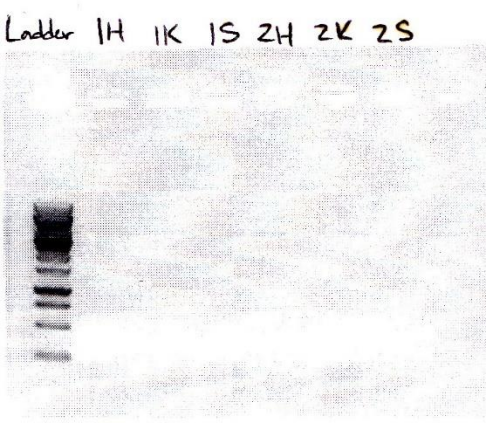

Figure A3.1: Although we were able to extract RNA with the proper 28s and 18s bands (**a**), we were unsuccessful in amplifying PCR products from the resultant cDNA (**b**); this is an example of a 1% agarose gel after PCR cDNA derived from heart, (1H, 2H), (1K, 2K), and spleen (1S, 2S). Sample 1 from each was performed with Pfx buffer and protocol, and sample 2 was Mihara buffer (**Table A3.1**). Ladder was GeneRuler 1kb DNA Ladder (ThermoFisher Scientific, Carlsbad, CA, USA).

A3.2: Synthesizing the Receptor Directly from the Predicted Sequence

After attempts to amplify the clone using RT-PCR failed, we decided to commercially synthesize the receptor directly from the predicted protein sequence (NCBI: XP_004942333.2) through Integrated DNA Technologies (IDT; Coralville, IA, USA); a 3X HA tag was added to the n-terminal of the receptor sequence, and the sequence was ligated into a pcDNA™3.1+ vector. Upon transfection, the synthesized clone did not express in the cell membrane as expected (**Fig. A3.2a**), nor did agonist-treatment result in any significant changes in CRE-Luc expression as assayed by the Dual Glo® Luciferase Assay system (Promega; **Fig. A3.2b**). During testing of the cADRA2A receptor, the predicted sequence was updated online to include a 17 amino acid addition onto the n-terminal, so we synthesized the new sequence and retested it; but, we still could not obtain a conclusive change in CRE-Luc expression upon agonist-treatment (**Fig. A3.2c**).

Figure A3.2: Agonist-Treatment and Receptor Localization of Commercially Synthesized cADRA2A Clone and cADRA2A Clone + 17 aa Sequence

(a)

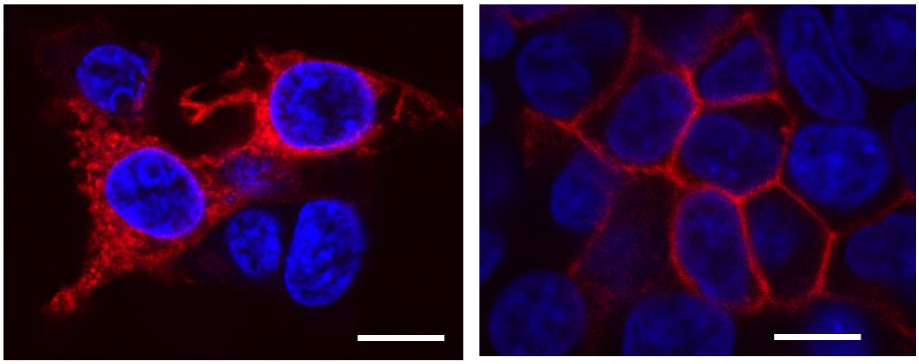

cADRA2A cM_4

(b)

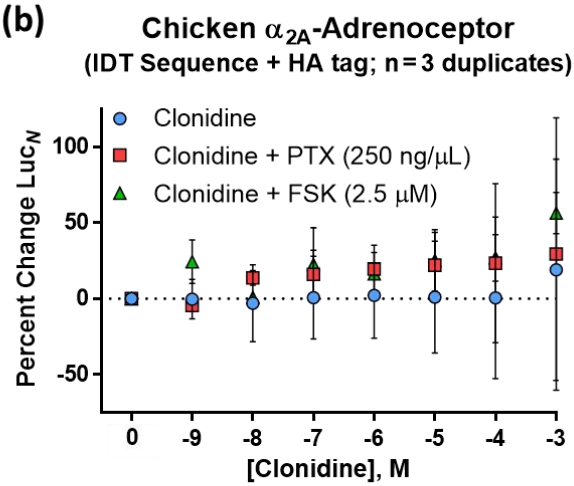

(c)

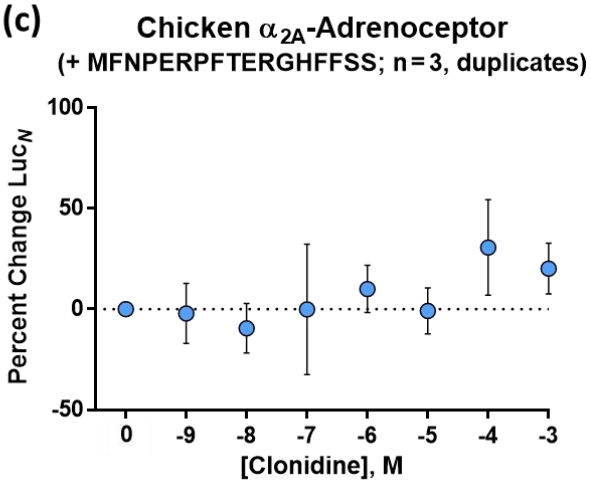

Figure A3.2: Experimental data obtained for the synthesized cADRA2A receptor. The receptor sequence was commercially-produced according to the predicted sequence published online, and a 3X HA-tag was added later to aid localization in the cell. Once the receptor was transfected into CR-M_3 cells, they failed to localize to the membrane as expected – membrane localization of cM_4 (right) is included for comparison (**a**), or produce any functional changes in normalized CRE-Luc expression even in varying experimental conditions (**b**). During testing, the predicated sequence was updated to include 17 amino acids on the N-terminal (MFNPERPFTERGHFFSS). We re-made the clone, removed the HA tag, and tested its function using the Dual-Glo® Luciferase Assay (Promega), but there was still no response to clonidine-treatment (**c**). Image **A3.2a** was taken on the Olympus FV1000 laser-scanning confocal microscope (Live Cell Imaging Facility, Snyder Institute, Cumming School of Medicine, University of Calgary) using a 60x oil immersion objective (NA = 1.42); scale bar = 10 µm.

A3.3: Human-Chicken Chimera

The n-terminal of the cADRA2A receptor is missing glycosylation and myristylation sites compared to the human ADRA2A receptor n-terminal. Because we were expressing these receptors in a human cell line, we hypothesized that the lack of these sites in the cADRA2A receptor may be interfering with trafficking the receptor to the cell membrane, resulting in a non-functional receptor. To test this, we created a chicken ADRA2A receptor with a human ADRA2A receptor n-terminal, termed the chicken chimera ADRA2A receptor (ccADRA2A; **Fig. A3.3a**). This receptor did not have an HA tag, so we have not examined whether the human n-terminus had an effect on localization, but functional assay of the receptor determined that treatment with high concentration agonist (2-4 mM clonidine) resulted in a small (≤ -100%) percent change in CRE-Luc expression in the presence of 2.5-5 µM forskolin (FSK) that was different than plasmid-only controls (**Fig. A3.3b,c**). Unfortunately, however, there was no obvious effect of yohimbine-treatment at a concentration of 1 mM clonidine (ca. 30% effective dose) in the presence of 2.5 µM FSK (**Fig. A3.3d**). Due to the nearly toxic concentration of clonidine required to elicit any effect from ccADRA2A, and the inability to measure accurately the small changes in CRE-Luc expression, we decided to abandon these experiments. It is likely that any results obtained from this system would not be broadly applicable to ligand binding behavior at the chicken ADRA2A.

Figure A3.3: Sequence and Agonist-Treatment of Human-Chick Chimera (ccADRA2A)

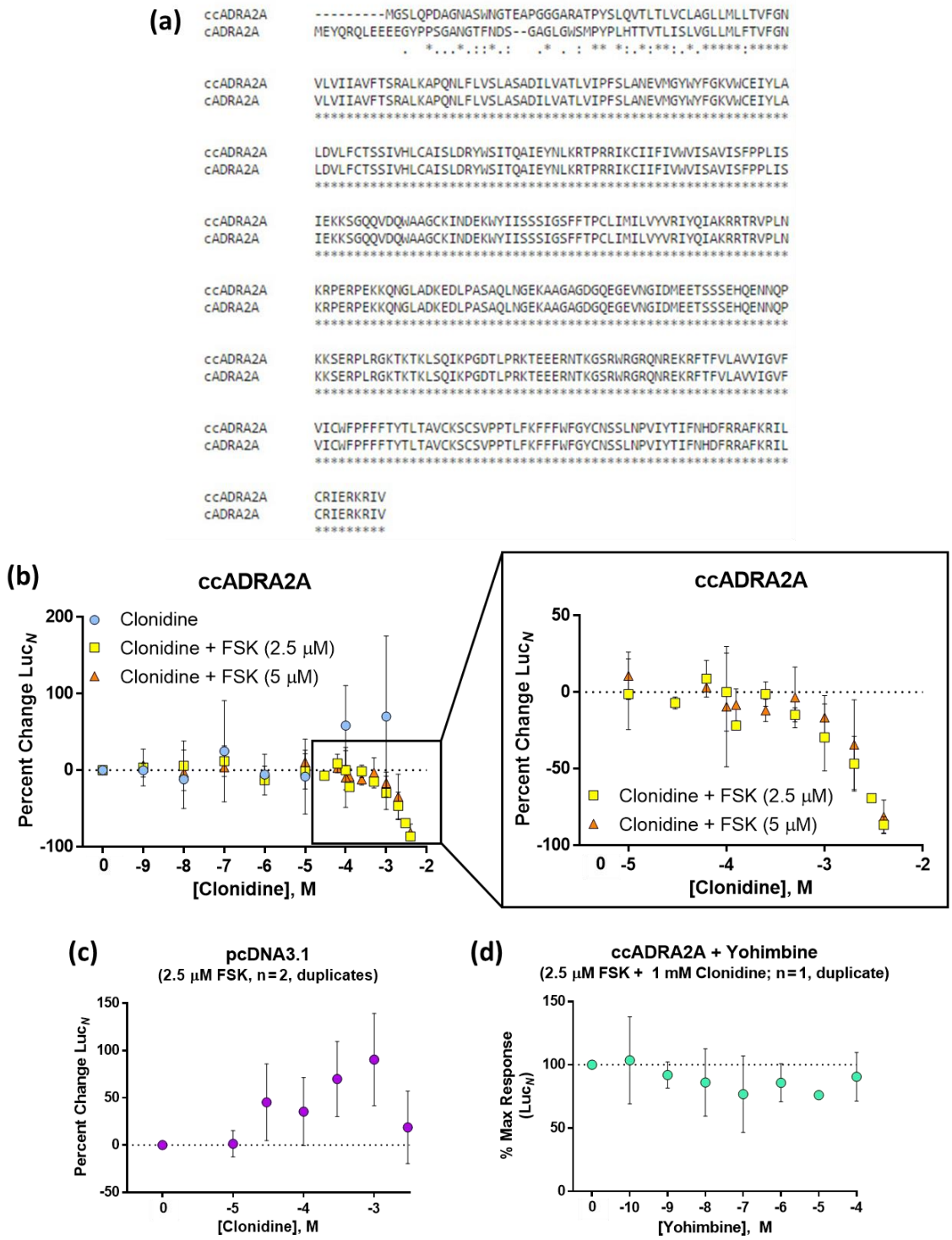

Figure A3.3: Experimental data from experiments using the human n-terminal chicken chimera receptor (ccADRA2A). The receptor sequence matched that of cADRA2A, with the exception of the n-terminal amino acids 1-42 (**a**) which were substituted with the human ADRA2A sequence. High concentration agonist-treatment (clonidine, 2-4 mM) did result in changes in CRE-Luc expression in the presence of 2.5 µM FSK (**b**) that differed from pcDNA™3.1+-transfected cells (**c**), but there was no effect of yohimbine-treatment on these changes at concentrations ≤ 100 µM (**d**).

Discussion

We were unable to get satisfactory results from multiple attempts at cloning and expressing a functional chicken α_{2A}-adrenoceptor. It is possible that we did not use tissues with high enough expression of cADRA2A mRNA (retina, heart, spleen, kidney) to clone the receptor via RT-PCR. We chose these tissues on the basis of expression data for humans (human protein atlas), and for ease in removal of these tissues from the chick; but expression levels in these tissues (human) is not high. The published sequence for cADRA2A (NCBI: XP_004942333.2) is only a *predicted* sequence based on homology with mammalian receptors; it has not been verified experimentally. If the sequence is incorrect at even very few base pairs, it could impact our ability to design primers (for RT-PCR) or get expression of a functional receptor from commercial synthesis. We have some evidence that the commercially synthesized cADRA2A receptor was not able to be trafficked and localized correctly to the cell membrane (**Fig A3.2b**). The receptor sequence was missing glycosylation and myristylation sites which *are* present on the human receptor; missing important protein modification sites such as these could explain why the receptor seemed to be "stuck" in the golgi/ER (not shown) or was mislocalized to the cytoplasm of the human HEK293T host cells. Another issue with using human cells to host a chicken receptor is that the correct G protein alpha subunit required for coupling to a chicken receptor may not be present; if the receptor cannot couple with the existing G proteins in the cell, no signalling can occur[220].

Copyright Permissions

Journal of Biological Chemistry

1. Kukkonen, A., Perakyla, M., Akerman, K. E. & Nasman, J. (2004). Muscarinic toxin 7 selectivity is dictated by extracellular receptor loops. *J Biol Chem* **279**, 50923-50929 (**Figure 5.7**)

© Association for Research in Vision and Ophthalmology (ARVO)

Investigative Ophthalmology and Visual Science (IOVS)

1. Strang, C. E., Renna, J. M., Amthor, F. R. & Keyser, K. T. (2010). Muscarinic acetylcholine receptor localization and activation effects on ganglion response properties. *Invest Ophthalmol Vis Sci* **51**, 2778-2789 (**Figure 1.4**)
2. Harun-Or-Rashid, M., Lindqvist, N. & Hallbook, F. (2014). Transactivation of EGF receptors in chicken Muller cells by alpha2A-adrenergic receptors stimulated by brimonidine. *Invest Ophthalmol Vis Sci* **55**, 3385-3394 (**Figure 1.5**)

RE: Copyright Permissions for PhD Thesis

Debbie Chin

Tue 2/28/2017 3:31 PM

To: Brittany Jane Carr

Hi Brittany,

Thank you for the information.

Permission is hereby granted to reprint the following figures in your PhD thesis for the University of Calgary:
Figure 6 from Strang CE, Renna JM, Amthor FR, Keyser KT. Muscarinic acetylcholine receptor localization and activation effects on ganglion response properties. *Invest Ophthalmol Vis Sci*. 2010;51:2778-2789.
Figure 1 from Harun-Or-Rashid M, Lindqvist N, Hallböök F. Transactivation of EGF receptors in chicken Müller cells by α2A-adrenergic receptors stimulated by brimonidine. *Invest Ophthalmol Vis Sci*. 2014;55:3385-3394.
A reprint of this material must include full article citations and acknowledge ARVO as the copyright holder.

Regarding the material from your past ARVO abstracts, ARVO only owns the copyright for the abstracts. You and your co-authors own the copyright for the posters, so you are free to reuse it.

For the material from your upcoming ARVO poster, you said your thesis will be submitted before the Annual Meeting. But will it be approved and published after the Meeting? I think the material must be presented at the Meeting before it is published elsewhere, but I can double-check this if you think your thesis will be published before the Meeting. If you know it will be published after the Meeting, then I think you could cite the material as 'submitted' or 'in press' now, and then update the citation after the Meeting.

Best regard,
Debbie

© Cambridge University Press

Visual Neuroscience (Vis Neurosci)

1. Woldemussie, E., Wijono, M. & Pow, D. (2007). Localization of alpha 2 receptors in ocular tissues. *Visual neuroscience* **24**, 745-756 (**Figure 1.5**)
2. Wilson, M., Nacsa, N., Hart, N. S., Weller, C. & Vaney, D. I. (2011). Regional distribution of nitrergic neurons in the inner retina of the chicken. Vis Neurosci 28, 205-220 (**Figure 1.6**)
3. Tekmen-Clark, M. & Gleason, E. (2013). Nitric oxide production and the expression of two nitric oxide synthases in the avian retina. *Visual neuroscience* **30**, 91-103 (**Figure 1.6**)

RE: Permission Request

Adam Hirschberg

Wed 3/22/2017 9:43 AM

To: Brittany Jane Carr

Cambridge University Press grants permission freely for the reproduction in another work of a short prose extract (less than 400 words), a single figure or a single table in which it holds rights. In such cases a request for permission need not be submitted, but the reproduced material must be accompanied by a full citation of the original source. Always check the caption or citation to ensure that Cambridge is the rights holder before proceeding.

Regards,

Adam

Adam Hirschberg
Senior Permissions Associate

© John Wiley & Sons, Incorporated

Journal of Comparative Neurology (JCN)

1. Fischer, A. J., McKinnon, L. A., Nathanson, N. M. & Stell, W. K. (1998). Identification and localization of muscarinic acetylcholine receptors in the ocular tissues of the chick. J Comp Neurol 392, 273-284 (**Figure 1.4**)

JOHN WILEY AND SONS LICENSE TERMS AND CONDITIONS

Mar 30, 2017

This Agreement between Brittany Carr ("You") and John Wiley and Sons ("John Wiley and Sons") consists of your license details and the terms and conditions provided by John Wiley and Sons and Copyright Clearance Center.

License Number	4061720433433
License date	
Licensed Content Publisher	John Wiley and Sons
Licensed Content Publication	Journal of Comparative Neurology
Licensed Content Title	Identification and localization of muscarinic acetylcholine receptors in the ocular tissues of the chick
Licensed Content Author	Andy J. Fischer,Lise A. McKinnon,Neil M. Nathanson,William K. Stell
Licensed Content Date	Dec 6, 1998
Licensed Content Pages	12
Type of use	Dissertation/Thesis
Requestor type	University/Academic
Format	Electronic
Portion	Figure/table
Number of figures/tables	1
Original Wiley figure/table number(s)	Figure 1
Will you be translating?	No
Title of your thesis / dissertation	Mechanisms of Myopia-Inhibiting Muscarinic Antagonists in Chick: A Case of Mistaken Identity?
Expected completion date	May 2017
Expected size (number of pages)	150
Requestor Location	Brittany Carr
Publisher Tax ID	EU826007151
Billing Type	Invoice
Billing Address	Brittany Carr
Total	0.00 CAD

2. Fischer, A. J. & Stell, W. K. (1999). Nitric oxide synthase-containing cells in the retina, pigmented epithelium, choroid, and sclera of the chick eye. *J Comp Neurol* **405**, 1-14 (**Figure 1.6**)

JOHN WILEY AND SONS LICENSE TERMS AND CONDITIONS

Mar 30, 2017

This Agreement between Brittany Carr ("You") and John Wiley and Sons ("John Wiley and Sons") consists of your license details and the terms and conditions provided by John Wiley and Sons and Copyright Clearance Center.

License Number	4061720304521
License date	
Licensed Content Publisher	John Wiley and Sons
Licensed Content Publication	Journal of Comparative Neurology
Licensed Content Title	Nitric oxide synthase-containing cells in the retina, pigmented epithelium, choroid, and sclera of the chick eye
Licensed Content Author	Andy J. Fischer,William K. Stell
Licensed Content Date	Jan 27, 1999
Licensed Content Pages	14
Type of use	Dissertation/Thesis
Requestor type	University/Academic
Format	Electronic
Portion	Figure/table
Number of figures/tables	2
Original Wiley figure/table number(s)	Figure 4, Figure 5a
Will you be translating?	No
Title of your thesis / dissertation	Mechanisms of Myopia-Inhibiting Muscarinic Antagonists in Chick: A Case of Mistaken Identity?
Expected completion date	May 2017
Expected size (number of pages)	150
Requestor Location	Brittany Carr
Publisher Tax ID	EU826007151
Billing Type	Invoice
Billing Address	Brittany Carr
Total	0.00 CAD

© Molecular Vision

1. McBrien, N. A., Jobling, A. I., Truong, H. T., Cottriall, C. L. & Gentle, A. (2009). Expression of muscarinic receptor subtypes in tree shrew ocular tissues and their regulation during the development of myopia. Mol Vis 15, 464-475 (**Figure 1.4**)

Fwd: Agii: Copyright permission for PhD thesis

Nickerson, John

Wed 3/1/2017 1:32 PM

To: Brittany Jane Carr

Hi Brittany,

Yes, you have permission to reprint the figures as you indicated below.

Congratulations on reaching this milestone in your career. Were/are you working in Bill Stell's lab?

Best wishes,

-JN

John M. Nickerson, Ph.D.
Editor-in-Chief, Molecular Vision

© Osram Sylvania

Spectral power distributions of Sylvania Octron®XP®ECO3 fluorescent lamp and daylight at 6500 K (**Figure 2.1**)

approval

Tue 3/21/2017 9:27 AM

Hello Brittany,
I have checked with our legal department and they approved the use of the graphs that you attached. If you need further assistance, please let me know.

Thank you,

Misty

© Webvision: The Organization of the Retina and Visual System (Online)

1. Kolb, H. (2012). Gross Anatomy of the Eye. *Webvision: The Organization of the Retina and Visual System*, (Online) http://webvision.med.utah.edu (**Figure 1.2**)

Re: Copyright permission

Hello Brittany
There is no copyright on webvision images. I can give you permission to use the image personally, and I do just that. Go ahead and use any image that is in any chapter I wrote for web vision. If you want to use an image from a chapter written by any other author you could write directly to the author. Again there is no copyright but it would be polite. Hope this is clear. We have a copyright clause in the first pages of webvision that gives facts and information. Hope to hear from you soon concerning the myopia chapter. All the best and good luck, Helga Kolb

Helga Kolb